Progress in Materials Science 154 (2025) 101506

Contents lists available at ScienceDirect

Progress in Materials Science

journal homepage: www.elsevier.com/locate/pmatsci

The wide range of battery systems: From micro- to structural batteries, from biodegradable to high performance batteries

Carlos M. Costa [a,b,1,*], Manuel Salado [c,d], Chiara Ferrara [e], Riccardo Ruffo [e], Piercarlo Mustarelli [f], Rui Mao [f], Sheng Feng [f], Yuxiang Shang [f], Xiaochen Wang [f], Zhenkun Lei [f], Ruixiang Bai [f], Cheng Yan [g], Kwon-Hyung Lee [h], Sang-Woo Kim [i], Tae-Hee Kim [j], Sang-Young Lee [k], Long Kong [l], Qiang Zhang [m], Harsha Devnani [n,o], Shikha Gupta [p], James F. Rohan [q], Neil S. Curtis [q], Abhishek Lahiri [r], Yinghe He [r], S. Lanceros-Mendez [a,c,d,*]

[a] *Physics Centre of Minho and Porto Universities (CF-UM-UP) and Laboratory of Physics for Materials and Emergent Technologies, LapMET, University of Minho, 4710-057 Braga, Portugal*
[b] *Institute of Science and Innovation for Bio-Sustainability (IB-S), University of Minho, 4710-053 Braga, Portugal*
[c] *BCMaterials, Basque Center for Materials, Applications and Nanostructures, UPV/EHU Science Park, 48940 Leioa, Spain*
[d] *IKERBASQUE, Basque Foundation for Science, Bilbao 48009, Spain*
[e] *Department of Materials Science, University of Milano-Bicocca, and GISEL-INSTM, Via Cozzi, 55, 20125 Milano, Italy*
[f] *State Key Laboratory of Structural Analysis, Optimization and CAE Software for Industrial Equipment, Dalian University of Technology, Dalian 116024, China*
[g] *School of Mechanical, Medical and Process Engineering, Queensland University of Technology, Brisbane, QLD 4001, Australia*
[h] *Ulsan Advanced Energy Technology R&D Center, Korea Institute of Energy Research (KIER), Ulsan 44776, Republic of Korea*
[i] *Department of Energy and Chemical Engineering, Ulsan National Institute of Science and Technology (UNIST), Ulsan 44919, Republic of Korea*
[j] *School of Chemical Engineering, University of Ulsan, Ulsan 44610, Republic of Korea*
[k] *Department of Chemical and Biomolecular Engineering, Yonsei University, Seoul 03772, Republic of Korea*
[l] *Institute of Flexible Electronics, Northwestern Polytechnical University, Xi'an 710129, China*
[m] *Beijing Key Laboratory of Green Chemical Reaction Engineering and Technology, Department of Chemical Engineering, Tsinghua University, Beijing 100084, China*
[n] *Department of Sciences, School of Sciences, Manav Rachna University, Faridabad 121004, India*
[o] *University Instrumentation Center, Manav Rachna University, Faridabad 121004, India*
[p] *Department of Chemistry, Faculty of Engineering and Technology, Manav Rachna International Institute of Research & Studies, Faridabad 121004, India*
[q] *Tyndall National Institute, Lee Maltings, University College Cork T12 R5CP Cork, Ireland*
[r] *Department of Chemical Engineering, Brunel University of London, UB8 3PH Uxbridge, United Kingdom*

ARTICLE INFO

Keywords:
Different battery systems
Smart capabilities
Circular Economy
Recycling issues

ABSTRACT

Battery systems are essential components of the on-going energy transition and digitalization of society. With the need to power an increasing variety of portable and stationary systems, ranging from disposable point-of-care devices or smart packaging systems to applications in portable computers and electric cars, an increasing variety of batteries and battery systems are being developed, each aiming to specific sets of required performance parameters, including energy and

---

[*] Corresponding authors at: Physics Centre of Minho and Porto Universities (CF-UM-UP) and Laboratory of Physics for Materials and Emergent Technologies, LapMET, University of Minho, 4710-057 Braga, Portugal.

E-mail addresses: cmscosta@fisica.uminho.pt (C.M. Costa), senentxu.lanceros@bcmaterials.net (S. Lanceros-Mendez).

[1] All authors contributed equally to the review, by being in charge of different sections.

https://doi.org/10.1016/j.pmatsci.2025.101506
Received 16 January 2024; Received in revised form 18 January 2025; Accepted 7 May 2025

power density, cycling stability, flexibility, degradability, environmental impact or improved integration into the specific application context.

This work analyzed the state of the art of the different materials and geometries, performance parameters and applications of the different battery systems.

We discuss the rationale behind each material selection, the processing technologies and the integration into the specific application, taking into account the whole life-cycle of the battery. Further, the main challenges posed for each battery type will provide a roadmap for their successful development and application.

---

1. Introduction: performance parameters and main characteristics of batteries systems

Energy and environmental issues are the two most pressing global issues that society will face in the next half century, considering that fossil fuels are currently the main source of energy used to satisfy human needs and that the reduction of their is necessary, as they decisively contribute to climate change and global warming [1–3]. Given the need to reduce greenhouse gas emissions from fossil fuels and the increasing energy demand, related to population growth and improved socio-economical conditions, the focus is directed towards the development and implementation of technologies and devices related to renewable energies, i.e. sustainable energy generation and storage, also related to the electrification of the economy and society [4,5].

There are a variety of systems to generate energy in a sustainable way, including solar, wind, or hydroelectric, among others, in which energy efficiency is often also closely linked to energy storage and conservation [6,7].

After electricity is produced, it needs to be effectively stored for its use in various applications or during times of low demand [8] where energy storage devices are also required [9].

Research and technology related to energy storage systems is a rapidly evolving area based on the objective challenges posed by energy transition and the need to power an increasing number of very different portable electronic devices, as well as by the rapid implementation of the electric car, among the most relevant areas [10,11]. In this scope batteries are one of the most suitable systems for a wide range of applications, for which it is necessary to properly tailor capacity, energy and power density, and operational potential window, all dependent on the materials used for battery development [12]. Further, rate capacity, cycle life and coulomb efficiency of the batteries must be optimized, while properly addressing the detrimental aspects leading to leakage current and self-discharge [13]. Furthermore, additional issues such as safety, economic viability, material recovery and recyclability are important in the field of batteries [14].

A separator with electrolyte, and two electrodes with different potentials (i.e., cell voltage), together with the collectors, make up a traditional battery [15]. The electrodes (anode and cathode) are composed of a range of materials with various functions (active material, polymer binder and conductive additive) that vary depending on the type of battery [16,17]. Thus, innovations in battery systems are being implemented at different levels, mainly driven by the novel materials applied to their different components to improve performance and safety, while reducing environmental footprint [18].

The most implemented and efficient energy storage devices for a variety of uses, including computers, smartphones, electric cars, and even home storage systems, are lithium ion batteries [19]. With the growth of the electric vehicle market, there is a strong dependence on this technology which will lead to an increasing demand for lithium and other materials needed to manufacture batteries, creating dependence on these resources and bringing scarcity problems similar to those observed nowadays with fossil fuels [20].

Furthermore, using liquid electrolytes in lithium-ion batteries still has certain drawbacks, primarily related to durability and safety concerns [21]. Solid-state batteries, which are based on solid polymeric electrolytes, are an efficient way to get around these limitations [22]. These battery types have been developed and are implemented in applications that require high energy value and efficiency, but recently, the field of batteries is experiencing a strong evolution to develop batteries matching the specific application and performance parameters requirements instead of implementing a single battery concept for all applications.

Thus, printed batteries, microbatteries, organic batteries or batteries following the life-cycle of a specific application (from disposable point-of-care systems to smart packaging or agriculture 4.0) are being developed [23–25]. Similarly, structural batteries are a focus of important developments to take advantage of the energy provided by renewable sources [26].

The structure of this review is presented schematically in the Scheme 1. The review is basically divided in 4 sections: fundamentals of batteries, wide range of batteries, smart capabilities for different battery systems and circular economy and recycling issues.

Thus, in contrast to any other review on the area, the present one focus on all types of batteries, analyzing their most relevant materials, geometries, performance parameters, and applications areas. Further, the main challenges to be addressed in the near future for each battery type are also addressed.

This contribution does not pretend to be just a summary of the relevant state of the art, but to critically analyze it and provide a roadmap for future developments in order to positively contribute to the implementation of the wide range of battery types in the areas for which they are more appropriate, contributing to the energy transition in the most efficient and sustainable way.

2. Processing and fabrication technologies

The rapid expansion of the lithium-ion battery (LIB) market, driven primarily by the electric vehicle (EV) sector, has boosted

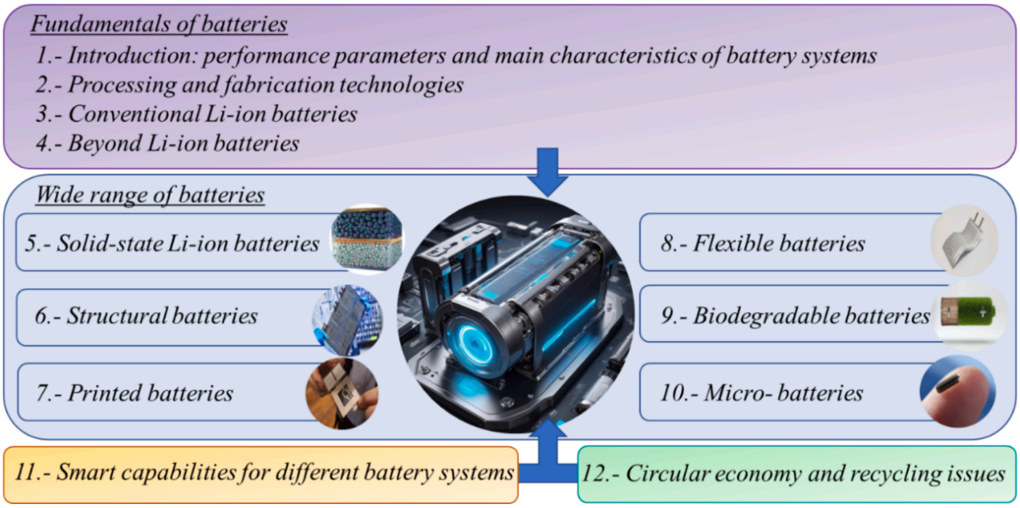

Scheme 1. Schematic diagram illustrating the various sections into which the review is organized.

substantial advances in battery processing and manufacturing. This growth encompasses the complete LIB production cycle, from raw material preparation to cell assembly (Fig. 1), effectively bridging the gap between academic research and industrial-scale applications in a variety of ways [27]. The EV battery industry is driven by a commitment to efficiency and sustainability, with yield optimization emerging as a key priority. In this context, yield—the proportion of high-quality products within the total production output—serves as a vital measure of manufacturing efficiency, cost-effectiveness, and environmental impact.

Due to the inherent complexities of the manufacturing process, battery cell production lines often face yield rates around 40–60%. However, as production lines mature (e.g. Asian battery manufacturers) and incorporate advanced technologies, this yield can be improved (e.g. 99%) [28]. As a result of the manufacturing process optimization, a significant sharp reduction in LIB pack costs, which declined by approximately ~90% between 2011 and 2024, reaching around $88 per kilowatt-hour, has been achieved [29]. Nevertheless, sustaining this trend of cost reduction will require continuous improvements in both material innovation and manufacturing processes.

Materials remain the most substantial contributor to LIB costs, and integrating new active materials introduces additional challenges for established manufacturing techniques. For instance, the inclusion of silicon in graphite anodes (that will increase by a factor of 10 the capacity of the cell: graphite: 372 $\text{mAh}\cdot\text{g}^{-1}$ vs silicon: 3579 $\text{mAh}\cdot\text{g}^{-1}$) demands extra processing steps, such as surface passivation of silicon [30]. Also, due to the high cost of cobalt, there has been increasing interest in developing nickel-rich cathodes. However, due to the oxidation state of nickel in the material (e.g. Ni^{+3} in high-nickel NMCs), it is also important to understand the reactions between cathode materials and water that occur within industrially relevant time scales and processes to prevent gas generation [31]. Developing advanced processing methods that can accommodate new materials is essential for further progress. In

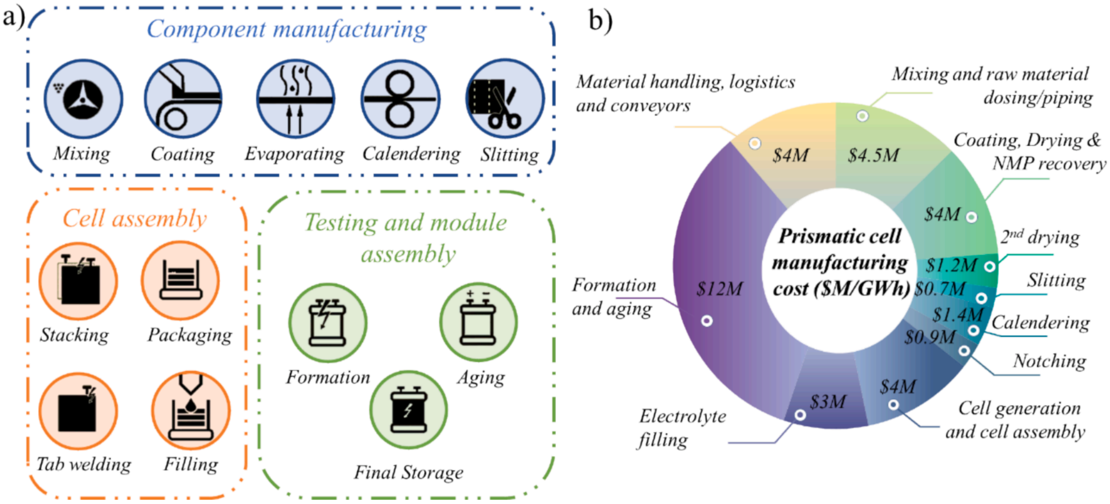

Fig. 1. A) typical process steps applied in a lib cell production plant. b) average prismatic cell manufacturing cost (data adapted from Bonsai Technology Srl) [48].

addition to materials innovation, the approaches, challenges, and constraints in key stages of electrode fabrication and cell assembly are crucial. The energy-intensive electrode drying process (Fig. 1a and b), in particular, is a focal point for optimization due to its influence on both manufacturing costs and the final performance of the battery. Techniques including optimizing the mixing sequence, increasing solid content in slurries, applying multiple drying zones, and adopting radiative drying methods offer significant potential for reducing energy demands in this step [27,29,32,33].

Emerging electrode processing materials and methods, such as NMP-free [34], aqueous [35], and dry processing [36,37], promise to further decrease manufacturing costs, reduce energy use, and cut greenhouse gas emissions. For instance, while NMP-free electrode fabrication entails key advantages such as improved electrode quality (e.g. stronger adhesion and cohesion of the electrode components) as well as the potential for new applications (e.g. all-solid-state batteries (ASSBs) and pre-lithiation in LIBs), several challenges need to be addressed before widespread commercialization. Among them, 1) the tendency of different electrode materials to agglomerate during dry mixing makes it challenging to achieve a uniform distribution and good interfacial interactions between the active material, binder, and conductive additives. 2) Maintaining a consistent mass loading of electrodes is critical for ensuring reliable LIB performance. The dry mixture used in the solvent-free processing presents a lower fluidity than the slurry in the SC process, making it more challenging to achieve the same level of mass loading consistency and 3) Different binders are required for the various dry electrode fabrication techniques (e.g., PVDF for dry spraying, thermoplastics for 3D printing and melting extrusion) [38,39]. The stability and flexibility of these binders, especially for use with different active materials, need to be further investigated. Enhancing energy density through minimizing inactive components, developing self-supporting electrodes, and increasing electrode areal loading is also crucial. However, producing high-loading, thick electrodes introduces mechanical challenges related to their integrity and adhesion [40].

To address these technical hurdles, new electrode architectures are being developed, including gradient-structured electrodes [41] and vertically aligned pore designs [42]. Techniques such as laser processing [43], freeze casting [44], and co-extrusion [45] facilitate these innovative architectures, though the scalability, throughput, and cost-efficiency of these methods are yet to be fully proven. One of the most promising approaches is laser structuring of composite electrodes [46], as part of the 3D battery concept [43,47]. This can improve battery performance and safety, as well as production reliability. The key advantage is that laser-generated artificial porosity enables more homogeneous and rapid wetting of the electrode with the liquid electrolyte. As a result, inhomogeneous wetting with dry electrode areas are avoided which can initiate electrochemical degradation and cell failure. This offers a significant reduction in production costs, increased battery lifetime, and easier translation into high-energy and high-power thick-film batteries.

Given the high standards for cycle life, calendar life, and defect tolerance—particularly in large-scale applications like EVs—LIB manufacturing increasingly relies on continuous processes, automation, and stringent quality control systems. Establishing the connection between defects and cell performance is critical for creating effective criteria for scrap and quality determination. Bearing this in mind, it has been proposed the use of a digital twin that consists on a dynamic, virtual replica that mirrors a physical product, process, or system in real time [49]. This sophisticated model serves as both a window into current operations and a laboratory for future possibilities (e.g. beyond lithium technologies). Engineers and operators can use it to predict performance, optimize maintenance schedules, and test scenarios without risking the actual asset.

The true benefit of digital twins lies in their bi-directional connection with physical assets. As conditions change in the real world, sensors relay this information to update the digital model automatically. This continuous feedback loop enables predictive

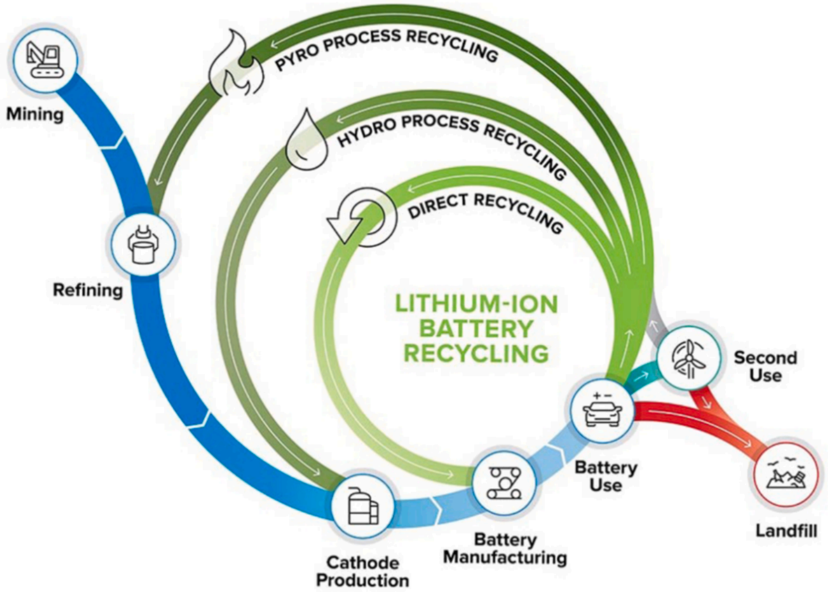

Fig. 2. Recycling processes in order to promote a circular economy. Adapted from Ref. [50] with permission from Wiley, Copyright 2022.

maintenance, performance optimization, and data-driven decision making.

As the first generation of EV batteries reaches the end of its operational life, LIB recycling has become increasingly important [48]. By 2040, projections indicate that electric vehicles will comprise about two-thirds of all cars. However, current LIB designs rarely account for recyclability, complicating the recovery of battery-grade materials. Europe is addressing this challenge by implementing new policies to foster battery circularity and improve the recovery of critical materials like lithium, cobalt, and nickel. These policies aim to mitigate environmental impact and reduce dependency on imported resources. Currently, however, European recycling rates remain low, with only 8–22% of materials successfully recovered [28]. As schematically illustrated in Fig. 2, when a LIB reaches its end of life, several pathways are possible. It can be disposed of in a landfill (an undesirable scenario), repurposed for a second-life application in a less demanding setting – typically stationary energy storage – or recycled to close the loops for both materials and energy [50].

While LIBs will continue to dominate the EV market, new battery technologies, including lithium-sulfur and solid-state batteries, are on the horizon. Developing specialized manufacturing processes for these next-generation battery systems will be essential to realize their potential and overcome unique challenges, such as stability, compatibility, conductivity, and interface issues between the cathode and solid-state electrolyte.

3. Conventional lithium-ion batteries

The most widely used energy storage system is lithium-ion batteries (LIBs), which are expected to expand at a compound annual growth rate of 14.2% between 2023 and 2032 [51] due to the expansion of the electric vehicle market and applications in electronic devices like computers and smartphones [52]. Relaying on the discoveries achieved by M. Stanley Whittingham, John B. Goodenough, and Akira Yoshino— Nobel Prize in Chemistry in 2019—Sony commercialized the first battery prototype in 1991 [53].

In comparison to other battery systems like NiMH (nickel-metal hydride) and Ni-Cd (nickel–cadmium), lithium-ion batteries are characterized by improved characteristics including lightweight, higher power and energy density value, more charge/discharge cycles, and no memory effect, among others [52]. Fig. 3 shows the evolution of the different generations of these batteries in terms of materials, with the current generation 3 being based on different materials for both anodes and cathodes.

Despite the success, more work is required to enhance the characteristics and features of its various components, including the electrodes and separator/electrolyte. The cathode, or positive electrode, establishes the battery's capacity, while the anode, or negative electrode, needs to sow a low potential in order to deliver a high voltage to the cell [54]. Whatever the electrode type, it is formed by an active material, conductive additive, and binder polymer [55]. The conductive additive improves the electrode's electrical characteristics, the polymer binder connects the other components (active material and conductive additive) and increases the electrode's mechanical stability, whereas the active material is responsible for the intercalation and deintercalation process [55].

Because of its long life cycle, abundance, electrochemical stability, ease of production, and affordability, graphite is the most commonly used active material for anodes [56].

With respect to active materials for the cathode, it is selected depending on the specific application requirements. Lithium cobalt oxide ($LiCoO_2$) was the first active material used due to its good capacity retention, high structural reversibility (below 4.2 V vs Li^+/Li) and good rate capability [57]. Among the different active materials, the ones that stand out are lithium iron phosphate ($LiFePO_4$, LFP) and lithium-nickel–cobalt-manganese oxide ($LiNiCoMnO_2$, NMC), often used in electric vehicles due to their as low-cost and non-

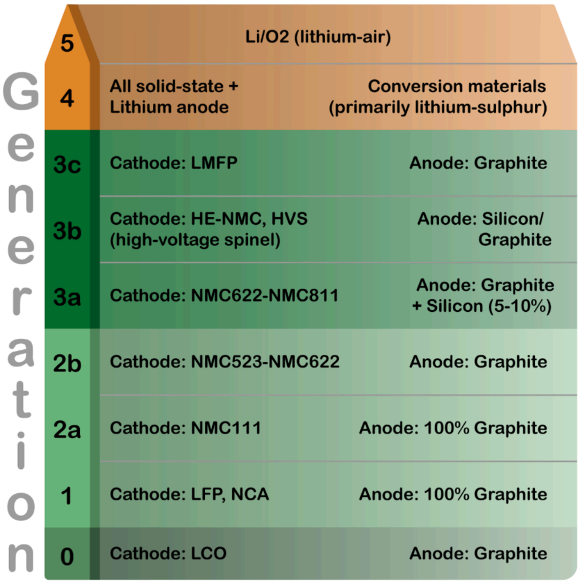

Fig. 3. Roadmap of the different generations of lithium batteries.

toxicity, no memory effect, good thermal stability, and environmental friendliness, among others [58].

NMC active material exhibits higher capacity and tap density compared to other active materials, with both Ni and Co participate in surface redox, whereas Mn is non-redox active [59].

By preventing contact between the two electrodes, the separator—which takes the shape of a porous or gelatinous electrolyte—improves the battery's mechanical flexibility and resilience while supplying the required ionic conductivity without electronic conductivity [60].

Currently, these battery systems are the most studied, developed, produced and integrated in devices. Every year, an increasing number of works are published that address fundamental concerns related to energy, power, safety, sustainability, processability and reliability in order to improve their performance [21,61].

Additionally, attempts are being made to develop new capabilities for the batteries, like self-sensing, self-healing, and thermal shutdown [62–64]. The development of solid electrolytes for solid-state batteries represents another strategy for improved durability and safety [65].

4. Beyond lithium-ion batteries

As discussed in Section 2, recycling spent lithium-ion batteries (LIBs) is essential for addressing environmental and resource-related challenges. Another possibility to address those issues is by developing alternatives to current main stream technology, the mains ones – sodium-ion, solid-state electrolyte, and lithium-sulfur (Li-S) batteries – offering potential advantages in safety, environmental impact, or energy capacity [66].

Sodium-ion batteries represent a promising alternative to traditional lithium-ion technology, offering a complex mix of benefits and limitations tailored to specific applications. One significant advantage is the abundant availability of sodium – approximately 1,000 times more prevalent than lithium – and its significantly lower water requirements for extraction, reducing production costs by 30–50% compared to lithium-ion [67,68]. Additionally, sodium batteries can be manufactured in existing facilities and safely transported due to their ability to discharge fully to zero volts. However, they currently fall short in energy density, with a range of 140–160 Wh kg^{-1} compared to lithium's 150–220 Wh kg^{-1}, and they support fewer charging cycles. This lower density makes sodium-ion batteries less suitable for applications where space and weight are critical, such as portable electronics or high-performance EVs [69]. Furthermore, limited commercial availability and fewer manufacturers restrict their current application potential. Nonetheless, sodium-ion batteries show promise in stationary energy storage, grid-scale implementations, and budget-focused EVs where cost benefits could outweigh density limitations.

Solid-state batteries, which use solid electrolytes instead of liquid ones, offer several advantages, including a reduced risk of dendrite formation, higher energy density (potentially 2–3 times greater than lithium-ion batteries, enabling longer EV ranges), and faster charging [70]. They also perform well in extreme temperatures and show promising cycle longevity, with some prototypes enduring thousands more charge–discharge cycles than traditional batteries. Various solid-state electrolyte (SSE) materials are under study, such as polymeric, oxidic, and sulfidic types, each with unique ionic conducting and mechanical characteristics [71]. Emerging materials like metal–organic frameworks (MOFs) offer tunable functionality and structured ion channels [72], while chloride-based SSEs exhibit high ionic conductivity and compatibility with oxide cathodes [73]. However, high production costs and scaling challenges currently limit solid-state battery applications to smaller devices like wearables and IoT products. Technical issues related to the solid-electrolyte interface, dendrite prevention, and mechanical stress during charge–discharge cycles also impact their longevity. Despite these challenges, major companies continue to invest in solid-state technology, viewing it as a potential future standard for energy storage. This battery type is explained in more detail in the next section.

Aqueous Zn-ion batteries (ZIBs) operating within a pH range of approximately 4 to 5.5, offer a compelling alternative to lithium-ion batteries for stationary grid energy storage. Their key advantages include high safety, environmental friendliness, non-toxicity, high specific power, excellent reversibility, and affordability due to the abundance and low cost of zinc [74]. These characteristics make ZIBs a viable, green, and cost-effective technology for large-scale applications. However, achieving widespread adoption requires overcoming specific challenges, such as enhancing energy density and addressing parasitic hydrogen evolution during zinc electrodeposition. In order to overcome these challenges, focused research on enhancing energy density (e.g cathode materials should be designed to deliver an average discharge voltage of at least 1.0–1.2 V) [75], optimizing electrolyte formulations (including the use of additives [76], e.g propylene glycol, 1,2-butanediol or pentanediol), and adhering to standardized testing [77], such as conducting long-term cycling tests at around 1C or testing under "electrolyte-starving" conditions to better simulate real-world scenarios rather than flooded conditions, will accelerate their readiness for deployment in power grid applications.

Lithium-sulfur batteries combine lithium anodes with sulfur cathodes, offering an alternative that maintains lithium's benefits while replacing critical materials with more abundant sulfur. These batteries have a theoretical energy density up to nine times higher than lithium-ion batteries but currently face issues with limited chargeability and cycle life. Research efforts focus on enhancing performance through several strategies: (a) modifying electrolyte solvation properties to improve voltage profiles, polysulfide solubility, and cyclability [78], (b) using sulfurized polyacrylonitrile (S@PAN) as a cathode material to reduce polysulfide dissolution and enhance cell stability [79], (c) incorporating kinetic promoters to accelerate sulfur cathode reactions (e.g., heterogeneous, homogeneous, and semi-immobilized promoters) [80], and (d) utilizing redox mediators (both solid and soluble) to catalyze sulfur redox reactions, which has shown promise in improving Li-S cell performance [81]. These advancements aim to address key limitations in Li-S battery technology, making them increasingly viable for practical applications.

Several other promising but commercially immature technologies, including lithium-air (Li-air), zinc-air (Zn-air) batteries, and multivalent systems like calcium (Ca^{2+}), magnesium (Mg^{2+}), and aluminium (Al^{3+}) batteries, are under active development. Recent advancements have focused on improving catalysts, electrolytes, and electrode materials to enhance the performance, stability, and scalability of these alternatives (Table 1):

- **Li-Air Batteries**: Research into NiO/ZrO_2 [82] and lattice-activated SnTe [83] catalysts has shown promise for improving LiOH decomposition and oxygen diffusion, as well as reducing exposure to CO_2 and H_2O. Polymer electrolyte innovations also enhance stability and cycling under ambient conditions, addressing critical issues in cathode and electrolyte efficiency [84].
- **Zn-Air batteries**: Limited energy density remains a significant challenge for Zn-air batteries as practical applications have been struggled to achieve the potential high theoretical energy density. Research focused on pore size engineering of the electrode materials allows to increase the density of active sites, including core–shell design, space confinement, and hierarchical structures [85]. Additionally, electrolyte additives, such as zinc acetate and citric acid, or solid-state electrolytes such as polyacrylamide polymer with a highly amorphous dual-cation ionomer [86] can enhance the performance of Zn-air batteries by improving the shape change of the zinc electrode.
- **Calcium Batteries**: Notable developments include a rechargeable Ca/Cl_2 system and enhanced cathode materials, such as carbon-confined sulphur and $BaV_6O_{16}\cdot 3H_2O$ composites, offering high specific capacities and extended lifespans [87]. A solvation strategy using low-donor number (DN) propylene carbonate has also improved rate performance in vanadium-based systems [88].
- **Magnesium Batteries**: Efforts to stabilize FeS_2 cathodes aim to reduce shuttle effects and improve cycling stability, though challenges remain with dendrite formation and electrolyte flammability [89]. Ongoing work focuses on enhancing safety and scalability for large-scale applications.
- **Aluminium Batteries**: Advances in chloroaluminate-based solid polymer electrolytes have achieved higher electrochemical stability and ionic conductivity, which are important for aluminium-graphite cells' performance [90].

Rather than relying on a single replacement for lithium-ion batteries, a diversified approach tailored to specific applications is likely to be more sustainable. By developing multiple "fit-to-purpose" battery technologies, this approach could help mitigate the environmental and social impacts of lithium mining—such as high water usage, CO_2 emissions, and disruptions to Indigenous communities—while meeting the growing global demand for energy storage.

5. Solid-state lithium-ion batteries

5.1. *Introduction*

Lithium-ion batteries (LIBs) have become ubiquitous electrochemical energy storage systems for portable electronics and electric vehicles [28,91]. The expansion of their market and fields of applications have been driven by their remarkable energy density, long cycle life, and low cost [92]. However, conventional LIBs on the market today rely on the use of liquid electrolytes composed of highly flammable organic solvents, which pose inherent safety risks. Today, commercial LIBs contain lithium hexafluorophosphate ($LiPF_6$), lithium bistrifluoromethanesulfonimide (LiTFSI), lithium bismethanesulfonimide (LiFSI), lithium- bis oxalateborate (LiBOB) dissolved in carbonate-type such as dimethylene carbonate (DMC), diethylene carbonate (DEC), ethyl methyl carbonate (EMC) and cyclic carbonates (like ethylene carbonate (EC) and propylene carbonate (PC)), sulfone-type (dimethyl sulfite, DMS) or sulfolane-based solvents. This liquid electrolyte is supported by a mechanical separator in polypropylene (PP) or/and polyethylene (PE), with addition of glass fiber providing the physical separation of the electrode [93,94]. The risks associated with this type of electrolyte include leakage, short-circuiting, and consequently the possibility of fires or explosions. Furthermore, the limited electrochemical window of liquid electrolytes hinders the use of high-capacity and high-voltage electrode materials, thus restricting the battery performance

Table 1
Some representative battery technologies under research and development for next generation energy storage.

Technology	Advantages	Drawbacks
Li-air batteries	• high theoretical energy density (10 times greater than that of lithium-ion) • specific energy (3000 Wh·kg^{-1} vs 250 Wh·kg^{-1} of Li-ion).	• complex chemistries involved in the charge/discharge cycles • poor reversibility and cyclability • electrolyte instability • lithium metal anode instability
Zinc-air batteries	• theoretical energy density (3 times greater than that of lithium-ion) • minimal fire risk and non-toxic components • abundance of zinc, entails a lower cost compared to lithium	• short cycle life due to zinc dendrite formation • sluggish oxygen reduction reactions
Calcium batteries	• abundant element in Earth's crust • lower cost compared to lithium • higher energy density than lithium-ion batteries due to the transfer of multiple electrons	• suitable cathode materials that can accommodate the larger size of calcium ions • dendrite formation and electrode deterioration
Magnesium batteries		• slow diffusion of magnesium ions in conventional electrolytes and cathode materials • cathode materials that can accommodate the insertion of Mg^{2+}
Aluminium batteries		• parasitic hydrogen evolution reaction during charging, which reduces efficiency and can cause corrosion issues • cathode materials that can accommodate the insertion of Al^{3+}

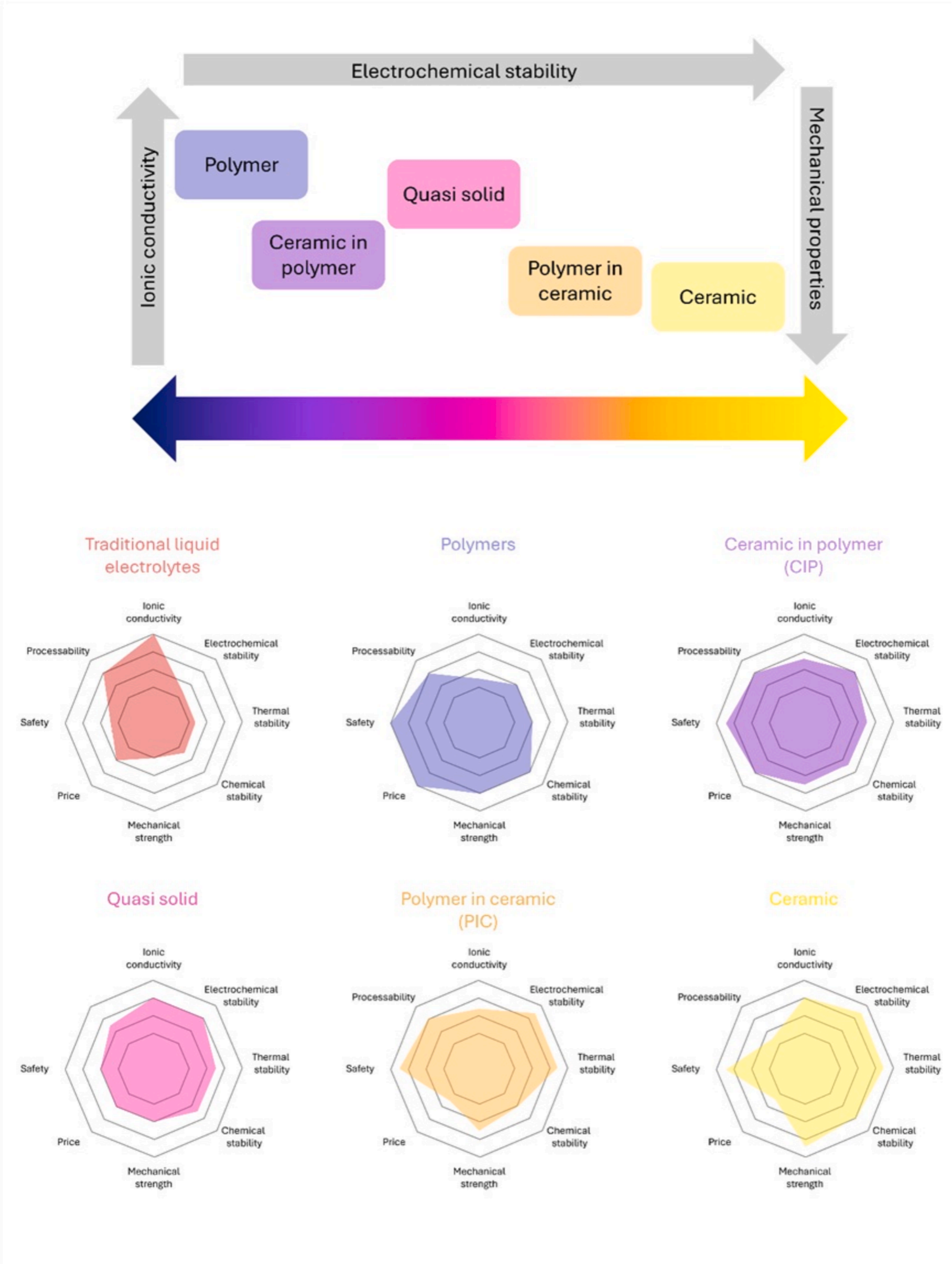

Fig. 4. Proposed classification for the solid-state electrolytes, identifying the categories and correlating them with some relevant physical and transport properties.

[93–95].

All Solid-State Batteries (ASSBs) have emerged as a promising strategy to produce next-generation energy storage technology, aiming to address these limitations [96–98]. The definition of ASSBs thus is specifically referred to the nature of the electrolyte. The switch to ASSBs allows not only to overcome the main limitations of traditional liquid-electrolytes based batteries, but also to meet the required standards for the next generation batteries, particularly in the field of electric mobility. Today, commercial LIBs are approaching their performance limit in terms of energy density, assessed around 300 Wh kg^{-1}. ASSBs indeed represent the picklock to access the lithium-metal battery design (LMBs), exploiting the advantages of metal lithium (3860 $mAh.g^{-1}$ capacity, −3.04 V vs SHE potential) and allowing for super high energy density batteries. Indeed, the removal of the inert separator and the reduced electrolyte thickness can lead to energy density in the range of 500 $Wh.kg^{-1}$ [96]. At the same time, this poses extra challenges as the use of metal lithium involved the formation of dendrites, large volume changes, interfacial reaction and new phases formation, and overall safety issues. Moreover, the traditional cathode materials and lithium metal anode (LMA) present inherently different challenges and problems, difficult to address with the same approach and thus making the development of suitable electrolyte systems even more demanding.

ASSBs are distinguished by replacing the flammable liquid electrolyte and separator with a non-flammable and mechanically robust solid-state electrolyte (SSE). This fundamental shift offers mainly enhanced safety and improved cycle life stability [99,100].

Indeed, the ideal SSE should possess the following desirable characteristics:

- High ionic conductivity in a wide temperature range, enabling for improved battery's rate performance under different conditions (ideally $\sigma \geq 10^{-3}$ S cm^{-1} at RT, with practically null electronic contribution, i.e. below 10^{-10} S cm^{-1}). High Li transference number, $t_{Li}^{+} > 0.5$, ideally ∼ 1. This transference number is defined as the ratio between the current transported by cations and the overall current in the cell [101].
- Wide electrochemical stability window, ESW, up to 6 V vs Li^{+}/Li, opening the route for the exploitation of high-voltage cathode, nickel-rich and cobalt-free cathodes, boosting the overall energy density of the battery. At present, liquid organic electrolytes have ESW ∼ 4–4.5 V [102].
- Good chemical stability with traditional electrodes and new possible electrodes (metal anode), which is crucial for long cycle life and overall performance [102].
- Low interfacial resistance with the electrodes; minimizing the resistance at the interface between the SSE and the electrodes is vital for efficient battery charging and discharging [102].
- High safety, low flammability. Ideally, this should allow reaching EUCAR = 1–2 for the overall battery in automotive applications [97,103].
- High mechanical strength (Young modulus > 5.5 GPa to hinder dendrites formation). Resistance to dendrites' formation, so opening the way to the use of LMA with 3870 $mAh.g^{-1}$ capacity, density 0.59 $g.cm^{-1}$, the lowest possible potential −3.4 vs SHE, and improving the energy density [104].

5.2. *Materials, strategies, and applications*

Several approaches and classes of SSEs have been explored. In the early stage of this research's field, three main categories could be identified: polymer electrolytes, ceramic inorganic electrolytes, and composite electrolytes. These classes will be discussed in detail in the following sections [100,104–108]. Considering the "end members", i.e., the pure ceramic and pure polymer electrolytes, they have been considered and widely investigated, nevertheless their inherent weaknesses (such as poor ionic conductivity at room temperature for ceramic systems and mechanical properties not sufficient to block dendrite growth for the polymeric systems among the others), have led to the investigation of composite as main strategy to mitigate the drawbacks of these individual components. Today, the use of composites has overcome the other strategies, thus we here propose and discuss the specific classification of composite electrolytes, as following:

- Ceramic-in-Polymer, CIP [106,109,110].
- Polymer-in-Ceramic, PIC [104,111].
- Quasi-Solid Electrolyte, QSE [112–114].

To properly discuss this classification, the end members (polymeric systems and ceramic materials) are here discussed to highlight both pros and cons of the single components and thus better understand the synergistic effect of the preparation of a composite, as reported in Fig. 4.

5.2.1. *Ceramic materials*

Inorganic solid electrolytes (ISEs) can be further categorized into three main types based on the chemical composition, i.e. oxides, sulfides, and halides [115,116].

All these classes of materials share some common features. Generally, these systems are composed by a rigid (order or disordered) inorganic framework accommodating Li ions on sites ideally connected through planes or channels. The transport properties of Li ions within the structure are supported by the presence of point defects (such as vacancies, interstitial species, anti-site defects) allowing for the Li ion diffusion, generally controlled by proper doping and substitutions, and follow the activated diffusion described by the Arrhenius equation. This provides Li transference numbers close to 1; nevertheless, ISEs present lower ionic conductivity respect to the liquid systems (in the range of 10^{-6} – 10^{-3} S cm^{-1} at RT) but at the same time good electrochemical and thermal stability, while the chemical and mechanical properties should be discussed case by case [115,116]. Generally, they are also characterized by poor interfacial compatibility, high interfacial resistance, poor flexibility, high cost of production and scalability. Indeed, some of the materials reported below possess good chemical compatibility with the electrodes but extreme sensitivity to air and moisture. Although ceramic materials have globally good mechanical properties, the membrane of pure ceramic compounds ends up in being fragile and brittle (pristine and under working conditions). Moreover, the preparation and processing are not easily scaled up to give the final product at the industrial level.

5.2.1.1. Oxides. Oxide-based SSEs are generally represented by crystalline materials. The main classes belong to the family of NASICON, e.g. $Li_{1.3}Al_{0.3}Ti_{1.7}(PO_4)_3$ (LATP and derivates compositions [117,118]) $Li_7La_3Zr_2O_{12}$ garnet (LLZO and derived compositions [119,120]), lithium phosphorous oxynitride, Li_2PO_2N (LiPON and derived systems [121,122]). The NASICON structure was one of the first proposed by Goodenough, initially for Na transport in 1976 and followed by Li analogues in 1978 [123,124]. This represented the starting point for the research work in the field of oxide Li-ionic conductors. These systems share some peculiar and essential features such as presence of an open framed structure with channels or planes favorable for the Li diffusion, high band gap associated with the absence of electronic conductivity, high ionic character. Generally, they exhibit good ionic conductivity at room temperature (10^{-5} – 10^{-3} $S.cm^{-1}$) and can suffer from poor interfacial compatibility with electrodes, leading to high interfacial resistance. The production of dense pellets can be carried out, providing high conductivity values. Due to chemical stability, they are characterized by good processability also in presence of moisture and oxygen. Since their introduction, no substantial changes in

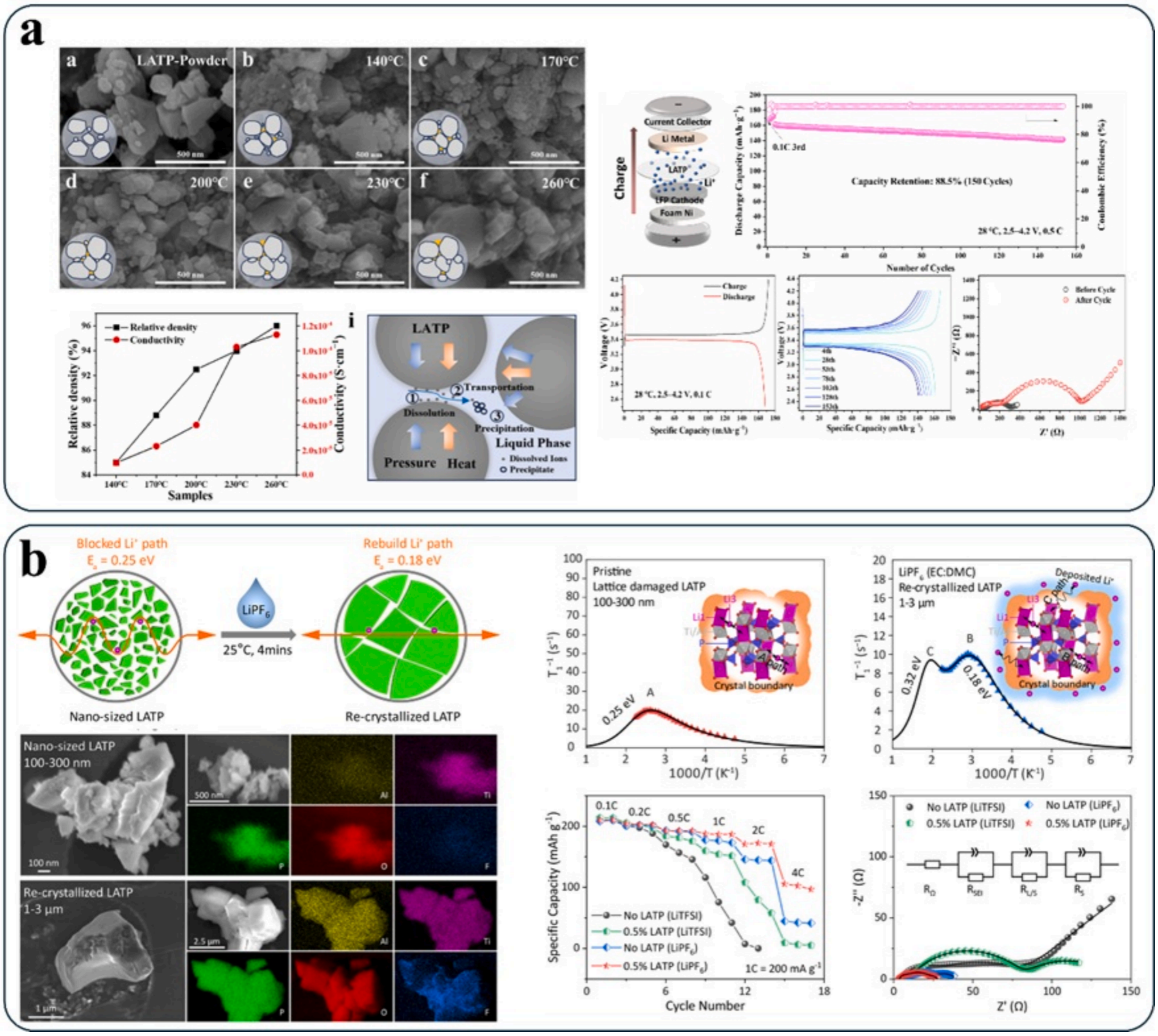

Fig. 5. (a) strategies for densification of LATP powders through new cold sintering procedure to enhance transport properties and the corresponding electrochemical performance in a LFP – metal Li based cell. Adapted from Ref. [117] with permission from Wiley, Copyright 2024; (b) enhancement of Li transport properties through liquid-electrolytes-induced secondary crystallization, the effect on the morphology, and the effect on the cell performance. Adapted from Ref. [118] with permission from American Chemical Society, Copyright 2023.

structure and compositions have been reported. The main trends in this field are represented by the study of possible doping, morphology control with surface engineering, as schematized in Fig. 5.

5.2.1.2. Sulfides. Sulfide-based SSEs include $Li_{10}GeP_2S_{12}$ (LGPS) [125,126], Li_2S-P_2S_5 glass [116,127,128], glass-ceramics [116,129], thio-LISICON types [130]. Compared to their oxide counterparts, sulfide-based SSEs exhibit higher ionic conductivity at room temperature, often comparable to that of liquid electrolytes. However, sulfide-based SSEs are often hampered by high chemical instability against moisture and air and are prone to lithium dendrite formation.

Sulfides represent an alternative to traditional ceramic materials as globally they are softer and denser with respect to oxides, which are harder and more difficult to densify. This is due to the lower Young's modulus of the sulfides. Moreover, also sulfide materials present both crystalline and amorphous structures. Glassy sulfides are ductile, and their processing is complicated by the requirement of high temperature for the cell assembly.

Crystalline LGPS presents high RT ionic conductivity (around 4×10^{-3} Scm^{-1}), whereas glassy systems generally have lower ionic conductivity, (in the range of 10^{-4} Scm^{-1}) which is strongly dependent on the actual composition.

Similarly to the oxide materials, the most relevant phases and compositions are unchanged with respect to the abovementioned

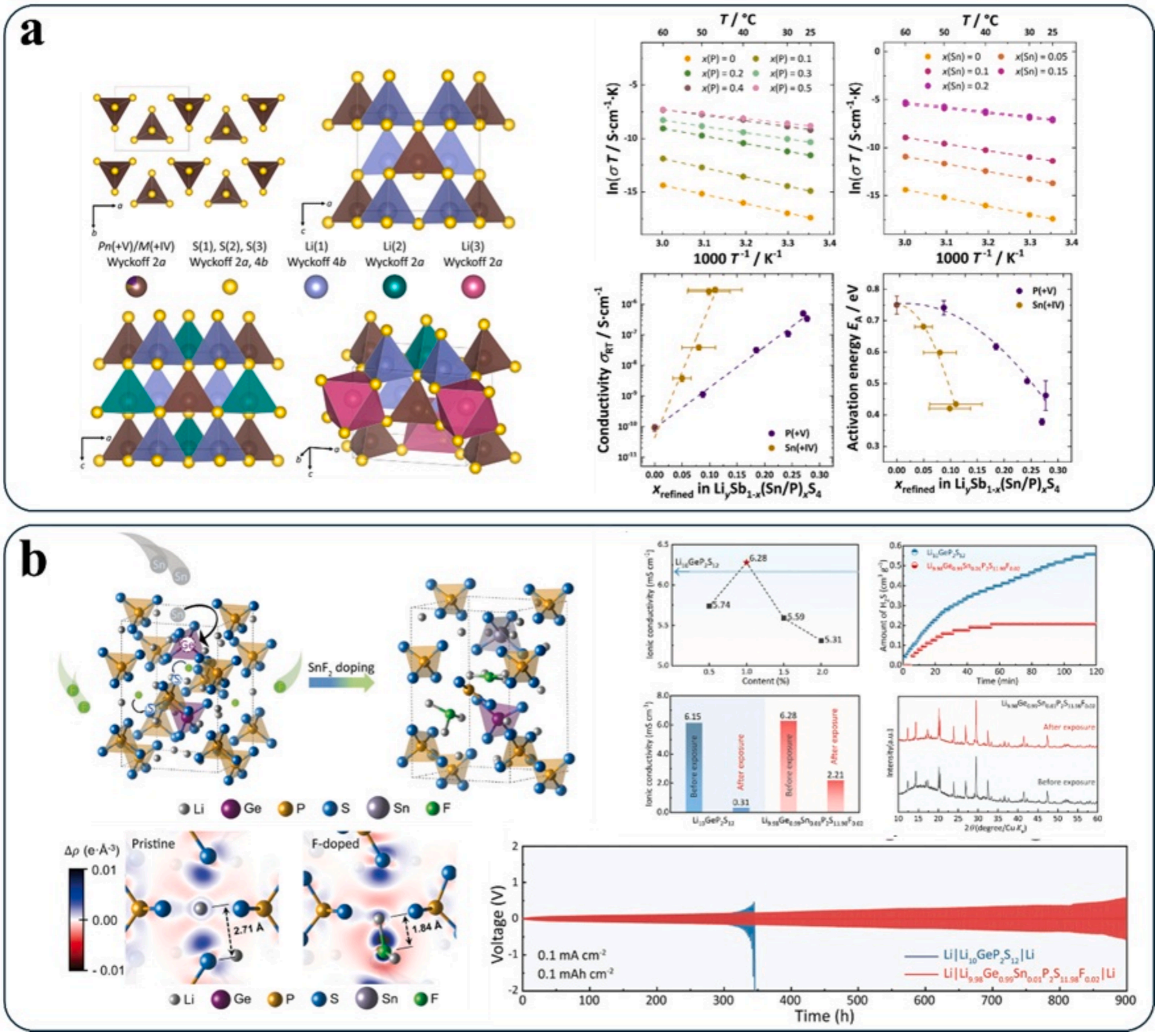

Fig. 6. (a) The effect of isovalent substitution $Li_3Sb_{1-x}P_xS_4$ ($0 < x < 0.5$) on the structure, stability, and conductivity of the sulfide system. The isovalent doping can improve the ionic conductivity of four order of magnitude. Reproduced from Ref. [134] with permission from American Chemical Society, Copyright 2024; (b) Fluorine doping of the $Li_{10}GeP_2S_{12}$ structure is considered for improvement of air stability; the fluorine surface modification reduces the hydrophilicity and postpone the degradation of the material that show high conductivity also after 20 min exposure at air. Reproduced from Ref. [135] with permission from Wiley, Copyright 2024.

classical systems and the effort in the development of such systems is now decreasing, focusing the attention on the preparation of composites, understanding of failure mechanism, and conduction mechanism at the interface [131–133]. In the field of development and exploitation of sulfides alone (not in composite), the main tendencies outlined at present are outlined in Fig. 6 and are represented by the introduction of surface coating, doping, and exploration of new synthesis and sintering for the improvement of the air stability, representing the main drawback of such materials.

5.2.1.3. Halides. Halide-based SSEs are an emerging class of materials including Li_3InX_6, argyrodite system Li_6PS_5X (X = Cl, Br), and oxyhalides $LiMOCl_4$, which are briefly discussed below.

5.2.1.3.1. Pure halides. Halides are characterized by remarkable ionic conductivity at room temperature (10^{-4} Scm^{-1}), a wide electrochemical window, and good mechanical properties. The most studied compositions belong to the chloride materials with general formula Li_3XCl_6 with X = In, Y, Zr, Sc and represent a new and emerging class of materials [136,137]. At the present various doping and substitution on the X site are explored with the aim to create Li defects and thus improve the conductivity; also, cation mixing among Li and X sites has been demonstrated to plays a role in the Li transport properties [138–140]. The possibility to explore

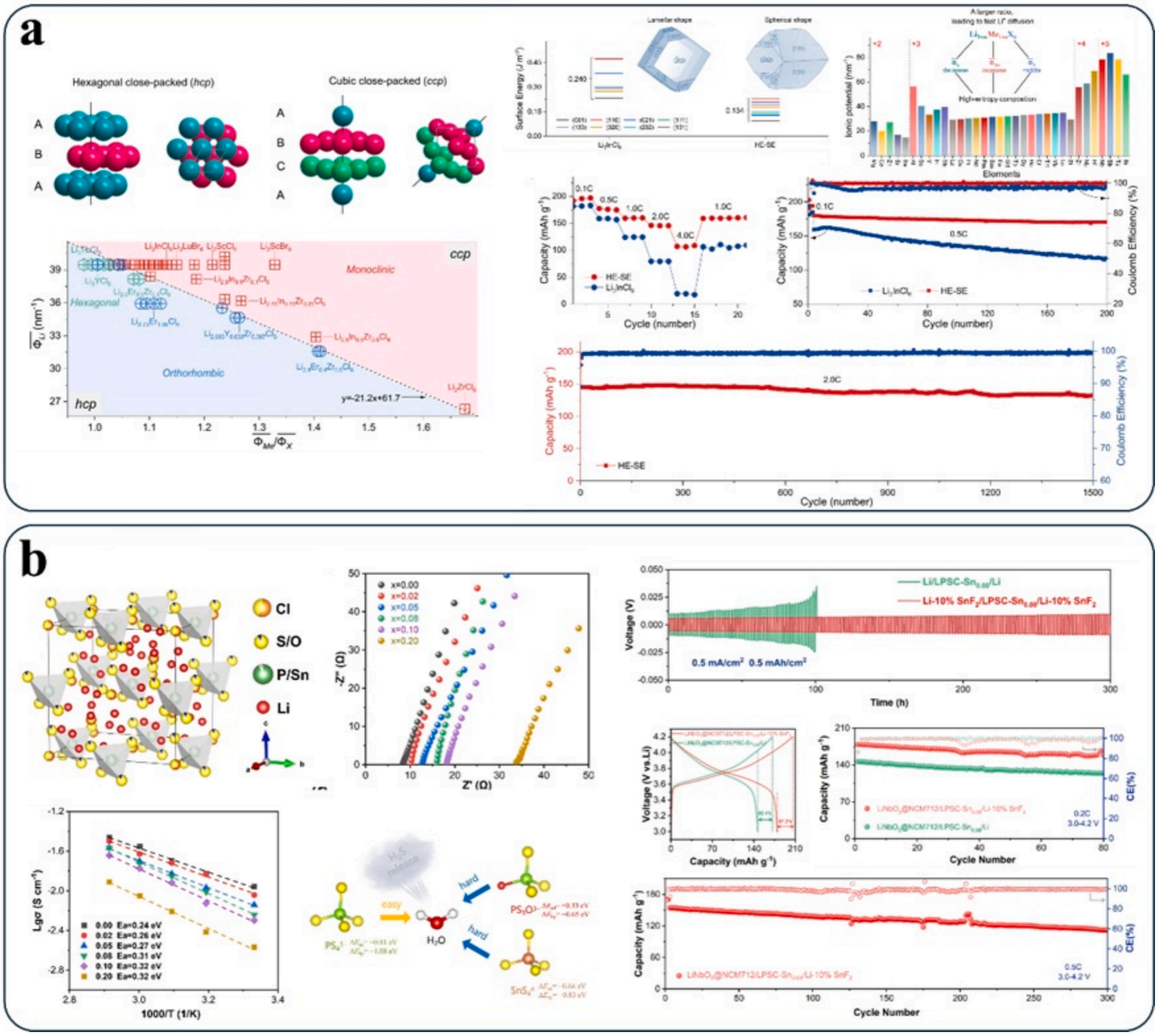

Fig. 7. (a) the systematic investigation of Li_3InCl_6 related materials accounting for the effect of ionic potential ratio and Li-ion potential, accounting for Li content, oxidation state, and composition of different Me ions, leading to the evaluation of high entropy compositions. Reproduced from Ref. [136] with permission from Springer, Copyright 2024; (b) tin and oxygen dual doping of $Li_{5.5}PS_{4.5}Cl_{1.5}$ system (with final composition $Li_{5.58}P_{0.92}Sn_{0.08}S_{4.34}O_{0.16}Cl_{1.5}$) as strategy to enhance the air stability of the material; the dual doping has a positive effect also on the electrolyte's compatibility with the Li metal anode and in the suppression of Li dendrite formation. Reproduced from Ref. [133] with permission from Elsevier, Copyright 2024.

the anion doping has been just very recently considered. Overall speaking, these systems offer good electrochemical properties (see Fig. 7).

On the other hand, halide-based SSEs suffer from high moisture sensitivity and air instability, which necessitates handling under inert atmospheres during the whole life cycle (synthesis and cell assembly processes). Also, the interfacial compatibility and chemical stability is low (especially with metallic lithium). To overcome these problems some strategies have been adopted such as doping [136,141], evaluation of other halides, e.g. bromides and fluorides, which generally show higher chemical stability and lower ionic conductivity [142], development of high entropy systems, addition of artificial SEI/CEI [136,137,143].

5.2.1.4. *Argyrodites.*

Argyrodites are chemical compounds with the general formula Li_6PS_5X, X = Cl, Br, I [144]. Argyrodites have been proposed to overcome the main problems of sulfide-based electrolytes as they offer excellent chemical compatibility with lithium metal thanks to the improved ionic character conferred by the presence of halide ions [145]. Moreover, they allow for the formation of a superior SEI and better contact if compared with oxide SSEs. Due to these interesting properties, a huge number of papers have been published since their first appearance in 2008 [146]. However, similarly to the other sulfides and halides material, they suffer of sensitivity to air and moisture. This problem can be partially addressed considering aliovalent substitution and high entropy systems [147–149].

5.2.1.5. *Oxyhalides.*

The introduction of oxyhalides with general formula $LiMOCl_4$ (M = Nb, Ta, etc. [150,151] is quite recent [150,151]. This effort is motivated by the need to enhance the ionic conductivity of halides, that despite the huge effort in doping exploration remains poor [150,151]. The mixed-anion strategy allows to obtain high ionic conductivity (10^{-3}-10^{-2} Scm^{-1}) and it is further corroborated by the use of cost-effective materials [150,152].

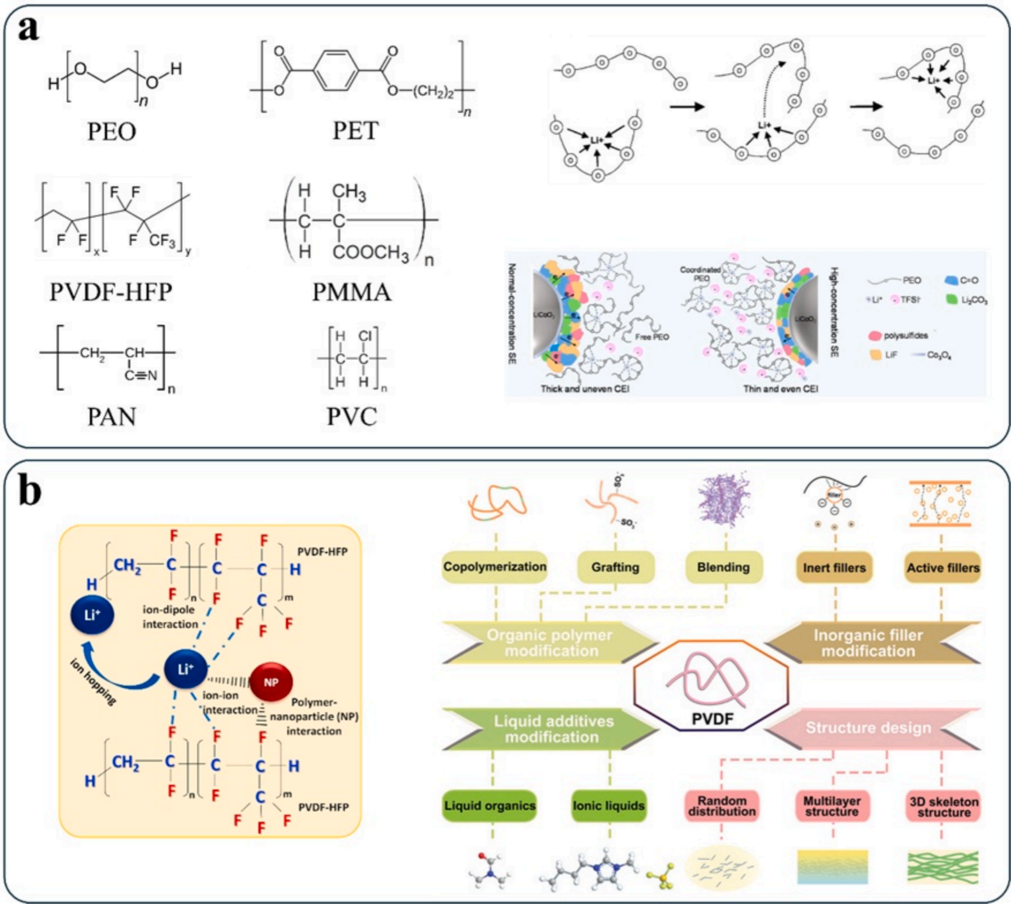

Fig. 8. (a) main polymer exploited for SPE and representation of the Li diffusion assisted by segmental motion in amorphous polymer and coordinating properties. Reproduced from Refs. [156,167] with permission from Wiley, Copyright 1998 and 2023; (b) PVDF conduction mechanism and possible strategies for improvement of transport properties Reproduced from Ref. [164,167] with permission from Elsevier and Wiley, Copyright 2024 and 2023.

5.2.2. *Polymer electrolytes*

Solid polymer electrolytes (SPEs) typically involve lithium salts dissolved in a polymer matrix thanks to its relatively high permittivity. This leads to the presence of mobile Li ions. However, anions are generally also free to move, and this leads to a cation transference number which can be as low as 0.1–0.2, being detrimental to the overall functional properties of the SPE [104,153–156]. Efforts have been made to overcome this problem by designing polyanions with reduced mobility [157].

The selection of proper polymeric materials allows to obtain flexible, elastic, and wettable electrolytes with improved interfacial properties with respect to the ISEs. With the aim of reducing the crystallinity of the systems (generally hindering the Li conductivity) the addition of plasticizing agents has also been considered. Ideal SPEs should offer high ionic conductivity, high t_{Li}^+, low crystalline fraction, low glass transition temperature and high melting temperature, good solubility properties for Li salts (thus good dielectric constant), high electrochemical stability. The transport mechanism in SPEs is driven by the coordination properties of the polymer, the flexibility of the polymeric chains, and is usually thermally activated, being described by the Vogel-Tammann-Fulcher (VTF) equation. For coordinating polymers such as poly(ethylene oxide) (PEO), the conduction mechanism is controlled by the formation and breaking of bonds among Li and the coordinating sites. Lithium can move in the free volume in the polymeric matrix with intra- or inter-chains hopping. The mobility of the chains (segmental motion) is thus relevant as occurs above the Tg temperature. For non-coordinating polymers, such as poly(vinylidene fluoride) (PVDF), the stronger interaction of Li is with the anion of the salts, that in turns can interact with the polymeric chains. The Li ions move through the ion's clusters hopping between possible stable positions [154–156].

These electrolytes offer several advantages, including flexibility, ease of fabrication, and good interfacial contact with electrodes. PEO stands out as one of the most widely used polymers for SPEs due to its remarkable ability to dissolve lithium salts. More recently, also PVDF and its copolymers, e.g. poly(vinylidene fluoride-hexafluoro propylene) (PVDF-HFP) have been widely studied. However, SPEs typically suffer from low ionic conductivity at room temperature and a limited electrochemical window, hindering their performance.

Other polymers considered as possible host matrices for lithium salts are poly(acrylic acid) (PAA), polyacrylonitrile (PAN), poly (methyl methacrylate) (PMMA), polyvinylidene chloride (PVC) (see Fig. 8) [97,108,109,154–156,158–160].

5.2.2.1. Poly(ethylene oxide). This is the most studied polymeric matrix for preparation of SPEs due to its ability to dissolve Li based salts thanks to the CH_2-CH_2-O structure and high mobility of the polymeric chains [108,161]. PEO and its copolymers have been explored for many years as suitable matrices for SPEs [108,162]. PEO is a semicrystalline polymer with T_g and T_m around −60 °C and 65 °C, respectively. Because of its high permittivity ($\varepsilon = 8$ in the amorphous phase), it can dissolve lithium (or other cations) salts. Several PEO_n-LiX systems were explored in the past, by changing both the molar ratio $n = [EO]/[Li]$, and the anion (X = halide, PF_6^-, N $CF_3SO_3^-$, $(CF_3SO_2)_2^-$, etc.) [115]. Carriers transport takes place based on an oxygen-assisted hopping mechanism involving long range segmental motion of the polymer amorphous phase above the T_g. For reasons previously stated, low lithium transport numbers ($t^+ < 0.3$) are typically obtained, which may be improved by choosing salts with larger organic anions and huge electron delocalization, like TFSI-, also acting as plasticizers for the polymer. [16] In fact, the addition of the salt increases the polymer amorphous fraction, that can reach 100 % for $8 \leq n \leq 30$ values, depending on the salt itself. Conductivity values $> 10^{-5}$ S cm^{-1} can be easily obtained in case of fully amorphous systems. However, the metastable amorphous phases generally undergo crystallization in a matter of hours/days, which determines a relevant decrease in conductivity. Moreover, the mechanical properties of amorphous systems are not optimal. At higher salt contents ($n < 6$), crystalline aggregates may be observed, which are responsible for the reduction of the conductivity and transport numbers, because of the formation of ion pairs and phase segregation [163]. The technological use of PEO-salt SPEs requires a compromise among the following features: i) acceptable ionic conductivity, ii) good mechanical properties, and iii) high transport number. Many efforts have been made to this aim, including blending and/or cross-linking with other compatible polymers, such polyacrylic acid (PAA), polymethylmethacrilate (PMMA). Polystyrene has been used to give a better dimensional stability to the polyether systems [163].

5.2.2.2. Poly(vinylidene fluoride). PVDF is a high-performance polymer widely used in battery technology. Its semi-crystalline structure, and ability to form flexible films make it useful for fabrication of separators, binders, and electrode coatings [155,164]. PVDF exhibits high dielectric strength and excellent compatibility with organic solvents commonly used in electrolytes. These characteristics contribute to its ability to maintain robust mechanical and chemical integrity in the harsh LIBs environment. Moreover, PVDF resistance to degradation in highly oxidative conditions and its strong adhesion to active materials enhance the overall stability and performance of electrodes [108,165]. However, pristine PVDF has low ionic conductivity and limited flexibility. To address these limitations, copolymerization of PVDF with other monomers, such as hexafluoropropylene (HFP) and trifluoroethylene (TrFE), followed by gelification with organic solvents and lithium salts has emerged as a promising strategy to develop highly performing gel polymer electrolytes (GPEs) [153].

In addition to copolymers, composite materials combining PVDF with inorganic fillers, such as ceramic nanoparticles (e.g., Al_2O_3, SiO_2, TiO_2), have shown promise in further enhancing the mechanical properties and thermal stability of separators and binders [110,166]. These composites leverage the synergistic effects of PVDF's flexibility and the thermal stability of inorganic fillers to produce separators with enhanced electrolyte wettability, reduced shrinkage, and improved safety in high-temperature environments. Such advancements are crucial for maintaining the integrity of lithium-ion batteries under extreme conditions, such as during rapid charge–discharge cycles or at elevated operating temperatures. Whereas the advantages in terms of performance are evident, from the point of view of fundamental knowledge the nature of ions transport mechanisms in non-coordinating matrices e.g. PVDF is not very clear. This aspect will be discussed in a further section. The state-of-the-art of PVDF-based SPEs and composite electrolytes has been recently reviewed [167].

5.2.2.3. Composite electrolytes. As already stated, the use of pure polymeric systems or pure inorganic systems has been overcome to go over the main drawbacks of these systems and at the same time benefit of the synergies of the combination of the two. Thus, the use of inorganic fillers (both active or inactive) in polymer electrolyte will improve the mechanical stability and reduce the polymeric crystallinity and consequently enhance the ionic conductivity [109–111,154,168,169]. At the same time, the use of fraction of polymers or polymeric electrolytes into the preparation of ceramic membranes has been explored for the improvement of interface contact and reduce the grain boundaries resistance, enhancing the overall ionic conductivity. Hereafter these categories are further discussed introducing the main merit figures, valuable examples, fields of application, limitations and perspectives.

5.2.2.4. Ceramic-in-Polymer. Ceramic-in-Polymer (CIP) systems are composed by a polymeric host matrix where a Li salt is dissolved and with addition of inorganic filler. This is one of the former strategies developed to overcome the limitations of SPEs [109,110,115,170]. The considered filler can be active (contributing to the Li transport properties) or inactive (no ionic conductivity) and address specifically some of the SPEs limitations (see Fig. 9). Inorganic fillers have been used to increase the polymer amorphous fraction (preventing crystallization), to enhance the polymer segmental motion, to increase the Li transport properties.

Inactive fillers are specifically used to prevent the crystallization of the polymer and increase the Li salt dissociation; among this SiO_2, Al_2O_3, TiO_2, ZrO_2 have been mainly explored [106,166,169,171,172]. Although the Li transport mechanism in such system is believed to be similar to that in filler-free SPEs, the presence of the filler has a beneficial effect on the ionic conductivity as it can amorphized the polymer and enhance the Li salt dissociation [106,169].

In addition to the advantages of inactive filler, the use of active filler can also contribute to the improvement of the transport properties. Most of the inorganic materials discussed in the previous section have been explored in this sense, such as Nasicon garnet [173], LIPON [174], etc. The mechanism for Li transport is getting more and more complicated as three different contributions must be

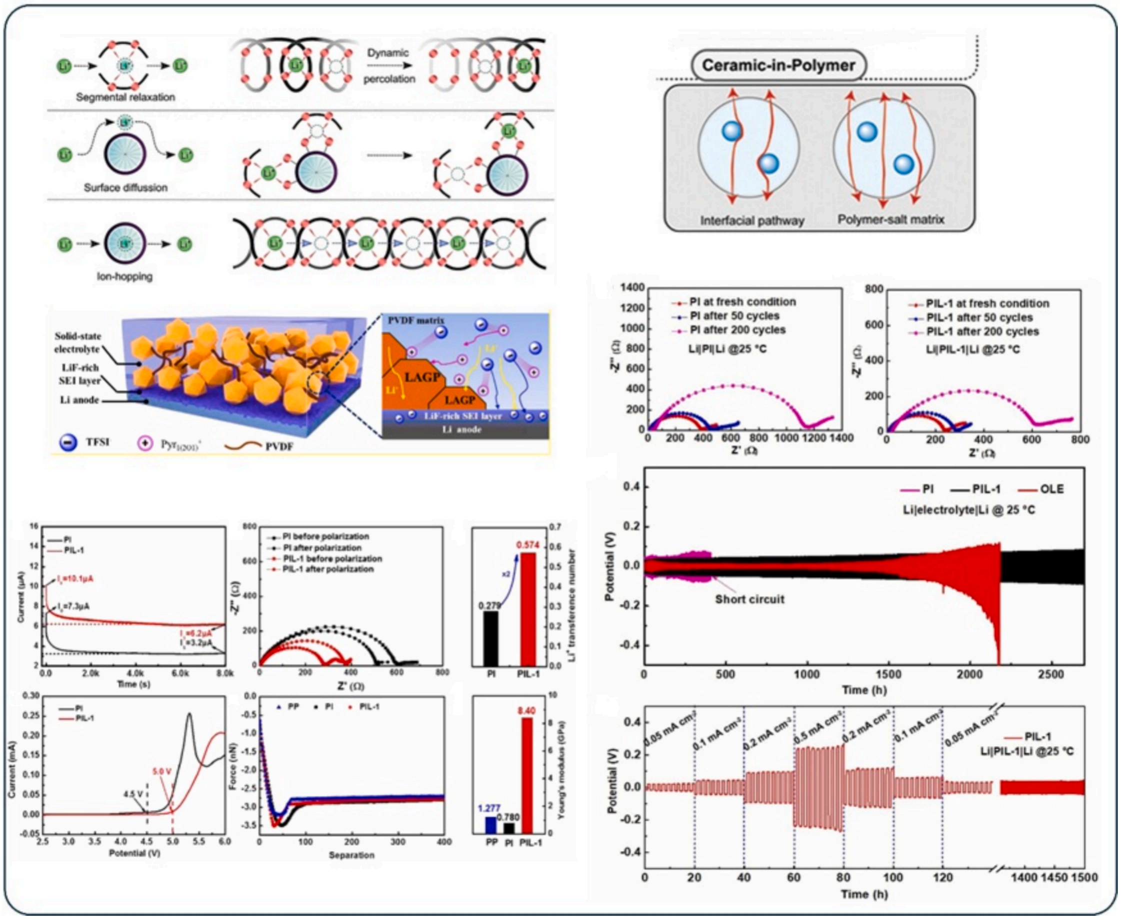

Fig. 9. Scheme of mechanism of li transport in amorphous, crystalline/amorphous mixture, crystalline phase for the cip systems and pvdf-latp based cip electrolyte showing the synergistic effect of the polymer / ceramic composition. reproduced from ref. [178] with permission from Springer, Copyright 2023.

considered: the polymeric matrix, the ion-conducting filler, and the polymer-ceramic interface [106,111,168,169].

Critical aspects within CIPs are related to particles' dimensions and filler-to-polymer ratio. If the filler is passive, a major role is played by the particles' dimensions and, consequently, by the overall surface area. For particles in the micrometer range, which means surface area of the order of few m^2/g, filler addition only determines an improvement of mechanical properties, whereas the conductivity decreases by dilution of the active phase. If the particles are in the nanometer range (i.e. specific areas of hundreds m^2/g) there is an initial increase of the ionic conductivity, even by one order of magnitude or more due to space-charge effects [175]. The conductivity maximum is in the range 5-15 wt% of filler, followed by decrease for dilution. If the filler is active, the particles' dimension plays a minor role, and it is possible to increase the filler phase content up to several tens wt.%. This leads to the possibility to fabricate PICs (see below).

The introduction of an inorganic insoluble filler complicates the preparation of the electrolyte, that strongly affect the final performance of the final device. Indeed, the homogeneous dispersion of the filler, avoiding clustering or precipitation need to be controlled. Preparation methods include dry methods (dry mixing of components followed by cold or hot pressing), wet chemical methods (dispersion of components in a solvent of the polymer and non-solvent for the filler, casting, and evaporation of the solvent), high viscosity methods (formation of a paste without the use of a solvent, formation of the membrane with desired thickness) [176,177].

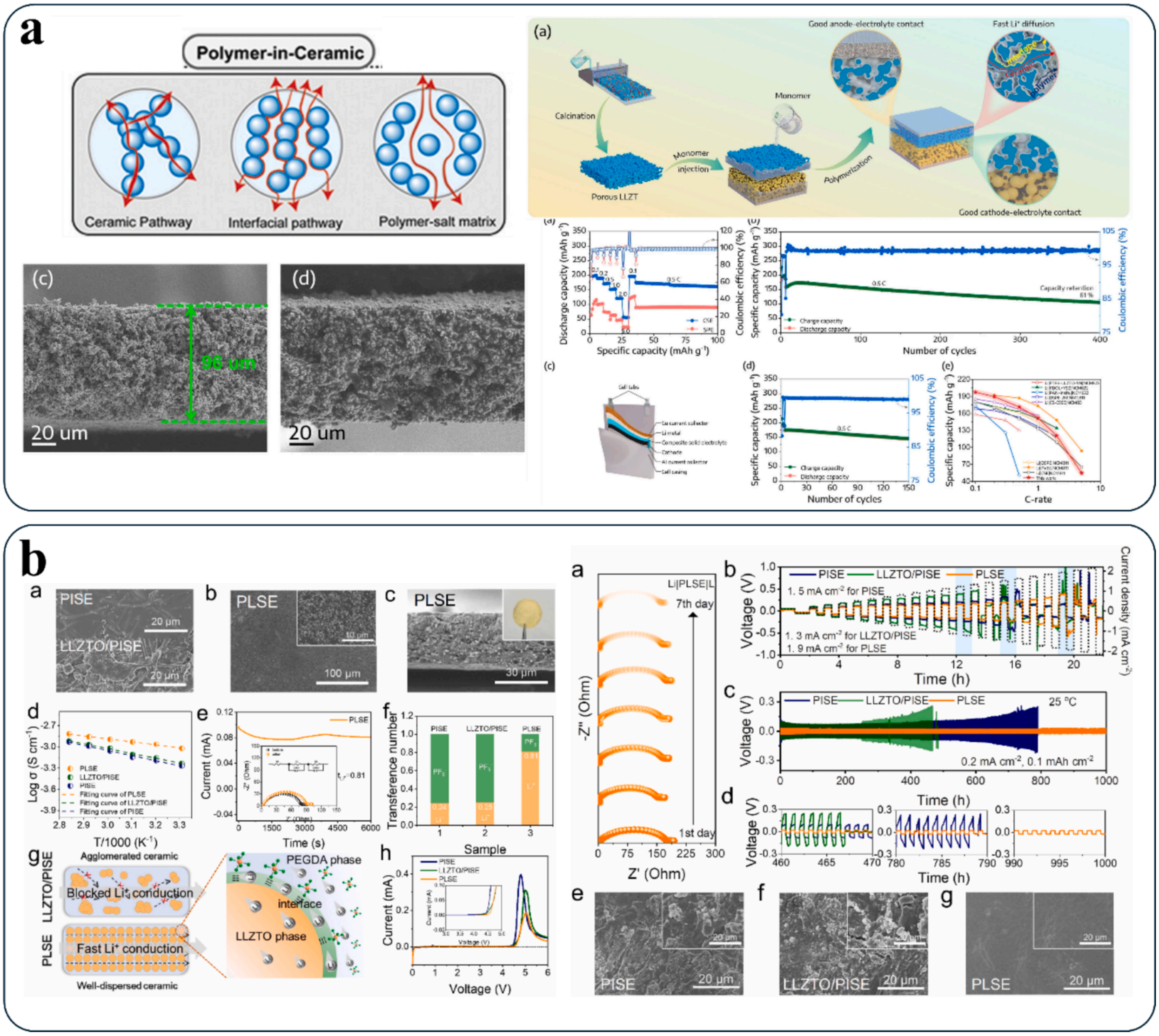

Fig. 10. (a) Scheme of mechanism of Li transport in the PIC system with LLZT and in situ polymerization. Reproduced from Ref. [98] with permission from Springer, Copyright 2024; (b) example of PIC based on garnet. Reproduced from Refs. [178,186] with permission from Springer and Elsevier, Copyright 2023, 2024.

5.2.2.5. Polymer-in-ceramic. The polymer-in-ceramic (PIC) approach was initially developed to overcome the main limitation of ceramic electrolytes, essentially the poor mechanical properties, poor interface contact and grain boundaries resistance. In principle, the polymer is added in small or at least minority fraction (<50 % by weight) and can be an inert component (i.e. non-participating in the ionic conductivity) or an active one if present ionic conductivity [179]. The fine calibration of the weight ratio among the components is crucial for the enhancement of the mechanical and transport properties. Moreover, if the polymer fraction is inert, the existence of percolation thresholds should be considered. According to standard General Effective Medium theories, thresholds of inert around 33 wt% should be considered [180].

The morphology and particle size of the inorganic fraction should be carefully controlled. The electrolyte disks are obtained by mixing the polymer and inorganic components and subsequent hot pressing of pellet preparation by heating. However, free-standing membranes with high content of ceramic are not easy to achieve; thickness is relevant but contributes to determining the energy density of the cell. Other typical preparation procedures include dry methods (dry mixing and casting and tape casting, in situ polymerization, infiltration method with the use of solvents [181,182].

The contact with the electrode is also extremely relevant and different from the case of liquid electrolytes (LEs). Indeed, LE can penetrate the pores of the electrodes and wet the electrodes, forming a deep ionic connection, while with SE the ion transport is limited to the surface region as SE cannot penetrate the electrode. In addition, the electrodes can undergo volume variation during charge and discharge, and SE can undergo cracking due to the induced stress. These problems can be partially overcome with the use of a polymer fraction (active or inactive), used also as a binder in the electrode formulation. This not only provides intimate contact between the electrode and electrolyte components, with continuous ionic paths for ion diffusion, but also enhances the compatibility of the components. The use of active polymer eliminates the need of inactive binder in the cathode preparation, providing an additional beneficial effect.

Several examples of PIC electrolytes have been recently reported by our group, including poly(ethylene oxide)/$Li_{1.3}Al_{0.3}Ti_{1.7}(PO_4)_3$ (PEO/LATP) [183], PEO-grafted TiO_2 nanocrystals [184] (Fig. 10). The PIC concept has been also linked to the CIP one to obtain Janus membranes to separately optimize the interfaces towards anode and cathode. Jiang et al reported a bilayer ultrathin (~11 μm) composite solid electrolyte membrane by exploiting a spontaneous precipitation of $Li_7La_3Zr_2O_{12}$ in a polymer-lithium salt matrix. The PIC layer is toward a high-voltage cathode, which can effectively inhibit oxidative decomposition of electrolytes. The CIP layer is toward the anode can provide good flexibility. Experimental results show that the CSE bilayer membrane has not only high ionic conductivity but also satisfactory Li^+ transference number [185].

5.2.2.6. Quasi solid electrolytes. The interfacial issues between the SSE and the electrodes, both with the anode (SEI) and the cathode (CEI), may strongly limit the cyclability and the long-time performance of the cell. In the last few years, there has been growing evidence that some residual fraction of solvents or non-solvents from membrane fabrication can strongly influence the functional properties of the electrolyte. This was reported chiefly for PVDF-based systems due to excellent mechanical and chemical properties of the fluorinated backbone. PVDF–$LiClO_4$ solid electrolyte membranes were prepared via solution-casting method employing a N,N-dimethylformamide (DMF)-tetrahydrofuran (THF) binary solvent. The electrolytes showed conductivity values as high as 2.03 ×

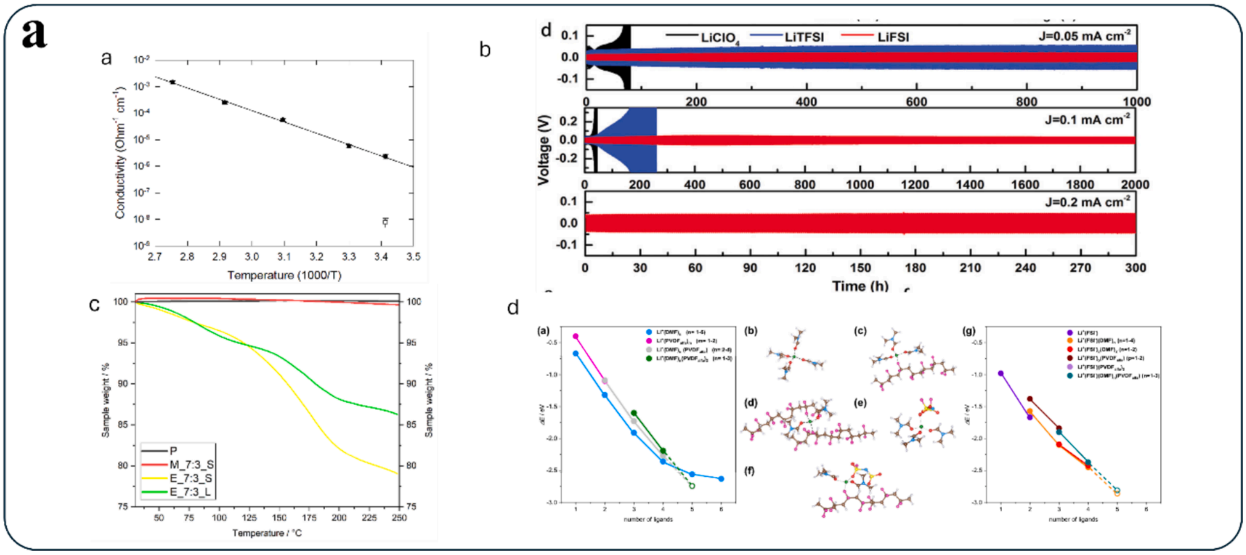

Fig. 11. (a) Ionic conductivity of PVDF-based QSE vs. residual DMF content. Reproduced from Ref. [188] with permission from Wiley, Copyright 2020; (b) cycling capability of QSE with different lithium salts. Reproduced from Ref. [187] with permission from Wiley, Copyright 2019; (c) thermogravimetric curves of samples with different aging. Reproduced from Ref. [189] with permission from American Chemical Society, Copyright 2024; (d) DFT modeling of the interactions among the different components in PVDF-based QSE. Reproduced from Ref. [189]. with permission from American Chemical Society, Copyright 2024.

10^{-4} S cm^{-1} at 25 °C and excellent cyclability in lithium metal cells (Fig. 11) [187]. The exact nature (true solid or semisolid) of these electrolytes was strongly questioned in the literature, chiefly as far as the exact nature of the ion transport mechanism is concerned. In fact, residual (or better permanent) DMF amount in the range 10–20 wt% were observed in the membrane, which could give origin to liquid-assisted transport [187,188]. In a recent paper, we studied the Li^+ transport mechanism in a model system consisting of PFDF-HFP, lithium bis(fluorosulfonyl)imide (LiFSI) salt and DMF as permanent residue, combining a large set of experimental techniques (thermal analysis, NMR, IR and Raman spectroscopy, impedance spectroscopy) and Density Functional Theory (DFT) modeling. We showed that Li^+-DMF interactions are predominant in these quasi solid electrolytes (QSEs) and are the basis of the effective ion transport mechanism. Permanent solvent amounts of the order of $[DMF]/[Li^+] \sim 2$–3 are needed to make QSEs able to practically work in a real environment [189].

Further improvements of QSEs properties could be obtained by preparing nanocomposite membranes. Silica-based hybrid nanofillers were obtained by grafting chains of poly(ethylene glycol) methyl ether (PEG) with different molecular weight on the surface of silica nanoparticles. The functionalized nanofiller improved the mechanical, transport and electrochemical properties of the QSEs, which showed good ionic conductivity values and high resistance against dendrite penetration, ensuring boosted long and safe device operation. The most promising result was obtained by dispersing 5 wt% of SiO_2 functionalized with short PEG chains (Mw = 750 g mol^{-1}). This system displayed ionic conductivity of 0.1 mS cm^{-1} at 25 °C, more than 250 h resistance to stripping/plating, and impressive results during cycling tests in LMB with $LiFePO_4$ cathode [190].

Other QSEs were recently reported in the literature to allow efficient strategies towards the improvement of functional properties, including: i) maximum attainable power density, ii) chemical and electrochemical stability, and iii) safety. These systems included patterned microporous and mesoporous membranes, metal–organic-framework based systems, and "soggy sand" electrolytes. Full details on these solutions could be found in this work [104].

5.3. *Emerging Horizons and outlook*

Despite the promising advantages of ASSBs, some major challenges need to be faced to reach the widespread commercialization of such devices. Overcoming these issues is crucial to unlocking the full potential of ASSBs. The key aspects to be addressed can be outlined in the following.

- *Enhancing ionic conductivity at room temperature*. Efforts are underway to develop new SSE materials with higher ionic conductivity, especially at room temperature. This includes exploring novel electrolyte compositions, designing innovative electrolyte structures, and engineering ionic conduction pathways and mechanisms within SSEs. Considering the single components, several strategies can be developed. The ionic conductivity in the polymeric fraction can be improved by: i) suppressing the crystallization, ii) lowering the Tg, iii) modifying the intra- and inter-chain path and coordination sites for Li ions. Functionalization, branching, copolymerization, polymer blending should be considered [159,191,192].

  As the Li^+ transport number in the polymeric matrix is known to be low, work can be done in restricting or blocking the mobility of the anion. The anion groups could be immobilized within the polymeric chains by functionalization through covalent bond formation [193,194].
  Due to the relevance of the polymer-ceramic interface as a possible fast ion pathway, the surface engineering of the filler can open new possibilities. Particle size, surface orientation, morphology could be tuned to modify the interface properties of the final systems [195].

- *Improving interfacial stability*. The electrode–electrolyte interface plays a crucial role in determining the performance of the whole battery, both in terms of power density and cyclability [195–197]. The SSEs are characterized by low contact area, resulting in limited transport properties at the interface; moreover, the resistance as the interphase generally increases with cycling due to electrode volume variations and SEI/CEI formation. Interfacial engineering strategies should be thus considered, including the introduction of buffer layers, modifying electrolyte compositions, and optimizing fabrication processes to stabilize these interfaces and reduce interfacial resistance. Introduction of bilayer systems (so called Janus membrane type), multilayer electrolyte (symmetrical and asymmetrical) could represent a strategy to properly face the specific cathode and anode interface problems [198,199].

  Considering the cathode side, it must be considered that the problem of poor interfacial contact is here even more relevant as the cathode materials present a complex and inhomogeneous surface. The main strategy is represented by the preparation of composite catholyte, mixing the traditional cathode materials with the SCE. This can represent a further benefit for the aspect of energy density as the inactive binder can be substituted with the ionically conductive SCE [200,201].

- *Suppressing dendrite growth*. Preventing lithium dendrite formation and propagation is essential for ensuring the safety and longevity of ASSBs and the main challenge related to the use of LMA. Research in this area focuses on understanding dendrite growth mechanisms, developing SSEs with high mechanical strength, and exploring innovative cell design strategies to mitigate dendrite growth. Dendrite formation is not completely suppressed by SSE due to a combination of contributions such as the low Li metal hardness, the surface and bulk defect in the SE, imperfect and poor interfacial contact. Actually, the first step is the deep and complete comprehension of the dendrite growth mechanism and the parameters affecting their growth, the electrode and SE degradation. The main strategy is suppressing the dendrite growth using high shear modulus SCEs, the minimum values required is 6.8 GPa. To this the implementation of rigid ceramic filler has been proposed [170,174,202,203].

- *Large scale production and cost-effectiveness*. Scaling up ASSB fabrication processes at competitive costs is essential for their commercial adoption. Efforts are underway to develop scalable and cost-effective manufacturing methods for SSE materials and cell assembly, paving the way for mass production of ASSBs [152,204].
- *Design-for-recycling*. This sector is becoming progressively more important considering the expected exponential growth of the automotive market. This growth, soon, will increasingly concern the ASSB sector. It will be necessary to design cells that can be disassembled with simple mechanical methods, reducing as much as possible the processes of formation of extensive interphases during the life of the battery. Furthermore, the materials will have to be reprocessable in a safe way and with low environmental impact. Being able to use processes in an aqueous environment will be of fundamental importance [205].

The most recent research is pointing out that CIP approach can lead to flexible and down-sizable devices, thanks to their high flexibility, low cost of components and scalable production. In contrast, the PIC approach is more appealing for EVs applications due to the high energy density, high mechanical properties and globally increased safety. Wide development possibilities are connected to the realization of quasi-solid systems with the introduction of optimal quantities of ionic liquids, solvents or non-solvents, etc. Also, the fabrication of Janus-type systems, optimized separately for the two anodic and cathodic interfaces, will allow to improve the long-term performance, the safety and the possibility of direct recycling-recovery of the components.

In conclusion, solid-state batteries represent an exciting path toward safer, more energy-dense, and longer-lasting energy storage systems. Solid-state electrolytes are key to realizing the transformative potential of ASSBs. Addressing the remaining challenges through continuous research and development efforts will pave the way for the widespread adoption of ASSBs, revolutionizing the energy storage landscape across various sectors.

6. Structural batteries

6.1. Introduction

The transportation industry is the largest contributor to greenhouse gas emissions, responsible for approximately 29 % of global emissions [206]. To protect the environment and expedite the transition towards green, low-carbon energy, industries such as new energy vehicles and aerospace are being heavily promoted. One of the primary challenges faced by batteries today is their capacity. Both electric vehicles (EVs) and aircraft require multiple battery packs for extended range; however, this leads to increased weight, larger battery volumes, and reduced energy density [207,208]. Although significant efforts are underway to develop high-energy–density electrode materials, such as lithium-sulphur batteries [209,210] and metal-air batteries [211–213], these technologies remain some way from widespread commercialization and application [214]. As a result, an alternative research direction involves enhancing the functionality of batteries. In addition to providing energy storage, batteries can also serve as structural components, which are expected to meet the stringent demands for lightweight structures, reliability, spatial integration, and high energy density in sectors such as automotive and aerospace.

Common structural materials, such as fibre-reinforced polymers, can reduce structural weight by 50 % to 70 % [215]. Among the various reinforced composite materials, carbon fibre (CF) is frequently utilized in the production of lightweight structural components due to its high specific strength and stiffness. Moreover, CF exhibits excellent electrical conductivity [216], presenting innovative possibilities for the development of lightweight batteries. The U.S. Army Research Laboratory (ARL) was the first to propose the combination of CF with battery materials, including CF as the anode, $LiFePO_4$ (LFP) and $LiCoO_2$-coated metal substrates as the cathode,

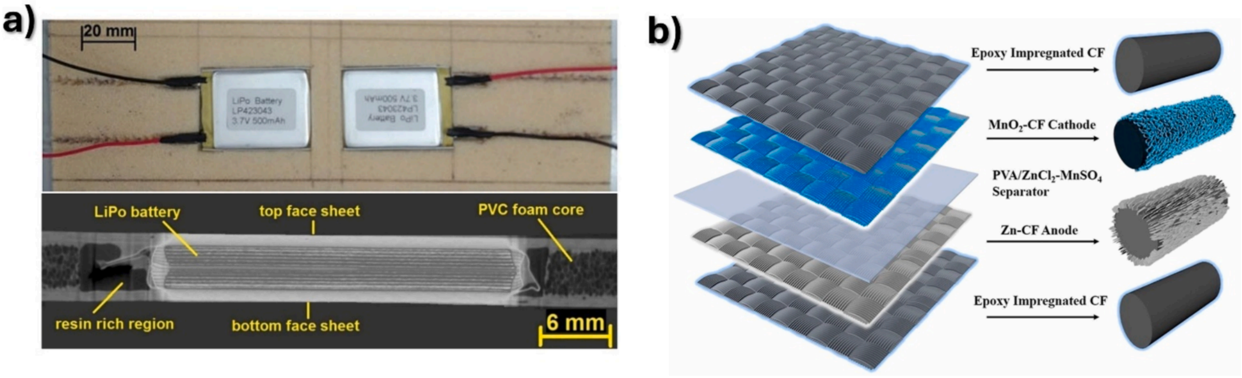

Fig. 12. A) uncoupled structural battery. reproduced from ref. [222] with permission from Elsevier, Copyright 2020, and b) coupled structural battery. Reproduced from Ref. [223] with permission from Elsevier, Copyright 2021.

glass fibre as the separator, and integrating electrolyte into resin to preserve ion transport capability while providing structural support [217,218]. Subsequently, the potential of this structure for use in composite fuel cells and composite capacitors was also investigated [219]. Johannison et al. [220] estimated that employing a composite structural battery (CSB) with a similar design could reduce mass by 22 % when replacing traditional steel car roofs, by 4 % when replacing interior panels in aircraft, by 12 % when replacing electric ferry hulls, and by 20 % when replacing laptop chassis. Consequently, CSBs offer significant potential across multiple sectors, including electric vehicles, aircraft, spacecraft, marine vessels, sports equipment, and robotics.

Current methods for CSBs can be classified into two categories [221]:

Uncoupled structural battery: The battery and the structure remain as two distinct components. Specifically, a battery system is integrated into the composite structure, with the battery positioned within the interlayer of the composite material, as illustrated in Fig. 12a) [17–19].

Coupled structural battery: In this method, the energy storage material is combined with the structural material, often by coating or depositing the active material onto CFs. These CFs can serve as current collectors or active materials. Furthermore, both traditional liquid electrolytes and solid-state electrolytes (SSE) can function as the electrolyte, allowing materials such as anodes, cathodes, and electrolytes to demonstrate both structural and energy storage properties. In this case, the structure itself effectively becomes a “large battery,” as shown in Fig. 12b) [19–21].

To broaden the application of structural batteries, these batteries also exhibit significant plasticity and high flexibility. Depending on varying operational conditions, different structural forms, such as tubular [224] and wavy designs [225], have been developed. Additionally, advanced manufacturing techniques like co-extrusion deposition and 3D printing technology [226–228] are employed to create these innovative designs as shown in Fig. 13.

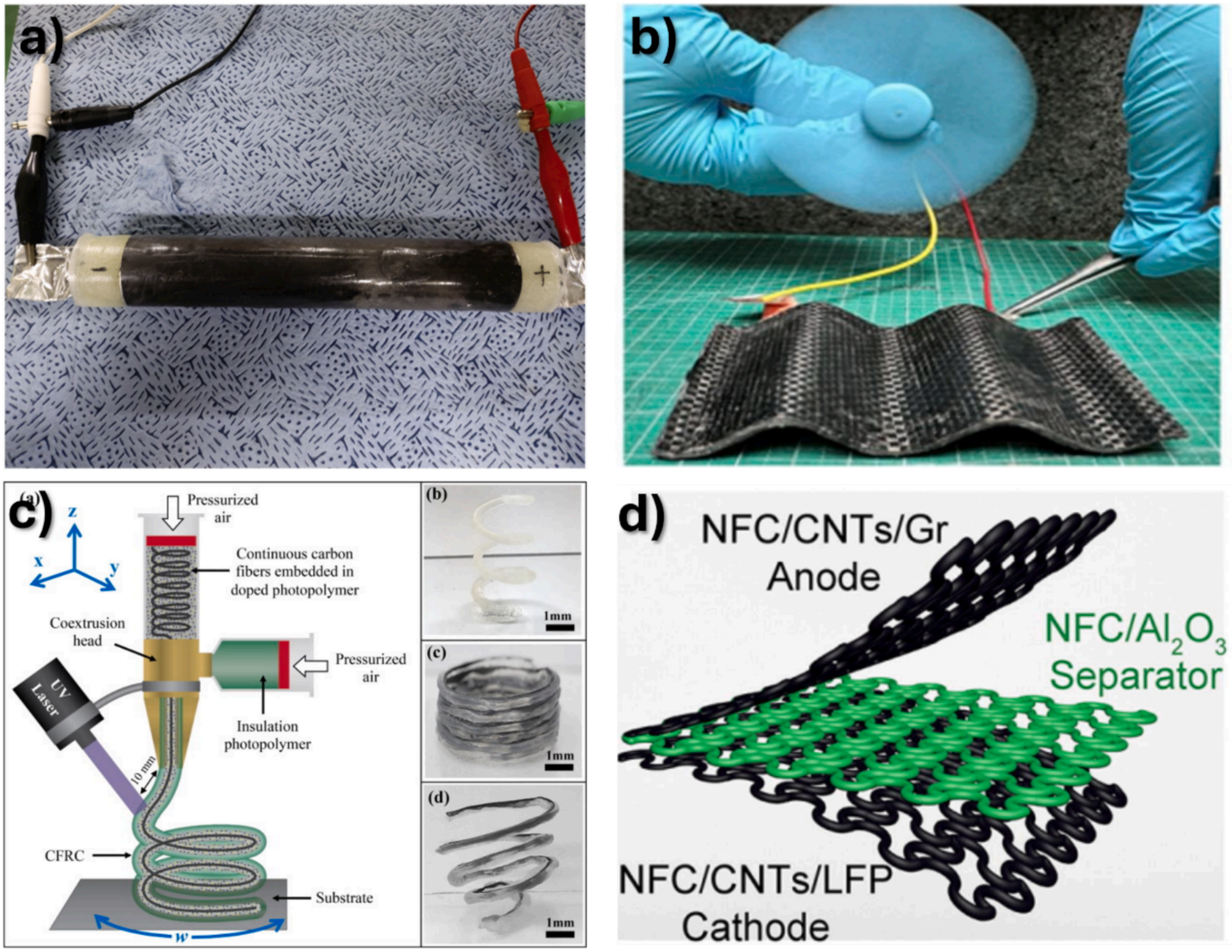

Fig. 13. A) tubular csb. reproduced from ref. [224] with permission from Elsevier, Copyright 2021, b) wavy CSB. Reproduced from Ref. [225] with permission from Elsevier, Copyright 2023, c) and d) 3D printed CSB. Reproduced from Ref. [226,228] with permission from Elsevier, Copyright 2020 and 2022.

6.2. Main materials and geometries

Structural batteries are composed of five key components: anode, cathode, electrolyte, separator, and collector. However, as uncoupled structural battery electrode materials are predominantly used in as same as commercial batteries. So, the technology is well-established, this section will not delve into extensive detail on that aspect. Instead, the focus will be on coupled structural batteries.

(1) Anode.

The main forms of anodes in CSB can be categorized into two approaches. The first involves directly using CF as anodes. A notable example is developed by Leif's research group at Chalmers University of Technology [229,230], which employs ultrathin

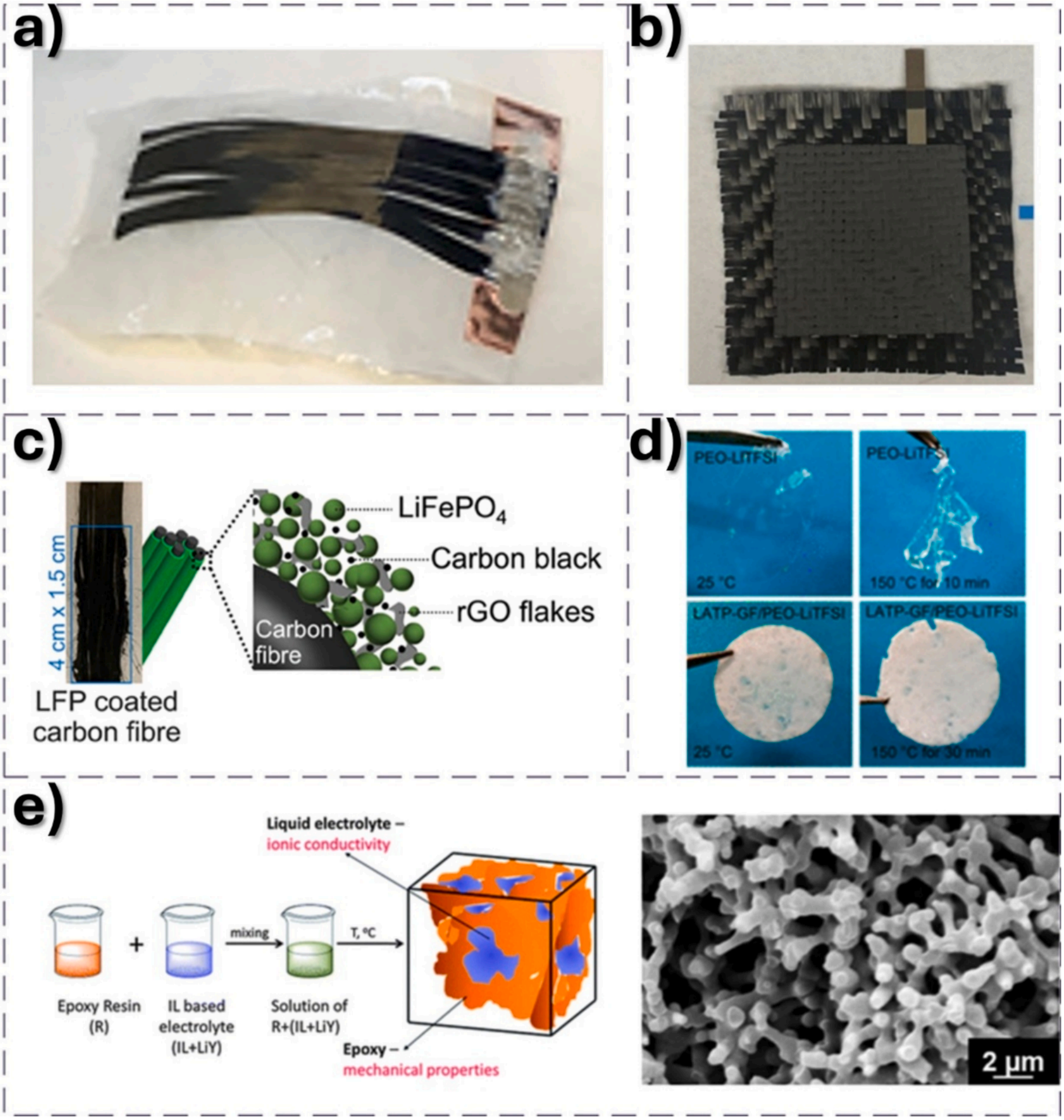

Fig. 14. a) and b) structural battery anode. Reproduced from Ref. [230,233] with permission from Wiley and Royal Society of Chemistry, Copyright 2022 and 2020. c) Structural battery cathode. Reproduced from Ref. [229] with permission from Wiley, Copyright 2024. d) GPE. Reproduced from Ref. [249] with permission from American Chemical Society, Copyright 2021 e) Heterogeneous electrolyte and the corresponding SEM micrographs Reproduced from Ref. [250] with permission from Royal Society of Chemistry, Copyright 2013.

unidirectional (UD) tapes made from polyacrylonitrile (PAN)-based CFs, as illustrated in Fig. 14a). To optimise the selection of CF, Kjell [231] and Snyder [216] evaluated the factors influencing the reversible capacity, microstructure, and the mechanical–electrical properties of common commercial CF, ultimately identifying the model with the best performance. The second approach utilizes conventional active materials such as graphite [232–235], which are mixed with binders and conductive agents to form a slurry. This slurry is then coated or deposited onto a CF collector, as shown in Fig. 14b).

It is worth noting that the insertion and extraction of lithium ions into and from the electrode during electrochemical cycling (lithiation and delithiation) can cause volume changes of the active material. Especially for carbon materials, the volume expansion is approximately 10 % [236,237]. Conventional metal collectors do not experience changes in volume or modulus, which leads to interlayer mismatch strain and high stress concentration between electrodes. In severe cases, this can result in the delamination and peeling of electrode materials from the metal current collectors, ultimately causing electrode structure failure. Such failure significantly affects the electrochemical processes within the electrode and leads to a decline in electrode cycling performance and reduced battery lifespan [238–240]. In composite electrode structures where CF is used as the collector, the fibre has a disordered core surrounded by a graphite sheath and can also undergo lithium insertion. The expansion and contraction of CF as an electrode material during battery cycling can induce stress changes of CF. The lateral expansion of fully-lithiated CF is around 10 %, while the longitudinal extension along the fibre axis is about 1 % [241]. Mao et al. [242] studied the lithium insertion-induced deformation behaviour of dual graphite-CF electrodes during electrochemical cycling and developed a theoretical model of electrochemical stress for a bi-layer electrode cantilever structure. Their findings demonstrated that CF, when used as a collector, can effectively mitigate electrode volume expansion mismatch strain.

(2) Cathode.

The design of the cathode in structural batteries is relatively straightforward. In most cases, a cathode active material is mixed into a slurry and applied to CFs. For instance, Park [243] mixed LFP with polyvinylidene fluoride (PVDF), dried the mixture, and then added it to N-methylpyrrolidone (NMP), stirring the components to form a mud-like electrode slurry. This slurry was coated onto woven carbon fibre (WCF) and treated with silicone rubber in a high-pressure reactor within a vacuum bag to form the cathode. As shown in Fig. 14c), the electrode achieved a maximum capacity of 114 $mAh.g^{-1}$ at a rate of 0.1C. Additionally, the LFP/WCF single electrode, measuring 35 mm × 5 mm, demonstrated a tensile strength of 250 N.

(3) Electrolytes and separators.

Some structural batteries retain the traditional design of separators and liquid electrolytes. For instance, Ladpli et al. [224,225,232–235] utilized liquid electrolytes in various battery systems, including conventional lithium salts like $LiPF_6$ or electrolyte solvents dissolved in organic compounds such as ethylene carbonate (EC), diethyl carbonate (DEC), and dimethyl carbonate (DMC). In these systems, the separators are immersed in the electrolyte solution. The separators are typically made of polypropylene or glass fibre.

For structural batteries, an electrolyte that provides both structural support and ion transport channels is essential. SSE offer several advantages over liquid electrolytes, as they are less prone to issues such as corrosion, combustion, leakage, and internal short circuits. Additionally, they are inert to metallic lithium and can act as separators while also helping to suppress dendrite growth [244,245]. One type of solid electrolyte is gel polymer electrolyte (GPE), which is formed by expanding a thinly-crosslinked thermoset polymer with a liquid electrolyte [246]. For example, Tikekar's research [247] demonstrated that fixing only a small portion (5 %) of anions on the membrane can inhibit dendritic growth by more than 20 times. Some structural cells utilize gel electrolytes. For instance, Liu et al. [248] used a polymer blend of PVDF-HFP (polyvinylidene fluoride-hexafluoropropylene) and polyethylene glycol dimethacrylate to form a high-strength polymer gel electrolyte with $LiPF_6$ electrolyte solution. Chen added monomer PVA to the $ZnCl_2$ and $MnSO_4$ electrolyte and injected it into a fibre film to create a solid electrolyte. Dong et al. [249] mixed and ground PEO, lithium aluminium titanium phosphate (LATP), and LiTFSI powders into a thin SSE layer, which was then fused with a glass fibre separator through hot pressing, as shown in Fig. 14d). This electrolyte material exhibited a high Young's modulus of 1.62 GPa and a conductivity of 6.3×10^{-2} mS cm^{-1} at 25 °C, with conductivity increasing as the temperature rises.

Another is heterogeneous electrolyte, comprising a uniform bi-continuous network of two pure phases, one phase for mechanical properties (monomers) and the other for ion transport (electrolytes) as shown in Fig. 14e). While high concentrations of lithium salts can improve the ion conductivity of polymers but reduce mechanical strength. To address this, Shirshova et al. [250,251] investigated the relationship between conductivity and Young's modulus by adjusting the volume/weight ratio of monomers to electrolytes, identifying the optimal balance between mechanical strength and ion transport. A systematic study on electrolyte structure was carried out by the Chalmers University of Technology and the KTH Royal Institute of Technology team. Ihrner et al. [252] combined dimethyl methylphosphonate (DMMP) with LiTFS and cured it with ultraviolet light to form a solid-state electrolyte (SSE) film on the outer layer of CFs. The Young's modulus is about 0.5 GPa and ion conductivity is 0.2 mS cm^{-1}. The following year, Johannison et al. [220,253,254] made further improvements by using different materials to create a uniform, low-viscosity solution. This solution was then vacuum-assisted and applied to CFs, followed by UV curing at 100 °C for 3.5 min to form a half-cell electrode. This process increased conductivity to 0.3 mS cm^{-1}, and the elastic modulus to 0.69 GPa. As structural batteries are typically composed of sealed and opaque materials, ultraviolet radiation is not always effective for curing. Subsequently, Schneider et al. [255] improved this electrolyte solution, which could be heated to form a solid electrolyte with a conductivity of 0.15 mS cm−1, showing great promise for use in composite structural batteries. Schneider's group later applied this electrolyte to produce high-performance composite structural batteries [256].

6.3. Figures of merit and functional characteristics

The evaluation of structural batteries can be approached from two key aspects: electrical performance and mechanical performance. Electrical performance is typically characterized by battery capacity, while mechanical performance is assessed through various mechanical tests, including conventional methods such as tensile, compression, and bending tests.

(1) Electrical performance.

The energy density of various reported structural batteries has been compared as shown in Fig. 15. Batteries 1–5 represent uncoupled structural batteries, while 6–11 are coupled structural batteries. Uncoupled structural batteries 1 and 2 consist of commercial batteries embedded in CF or CF-foam sandwich structures, whereas batteries 3, 4, and 5 were prepared in the laboratory, where the battery packaging was directly replaced with CF. It is evident that these batteries exhibit much higher energy densities compared to other types.

In particular, Ladpli et al. [232] used carbon fiber reinforced polymer (CFRP) laminates to replace traditional battery packaging, reinforcing the electrode stacks mechanically with interlocking polymer rivets. Their battery featured multi-layer electrodes, fixed by polymer rivets and clamped between CFRP panels, achieving an energy density of up to 130 Wh/kg. Dong et al. [257] 's structural battery, designed with a self-supporting LFP (SS-LFP) cathode, incorporates LFP particles uniformly distributed within the SS-LFP cathode, surrounded by MXene nanosheets, CNTs, and cellulose, enhancing both electron transfer efficiency and structural stability, resulting in a high energy density.

Coupled structural batteries also demonstrate strong electrical performance. For instance, Chen et al. [223] developed a Zn-MnO_2 battery, and Moyer et al. [234] created a lithium battery, both of which involve depositing or coating electrode slurry onto a CF current collector, significantly reducing the weight of the battery. Scholz et al. [258] suggested that battery for small electric aircraft would require a minimum energy density of 51.8 Wh/kg. Several structural batteries can meet or exceed this requirement, showcasing promising potential for future applications.

(2) Mechanical performance.

Based on reported mechanical properties in the literature, the electrical performance of structural batteries has been compared with commercial batteries. Due to the varying sizes and strengths of these batteries, elastic modulus or stiffness was chosen as the basis for comparison. As listed in Table 2, both forms of structural batteries have significantly enhanced mechanical performance. To date, the coupled structural battery produced by Richa et al. [229] demonstrates the best mechanical performance. The structural battery boasts an elastic modulus exceeding 76 GPa, an energy density of 30 Wh/kg, stability for up to 1000 cycles, and a coulombic efficiency of nearly 100 %, achieving a balance between energy and mechanical performance. Structural batteries with excellent mechanical properties are often analyzed to ensure the continuity and integrity of the structure. Coupled structural batteries, particularly those using heterogeneous electrolytes or packaged with CF, exhibit superior mechanical performance. However, due to a lack of adhesion

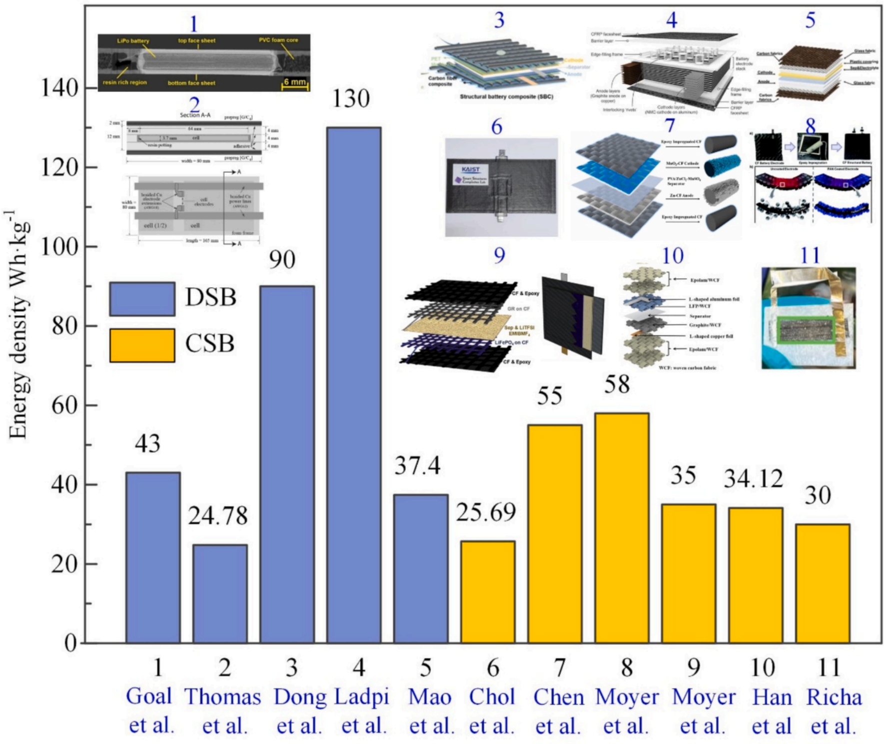

Fig. 15. Comparison of the energy density of structural batteries [222,223,225,229,232–235,257,259,260].

Table 2
Comparison of mechanical properties of structural batteries.

Reference	Catergory	Mechanical propties	Value
Elham [263]	lithium polymer pouch cells	Young's ModulusShear modulus	180 Mpa 300 MPa
Goal [222]	DSB	Flexural modulus	12.8 ± 0.48 GPa
Thomas [259]	DSB	Bending stiffness	985 ± 31 $N{\cdot}m^2$
Dong [257]	DSB	Flexural modulus	42.1 GPa
Ladpi [232]	DSB	Flexural Rigidity.	12 $N{\cdot}m^2$
Mao [225]	DSB	Flexural modulus	7.7 GPa
Chen [223]	CSB	Young's ModulusFlexural modulusCompressive modulus	12.8 Gpa4.4 GPa5.0 GPa
Moyer [234]	CSB	Young's Modulus	1.8 GPa
Han [260]	CSB	Young's Modulus	13.07 Gpa
Richa [229]	CSB	Young's Modulus	76 GPa

between electrode materials, these batteries are susceptible to interface debonding, delamination damage, and other issues during mechanical loading [261,262]. These challenges can lead to a lower modulus, reduced energy storage capacity, and diminished electrical performance.

(3) Multifunctional coefficient.

However, the electrical performance of most structural batteries is still far below traditional batteries capacity, but their mechanical performance has improved by thousands or even higher. Therefore, in order to verify if it is worth to sacrifice electrical performance to improve mechanical performance, O'Brien et al. [264,265] proposed the concept of multifunctional efficiency of overall system performance to compete design criteria between the electrochemical and mechanical properties of structural batteries.

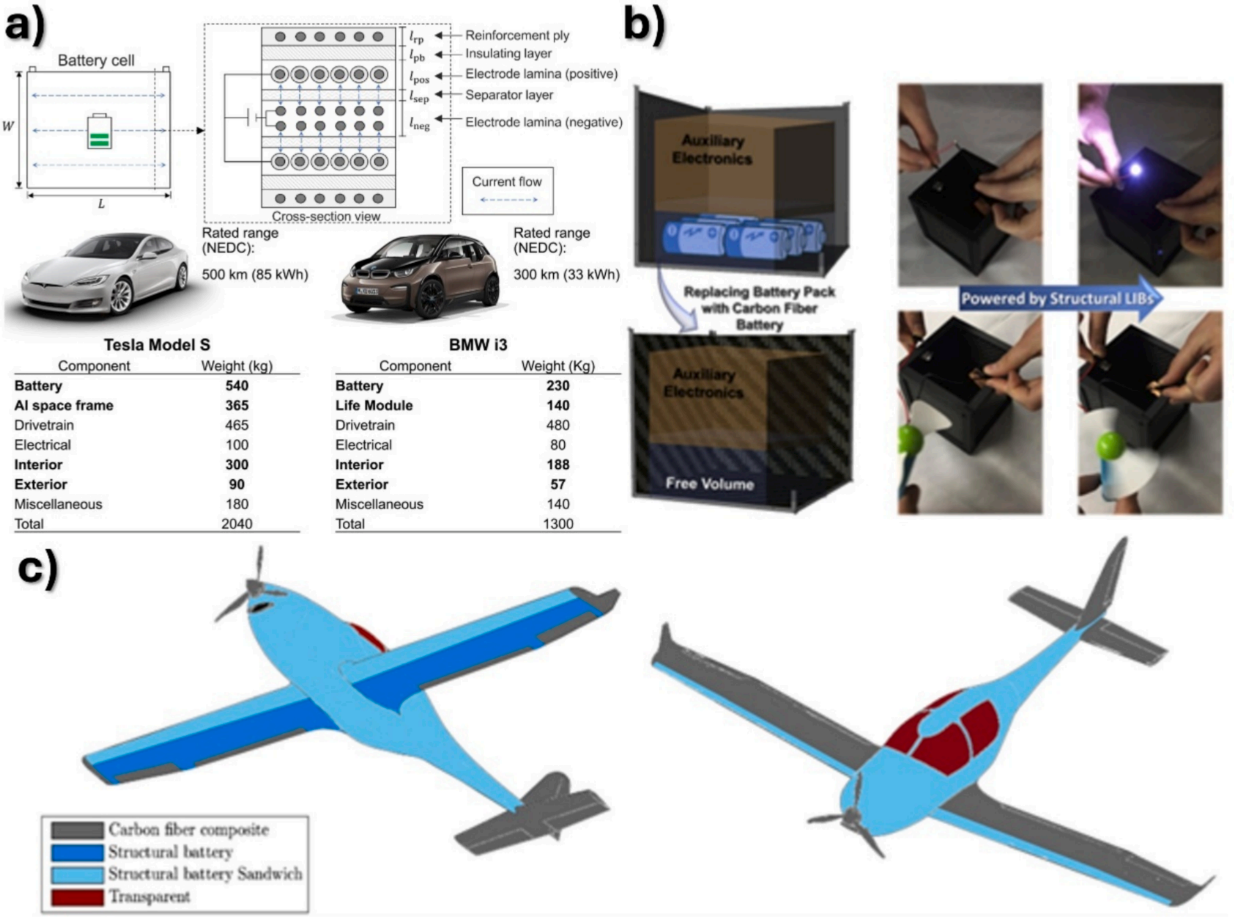

Tesla Model S

Component	Weight (kg)
Battery	**540**
Al space frame	**365**
Drivetrain	465
Electrical	100
Interior	**300**
Exterior	**90**
Miscellaneous	180
Total	2040

BMW i3

Component	Weight (Kg)
Battery	**230**
Life Module	**140**
Drivetrain	480
Electrical	80
Interior	**188**
Exterior	**57**
Miscellaneous	140
Total	1300

Fig. 16. A) CSB in EV application. Reproduced from Ref. [267] with permission from Elsevier, Copyright 2020, b) integrating CSB within a 1U CubeSat. Reproduced from Ref. [241] with permission from Elsevier, Copyright 2013, c) CSB in hybrid aircraft (CS-23). Reproduced from Ref. [273] with permission from American Society of Civil Engineers, Copyright 2020.

Multi functional efficiency is divided into the ratio of energy density and modulus (or stiffness) to that of a single functional system, η_{e} andη_{s} (equations (1) and (2).

$$\eta_e = \frac{\overline{\Gamma_{m_f}}}{\overline{\Gamma}} \tag{1}$$

$$\eta_s = \frac{\overline{E_{m_f}}}{\overline{E}} \tag{2}$$

The sum of two ratios is the multifunctional efficiency, and each term cannot be 0. When the multifunctional coefficient is greater than 1, it means that the multifunctional system has achieved an improvement in the balance of electromechanical performance (equation (3),

$$\eta_{mf} \equiv \eta_s + \eta_e > 1 \tag{3}$$

Snyder et al. [266] further enhanced the multifunctional coefficient by taking into account that structural batteries often employ anisotropic materials. In such cases, the modulus can be replaced by plane shear stress or shear modulus, and the minimum value of stress or modulus in each direction of anisotropy should be selected for comparison. Similarly, the electrical coefficient should be calculated by choosing the minimum value of energy density and specific power.

Johannison et al. [220] introduced a new multifunctional coefficient to evaluate the weight savings of structural batteries, assuming that these batteries possess the same mechanical stiffness as traditional CFRP laminate under specific loads. Additionally, they assumed that both structural batteries and standard lithium-ion batteries store an equal amount of electrical energy. If based on this situation, the structural battery has a lower mass than the combined mass of the laminated panel and battery, it indicates that the structural battery outperforms the traditional single-function panel and battery.

6.4. Applications

David Carlstedt and Leif E. Asp [267] evaluated the potential application of structural batteries in EVs based on their designed battery structure [246]. Using the BMW i3 and Tesla Model S as examples, as illustrated in Fig. 16a), they assumed the complete removal of all traditional batteries from the vehicle. In their scenario, 70 % of the inner and outer panels, as well as 60 % of the space frame and lifespan module, were replaced by their heterogeneous electrolyte structural battery. This modification resulted in a mileage increase of approximately 70 %, while maintaining the vehicle's original weight. Reza et al. [268] conducted a similar study, using the Tesla Model S as a case example. They proposed that by replacing components such as the roof and hood with structural batteries, the vehicle's mileage could increase by 23 %, all while maintaining good mechanical performance.

CubeSats are a type of micro- and nano-scale scientific research spacecraft that utilize novel packaging and integration methods, multifunctional composite structures, embedded microsystems, and miniaturized propulsion systems. They are employed in various applications such as small payload delivery, rendezvous and docking operations, and satellite constellation arrangements in low Earth orbit (LEO) [269]. Typically, CubeSats have a standard size of 10 × 10 × 10 cm^3 and weigh 1.33 kg, known as 1U (one unit), as illustrated in Fig. 16b) [270]. Due to their small size and modular nature, CubeSats help reduce costs while presenting greater technological innovation challenges for system integration, miniaturization, multifunctionality, and intelligence. Batteries are critical to CubeSat operation, as the average daily power generation and consumption of onboard solar panels range from 2 to 6 W, necessitating energy storage for operations during periods of solar eclipses. To increase payload capacity and maximize usable space, CubeSat power systems have increasingly adopted new energy storage technologies, especially lithium-ion batteries. Batteries typically account for about 13 % of the total CubeSat mass. Moyer et al.[234] demonstrated that integrating CSB within a 1U CubeSat frame reduced battery mass by 30 % and increased available space, aligning CubeSat designs more closely with NASA's operational requirements for mission injection.

In terms of aircraft, Thomas et al. [271,272] designed and developed lithium cobalt oxide ($\mathrm{LiCoO_2}$)-graphite batteries, which were encased in DaiNippon EP-40 and used as structural wing materials for drones. This innovation allowed drones to increase their flight time by up to 26 %, while maintaining the same specific energy as traditional battery structures. Riboldi et al. [273] investigated the use of CSBs in hybrid aircraft (CS-23), incorporating them into 38 % of the wings and 66 % of the fuselage, as shown in Fig. 16c). They found that, while maintaining the original power performance, the overall weight of the aircraft structure and battery could be reduced by approximately 20 % compared to traditional carbon fibre-reinforced polymer (CFRP) structures, and by about 29 % compared to aluminium alloy structures with traditional battery packs. Mauro et al. [274] expanded on this research by replacing 38 % and 75 % of the wing and fuselage structures with structural batteries for the P2012 Traveller aircraft. This resulted in a fuel savings of approximately 18 % for the design mission (1100 km) and 20 % for a typical mission (370 km). Elitza et al. [275] examined the A320 aircraft and found that replacing 50 % of the fuselage with CSBs could increase fuel efficiency by 15 % during a 1500 km mission, compared to the traditional hybrid A320. Compared to a fully electric A320, structural batteries could halve the specific energy or mass required for 1000 km of flight. In another case, Sang et al. [276] replaced the floor of the Airbus A220-100 with a clip-on CSBs to power the in-flight entertainment system. This modification saved approximately 260 kg in weight and 510 L in volume.

6.5. Outlook and future challenges

This section reviews the current development of both uncoupled and coupled structural batteries, focusing on materials, electromechanical properties, and applications. Structural batteries integrate energy storage materials with structural components, significantly enhancing mechanical properties while contributing to weight reduction and space efficiency.

However, there remains a gap between the capacity, cycling, and rate performance of structural batteries compared to conventional commercial batteries. To narrow this gap, it is necessary to develop high-performance electrode materials that can withstand mechanical loads. As structural batteries become increasingly applied in fields such as aerospace, automotive, and marine industries, they are subjected to static and complex dynamic loads, particularly under high discharge rates, overheating, and uneven temperature distribution. Long cycling or intermittent charging and discharging can result in significant performance degradation, reduced reliability, and early failure of electrochemical systems.

Research on the reliability of structural batteries under complex mechanical loads and fatigue conditions remains insufficient. Furthermore, to deploy these batteries in aerospace, the limited temperature range of conventional electrolytes must be addressed, and the performance of batteries under extreme temperatures and vacuum conditions should be carefully considered.

Additionally, the intricate behavior of electrolytes and their interfaces in structural batteries remains a challenge. The structural and compositional characteristics, chemical and electrochemical reactions, and thermodynamic and kinetic behavior at the solid electrolyte interphase (SEI) are not yet fully understood. This area requires further research and interdisciplinary collaboration in chemistry, physics, materials science, and nanoscience. By leveraging data science methods, optimizing design structures can help reduce experimental costs and enable data-driven approaches to evaluating and predicting key parameters and electromechanical performance. This is essential for advancing the development of structural batteries in a meaningful and innovative way.

Fig. 17. Schematic illustration of printed power sources, emphasizing printable ink materials, printing techniques, and their applications in upcoming diverse structured electronic devices.

7. Printed batteries

7.1. Introduction

The surge in demand for state-of-the-art electronics, such as flexible and wearable devices, wireless technologies, and the Internet of Things (IoT), has driven the need for power sources that break free from conventional design constraints [277–279]. Energy storage devices, such as batteries and supercapacitors (SCs), often manufactured by stacking electrode sheets and separator membranes and injecting liquid electrolytes into rigid package materials, lack the versatility and seamless integration capabilities essential for advanced electronics [280–282]. This has prompted the development of innovative, form factor-free, high-performance power solutions. Among these innovations, printed batteries have emerged as a paradigm-shifting approach, offering exceptional design flexibility and cost-effective manufacturing processes [283–285]. By utilizing various printing techniques and rationally designed ink materials, the printed batteries can be directly fabricated onto target substrates with complex and unconventional shapes. This capability enables monolithic integration with a wide range of electronic devices while ensuring high electrochemical performance, meeting the demands of next-generation electronics.

This section discusses recent advancements in printed battery technology, exploring design diversity, material breakthroughs, and applications, thereby highlighting their potential impact on the future of electronic power sources (Fig. 17).

We outline a range of printing techniques and their requirement for ink design. This is followed by an exploration of the intricate chemistry and material composition of printable component inks, including electrodes, electrolytes, separator membranes and current collectors. Understanding these foundational elements in printing techniques and core materials is essential for exploring the diverse applications of printed power sources. The application section emphasizes printed batteries' outstanding design flexibility and reliable electrochemical performance when integrated into electronic systems. We categorize the application of printed batteries into shape-versatile form factors, target-oriented designs, and performance-oriented designs. In addition, future development and outlook for printed batteries are proposed from the viewpoint of commercialization and practical application as device-tailored energy storage solutions.

7.2. Key materials and fabrications for printed batteries

7.2.1. Printing techniques

Selecting appropriate printing techniques is critical for satisfying the design diversity and electrochemical requirements of printed batteries. Printing techniques can be classified into (i) mask-based printing and (ii) direct-ink-write (DIW) printing, depending on whether predesigned masks are utilized during the ink deposition process. The selected techniques are closely linked to the design and preparation of cell component inks. This chapter reviews the design principle of ink, various printing methods, representative examples, and their underlying mechanism, highlighting the necessity of meticulously designed inks to ensure stable printability and reliable electrochemical performance.

7.2.1.1. Rationale of ink formulation. Battery component inks must be rationally designed to ensure compatibility with printing technologies and achieve optimal electrochemical performance. Key requirements for these inks include (i) stable dispersion of components, (ii) rheological properties, such as viscosity and viscoelasticity, suitable for the specific printing process, (iii) structural and dimensional stability after printing, including cohesion between the components, adhesion to the substrate, and mechanical integrity under stress, and (iv) the electrochemical performance of the resulting printed battery.

Generally, the component inks of printed batteries are colloidal dispersions composed of various solid particles, polymers, and solvents. Therefore, an in-depth understanding of colloidal interactions is essential for appropriate ink design. Colloidal particle interaction is theoretically explained by the Derjaguin–Landau–Verwey–Overbeek theory, which provides a framework for describing these interactions. This theory explains interparticle potential energy by combining several attractive and repulsive forces (Fig. 18a), which can be expressed as (equation (4):

$$V_{total} = V_{vdW} + V_{elect} + V_{steric} + V_{structural} \tag{4}$$

where V_{total} is the total interparticle potential energy, V_{vdW} is the attractive potential energy driven by long-range van der Walls interaction, V_{elect} is the electrostatic repulsive potential energy by charged surfaces, V_{steric} is the steric repulsive potential energy by polymeric species absorbed on particle surfaces, and $V_{structural}$ is the potential energy resulting from the nonadsorbed species in solution [286].

Control of the electrostatic force (i.e., V_{elect}) is an effective way to manipulate colloidal particle interactions; thus, many previous studies on printable batteries have focused on controlling the surface potential of printable inks. Zeta potential is a common term for describing the surface potential of colloidal particles. It refers to the electrical potential at the slipping plane within the interfacial double layer, measured relative to a point in the bulk fluid distant from the interface. There are several ways to manipulate the zeta potential, including utilizing ionic surfactants, particle surface modification, and solvent processing (i.e., adjusting pH or ionic strength). A schematic of colloidal particle behavior according to the zeta potential is presented in Fig. 18b. A high zeta potential results in a well-dispersed suspension, leading to excellent sedimentation stability and high solids loading capacity [287]. Such suspensions exhibit fluid-like characteristics, including low viscosity and relatively linear viscoelastic behavior as a function of shear or strain. In contrast, a low zeta potential leads to particle aggregation, forming a strong network structure that provides good

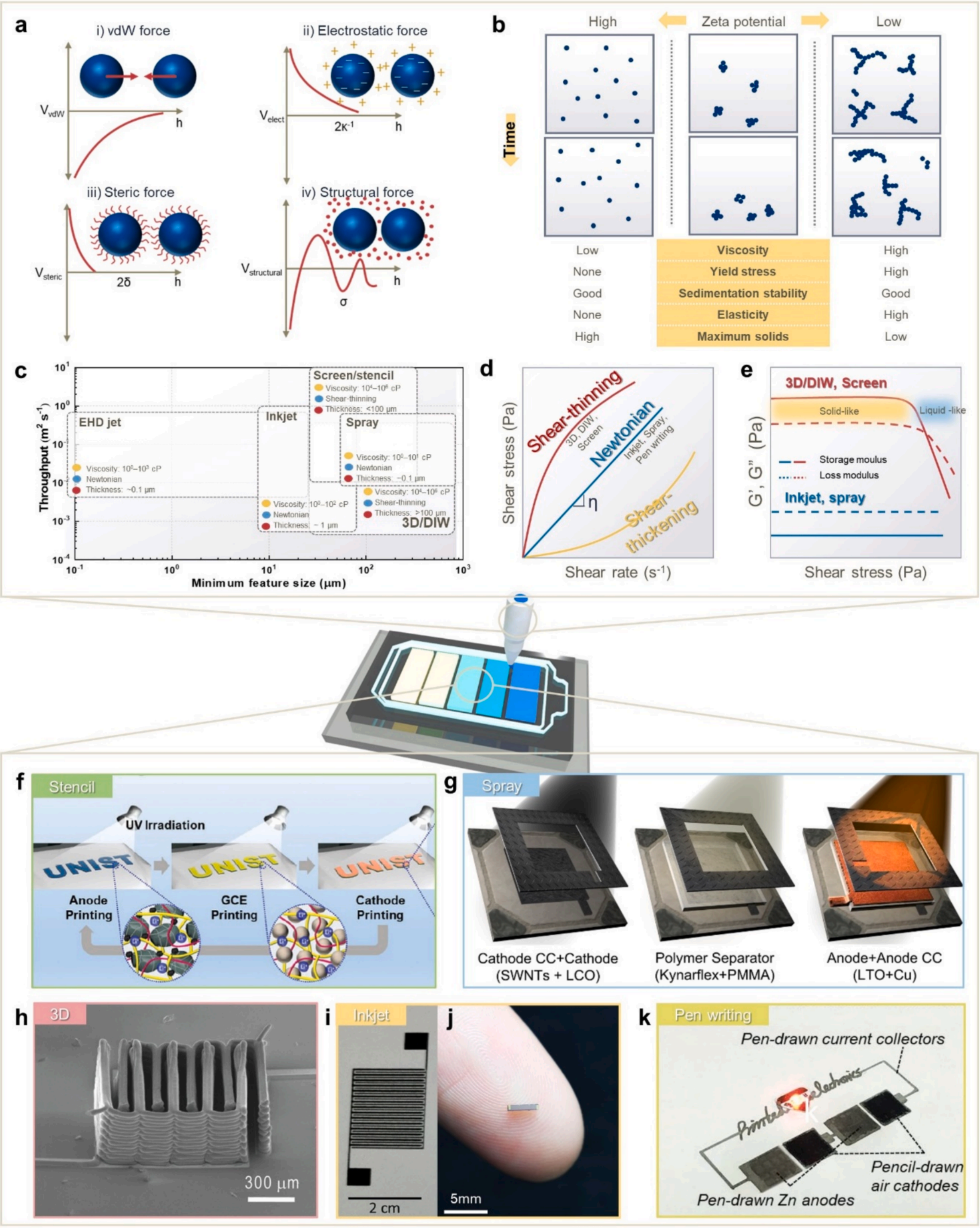

Fig. 18. a) Schematics representation of the colloidal particle interaction potential energy and relevant lengths scale. Reproduced from Ref. [286] with permission from Wiley-VCH GmbH. Copyright 2000. b) Effect of Zeta potential in colloidal suspension properties [287]. c) Comparison of minimum feature size, throughput and rheological properties for different printing techniques. Schematic diagram representing suitable ink characteristics corresponding printing techniques based on the relationship between d) shear rate and viscosity, and e) shear stress and viscoelastic properties. Reproduced from Ref. [282] with permission from Elsevier, Copyright 2022. f) Schematic of the fabrication of stencil-printed flexible LIB prepared via UV-curing-assisted printing processes. Reproduced from Ref. [288]. with permission from Royal Society of Chemistry, Copyright 2018. g) Direct fabrication of spray-printed LIB on the surface of interest. Reproduced from Ref. [289] with permission from Nature Publishing Group, Copyright 2012. h) 3D-printed LIB composed of 16-layer LFP cathodes and LTO anodes. Reproduced from Ref. [290] with permission from Wiley-VCH GmbH, Copyright 2013. Photographs showing the i) inkjet-printed Zn-MnO_2 battery on a paper substrate and j) EHD-printed MSCs.

Reproduced from Ref. [291] with permission from Nature Publishing Group, Copyright 2024. Reproduced from Ref. [292] with permission from American Association for the Advancement of Science, Copyright 2020. k) A photograph of pen-written Zn-air battery composed of silver current collectors, pen-drawn Zn anodes, pencil-drawn air cathodes, and pen-drawn gel electrolytes. Reproduced from Ref. [293] with permission from Wiley-VCH GmbH, Copyright 2018.

sedimentation stability but significantly reduces solids loading capacity. This results in rheological behavior characterized by high viscosity, high elasticity, and a yield point at a critical strain. Steric force (i.e. V_{steric}) provides an alternative route for controlling colloidal particle behavior. Generally, polymeric or low molecular weight organic surfactants are utilized as steric force control agents. For effective steric repulsion, the adsorbed layers must possess sufficient thickness and density to overcome the van der Waals attraction between particles and prevent bridging flocculation. These species should be securely anchored to the particle surfaces to prevent desorption during particle collisions.

Based on the colloidal particle interactions, the rheological properties of printable inks should be tailored for specific printing processes. Various printing techniques such as screen, stencil, spray, 3-dimentional (3D), inkjet, electrohydrodynamic jet, and pen writing are available. Depending on the application fields and the configuration of the printed batteries, an appropriate printing technique is chosen based on factors such as throughput, feature size, thickness, and substrate characteristics. These printing techniques require distinct ink characteristics, including viscosity, viscoelasticity, and fluidic properties (Fig. 18c). Viscosity is a key parameter in characterizing the fluidic properties of inks. Fluids can be categorized into Newtonian and non-Newtonian (shear-thinning and shear-thickening) fluids based on how their viscosity changes with shear stress (Fig. 18d). In addition, viscoelastic properties are essential for preserving the structure after printing (Fig. 18e). For example, inks with high viscosity, utilized in 3D or screen/stencil printing, should behave like liquids during printing (i.e., under high shear stress). In contrast, these inks should behave like solids immediately after printing (i.e., under low shear stress) to maintain their shape without structural collapse.

7.2.1.2. Mask-based printing. Mask-based printing techniques, including screen printing, stencil, spray, and flexography, are cost-effective and enable high-throughput manufacturing. These methods are commercially viable and compatible with various inks exhibiting different rheological properties. However, the necessity for pre-patterned masks limits form factor diversity and impedes monolithic integration with other devices.

7.2.1.2.1. Stencil/screen printing. Stencil and screen-printing techniques utilize a pre-cut stencil or woven-mesh screen to transfer ink through open areas onto a substrate. These methods are simple, cost-effective, and well-suited for large, bold designs but lack the precision required for detailed work and are constrained by the stencil design. These techniques can produce relatively thick printed features approximately tens of micrometers utilizing highly viscous inks (10^4–10^6 cP). As a typical example, Kim et al. developed stencil-printed flexible lithium-ion batteries (LIB) that are easily fabricated via solvent-drying-free, ultraviolet (UV)-curing-assisted printing processes [288]. The stencil-printable, highly viscous electrode/electrolyte inks exhibited shear-thinning and thixotropic behavior, making them suitable for stencil printing processes. Furthermore, the inks contained sebaconitrile-based UV-curable solid-state gel polymer electrolyte as a drying-free solvent, facilitating the easy and straightforward fabrication of the printed LIBs (Fig. 18f).

7.2.1.3. Spray printing. Spray printing deposits micro- or nano-sized ink droplets onto a substrate via pre-patterned masks utilizing a carrying gas, typically air. This technique allows for the printing of thin layers, usually less than a few micrometers in thickness, over large areas. However, precise control over droplet size and continuous drying is required. Spray printing necessitates very low viscosity inks (< 10 cP), which are highly dispersive and quick-drying to prevent nozzle clogging and ensure stable ink deposition. Singh et al. reported a prototype of spray-printed LIBs composed of single-walled carbon nanotube (SWNT) cathode current collector, $LiCoO_2$ (LCO) cathode, Kynaflex-based separator, $Li_4Ti_5O_{12}$ (LTO) anode, and Cu anode current collector (Fig. 18g) [289]. The spray-printed LIBs were successfully integrated with various devices, such as photovoltaic cells and light-emitting diodes. In the early stage of printed battery research, several spray-printed batteries were reported. Unfortunately, owing to the difficulty in increasing the areal mass loading, spray printing is primarily employed to fabricate micro- or transparent power sources [294–300].

7.2.1.4. DIW. DIW printing involves the on-demand deposition of ink droplets or filaments, eliminating the need for pre-patterned masks and enabling the fabrication of intricate geometries. DIW printing techniques, often called additive manufacturing, include dispenser, inkjet, electrohydrodynamic (EHD) jet, 3D, and pen writing. A major difference from mask-based printing techniques is that DIW techniques deposit ink directly onto the target point through a nozzle. To achieve high printing precision, these techniques generally utilize micro-sized nozzles, which complicate the design of printable inks to prevent nozzle clogging.

7.2.1.5. 3D printing. 3D printing, also known as additive manufacturing (AM), is an innovative technology that utilizes digital programming to design and create complex patterns and structures with high precision. This method constructs 3D objects layer by layer utilizing materials such as light-cured monomers, heat-melted filaments, or laser-sintered powders. Among these methods, mechanical shear-ink printing is particularly favorable owing to its material diversity and ease of fabrication. 3D printing can achieve high-precision printing resolutions (approximately tens of micrometers) and produce layers with thicknesses exceeding a millimeter. For successful 3D printing, the inks must have high viscosity (10^4–10^6 cP) and viscoelastic properties to retain their quality after extrusion through the nozzle. Recently, 3D printing has garnered significant attention for its ability to increase areal mass loading, leading to advancements in areal energy density. In a pioneering study, Sun et al. demonstrated a 3D-printed LIB composed of a 16-layer $LiFePO_4$ (LFP) cathode and LTO anode with a narrow-printed feature of 30 μm (Fig. 18h) [290]. The utilization of nanosized colloidal particles and precise tuning of rheological properties enabled a stable printing process and efficient electrochemical operation. Despite being published over a decade ago, this study has significantly influenced numerous subsequent research efforts into 3D-printed batteries, as it represents the first successful demonstration of a 3D-printed LIB.

7.2.1.6. Inkjet/EHD jet printing. Inkjet printing is highly preferred in electronics applications because of its fine resolution (tens of micrometers) and compatibility with a diverse range of ink materials. It is ideal for creating thin-film power sources and integrating them with complex-shaped devices. Successful inkjet printing depends on ink properties such as particle size, dispersion stability, fluid characteristics (viscosity, density, surface tension, and rheology), and ink-substrate affinity. To avoid unwanted ink dripping or issues with droplet formation, optimal inks should have an inverse Ohnesorge number (Z) between 1 and 10 [301]. This is typically achieved with inks having low viscosity (1–25 cP), low surface tension (25–50 $mN \cdot m^{-1}$), and Newtonian behavior. Choudhury et al. reported a fully inkjet-printed zinc (Zn)-MnO_2 battery on a paper substrate (Fig. 18i) [291]. All component inks, including those for the current collector, curing agent, anode, and cathode, were designed to exhibit Z values ranging from 5.26 to 5.95. This fine-tuning was achieved by adjusting the co-solvent and particle concentration, ensuring optimal inkjet printing performance.

Recently, EHD jet printing has emerged as a high-fidelity printing technique capable of achieving submicrometer-scale resolutions, which are unattainable with conventional inkjet printing. Unlike inkjet printing, which pushes ink through the nozzle, EHD jet printing utilizes an electric field between the nozzle and substrate to pull the ink. In a representative study, Lee et al. successfully demonstrated EHD-printed microsupercapacitors (MSCs) utilizing highly dispersed carbon electrode inks and solid-state gel electrolyte precursors (Fig. 18j) [292]. Owing to the advantages of the EHD printing technique, the printed features exhibited the finest size (electrode width = 10 μm) among previously reported printed MSCs.

7.2.1.7. Pen writing. As an alternative to DIW techniques, pen writing offers a straightforward, rapid, and highly cost-effective approach to fabricating printable batteries. Various types of pens, such as ballpoint pens, fountain pens, and brush pens, can deposit ink materials onto substrates by applying pressure to the pen, causing the ink to flow through the tip. In the case of pencils, graphite is transferred from the pencil lead to the substrate, commonly adopted as a simple method for fabricating graphite electrodes. Choi et al. demonstrated fully hand-drawn Zn-air batteries on an A4 paper substrate, which comprised pen-drawn silver current collectors, pen-drawn Zn anodes, pencil-drawn air cathodes, and pen-drawn gel electrolytes (Fig. 18k) [293]. The pen-writable Zn anode ink exhibited an apparent viscosity of 10 cP, ensuring stable flowability without leaking, skipping, or clogging.

7.3. Materials for printable component inks

One of the most significant advantages of printing techniques is their material diversity, which allows for the application of various materials in printed batteries utilizing diverse electrochemical systems such as lithium-ion, lithium-sulfur, Na-ion, Zn-ion, and supercapacitors. This section reviews printable materials for ink design according to their respective electrochemical systems and material characteristics.

7.3.1. Printed electrodes

Printable electrodes are a key component determining the electrochemical performance of batteries. For optimal printable electrodes, the inks should be rationally designed to meet the requirements of the printing technique (i.e., printability), as discussed in Section 7.1. In addition, the printed electrode should exhibit reliable electrochemical performance, which can be achieved via several approaches, including introducing advanced active materials, structuring internal topology, and optimizing battery configuration. The most significant design factor for printable electrode inks is ensuring the electron/ion conducting pathways of the electrodes. Dispersing carbon conductive materials (e.g., carbon black, carbon nanotubes), essential for securing the electrical conductivity of electrodes, is crucial for maintaining both electron/ion pathways and printability. This is particularly challenging owing to the strong van der Waals attractive forces between carbon materials, which make them difficult to disperse. Therefore, the design of printable electrode inks must extensively consider various properties to address these challenges.

7.3.1.1. Lithium batteries. Lithium-based electrochemical systems, including Li-ion, Li-metal, Li-S, and Li-air, have been prevalently utilized in printed batteries because of their high energy density. Therefore, 3D-printed lithium batteries have been widely studied to demonstrate ultra-high areal energy density, owing to their ability to fabricate high aspect ratio electrodes. Wei et al. presented all-3D printed Li-ion batteries comprising printable LFP cathodes, LTO anodes, UV-curable gel electrolytes, and packaging inks [302]. To ensure the electrical conductivity and colloidal stability of the printable electrode inks, they controlled the colloidal interactions by varying the composition ratios of attractive conductive carbon and repulsive silica particles (Fig. 19a and b).

Cellulose nanofibers (CNFs) are highly suitable for 3D printing owing to their unique viscoelastic properties, surfactant effect driven by hydroxyl groups, and high Young's modulus (approximately 145–150 GPa) [315]. These characteristics facilitate the stable structural integrity of 3D-printed CNF/LFP electrodes after thermal carbonization, providing a robust scaffold for lithium-metal batteries (Fig. 19c) [303]. The carbonized CNF scaffold allowed stable electrochemical operation without any conductive additives because of its high electrical conductivity.

Recently, 2-dimensional (2D) materials have attracted significant attention because of their unique morphological features and chemical structures. The self-assembly of 2D materials significantly contributes to the formation of long-range electron and ion transport pathways within electrodes. Graphene and its derivatives have been extensively studied as fundamental components for

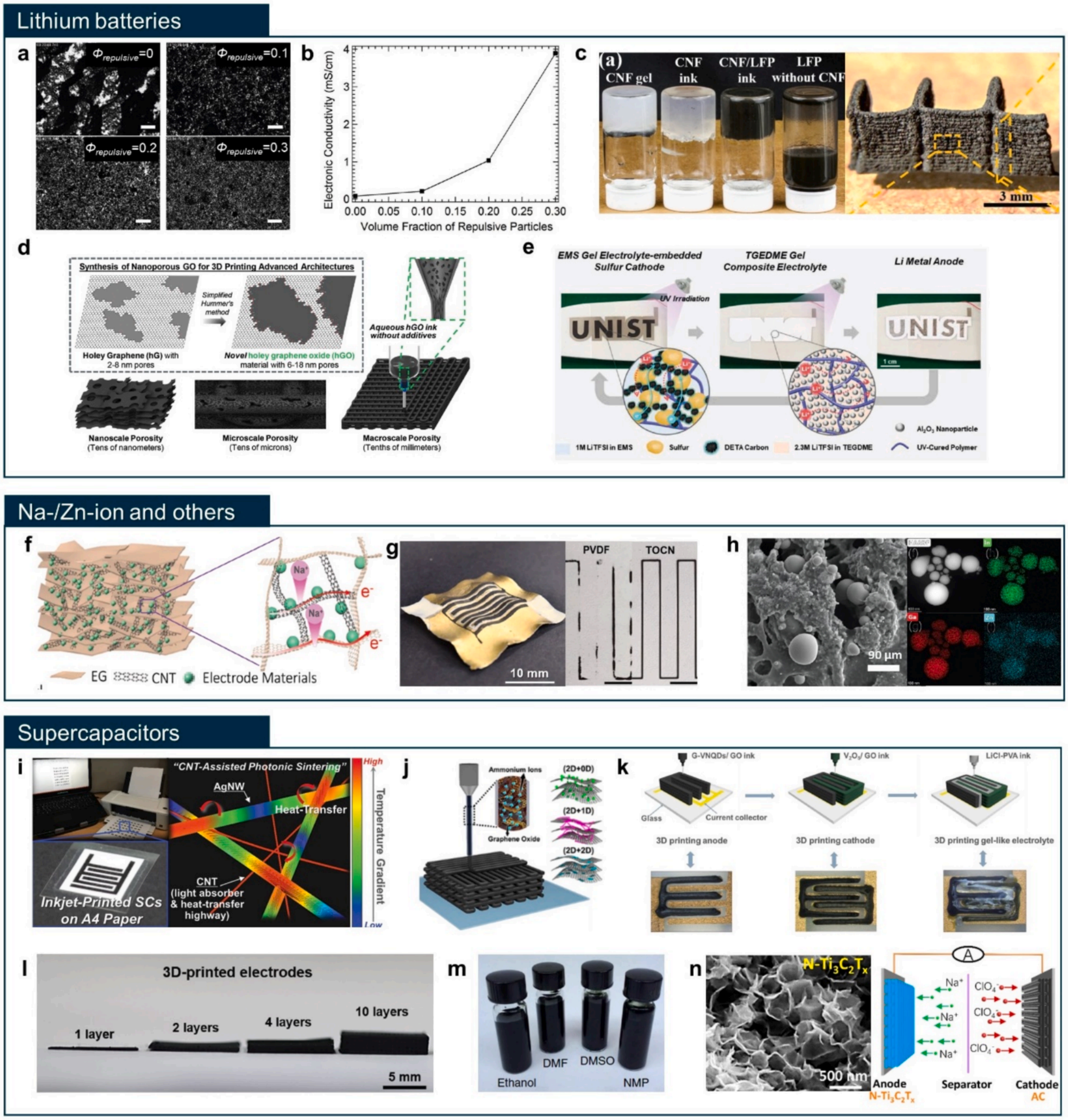

Fig. 19. a) optical microscopy images of biphasic mixtures of attractive conductive carbon particles and repulsive PVP-stabilized SiO_2 particles (1.5 vol% in water–glycerol solution). b) Electronic conductivity as a function of repulsive particle content. Reproduced from Ref. [302] with permission from Wiley-VCH GmbH, Copyright 2018. c) Photographs showing CNF-based 3D printable inks and 3D-printed carbonized CNF/LFP electrodes with 18 layers. Reproduced from Ref. [303]. with permission from Wiley-VCH GmbH, Copyright 2019. d) Schematic representation of hGO synthesize process as well as 3D printable hGO ink for extruding complex 3D architectures with hierarchical porosity. Reproduced from Ref. [304] with permission from Wiley-VCH GmbH, Copyright 2018. e) Schematic of the printed all-solid-state lithium-sulfur batteries through UV-curing-assisted stepwise printing process. Reproduced from Ref. [305] with permission from Wiley-VCH GmbH, Copyright 2019. f) The hierarchical conductive network structure of the 3D-printed SIB electrodes on conductive EG nanosheets and CNT. Reproduced from Ref. [306] with permission from Wiley-VCH GmbH, Copyright 2022. g) (left) A photograph of the nonplanar 3D-printed conformal ZIBs on the non-developable curvilinear substrate with a curvature radius of 4 mm. (right) Photographs of the TOCN-based and PVDF-based MnO_2 cathode. Reproduced from Ref. [307] with permission from Wiley-VCH GmbH, Copyright 2023. h) (left) Scanning electron microscopy (SEM) image and (right) EELS elemental mapping result of the EGaIn nanoparticles with electrochemically deposited Zn. Reproduced from Ref. [308] with permission from Wiley-VCH GmbH, Copyright 2023. i) (left) A photograph of the inkjet-printed SC using desktop inkjet printer and (right) schematic illustration depicting the CNT-assisted photonic sintering. Reproduced from Ref. [309] with permission from Royal Chemistry Society, Copyright 2016. j) Schematic illustration of 3D printing of graphene-based mixed-dimensional materials. Reproduced from Ref. [310] with permission from American Chemical Society, Copyright 2018. k) Schematic representation of 3D printing an asymmetric MSCs composed of V_2O_5 for cathodes and G-VNQDs for anodes. Reproduced from Ref. [311] with permission from Wiley-VCH GmbH, Copyright 2018. l) A photograph showing the thickness of the 3D-printed supercapacitor electrodes as a

function of printed layers. Reproduced from Ref. [312] with permission from Wiley-VCH GmbH, Copyright 2019. m) A photograph of the MXene ink with various organic solvents. Reproduced from Ref. [313] with permission from Nature Publishing Group, Copyright 2019. n) (left) A SEM image of 3D-printed N-$Ti_3C_2T_x$ electrodes featuring abundant open pores, and (right) Schematic representation showing charging process of the n-$Ti_3C_2T_x$ // activated carbon hybrid capacitor. Reproduced from Ref. [314] with permission from American Chemical Society, Copyright 2020.

constructing printed electrodes with macro- and microscopic 3D porous structures [310,316,317]. Graphene oxide (GO), in particular, offers beneficial properties for designing 3D printable electrode inks. The numerous oxygen-containing functional groups on the GO surface enable high dispersion in aqueous solutions. Furthermore, GO can achieve high electrical conductivity after reduction (i.e., reduced-GO). Lacey et al. introduced holey graphene oxide (hGO) as a hierarchically porous cathode for Li-O_2 batteries utilizing 3D printing (Fig. 19d) [304]. The trimodal porosity—nanoscale (4–25 nm on hGO sheets), microscale (tens of micrometer-sized pores introduced by freeze-drying), and macroscale (<500 μm square pores of the mesh design by 3D printing)—enables full active-site utilization of the air electrodes.

Electrolyte-embedded printable composite electrodes present a fascinating alternative by incorporating a liquid-state electrolyte precursor as the dispersion solvent for electrode inks. This approach ensures that the electrolyte-containing electrodes remain free from structural collapse and component migration issues during the drying process. Kim et al. and their colleagues have reported a series of electrolyte-embedded printable electrodes, demonstrating their versatility across various electrochemical systems. For instance, printable LIB electrodes have been successfully produced via the stencil printing technique. These electrodes comprise electrode powders (e.g., LCO or LTO and a conductive agent) and a UV-curable solid-state gel electrolyte precursor ink (composed of lithium salt and carbonate/nitrile solvent with acrylate monomers) [288,318]. This type of printable electrode has also been successfully utilized to demonstrate a printed Li-S battery [305]. Two thermodynamically immiscible and nonflammable gel electrolytes, derived from ethyl methyl sulfone and tetraethylene glycol dimethyl ether, were employed to address longstanding concerns related to the polysulfide shuttle effect (Fig. 19d).

7.3.1.2. Sodium-/zinc batteries. While lithium batteries offer several advantages, they also have significant drawbacks, such as high material costs and safety concerns, leading to increased interest in post-lithium battery systems. Sodium-ion batteries (SIBs) have attracted considerable attention recently owing to their abundant sodium resources, lower cost, smaller solvation shell, and operational principles similar to those of lithium-ion batteries. However, Na^+ ions (1.02 Å) are larger than Li^+ ions (0.76 Å), leading to phase instability in the electrode active materials during electrochemical reactions. Moreover, sodium is heavier than lithium (23 g mol^{-1} vs. 6.9 g mol^{-1}) and has a higher standard electrode potential (−2.71 V vs. SHE compared to −3.02 V vs. SHE for lithium), which results in a lower energy density for sodium-ion batteries compared to lithium-ion batteries [319–321]. To address these challenges, much research has focused on increasing the energy density and material stability of active materials. Recently, 3D-printed SIBs have been demonstrated with 3D interconnected conductive thick microelectrodes, achieving ultrahigh areal capacity and enhanced rate capability [306]. The 3D-printed SIB electrodes, featuring adjustable viscosity and superior rheological properties, were composed of well-dispersed high-capacity $Na_3V_2(PO_4)_2O_2F$ or high-rate carbon-coated $NaTi_2(PO_4)_3$, along with highly conductive additives such as 2D electrochemically exfoliated graphene (EG) nanosheets and 1D carbon nanotubes (CNTs) (Fig. 19f).

Zn-ion batteries (ZIBs) have recently garnered significant attention owing to the abundance of zinc, which provides a high theoretical capacity (820 mAh g^{-1}_{Zn}) and cost-competitive cell fabrication [322,323]. Notably, utilizing aqueous electrolytes ensures excellent safety compared to organic electrolytes, making ZIBs suitable for human-oriented applications such as wearable devices and implantable electronics. Furthermore, aqueous electrolytes are advantageous for various printing techniques because they do not require a dehumidified environment (i.e., dry room). Recently, Ahn et al. reported on-demand conformal (ZIB) on non-developable surfaces utilizing DIW-based nonplanar 3D printing (Fig. 19g) [307]. The manganese dioxide (MnO_2) cathodes consisted of α-MnO_2 nanorod active particles, carbon black (CB)/multi-walled carbon nanotube (MWNT) conductive additives, and Tempo-oxidized cellulose nanofiber (TOCN) as an anionic 1D binder. The TOCN binder effectively enhanced dispersion state via non-covalent hydrophobic attraction and interparticle electrostatic repulsion. Zn particles were combined with activated carbon (AC) for the anodes to improve Zn plating/stripping cyclability because of their highly developed micropores. The rationally designed ZIB component inks enable geometrical matching of the printed batteries with arbitrary curvilinear substrates without experiencing deformation strain.

Liquid metal is another fascinating candidate for fabricating printable electrodes owing to its liquid state, which ensures high printability and electrical conductivity comparable to conventional metals. Recently, eutectic gallium-indium (EGaIn) has been introduced as a structuring agent for Zn anodes in ZIBs, leveraging the unique physical properties of liquid metal, such as extremely high surface tension and high electrical conductivity [324]. A 3D-printed polyacrylamide-hemicellulose/EGaIn microdroplet hydrogel was developed as a self-standing scaffold [308]. This EGaIn-based hydrogel acted as an electrically and ionically conductive microporous matrix, enabling isotropic deposition of Zn^{2+} to form a stable anode host capable of stress dissipation (Fig. 19h). It was confirmed that the EGaIn-based hydrogel exhibits a double-covalent hydrogen-bonding system with self-healing and shear-thinning behavior, which is crucially advantageous for preventing liquid metal loss and facilitating 3D printing processes.

7.3.1.3. Supercapacitors. Supercapacitors are the most widely adopted electrochemical systems in printable power sources owing to their ease of fabrication, material versatility, long cycle life, and fast charging/discharging rates. Previous studies have employed various printing techniques for printable supercapacitors, including stencil [325], spray [326,327], inkjet [309,328,329], EHD jet [292], dispenser [330], 3D [331–335], and stamping [336]. Inkjet printing is one of the most frequently utilized methods to fabricate the printed supercapacitors owing to its capability for monolithic integration with inkjet-printed electronics. Choi et al. successfully integrated inkjet-printed supercapacitors onto A4 paper coated with a CNF nanomat-based primer to achieve high printing resolution [309]. To enhance electrical conductivity, the printed electrodes, composed of SWNT and AC, also functioned as a sintering agent for silver nanowires, in which the SWNT are exploited as UV light absorbers and hear-transfer pathways.

Although supercapacitors are attractive electrochemical systems for printable power sources, they have conventionally suffered from low energy density. To address this issue, many studies have focused on 3D-printed supercapacitors with thick electrodes to increase their areal energy density [331–335]. Tang et al. demonstrated the 3D printing of graphene-based aerogels for supercapacitors, achieving various arbitrary predesigned architectures and out-of-plane patterns on curved surfaces via mixed-dimensional materials (e.g., 0D quantum dots, 1D nanowires/nanorods, 2D boron nitrides, carbon nitrides, and transition-metal carbide nanosheets) (Fig. 19j) [310]. Furthermore, 3D-printed quasi–solid-state asymmetric MSCs with a high areal energy density of 73.9 μWh cm^{-2} were demonstrated (Fig. 19k). They utilized vanadium pentoxide (V_2O_5) for the cathode and graphene-vanadium nitride quantum dots (G-VNQDs) with highly concentrated GO-based anode inks, achieving electrode thicknesses exceeding 400 μm [311]. To achieve extremely high energy density, Gao et al. presented supercapacitor electrodes with a woodpile configuration, achieving an ultrahigh thickness of 3D-printed electrodes [312]. Their ten-layer printed electrodes exhibited a thickness of 2220 μm, resulting in an areal capacitance of 4.56F cm^{-2} and an areal energy density of 0.63 mWh cm^{-2}.

MXene has recently garnered significant attention as a high-capacitance material. The most extensively researched MXene, titanium carbide ($Ti_3C_2T_x$, with T_x representing the functional groups that terminate the structure), boasts a high electronic conductivity of up to approximately 10,000 S cm^{-1} and a surface chemistry similar to TiO_2, exhibiting extremely high volumetric capacitance (~1500F cm^{-3}). Zhang et al. demonstrated two types of MXene ink for both inkjet and dispenser printing to fabricate MSCs [313]. The negative surface charge on the hydrophilic $Ti_3C_2T_x$ nanosheets enabled a stable dispersion state in both aqueous and organic inks without adding surfactants or polymer stabilizers (Fig. 19m). Owing to the surface moieties of the MXene, a nitrogen-doped $Ti_3C_2T_x$ (N-$Ti_3C_2T_x$) was synthesized for the anode of sodium-ion hybrid capacitors (Fig. 19n) [314]. The 3D-printed N-$Ti_3C_2T_x$ electrodes feature abundant open and hierarchical pores, facilitating ion/electrolyte transport and accommodating volume changes during cycling. As a result, the 3D-printed hybrid capacitors exhibited high areal mass loading up to 15.2 mg cm^{-2} and areal energy density of 1.18 mWh cm^{-2}.

7.3.1.4. *Electrolyte or separator.*

Another key component of printed batteries is the printable electrolyte, which plays a crucial role in the design and flexibility of the resulting devices. Despite their important role as a medium for electrochemical reactions, electrolytes have not advanced as much as electrodes in the development of printed batteries [282,285]. Due to their fluid nature, conventional liquid electrolytes necessitate rigid and bulky packaging, which significantly hinders the shape diversity, safety, and miniaturization of printed batteries. Given these limitations, the focus has shifted to solid-state electrolytes, which can be classified into organic and inorganic categories. Each type of solid-state electrolyte has its own physical and electrochemical characteristics that affect the fabrication processes and battery performance.

7.3.1.5. *Inorganic solid-state electrolyte.*

Owing to their inherent single-ion conducting properties and the improvements in their ionic conductivity, solid inorganic electrolytes, especially those based on sulfides and oxides, have garnered substantial research interest [337,338]. However, severe interfacial issues and the necessity for harsh post-treatments (e.g., thermal sintering or mechanical pressing) pose hurdles in demonstrating printable solid-state electrolytes. Poor contact between the electrodes and electrolytes also results in increased internal cell resistance. To address this issue, McOwen et al. demonstrated the 3D-printed electrolyte comprising $Li_7La_3Zr_2O_{12}$ (LLZ) to enlarge contact area between the Li-metal electrodes and the electrolytes [339]. Based on the physical properties of binder materials, two types of printable LLZ inks were designed: self-supporting and conformal ink (Fig. 20a), which were utilized according to the final shape of the printed electrolytes. Hence, Li-metal symmetric cells with the 3D-printed LLZ electrolyte exhibited dramatically lower full-cell resistance and higher energy density (Fig. 20b and c).

One of the major drawbacks of oxide solid-state electrolytes is that the harsh sintering conditions (500–1100 °C) required to ensure moderate ionic conductivity result in severe lithium loss [348]. To address this issue, Ping et al. presented a printing and radiative heating fabrication method that allowed for the thin-film deposition and quick sintering of $Li_{6.5}La_3Zr_{1.5}Ta_{0.5}O_{12}$ solid-state electrolytes (Fig. 20d and e) [340]. The printed garnet electrolyte film exhibited a high Li ionic conductivity up to 10^{-3} S cm^{-1}, which is comparable to that of garnet bulk electrolyte.

Sulfide solid-state electrolytes are an attractive candidate for printable electrolytes owing to their high ionic conductivity (10^{2}–10^{3} S cm^{-1}) and ease of solution processability. Several studies have successfully demonstrated solution-processable sulfide solid-state electrolytes utilizing various fabrication techniques, highlighting their potential as printable electrolyte materials (Fig. 20f) [341,349].

7.3.1.6. *Organic solid-state electrolyte.*

Organic material-based solid-state electrolytes offer several advantages over inorganic ones, including ease of processability, mechanical flexibility, and intimate interfacial contact with electrodes. Generally, printable organic solid-state electrolytes comprise an ion-conducting medium (e.g., liquid electrolyte or polar polymer with salts) and a mechanical skeleton (e.g., polymer matrix or ceramic filler) mixed with a dispersing solvent. Typically, the printed electrolytes undergo a drying process to remove the dispersing solvent [282,285]. However, this drying process can induce unwanted shrinkage, resulting in structural disruption.

UV-assisted in-situ solidification of electrolyte inks is a facile method for developing scalable printable solid-state electrolytes without needing solvent drying (Fig. 20g). Various UV-curable printed solid-state electrolytes have been demonstrated to exhibit moderate ionic conductivity and excellent electrochemical performance. These electrolytes utilize a wide range of materials, such as

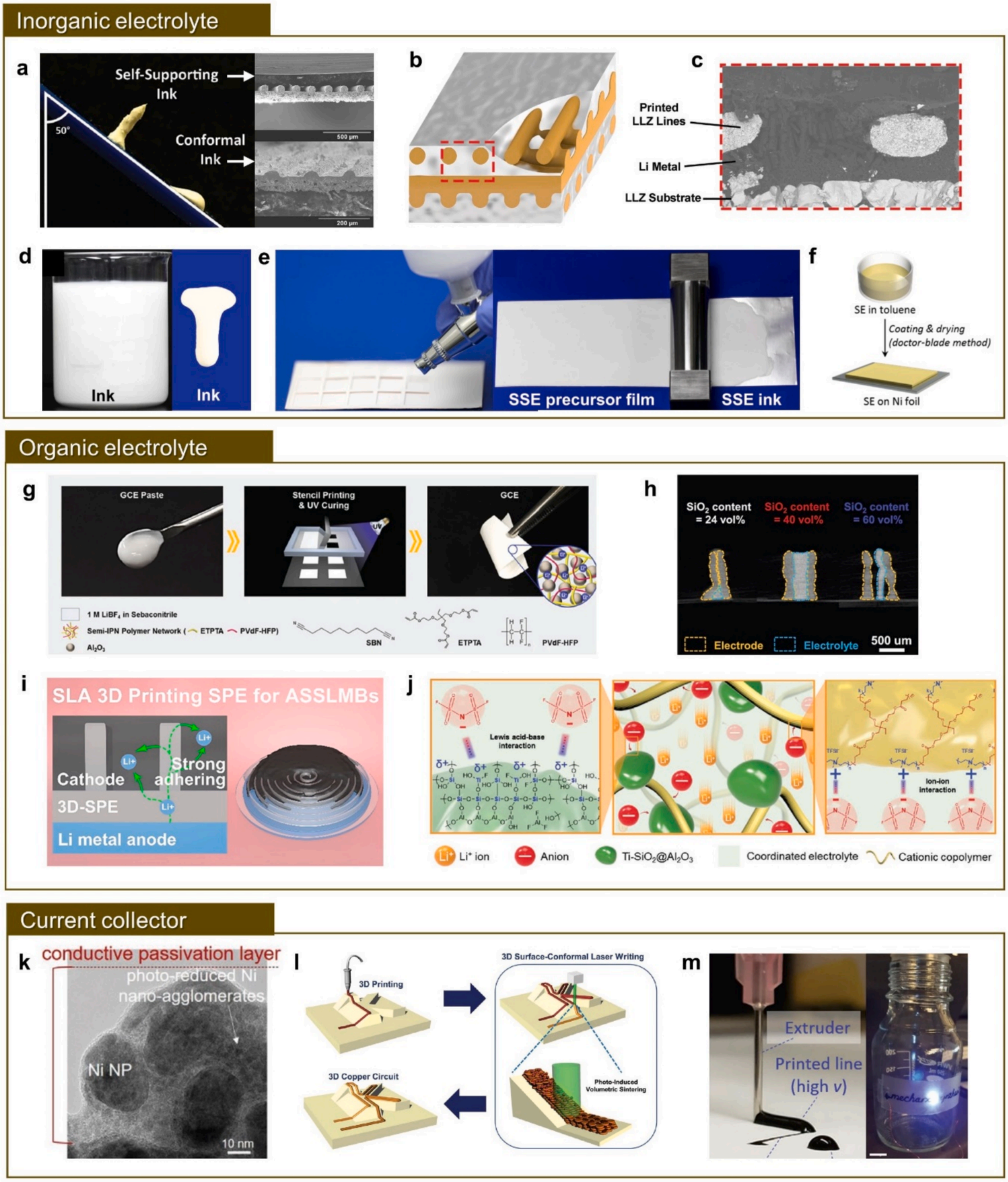

Fig. 20. a) A photograph of two-type of 3D-printable LLZ electrolyte ink deposited onto a tilted substrate. b) Schematic of Li-filled pores between 3D-printed LLZ grid in a stacked-array pattern on LLZ substrate. c) Cross-sectional SEM image of 3D-printed LLZ//Li metal interfaces. Reproduced from Ref. [339] with permission from Wiley-VCH GmbH, Copyright 2018. d) Photographs showing (d) appearance and e) printing processes of printable LLZTO solid-state electrolyte inks. Reproduced from Ref. [340] with permission from American Association for the Advancement of Science, Copyright 2020. f) Schematic representation of solution-processible sulfide solid-state electrolyte. Reproduced from Ref. [341] with permission from Wiley-VCH GmbH, Copyright 2018. g) Schematic of the procedure used to fabricate the stencil-printed solid-state electrolyte using UV-assisted in-situ solidification. Reproduced from Ref. [288] with permission from Royal Society of Chemistry, Copyright 2018. h) Micro-computed tomography (Micro-CT) image of UV-curable 3D-printed solid-state electrolyte infiltrated into interstitial voids between the 3D-printed adjacent electrode layers. Reproduced from Ref. [342] with permission from Wiley-VCH GmbH, Copyright 2022. i) Schematic representation of SLA 3D-printed solid polymer electrolyte. Reproduced from Ref. [343] with permission from Wiley-VCH GmbH, Copyright 2020. j) Schematics of printable single-ion conducting quasi-solid-state soft electrolyte. Reprinted with permission from [344]. Copyright 2021, Wiley-VCH GmbH. k)

High-resolution transmission electron microscopy (HRTEM) image showing the FLS-based printable Ni current collectors. Reproduced from Ref. [345] with permission from Wiley-VCH GmbH, Copyright 2020. l) Schematic showing the 3D printing and FLS process of 3D printable Cu circuit. Reproduced from Ref. [346] with permission from Wiley-VCH GmbH, Copyright 2020. m) Photographs showing the printing process and printed electric circuit using substrate-versatile CNT ink. Reproduced from Ref. [347] with permission from Wiley-VCH GmbH, Copyright 2021.

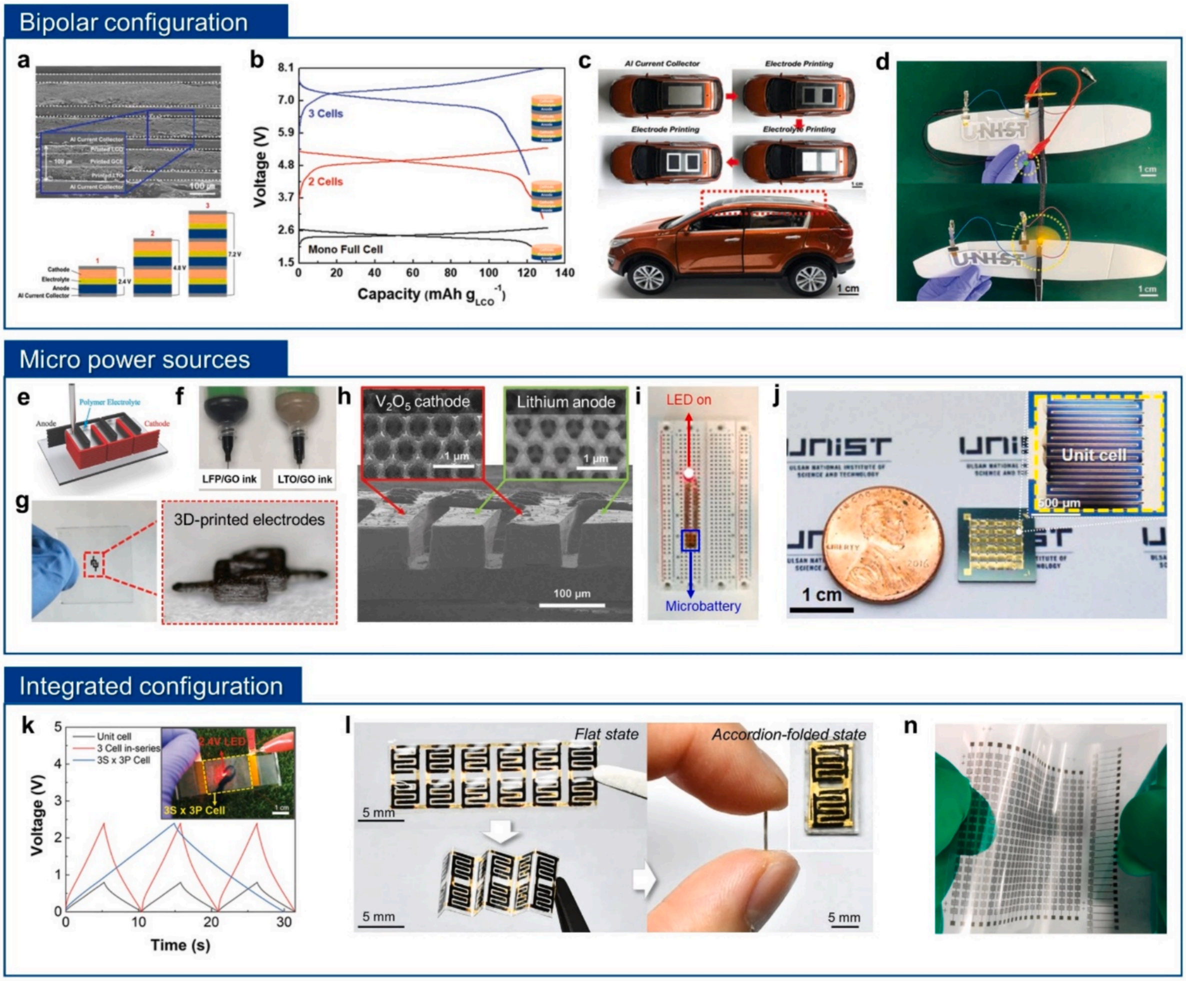

Fig. 21. Shape-versatile power sources. a) Cross-sectional SEM image of the printed bipolar cells, where three cells were connected in series, along with a schematic illustrating their structure. The Al foil is a common current collector shared between the LTO anode and LCO cathode. b) The charge/discharge profiles of the printed bipolar cells connected in series as a function of cell number (under charge/discharge current density of 0.1C/0.1C). c) Sequential photographs depicting the stepwise fabrication of the printed bipolar two-stacked cell on the curved roof of a miniature toy car. Reproduced from Ref. [288] with permission from The Royal Society of Chemistry, Copyright 2018. d) Bipolar ASSLSB in the shape of 'UNIST' letters (two cells connected in series) directly fabricated on a toy aircraft's surface. Photographs demonstrating the operation (LED and propeller) of the printed bipolar ASSLSB in the toy craft. Reproduced from Ref. [305] with permission from Wiley-VCH GmbH, Copyright 2019. e) Schematic of 3D-printed interdigitated micro-LIBs. f) Photograph of LFP/GO and LTO/GO inks in syringes. g) Digital images of micro-scale 3D-printed electrodes. Reproduced from Ref. [316] with permission from Wiley-VCH GmbH, Copyright 2016. h) Cross-section SEM image of the interdigitated electrodes, alternatively electroplated V_2O_5 cathode and lithium metal anode for Li-ion micro-batteries. i) Red micro-LED powered by a packaged cell. Reproduced from Ref. [353] with permission from Wiley-VCH GmbH, Copyright 2021. j) Photographs of on-chip UHD SS–MSCs (36 unit cells in series) with an area of 8.0 × 8.2 mm, smaller than a coin. Inset: optical microscopy image of a unit cell in the UHD SS–MSCs. Reproduced from Ref. [292] with permission from American Association for the Advancement of Science, Copyright 2020. k) GCD profiles of TNP-MSC configured with nine unit cells connected in series (3S) and in parallel (3P) in a combined 3S × 3P arrangement. The inset depicts a photograph of a micro-LED powered by the MSC. Reproduced from Ref. [299] with permission from Wiley-VCH GmbH, Copyright 2022. l) Photographs of the accordion-foldable MSC and the compact arrangement of its constituent cells. Reproduced from Ref. [330] with permission from Wiley-VCH GmbH, Copyright 2023. m) Photograph of flexible M−MIMSCs containing 400 cells. Reproduced from Ref. [354] with permission from Oxford University Press, Copyright 2023.

carbonate-, ether-, or nitrile-based liquid electrolytes as the ion-conducting medium, tri-acrylate UV-curable monomers, and linear polymers as the mechanical skeleton, and ceramic fillers as rheology modifiers [288,305,341,350,351]. Because of the ease of the solidification process and material versatility, UV-curable solid-state electrolytes are beneficial for fabricating 3D-printed solid-state batteries [302,307,352]. Lee et al. presented ionic liquid-based UV-curable 3D-printed solid-state electrolytes that enable dense infiltration into interstitial voids between the 3D-printed adjacent electrode layers [342]. The click-cross-linkable thiol-ene monomers quickly solidified the electrolyte inks after UV irradiation, which exhibited stable mechanical integrity without any collapse or unwanted void (Fig. 20h).

The material versatility of printable organic solid-state electrolytes can also be leveraged to enhance electrochemical performance. He et al. demonstrated stereolithography 3D-printing of a solid polymer electrolyte composed of lithium salt, succinonitrile, and poly (ethylene glycol) diacrylate [343]. The 3D-structured solid-state electrolyte successfully increased the contact area between the electrode and electrolyte, which reinforced interfacial adhesion, improved the mass loading of active materials, and enhanced mechanical strength (Fig. 20i). Furthermore, introducing single-ion conductive materials to printed solid-state electrolytes plays a crucial role in stabilizing the interfaces with electrodes. Recently, Oh et al. demonstrated a single-ion conducting quasi-solid-state soft electrolyte by utilizing a cationic copolymer-based ion-rectifying polymer and anion-trapping titanium/silica-modified alumina nanoparticles as the mechanical skeleton and rheology tuning agent, respectively (Fig. 20j) [344]. The single-ion conducting capability of the quasi-solid-state electrolyte enabled stabilizing the surface of the Li metal anode and $LiNi_{0.8}Co_{0.1}Mn_{0.1}O_2$ cathode, thereby prolonging the cyclability of the printed solid-state lithium metal batteries.

7.3.1.7. Current collector. To realize an all-printed battery, one of the key printable components is the current collector. However, there has been relatively little research on printable current collectors compared to other components. Metal foil is commonly utilized as a current collector in conventional bulk-type batteries, but it severely limits design diversity when utilized in printed batteries. Although metal particles-based printable inks are an alternative candidate to demonstrate printed current collector, common metal species for the current collector, such as aluminum (Al) and copper (Cu), tend to be easily oxidated, and they require harsh post-treatment processes, including thermal sintering or chemical reduction to reduce contact resistance between the metal particles.

To address these issues, printable nickel (Ni) current collectors were recently demonstrated through flash-light sintering (FLS) process in a timescale of 10^{-3} s [345]. During the FLS process, the printed particulate layer composed of Ni flakes and Ni nanoparticles was converted into a metallic current collector with an electrochemically robust and conductive surface passivation layer (Fig. 20k). The printed Ni current collector exhibited stable electrochemical operation in printed MSCs with an operating voltage of 3 V. A similar approach was applied to printed Cu circuits, which demonstrated a resistivity of 15 μΩ cm (corresponding to 670 kS m^{-1}) (Fig. 20l) [346], exhibiting potential as an anode current collector for printed batteries.

Carbon nanomaterials are typical alternatives to metal current collectors owing to their high electrical conductivity and good electrochemical stability without requiring additional post-treatments. Owens et al. presented a substrate-versatile printed CNT electric circuit with a conductivity of 10 kS m^{-1} (Fig. 20m) [347]. Owing to the mechanical properties of CNTs, the printed circuit exhibited excellent flexibility, exhibiting less than 3 % change in DC resistance with a bending radius down to 1 mm.

7.4. Applications of printed batteries for device-tailored energy storage solutions

7.4.1. Shape-versatile form factors

As the demand grows across various industries for diverse forms of electronic devices in daily life, shape-versatile batteries are increasingly spotlighted for their ability. Recent research has explored printed solid-state batteries and supercapacitors, which provide superior shape adaptability and aesthetic versatility beyond conventional batteries technologies.

7.4.1.1. Bipolar configuration. Bipolar configurations, utilizing solid-state electrolytes, enable straightforward electrical connections between individual cells in a single package through shared current collectors. Combined with advanced printing techniques, unit cells can be systematically assembled into a stable structure within a limited space. This technique enables the achievement of high voltages and high volumetric energy densities with a customizable cell design.

Kim et al. utilized stencil-printing and UV-light-assisted in situ processes to fabricate solid-state batteries [288]. They applied UV-curing-assisted multi-step printing to produce bipolar-stacked cells, where both stencil-printed anode and cathode shared an Al foil as a current collector. Fig. 21a) presents a cross-sectional SEM image illustrating a sequentially three-stacked bipolar cell featuring the battery components. The charge/discharge profile of series-printed bipolar cells depict a voltage increase from 2.4 to 7.2 V as the number of stacked cells increases (Fig. 21b). This multi-step printing technique enables the sequential printing of parallel bipolar cells on top of a target object (Fig. 21c).

Similarly, printable bipolar all-solid-state Li-S batteries (ASSLSBs) have also been reported [305]. These ASSLSBs, configured in the shape of the letters and comprising two cells connected in series (3.0–5.6 V), are manufactured without solvent drying directly on the surface of a toy aircraft. The printed ASSLSBs successfully powered a light emitting diode (LED) and a propeller integrated with the toy airplane (Fig. 21d).

7.4.1.2. Micro power sources. The rapid advancement of portable and wearable electronics has heightened the demand for lightweight, compact, and integrated microscale power sources. Advanced printing techniques are crucial tools for developing these miniaturized energy devices. They are noted for their efficient space utilization, adaptability for device-specific integration, reliable electrochemical performance, and capability for precise high-resolution electrode design.

3D-printed micro-scale LIBs with an interdigitated configuration of electrodes is a typical example of the micro power sources. (Fig. 21e) [316]. The rheology-tuned LFP/GO cathode and LTO/GO anode inks enable DIW printing (Fig. 21f). A micro-scale LIB was fabricated by injecting poly(vinylidene fluoride)–co-hexafluoropropylene (PVDF-co-HFP)-based solid-state electrolyte between the interdigitated electrodes. This configuration featured uniformly miniaturized electrodes with a high aspect ratio on a glass substrate (Fig. 21g).

Sun et al. proposed a novel 3D-structured battery (Li metal anode/gel electrolyte/V_2O_5 cathode) fabricated via imprint lithography for high-resolution micro-and nanofabrication [353]. Fig. 21h presents a cross-sectional SEM image of interdigitated microelectrodes. The electrodes are approximately 70 μm wide, with gaps of around 20 μm between them, demonstrating a highly precise microstructure. The packaged micro-battery exhibits an energy density of 1.24 J cm^{-2} and a power density of 75.5 mW cm^{-2}, successfully powering a red LED (Fig. 21i).

EHD printing is state- of-the-art technique to fabricate micro power sources owing to its high printing fidelity. Leveraging the high-precision capabilities, MSCs with interdigitated electrodes with a 10-μm resolution were printed onto the chip substrate [292]. To further emphasize the architectural and electrochemical performance of the downsized on-chip MSC, they successfully fabricated 36 unit cells connected in series on a chip with an area of 8.0 mm × 8.2 mm, smaller than a coin (Fig. 21j). The areal number density of the MSC was approximately 60 cells cm^{-2} with an areal operating voltage of 65.9 V cm^{-2}.

7.4.1.3. Integrated configuration. Conventional energy storage devices typically comprise a sandwich-type stacked configuration. However, this structure restricts performance customization within a single substrate for each unit cell. To overcome this challenge, the stepwise printing technique facilitates the construction of multiple cells on a single substrate, enabling easy integration and electrical connection in series or in parallel. This approach enhances either output voltage or capacity, depending on the configuration.

On-demand cell configuration could be easily demonstrated where nine unit cells of MSC were connected in series (3S) and in parallel (3P) to achieve tunable voltages and capacitances within a single transparent body (Fig. 21k) [299]. Via EHD printing, various micro-scale electrode structures were fabricated on a transparent nanocellulose paper with UV-curable mask ink. These structures were integrated with solid-state aqueous gel electrolytes that isolate MSC unit cells ionically, enabling the transparent power sources to maintain high transparency while offering customizable cell configurations.

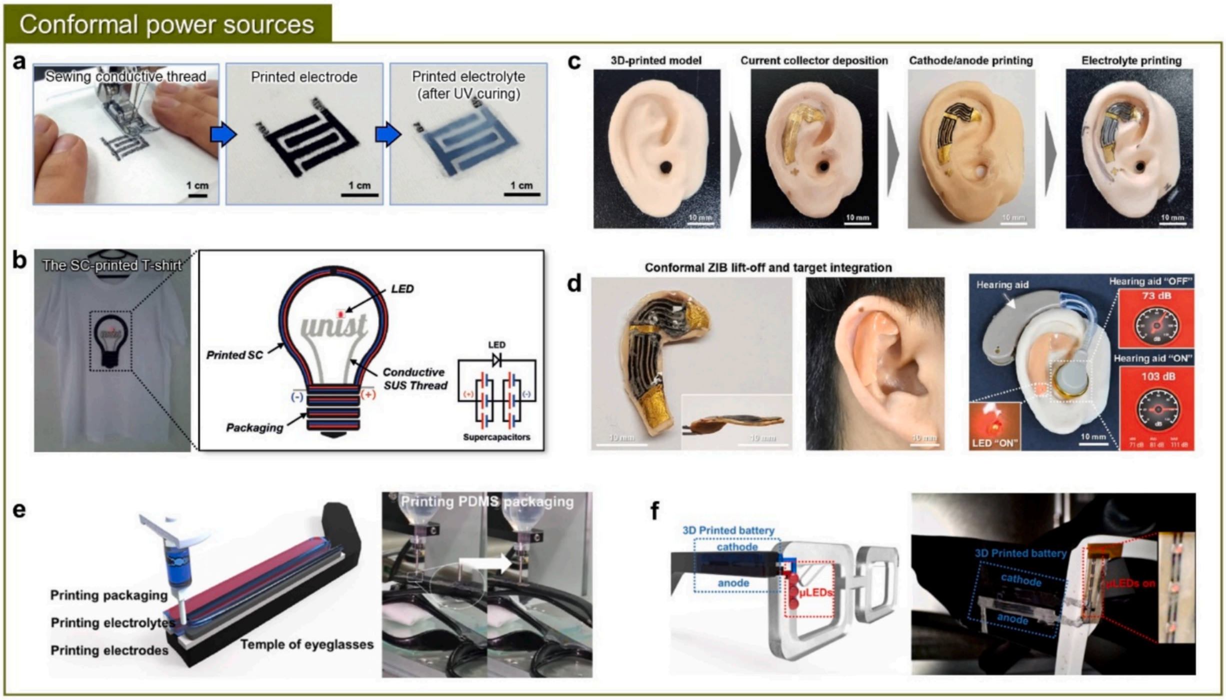

Fig. 22. Conformal power sources. a) Fabrication process of stencil-printed SC on T-shirts. b) Photograph of wearable electronic garments featuring SCs designed as a bulb symbol capable of operating LEDs. Reproduced from Ref. [325] with permission from Wiley-VCH GmbH, Copyright 2018. c) Photographs depicting the sequential fabrication and integration of conformal ZIB with human ear. d) Photograph of ear-shaped conformal ZIB connected to hearing aid connected with an LED, demonstrating successful operation of the LED and amplifier by the conformal ZIB. Reproduced from Ref. [307] with permission from Wiley-VCH GmbH, Copyright 2023. e) Schematic and photo images of a 3D DIW-printed LIB with packaging on an eyeglasses temple. f) Photographs of fabricated conformal printed battery onto 3D eyeglasses, powering connected micro-LEDs. Reproduced from Ref. [355] with permission from Elsevier, Copyright 2023.

Lee et al. employed an accordion folding strategy to compactly integrate on-demand MSCs with a high-fill factor-based cell design [330]. The DIW process of the metallic MoS_2-based inks allows for microscale manufacturing of MSCs with multiple integrated electrodes. This enables on-demand (in series/in parallel) in a footprint of 22.75 mm^2 and a thickness of 0.8 mm. The integrated 12 MSC unit cells achieve a high space utilization and demonstrate an areal capacitance of 180.7 $mF \cdot cm^{-2}$ and an areal energy density of 89.2 $\mu Wh \cdot cm^{-2}$ (Fig. 21l).

Recently, Wang et al. proposed a practical multi-step lithographic patterning and spray printing method for $Ti_3C_2T_x$ MXene-based microelectrodes.[78] They developed a mass production for these micro-electrodes, effectively enhancing the integration level with the high cell density of MXene-MSCs. By connecting 334 cells and precisely 3D printing the polyvinyl alcohol/H_2SO_4 (PVA/H_2SO_4) gel electrolyte, they achieved an extremely high voltage of 200 V in a small area of 3.5 cm × 3.5 cm (Fig. 21m).

7.4.1.4. Target-oriented applications. This chapter presents studies that have implemented specific target-oriented power sources, including conformal power sources, monolithic integration with devices, printed frameworks for Li-metal batteries, and 3D structural electrodes for high-mass loading. Building upon the materials and printing technologies discussed in earlier chapters, we review typical examples of printed batteries that ensure stable operation and enhance the electrochemical performance of flexible and

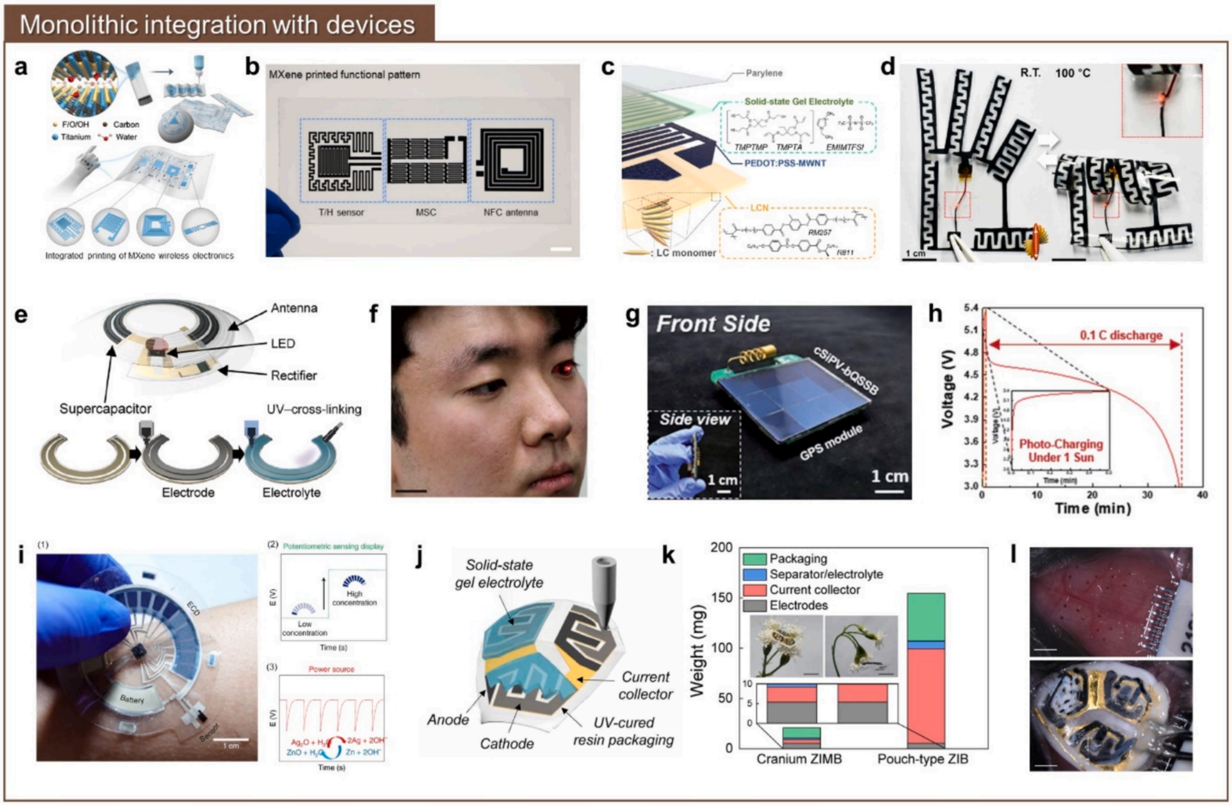

Fig. 23. Monolithic integration with devices. a) A diagram illustrating the direct printing of additive-free MXene aqueous inks at room temperature on diverse substrates, intended for flexible wireless electronics applications including sensors, MSCs, and antennas. b) Multi-functional pattern printed entirely with MXene for integrated electronics enabled with NFC. Reproduced from Ref. [356] with permission from Nature Publishing Group, Copyright 2022. c) Schematic depicting design of soft robot integrated with rechargeable power sources. d) Hand-shaped SL-PS with cells configured in series (3S) and in parallel (2P) at 100 °C autonomously morphing into a soft gripper. Reproduced from Ref. [327] with permission from Elsevier, Copyright 2022. e) Schematic of smart contact lens and DIW-based fabrication process of the monolithically integrated SC with an arc-shaped form factor. f) Photo of a person wearing soft smart contact lenses with operated LEDs. Reproduced from Ref. [357] with permission from American Association for the Advancement of Science, Copyright 2019. g) Photograph of printing-based cSiPV–bQSSB (h) Photo-charge and galvanostatic-discharge profiles of cSiPV–bQSSB with photo-charging from 3.0 to 5.4 V under 1-sun illumination, followed by galvanostatic discharge at a discharge current density of 0.1C. Reproduced from Ref. [358] with permission from The Royal Society of Chemistry, Copyright 2020. i) Photographic image displays the epidermal sweat sensing patch, illustrating instant target concentration readout (i), electrolyte concentration changes and sensor readout (ii), and the intermittent discharge mode of the Ag_2O–Zn battery powering the system (iii). Reproduced from Ref. [359] with permission from Nature Publishing Group, Copyright 2022. j) Schematic of nonplanar 3D printed quasi–solid-state ZIMB for cranium electronics. k) Comparison of the weight between the cranium-customized ZIMB and conventional pouch-type ZIMB. l) Optical stereomicrograph of liquid metal-based neural interface on a mouse cranium (top) and ZIMB integration on the neural interface (bottom). Reproduced from Ref. [291] with permission from American Association for the Advancement of Science, Copyright 2024.

wearable electronic devices tailored to specific applications.

7.4.1.4.1. Conformal power sources. Conventional batteries with rigid components are difficult to integrate seamlessly into wearable electronics. Direct integration into targe devices is most powerful advantages of the printed batteries. Lee et al. fabricated wearable SCs on cotton T-shirts via UV-assisted stencil-printing [325]. They utilized a commercial sewing machine to incorporate electrically conductive stainless steel threads as the current collector into the aesthetically designed structure. Then, electrode active ink (AC, MWNT, and ionic liquid) and ionic liquid-based UV-curable gel electrolytes were printed onto cotton to realize wearable energy storage textiles (Fig. 22a). Furthermore, they fabricated daily electronic garments employing a stencil printing method to create a bulb symbol. The printed SCs exhibit an areal capacitance of 15 $mF{\cdot}cm^{-2}$ and an output voltage of 3 V. They can operate the LEDs in various mechanical deformation modes and even when ironed at 140 °C (Fig. 22b).

Implementing nonplanar printing on arbitrarily curved substrates is challenging because of the gravitational deformation of the printed ink. To address these challenges, Ahn et al. optimized the composition by designing colloidal interactions for conformal printing (described in the section on Sodium-/zinc batteries) [307]. Fig. 22c showed the stepwise fabrication and integration procedure of the conformal ZIB with a human ear. They also emphasized versatile printing technology by monolithic integrating ZIBs with the human ear and then connecting them to LED-equipped hearing aids (Fig. 22d).

Recently, versatile-shaped electronics were successfully integrated within the scalable Li-ion system via the 3D DIW-printing technique, as illustrated in Fig. 22e [355]. The current collectors were printed conformally onto the desired target surface utilizing conductive silver and carbon paste. The rheological optimized LFP cathode and LTO anode inks were stably deposited on the surfaces of versatile-shaped objects, such as 3D eyeglasses. Subsequently, the LIB system was completed by sequentially printing a gel polymer electrolyte and UV-curable polydimethylsiloxane packaging ink, resulting in the successful illumination of micro-LEDs (Fig. 22f). Utilizing printable battery materials with sequential 3D DIW results in fully 3D-printed, shape-versatile batteries with a low device footprint. These conformal power sources offer a practical solution for powering specific applications, featuring flexible aesthetics, competitive electrochemical performance, and adaptable designs.

7.4.1.4.2. Monolithic integration with devices. Printed power sources provide optimal solutions for applications in flexible and wearable electronics, emphasizing mechanical properties and electrochemical performance in multifunctional devices. Combining energy storage systems with electronic devices and energy harvesting can sustainably power electronic devices without relying on external electrical charging.

MXenes ($Ti_3C_2T_x$) have been widely employed in numerous studies as a key material for supercapacitors and electrical circuits, owing to their outstanding electronic conductivity and dispersion stability as described in the section on Supercapacitors. (Fig. 23a) [356]. The printed MXene-based wireless sensors platform (T/H sensor/MSC/NFC antenna) is presented in Fig. 23b). This study incorporated the printed MXene patterns into a flexible printed circuit board containing a microcontroller unit, NFC antenna, and matching network. This integrated system responded to temperature and humidity changes, wirelessly sending the power/data to smartphones for monitoring the microenvironment of plant growth.

Soft electronics are garnering attention for their adaptability in complex environments, however, they encounter challenges such as restricted mobility due to tethered cords and bulky power sources. Recently, printed supercapacitors were monolithically integrated within an untethered soft robot to demonstrate light-triggered, shape-reconfigurable, and locomotive rechargeable power sources [327]. They fabricated supercapacitors utilizing flexible Poly(3,4-ethylenedioxythiophene) polystyrene sulfonate (PEDOT:PSS)/MWNT/solid-state gel electrolyte materials on a liquid crystalline polymer network (LCN) substrate *via* a dispenser printing process (Fig. 23c). The LCN-based soft robot demonstrates autonomous and reversible morphological changes upon exposure to light or heat without compromising the electrochemical performance of the power source. Experimental validation showcases its application as a soft robot, where the hand-shaped device exhibited stable capacitive behavior and reliably powered a red LED even as it autonomously transformed into a soft gripper at 100 °C (Fig. 23d).

As an application for the implantable devices, printed solid-state supercapacitors were monolithically integrated into a soft, smart contact lens with wireless charging. (Fig. 23e) [357]. This precision fine arc-shaped SC was fabricated via a DIW process. The smart contact lens system, including an antenna, rectifier, and LED, was monolithically integrated *via* microfabrication techniques. The printed SCs possess enough energy density to power the LED within the confined 9-mm diameter of the lens (Fig. 23f).

Interest in photovoltaics as a burgeoning energy-harvesting technology is rapidly growing. However, effective energy storage systems are indispensable for storing the harvested energy, and fully integrating these technologies poses substantial challenges. Recent advances have facilitated the development of integrated PV–battery systems utilizing printable solid-state LIBs. Kim et al. demonstrated printed bipolar quasi–solid-state LIBs (bQSSBs) with a bipolar cell configuration directly on the aluminum electrode of a crystalline silicon PV (cSiPV) module utilizing an in-series printing process [358]. This approach enables seamless architectural and electrical integration of PVs and energy storage systems (Fig. 23g). As depicted in Fig. 23h, the cSiPV–bQSSB system exhibited stable photo-charge and galvanostatic discharge behavior, achieving a rapid charge to 5.4 V within 30 s under 1-sun illumination, followed by a controlled discharge to 3.0 V over 36 min at a discharge current density of 0.1C.

Lu et al. introduce a robust, stretchable epidermal sweat-sensing platform integrating an Ag_2O-Zn battery and a low-power electrochromic display (Fig. 23i) [359]. This platform operates independently to directly display various electrolytes or metabolites concentrations, eliminating the need for external connections. The battery system was fabricated in a stacked configuration utilizing customized inks for the silver current collector, zinc anode, Ag_2O cathode, and titanium dioxide (TiO_2) separator. The sequential layer-by-layer construction ensured precise assembly and optimal performance, enabling the system to conduct sensing sessions over a week. The wearable patch features electrochemical sensors, ten individually addressable electrochromic pixels, and a microcontroller unit, all fabricated via screen printing. Furthermore, it maintained mechanical stability under 1,500 stretching cycles at 20 % strain and 10,000 on/off cycles.

Recent advancements in implantable neural probes have enabled precise monitoring of brain activity by converting neural signals into electronic signals. Conventional tethered connections restrict movement of subjects, underscoring the need for wireless neural recording devices to observe natural behaviors. Very recently, Kwon et al. reported that a conformal quasi–solid-state ZIB seamlessly integrated the power source with the biological system, utilizing an aqueous quasi–solid-state electrolyte (Fig. 23j) [352]. For optimal integration, the Zn-ion microbattery (ZIMB) was 3D conformally printed directly onto a model of a mouse's skull, produced via additive manufacturing. This approach resolves the mismatch challenge between flat batteries and curved surfaces, resulting in a streamlined battery system. Demonstrating superiority, the printed ZIMB proved significantly lighter than the pouch-type variant, with no discernible difference in active material mass loading (Fig. 23k). When implanted into a live animal for wireless neural recording, the preprinted skull model with ZIMBs exhibited promising results (Fig. 23l).

7.4.1.4.3. Performance-oriented applications. Novel 3D-shaped electrodes improve electrochemical performance across various applications, including lithium metal anodes and thick electrodes with complex structures. Various structural designs achieved *via* printing methods enhance efficient ion transport and stable high-mass loading, improving energy density. This achievement surpasses the performance of conventional slurry-cast electrodes.

An electrically active lithium host was successfully demonstrated for Li-metal batteries based on a micro-patterned Si electrode (MPS) [360]. The MPS host is manufactured by applying micro-scale direct ink writing technology (Fig. 24a). The printed MPS host is engineered with designed electrical conductivity and a porous structure onto the lithiophilic conductive substrate (lc-substrate). The fabricated MPS host stands at a height of 21 μm and enables customization of pitch sizes (Fig. 24b). Here, a pitch of 150 μm was determined to be optimal, supported by the uniform deposition of Li within the pores (Fig. 24c). The MPS host is designed with a regular structure, featuring an areal capacity of 3.8 mAh cm^2, high cell energy density (644 Wh kg^{-1}_{cell}/ 1538 Wh L^{-1}_{cell}), and stable cycling performance.

Lim et al. developed a safe Li anode with high areal capacity and high-rate capability by employing a 3D-printed Cu framework (3DP-Cu) (Fig. 24d) [361]. The framework possessed high mechanical robustness, effectively restraining Li dendrite growth and volume expansion. Porous structure and a large specific surface area, which simultaneously suppressed Li dendrite growth. The Li@3DP-Cu cell demonstrates superior performance even with an increased areal capacity of 2.5 mA h cm^{-2} at a current density of 1

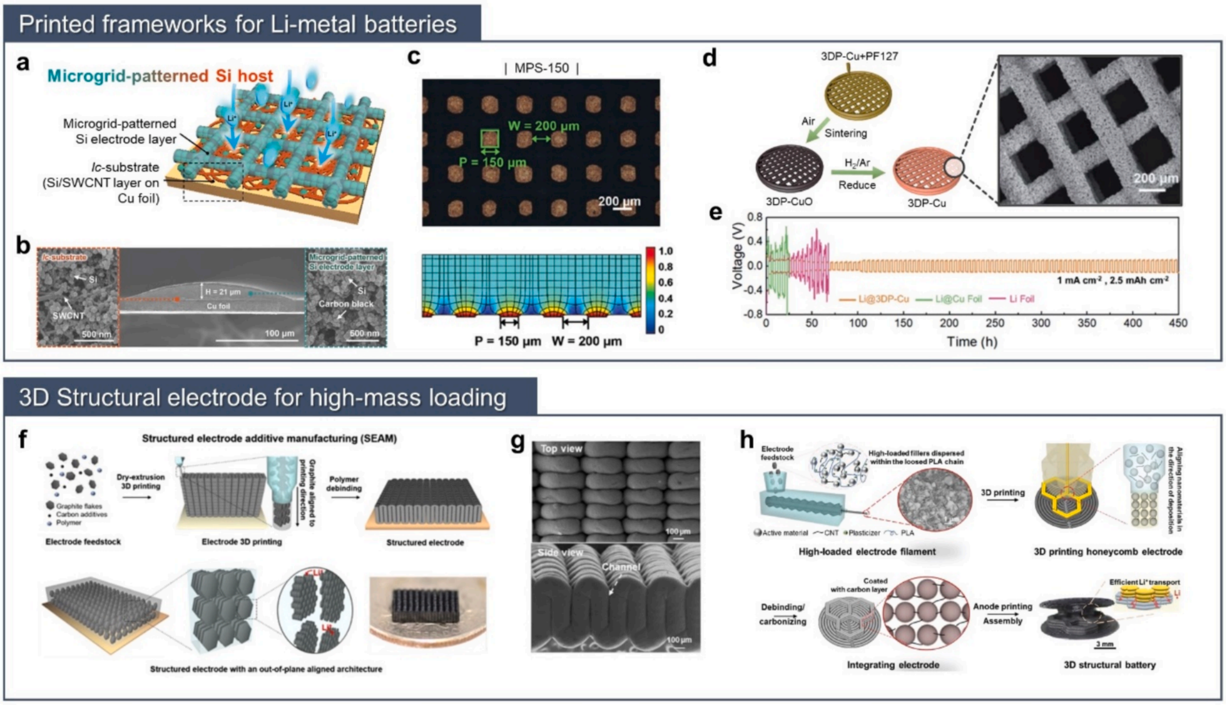

Fig. 24. Performance-oriented power sources. a) Schematic illustrating the structural and electrochemical characteristics of the printed MPS host. b) Cross-sectional SEM images of the MPS host consisting of the lithiophilic conductive (lc)-substrate (left) and the microgrid Si electrode active layer (right). c) Optical microscopy images and COMSOL simulation of the current density distribution of the MPS hosts (Pore size of 150 μm). Reproduced from Ref. [360] with permission from The Royal Society of Chemistry, Copyright 2022. d) Fabrication and SEM image of a 3D Printed Cu framework (3DP-Cu). e) The symmetric cell profiles at a current density of 1.0 mA cm^{-2} and a capacity of 2.5 mAh cm^{-2}. Reproduced from Ref. [361] with permission from The Royal Society of Chemistry, Copyright 2020. f) A schematic depicting the additive manufacturing process of structured electrodes for 3D graphite thick electrodes. g) SEM images of the 3D graphite electrode. Reproduced from Ref. [362] with permission from American Chemical Society, Copyright 2022. h) Schematic depiction of 3D printed honeycomb electrodes utilizing high-loaded filaments. Reproduced from Ref. [363] with permission from Wiley-VCH GmbH, Copyright 2023.

mA cm^{-2}. It maintains stable stripping/plating cycling with moderate charge/discharge profiles over extended periods compared to the compromised stabilities of Li@Cu and Li foil cells (Fig. 24e). This study provides an innovative approach employing 3D printing to fabricate copper-based framework for advanced Li metal battery systems.

To achieve higher areal energy density with thicker electrodes, 3D printing is fascinating approach to enhance the electrochemical performances that exceed that of conventional one. Park et al. developed a method known as structured electrode additive manufacturing (SEAM) [362]. This approach enables the production of thick electrodes without the need for solvents or drying processes. This approach aligns anisotropic active materials, such as graphite flakes, along their longitudinal directions through high-pressure induced shear flow. The multiscale porous structure through the thickness and oriented graphite flakes reduces lithium-ion path tortuosity, improving ion transport and providing more utilizing intercalation paths within the graphite flakes (Fig. 24f). A graphite anode fabricated with SEAM was densely stacked to a thickness of 2 mm, demonstrating no structural defects such as delamination or layer shifting (Fig. 24g). This precise alignment enhances areal and specific capacities at high current density, resulting in improvements of 260 % in specific and areal capacity at 1C when compared to slurry-cast electrodes.

Fused deposition modeling has been introduced to enhance the areal capacity of printable electrodes [363]. This technique provides superior design flexibility and scalability compared to conventional 3D printing and post-processing techniques (Fig. 24h). The researchers utilized highly loaded filaments composed of 65 wt% of active materials, conductive additives, and thermoplastics such as polyethylene glycol diglycidyl ether and polylactic acid. Hence, the structural full cell achieved a capacity of 12.28 mAh cm^{-2} at a current density of 0.92 mA cm^{-2}. Moreover, the honeycomb-shaped electrode designs enhance area loading and promote uniform electrolyte distribution, resulting in more durable and structurally stable electrodes.

7.5. Conclusion and outlook

In the past few years, printed batteries have attracted much attention owing to the ever-growing interest in portable/wearable electronics. We have briefly reviewed the recent developments and challenges of the printed batteries, with a focus on the printing techniques, ink materials/chemistry, and integration with devices of ink formulation, printing techniques, printable materials, and applications. Several notable progresses have been discussed in the printed batteries, surpassing the capabilities of conventional battery technologies. However, practical use and commercialization of printed batteries lie far behind those of conventional batteries. In this regard, the future development and practical prospects for the printed batteries can be summarized as follows:

Enhancement of the electrochemical performances: Compared to the rapid growth of conventional batteries, especially Li-ion, driven by the expanded global market of electric vehicles and energy storage systems (ESS), printable batteries have not yet been widely commercialized. One of the significant reasons is their inferior electrochemical performances compared with their conventional batteries. For instance, in traditional sheet-type electrodes, mechanical calendaring process is conducted to ensure effective electrical conduction and increase of energy density reducing the voids in the electrodes. However, the direct integration of the printed batteries with various devices makes it difficult to exploit mechanical pressing. To address this performances issue, it is desirable to adapt high-energy–density electrochemical systems such as Li-S and Li-metal as an alternative approach. For the stable operation of these post-Li-ion systems, there are several hurdles have to be tackled including polysulfide shuttling, lithium dendrite growth and formation of dead-lithium.

Defining the killer applications: Despite the performance of printed battery's lagging behind the conventional one, the most compelling strength of the printed batteries lies in their monolithic integration with other devices. For instance, batteries required for implantable devices often cannot be manufactured using traditional battery manufacturing processes because their fixed form factor. Printed batteries utilizing tailored printing technology for specific applications present a highly attractive means to achieve this goal. Another significant advantage of printed batteries is their micro-fabrication ability. Conventional roll-to-roll manufacturing processes lack the precision required for fabrication of microbatteries (device footprint < 1 cm^2) Furthermore, when the size of batteries shrank down, volumetric/gravimetric proportion of packaging substance within the battery increased exponentially [364]. In this regard, high-precision printing technologies are a very attractive way to fabricate the microbatteries, which also reduce the proportion of packaging materials through direct integrated with the target devices.

Scale up and cost reduction: For commercialization and wide distribution of printed batteries, scaling up production and reducing unit costs are essential. Particularly, with the rapid increase in battery production driven by the widespread adoption of electric vehicles, battery manufacturing based on roll-to-roll processes has achieved significant enhancement of the production speed (e.g. commercial electrode manufacturing speed: 100 m min^{-1}). However, the printing process, especially DIW printing method favorable for direct integration with device, exhibit lower throughput compared to roll-to-roll processes [285]. This low production rate consequently leads to increase of the battery cost. Therefore, scaling up and resulting decrease of the battery production cost can play a crucial role in practical application of commercialization of printed batteries.

The printed batteries described here hold great promise as an energy storage platform that can bring us closer to a battery of things (BoT) era featuring human-oriented technologies.

8. Flexible batteries

Flexible battery is a device that combines the considerable specific energy and the characteristics of being stretched, bended and twisted [365–369]. These characteristics are determinedly needed by the specific applications of powering wearable electronic devices, electronic skins, flexible displays and implantable medical equipment. In recent years, the development of powering devices towards diversification, flexibility, lightweight and thickness facilitates the rapidly evolution of flexible batteries [370–373], and meanwhile, parameters to evaluate the flexibility of flexible batteries are gradually clear and standard [374]. A comprehensive understanding of assessing parameters would direct the rational and ingenious designing to boost the implementation of high-flexibility and high-energy–density batteries.

$$f = 1/r \tag{5}$$

Geometric parameters and mechanical parameters are commonly combined to describe the capability of battery deformation. The flexibility (*f*) of batteries is identified by the reciprocal of the radius of tolerable curvature of materials (Equation (5) [374], referring to the minimum yield strain of all components of batteries.

The limitation of *f* is determined by the physical properties and the thickness of electrode, electrolyte, separator and current collector. The bending of components results in bipolar distribution of tensile strain and compressive strain [375]. Among them, the maximum bending strain before failure occurs in tensile strain, and the deformation (ε) of being tensile is related to the thickness of materials based on Equation (6) [373].

$$\in = \frac{[2\pi(\mathrm{r} + \frac{h}{2}) - 2\pi\mathrm{r}]}{2\pi r} = \frac{h}{2r} \tag{6}$$

The combination of Eqs. (5) and (6) emerges a critical result in geometry and mechanics: any material in sufficiently thin form is flexible, by virtue of bending strains that decrease linearly with thickness, as indicated in Eq. (7). Therefore, the concept of reducing-dimensionality for designing high-flexibility batteries is widely acceptable and practical.

$$\mathrm{f} = \frac{1}{\mathrm{r}} = \frac{2}{\mathrm{h}}\in \tag{7}$$

In the past few years, ultrathin current collector [376,377], flexible polymer electrolyte [378,379] and separators [380,381] have experienced tremendous progress to encounter the requirement of flexibility. Flexible solid Zn-Air batteries [382] based on polymer gel electrolyte [383], flexible sulfur batteries [384] with self-supported and flexible hosts [385] have been successfully contrived for powering electronic devices. Meanwhile, well designing of configuration structure gives more possible for highly flexible application. The configurations of flexible batteries are divided into origami-patterned flexible batteries (Fig. 25 a and b), belt-shaped flexible batteries (Fig. 25c), and fiber-shaped flexible batteries (Fig. 25d) based on the dimensionality and deformation.

Origami patterned designing (Fig. 25b) allows to incorporate commercially rigid packaging batteries into deformable electronic devices [387]. It is a convenient shortcut to achieve flexible batteries as it is completely compatible with industrial battery processing. The assembled rigid components of conventional batteries are deformed as a crease pattern to avoid large strain. Therefore, inspiring deformation (over 150 % stretchability) of lithium-ion batteries were achieved by the concept of kirigami pattern [388]. However, a paradigm shift that combines origami art, materials science, and energy storage devices simultaneously accompanies with non-negligible issues. The deformation centralizing in the region of crease cannot afford long-lasting repeated bending, leading to the localized breakage and disconnect and finally incurring the loss of capacity. Seeking the appropriate strategies to disperse deformation could largely mitigates this issue.

Belt-shaped designing (Fig. 25c) dissipates strain at the system level, which requires every component of batteries accommodating flexure [389,390]. The flexibility of components has been achieved by the concept of ultrathin designing (2D structure) based on

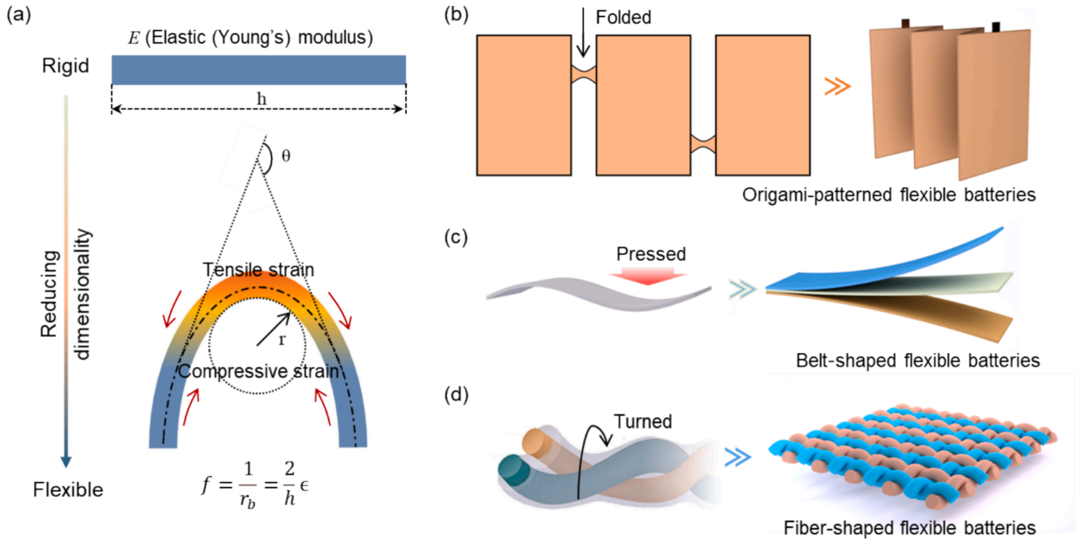

Fig. 25. Key parameters and battery configuration design for flexible batteries. (a) Schematics of key parameters and strain distribution to describe the flexibility of working devices. Reproduced from Ref. [386] with permission from Cell Press, Copyright 2019.; (b) Origami-patterned flexible batteries; (c) Belt-shaped flexible batteries; (d) Fiber-shaped flexible batteries.

Equation (7). For example, a small bending radius (13 mm) of batteries are attained by ultrathin electrode [391], which make it possible to be embedded in wearable electronic devices and E-skins. Considering the demands for higher energy density, the key issue of ultrathin belt-shaped batteries locates in increasing the loading of active materials with the adequate flexibility.

Fiber-shaped designing (Fig. 25d) further reduces dimensionality (1D structure) to cater to the flexible applications [392]. The cathode and anode wires are separated by flexible electrolyte to frame fiber-shaped batteries. Industrial scale production of fiber-shaped batteries with an energy density of 550 mWh m^{-2} has been reported [393]. However, such fiber-shaped batteries cannot deliver desired cycle life, which encourages the exploration of failure behavior and microstructure [394,395]. Besides, this unique 1D-structured batteries can be processed into textiles, representing the ultimate goal of powering wearable electronic devices. However, the possible leakage of electrolyte and plastic deformation under multiple-counts bending are the mountain challenges in the commercial applications.

The concept of reducing dimensionality for designing flexible batteries shows encouraging progresses. The rational approach to achieve the flexibility of batteries needs comprehensively considerations. These issues including energy density, technical flexibility,

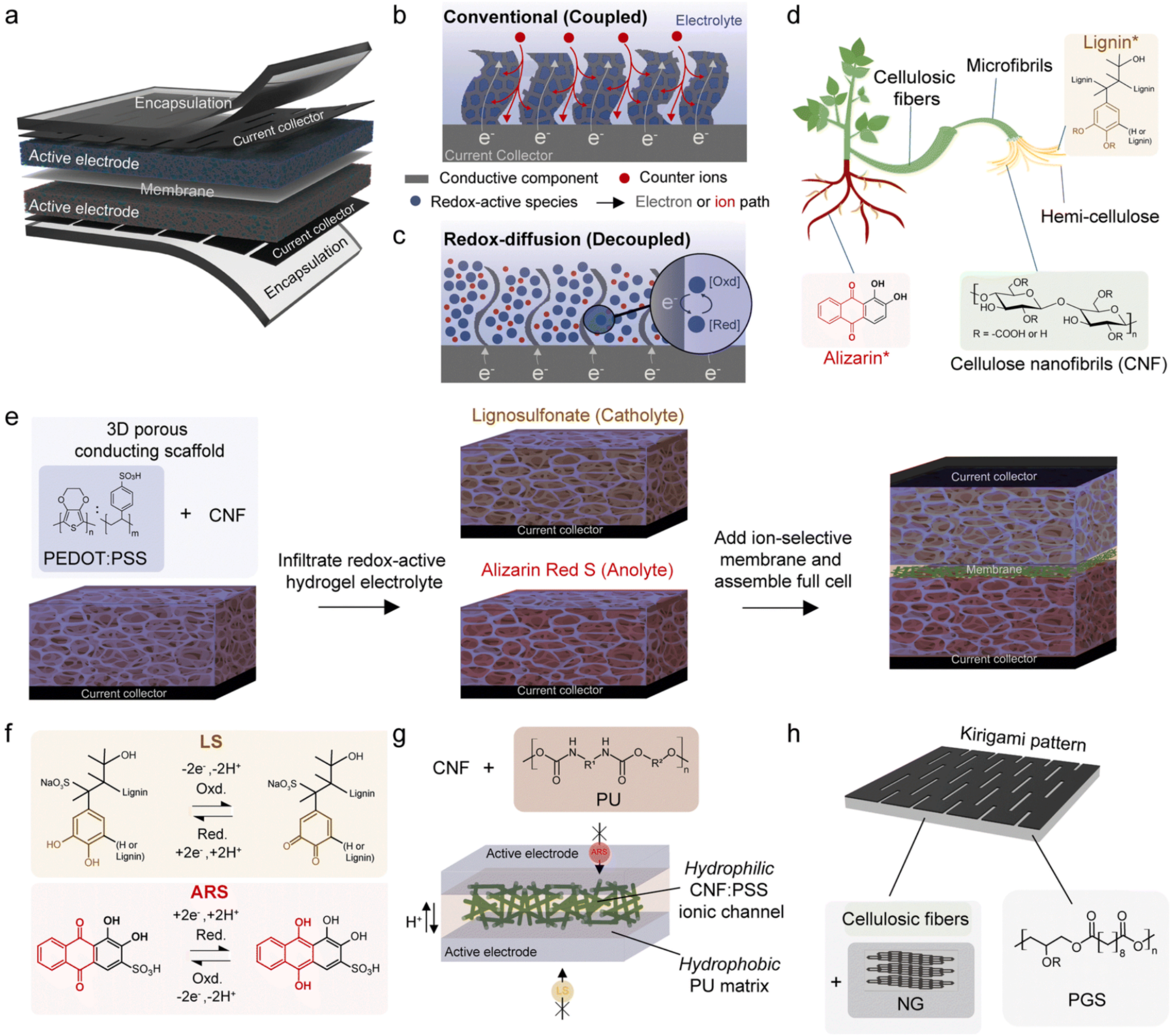

Fig. 26. Stretchable battery architecture and its components. Schematic representation: (a) the full cell, (b) conventional (coupled) and (c) the redox-diffusion electrode design (decoupled). (d) Biomaterials derived from various parts of a plant and the molecular structure of the cellulose nanofibrils (CNFs), alizarin and lignin. (*) indicates that the CNFs used were carboxymethylated cellulose and sulfonated ARS and LS were prepared post extraction of the materials. (e) The infiltration process. The 3D porous conductive scaffold is made from the conducting polymer PEDOT:PSS and CNF, with the dissolved redox-active biomolecules, LS (catholyte) and ARS (anolyte) in PVA/1 M H_2SO_4 within the pores. (f) The redox processes of LS and ARS. (g) Schematic of the selective ion conducting membrane with a hydrophobic elastomer and hydrophilic CNF:PSS network. (h) Schematic of the kirigami-patterned current collector made from nanographite and cellulosic fibers, and PGS (R = H or crosslinked chains) as the biodegradable elastomer encapsulation. Reproduced from Ref. [405] with permission from Roya Society of Chemistry, Copyright 2024.

and battery safety still restrict the revolutionarily proceeding towards the future wearable electronic devices.

9. Biodegradable batteries

9.1. Introduction

The search for environmentally sensitive and sustainable energy storage options has spurred research into novel materials that disintegrate spontaneously and have no effect on the environment. In the face of rising worldwide energy consumption driven by population growth and industrialization, the move to paper-based batteries presents a critical path [396]. This paradigm change represents a big step forward in the development of energy storage devices that are not only affordable and lightweight but also environmentally friendly. One such example is the development of sodium-ion hybrid electrolyte batteries, which have replaceable components. The organic sodium electrodes that come from renewable biomass resources significantly expand the scope of biodegradable battery materials [397]. These materials have the potential to revolutionize battery technology by bringing it into line with sustainable practices due to their inherent ecological significance. In broader sense, following materials and designs are more commonly being explored for biodegradable batteries.

9.2. Materials & design

9.2.1. Biodegradable Polymers/Gel electrolytes

Liquid electrolytes have basic drawbacks such as design constraints, environmental concerns, and safety risks from evaporation and leakage [398]. The development of solid-state polymer electrolytes is a result of these difficulties. Bio-based polymer electrolytes for lithium-ion batteries have been investigated recently employing cellulose, chitosan, and natural rubber [398–400]. Alternatives like sodium-ion batteries are becoming more popular since lithium-ion batteries, despite their superior performance, are dependent on expensive and limited resources [401]. Nevertheless, the research of bio-based polymer electrolytes for sodium-ion batteries is still in its early stages. Colò et al. [402] showed that sodium-ion battery electrolytes based on cellulose had a broad electrochemical stability window in addition to good thermal stability. There have also been reports of proton batteries that use bio-based polymer electrolytes such as chitosan, cellulose, and natural rubber. These materials not only provide ionic conductivity but also contribute to the overall biodegradability of the battery. The encapsulation of biodegradable batteries must also be environmentally friendly. Polylactic acid and other biodegradable plastics are often used to encase the battery components, ensuring that the entire device is biodegradable.

GelBat, a revolutionary biodegradable, edible, and rechargeable battery made of gelatin and activated carbon, was introduced by Chen et al. in 2023 [403]. With just 10 min of charging, this inventive device uses the water splitting process to create a basic, sustainable fuel cell. Water is the main output of GelBat's operation, highlighting its eco-friendliness. Potential biomedical applications are made possible by the gelatin matrix, which guarantees compatibility with biological systems and offers a safe and biodegradable substrate. The battery's overall performance is improved by activated carbon, which also increases the battery's conductivity and energy storage capacity. The GelBat represents a noteworthy progression in the creation of environmentally friendly energy solutions by fusing sustainability with useful energy storage and proving that employing edible and biodegradable materials in battery technology is feasible.

9.2.1.1. Natural organic materials. Quinones' inherent redox potential can be used as inspiration when creating new active electrode materials for rechargeable batteries. Tannins, lignin, and melanins are examples of quinone-based compounds that have been employed to increase the capacity of carbon electrodes to store charge [404]. Electron transfers between quinones in aqueous solutions occur via proton coupling. Next-generation sustainable energy storage devices could benefit from the use of biosourced, quinone-based organic electrode materials that function in aqueous electrolytes. Rahmanudin et al. [405] created a stretchable redox-diffusion battery that combines sustainable plant-based biomaterials for full-cell degradability with structural and material-level techniques for stretchability (Fig. 26). Due to the dissolved redox components, the electrode remains remarkably soft even at high mass loadings. To generate hydrophilic ionic transport channels, cellulose nanofibers (CNFs) were used to create a stretchy ion-selective membrane. Laser-structured cellulose graphite composites were fashioned into kirigami patterns for collectors, boosting stretchability and doing away with the necessity for metals. The entire cell demonstrated the mechanical robustness of all battery components during stretching, with an operating voltage of 0.6 V, a maximum volumetric capacity of 2.68 mA h cm^{-3} at 0.2 mA cm^{-2}, and steady capacity retention after 200 cycles at 30 % strain.

The electrochemical performance and mechanical stress tolerance of each component must be taken into account while designing stretchable batteries. This is accomplished by two key strategies: intrinsic material stretchability and structural design. Using techniques like layered twisted fibers, stiff cells on deformable substrates with stretchable interconnects, wavy/buckled structures, kirigami patterns, or ultrathin structures, structural designs isolate rigid components from strain [405].

9.2.1.2. Metal-Based materials. The creation of zinc dual-ion batteries (ZDIB), which combine the high energy density of zinc-ion batteries with the recyclability of carbon-based materials lessens reliance on harmful components. Sun et al. (2022) created a water-in-salt electrolyte (HiSE) for high-performance ZDIB that is based on PVA-gelatin hydrogel and is ecologically benign, while also offering the advantage of transitory degradation [406]. With an operating voltage of 2.0 V, superior rate performance, and remarkable stability—96.2 % of its capacity is retained after 8000 cycles— deeming the HiSE-based ZDIB a powerful device. Lately, there has been a lot of interest in magnesium-based biodegradable batteries because of their high specific capacity, energy density, extended shelf life, favorable biodegradability, physiological compatibility, affordability, and superior safety. Magnesium has a high rate of decay, though, which is mostly caused by its poor resistance to corrosion, especially in wet conditions. Controlling the rate at which magnesium anodes deteriorate is crucial and plausible solution to this is surface coatings, which offer a barrier against corrosion. A tight electrochemical window limits the performance of aqueous magnesium-ion batteries, but nonaqueous batteries often have weak ionic conductivity [407]. In response to these difficulties, Leong et al. previously created a water-in-salt battery that can operate at a voltage higher than 2 V [407]. However, this voltage is still lower than nonaqueous versions since the cathode mostly inserts protons rather than magnesium ions. In order to get around this restriction, they created a quasi-solid-state magnesium-ion battery (QSMB) that allows for genuine multivalent metal ion storage by confining the hydrogen bond network. Outperforming previous Mg-ion batteries, the QSMB attained an outstanding energy density of 264 $W \cdot h\ kg^{-1}$.

Due to the usage of metal sheets (such as Mg, Zn, Fe, W, and Mo) as electrodes, current biodegradable batteries frequently suffer from issues with bulkiness and rigidity. The surrounding tissues may sustain harm from these hard metal electrodes' potential adverse effects, which include corrosion and dissolution [408]. Mei et al. (2021) developed an aqueous fiber battery that is both rechargeable and biodegradable in order to overcome these problems. Body fluid serves as the electrolyte in their invention, which also includes a chitosan separator and biodegradable fiber electrodes [409]. The biodegradable fibre conductors incorporated with polydopamine/polypyrrole composite material serves as the anode and MnO_2 as the cathode. The fiber battery's one-dimensional design and great degree of flexibility enables less invasive integration because it may be injected straight into the body. Most importantly, the battery biodegrades after usage; the process is harmless and does not affect bodily functions in any way. The fiber-based power system is a major improvement that is created from an aqueous sodium ion battery through an eco-friendly and straightforward approach.

9.2.1.3. Conductive additives – Paper based batteries. Paper-based batteries have garnered interest as a portable, biodegradable, and environmentally beneficial energy storage solution. Paper substrates are used in these batteries to produce lightweight, flexible energy solutions. Highly conductive materials such as metals, conductive polymers, and carbon allotropes (graphite, fullerenes, graphene, carbon nanotubes, nanocrystals, and nanowires) are combined with regular paper in the creation process [410–416]. In the battery system, paper has three functions: it is a substrate for electrode deposition, a medium for electrolyte storage, and a current collector when coated with conductive material. Paper-like nanocomposite films, potentially scalable for industrial usage, can be made using regular paper as a foundation. Nanomaterials are applied to paper using a variety of printing techniques, with differing outcomes: spray coating, doctor blade, screen printing, inkjet printing, filtration, and photolithography [417–419]. Paper's structural characteristics, such as its rough and porous surfaces, improve power performance, particularly within the electrode, by facilitating ion and electron transport. Wang et al. [420] created a ground-breaking paper-based, liquid-free Al-air battery by storing an alkaline paper-based gel electrolyte within a porous cellulose framework. This design permits many reuses as a mechanically rechargeable Al-air battery by replacing both the electrolyte and the Al anode upon depletion in addition to eliminating the possibility of leakage and water management concerns.

9.3. Applications

The unique properties of biodegradable batteries make them suitable for a wide range of applications, particularly in fields where environmental impact and safety are critical considerations. In the medical field, biodegradable batteries are ideal for implantable medical devices like pacemakers and drug delivery systems, as they naturally break down within the body, eliminating the need for surgical removal and reducing long-term tissue damage. The most extensively researched transient batteries are those based on magnesium (e.g., Mg-Fe cells, Mg-Mo cells) and zinc (e.g., Zn-Cu cells, Zn-MnO_2 cells). These batteries are not only pivotal in the field of implantable medical devices but also offer multifunctional features such as self-powering capabilities, the ability to load drug-activated factors, flexibility, and biodegradability. For environmental monitoring, these batteries are well-suited due to their ability to decompose naturally, making them suitable for use in sensitive natural settings without posing pollution risks. In the realm of consumer electronics, biodegradable batteries can enhance sustainability by reducing electronic waste, powering devices like smartphones, tablets, and wearables while minimizing environmental impact. Additionally, for temporary power sources such as disposable medical devices, single-use sensors, and event-based electronics, biodegradable batteries provide reliable power during their operational life and degrade safely afterward, reducing waste. In fact, recently Navarro-Segarra et al (2022) have curated an ecodesign to monitor agricultural procedures wherein the FlowER battery passively transports reactants via a paper-based fluidic structure by imitating plant methods of fluid transport [421].

9.4. Challenges with existing biodegradable batteries

Despite their potential, biodegradable batteries face several significant challenges that need to be addressed before they can be widely adopted. The primary hurdles include achieving performance metrics comparable to those of conventional batteries, such as energy density, lifespan, and cost-effectiveness. One of the main challenges in the development of biodegradable batteries is ensuring that they offer sufficient energy density and longevity to be viable alternatives to conventional batteries. Additionally, the production of biodegradable materials can be more expensive than traditional materials, which poses a barrier to the widespread adoption of biodegradable batteries. Developing processes that allow for the mass production of biodegradable batteries without compromising their performance or environmental benefits is essential. The lack of standardization and regulation for biodegradable batteries poses another challenge for their commercialization. Extensive research and collaboration among industry and academia is needed to overcome these hurdles. Moreover, establishing industry standards and regulatory frameworks are crucial for ensuring the safety, performance, and environmental impact of biodegradable batteries. This will also facilitate the integration of biodegradable batteries into various applications and promote consumer confidence.

10. Micro-batteries

10.1. Introduction

Microbatteries are generally considered to be those fabricated using wafer-scale semiconductor electronics type processing equipment and techniques. As with the developments in lithium-ion technology, efforts to maximize the energy available have resulted in lithium-based microbatteries being the most commonly investigated materials. They differ from standard particle or slurry-based films, laminated on foils or coin cells in that they are typically all solid-state and thin-film in nature. Being solid-state confers advantages that are desirable for integration with electronic components. They are liquid-free and therefore, non-susceptible to leakage. It also means they can typically operate at higher temperatures or potentially withstand integration and packaging processes, such as solder reflow.

Non-flammable and solid electrolytes also increase safety. Solid electrolytes can suppress the growth of dendrites associated with lithium metal plating, making them more resilient to overcharging and short circuits, which can occur more readily with liquid electrolytes and polymer separators. Indeed, lithium metal can be utilized as the anode which obviates the need for lithium intercalation into a host material and either the lower capacity that results with carbon or tin-based anodes or the expansion and contraction that occurs during cycling of the higher capacity materials, such as silicon or germanium. Furthermore, the solid-state electrolytes can facilitate thousands of cycles to match the lifetime of the electronic device.

The low electronic and ionic conductivity of the cathodes and electrolyte, respectively, has limited the active material thickness to a few microns unlike the more common powder electrode and liquid electrolyte based, lithium-ion batteries. This has resulted in significant research efforts in 3D structuring of the materials to increase the energy per footprint while maintaining the advantages of solid-state materials. Recent developments in the use of multilayer microbatteries may prove to be an optimal electrode and electrolyte arrangement in which the 2D layers exhibit more uniform electrode materials access and reactions particularly at high charge and discharge rates. The schematic in Fig. 27 illustrates the advantage in energy and power density on going to 3D microbatteries together with some options to achieve such structures [422].

While lithium-ion batteries have seen considerable research, development and optimisation since their introduction in the early 90′s, all solid-state materials and microbatteries have had less investment for materials and product development. This is linked to the low capacity per footprint of the thin-film materials and the need to integrate an energy harvesting source to counter the low daily capacity of the batteries and provide a wireless recharge option for the microbattery. Typical energy harvesting options, such as solar and vibration are relatively large area or volume and require improved efficiencies to support the energy storage elements. Recent interest in solid-state materials for larger scale systems, such as electric vehicles, has accelerated the research effort in this area and will potentially lead to scalable options for improved electrodes, electrolytes and interfaces. It also brings into focus the need to decrease processing costs and increase throughput to deliver highly desirable solid-state options.

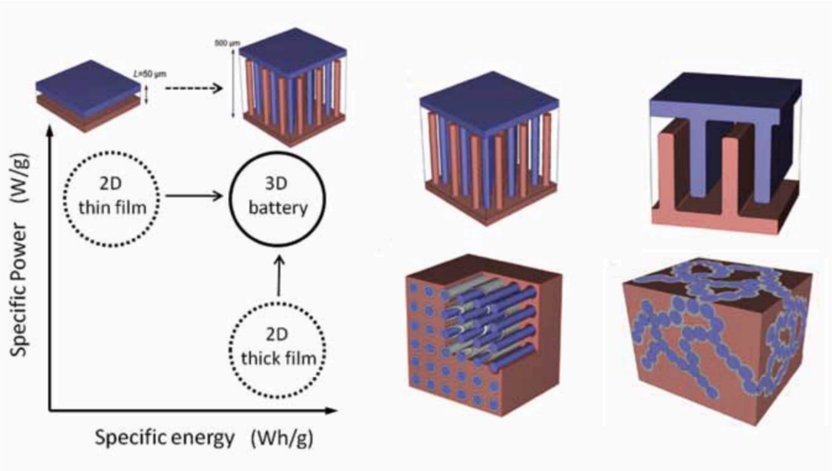

Fig. 27. Options to achieve 3 D architectures and benefits in terms of energy and power. Reproduced from Ref. [422] with permission from Institute of Physics Publishing, Copyright 2011.

10.2. Materials and geometries

This review will describe the materials utilised in rechargeable microbatteries and, as such, will not include primary small or coin cells. An all-solid-state thin-film microbattery that achieved over 1,000 stable cycles and supported periodic peak currents in the mA cm^{-2} range was first presented at the 6th International Meeting on Lithium Batteries in Münster, Germany in May 1992 and subsequently in manuscripts by Jones and Akridge [423,424]. A generic thin-film microbattery schematic is shown in Fig. 28a).

1992 also saw the patent filing for the now commonly used LiPON solid-state electrolyte [426], which exhibited superior electrochemical performance to those previously investigated, particularly in terms of enhanced lithium ionic conductivity (2×10^{-6} S cm^{-1} at 25 °C) and direct contact with lithium metal anodes [427–429]. The group at Oak Ridge National Laboratory extended their work to 'Li-free' anodes in which the lithium metal anodes were formed during cell operation by *in situ* plating on a copper current collector [430] to facilitate solder reflow and packaging of integrated cells in the discharged state. Micron scale individual battery units, down to 50 x 50 µm, and their connection in series is shown in Fig. 28b) for cells that used a nickel blocking anode contact, LiPON solid-state electrolyte, and *in situ* lithium metal formation. This permits the fabrication of thousands of cells per substrate wafer and was investigated for space based applications [425].

Efforts to develop solid-state lithium ion conductors with higher conductivity resulted in a superionic conductor $Li_{10}GeP_2S_{12}$ with conductivity of 1.2×10^{-2} S cm^{-1} at room temperature [126]. Despite this promising conductivity, the use of this material has been hampered by instability, surface interactions and breakdown products which impede kinetics at lithium metal [431] and at cathode interfaces [432]. An alternative oxide-based solid-state electrolyte, $Li_7La_3Zr_2O_{12}$ (LLZO) [433] has also attracted much attention, with reported conductivities of $\sim 4 \times 10^{-4}$ S cm^{-1} at room temperature. Despite the positive characteristics of this electrolyte, it was shown that lithium dendrites can perpetuate along grain boundaries in the electrolyte as a result of increased electronic conductivity in those areas resulting in short circuits [434]. A range of interfacial treatments or layers have been suggested and investigated to improve the characteristics and minimize resistance and contacting issues [435].

Since the initial realization of thin-film microbatteries and optimization of the materials processing that achieved long cycle life and high peak current capability, the major roadblock to widespread adoption and commercial success has been the relatively low energy storage capacity per unit footprint, or volume. Micro and nanoelectronic device development has relied upon continuous shrinking of the active materials or feature dimension in line with 'Moore's Law'. In contrast to this, the goal for batteries is to have as much energy storage active material as possible in the available volume. Therefore, except in situations where very low energy is required to power an electronic device, there has been an on-going effort to maximize the energy available through the utilization of advanced architectures to maintain the advantages of the thin-film structures in terms of short diffusion distances and all-solid-state materials, for electrode separation and safety. A selection of options to achieve this was presented at the first international three-dimensional microbattery architectures symposium held during the 204th Electrochemical Society meeting in Orlando in 2003. This was followed by a theoretical assessment of potential architectures in 2004 [436], and a comprehensive review of the field [437] published by some of the symposium co-organizers.

In essence, the drive to 3D is to improve the energy capacity per unit footprint. Some of the options presented included fin or pillar type either interdigitated or individually surrounded by electrolyte and capped with the second electrode, or aperiodic 'sponge' type structures as shown above in Fig. 27. To achieve these complex architectures requires the sequential and complete, pinhole-free, materials deposition of successive active layers, which remains a significant challenge for multi-element material layers, particularly those in the electrolytes and cathodes.

The baseline figures-of-merit for microbatteries are those achieved for single cells in 2D architecture thin-film format [423], with energy storage capacities of ~ 0.2 mWh cm^{-2} and short-term peak current densities of 0.3 mA cm^{-2}. The 'anode-free' version of the early microbatteries [430] achieved ~ 0.46 mWh cm^{-2} and peak current densities of 5 mA cm^{-2}. A commercial and packaged version

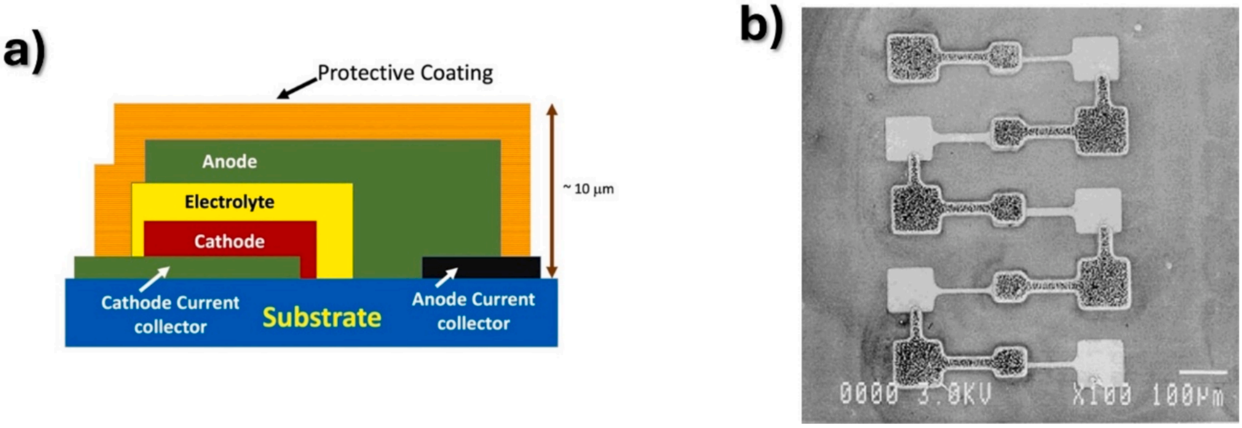

Fig. 28. A) 2d thin-film microbattery schematic and b) micrograph of a 5-cell lithium microbattery connected in series. reproduced from ref. [425] with permission from Institute of Physics Publishing, Copyright 2002.

of the ‘anode-free’ LiPON based 2D microbattery from Cymbet [438] delivered 0.3 mWh cm^{-2} and peak discharge currents of 0.46 mA cm^{-2} for 20 ms. This was based on the fully packaged, surface mount technology (SMT) compatible, 8 × 8 mm footprint battery. The cells achieved 1,000 cycles to 50 % depth of discharge. To go beyond the capacities and peak current capabilities of these 2D micron scale active materials in thin-film format researchers looked to 3D or even 1D nanowires as higher capacity options per unit footprint.

Some impressive results with non-planar micro and nanostructures [422,439–445] were reported, mostly for half-cells and efforts to integrate those as active materials in full cell microbatteries have been intensively pursued. Templates such as porous anodic alumina, with sub-micron diameter openings, have been used to form the 1D active materials and were even investigated to form an array of nanobatteries [446]. The alumina template was placed on a 400 nm SnO_2 thin-film anode material followed by infilling of the pores with 20 µm polyethylene oxide (PEO) electrolyte and 40 µm V_2O_5 ambigel cathode and with which they achieved ∼ 90 µWh cm^{-2} µm^{-1} for the arrays.

Another option to structure the battery materials [447] utilized high aspect ratio 3D etched structures, such as through holes in substrates or interposers, that connected the top and bottom surfaces and greatly increase the potential active surface area per unit footprint by up to 23 times. As in the previous case, this hybrid cell was not fully solid-state. The complex processing required that the substrate was activated and coated with a conductive electroless nickel barrier layer prior to molybdenum oxysulphide cathode electroplating. The electrolyte was poly(vinylidene difluoride) (PVDF) based polymer with conduction enhancers and the anode was carbon in bead format infiltrated into the structure with binder and solvent. Both of these layers were spin coated sequentially and vacuum processed to increase the coverage uniformity. Using a mid-discharge voltage of 1.7 V the energy achieved was 1.7 mWh cm^{-2}. The maximum discharge current investigated was 1 mA cm^{-2}.

Deep reactive ion etching (DRIE) of silicon has also been utilized to increase the surface area per unit footprint [448,449]. The small feature sizes enabled by the DRIE necessitate ultrathin-film active materials deposition in the high aspect ratio structures with vertical sidewalls. Etch depths of 135 µm can result in a surface area enhancement of 28 times for such substrates and an estimated 5 mWh cm^{-2} energy capacity. The difficulty with such structured substrate use, is the need to deposit successive, conformal, pinhole-free layers in even smaller features than previously envisioned to include, barrier layers, current collectors and the three active battery material layers. The timing of these efforts coincided with the commercial development of atomic layer deposition (ALD) precursors and equipment as a highly controlled and conformal method for materials deposition which is particularly well suited to oxide materials deposition, as required for most high energy battery cathodes.

Electrodeposition has been utilized on a number of occasions to achieve the 3D structuring of active materials or substrates [422,444,445,450,451]. In cases where an interdigitated structure can be realized, electrodeposition is a viable technique to deposit nm to mm scale materials in high aspect ratio, for both anodes and cathodes. Three-dimensional bi-continuous interdigitated microelectrodes [452], based on plated nickel supports was achieved by electrodeposition through self-assembled polystyrene (PS) spheres at a substrate. This resulted in a porous nickel scaffold onto which the active materials could be plated, a nickel-tin alloy for the anode and manganese dioxide for the cathode. The maximum active material thickness investigated was nanoscale, 90 nm for the anode and 67 nm for the cathode. The PS spheres diameter, and IDE width and separation were varied to modify the density and output characteristics of the cells. When tested in perchlorate-based ethylene carbonate (EC) / dimethyl carbonate (DMC) organic solvent electrolyte at 1.5C rate the energy density was 0.225 mWh cm^{-2}, limited by the nanoscale thin-film active material. The highly conducting and structured support did enable a power density of mW cm^{-2} even up to very high C rates. A modification of this work to improve manufacturability and extend the cycle life used holographic lithography and SU8 photoresist processing to structure the porous substrate [453]. The active electrode material thickness was again limited to 100 nm and for 10 µm thick electrode supports an energy density of 0.045 mWh cm^{-2} was achieved and 0.006 mWh cm^{-2} retained even at 1000C discharge rates. The cycle life was

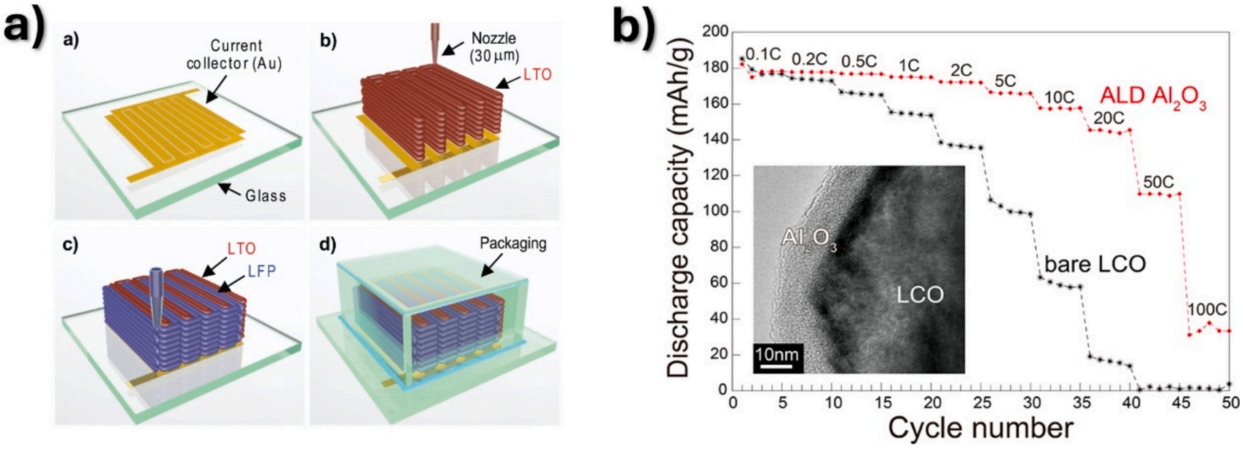

Fig. 29. a) Schematic of 3D printed and packaged microbattery. Reproduced from Ref. [290] with permission from Wiley, Copyright 2013. b) Interfacial nanoengineering by ALD coating of alumina on lithium cobalt oxide (LCO) and the resulting improved high rate capability by comparison with untreated bare LCO. Reproduced from Ref. [462] with permission from American Chemical Society, Copyright 2018.

extended to 200 with a 12 % decrease in capacity at that point.

A recent review has described the range of cathode materials that can electroplated to potentially go beyond the planar, conformal and low thickness levels of standard vacuum processed thin-films [454]. That work lists the wide variety of materials and processing media to achieve electrodeposition of cathodes such as $LiCoO_2$ from molten salts [455], MnO_2 [456], and V_2O_5 [457], from aqueous solutions and $LiFePO_4$ from ionic liquids [458]. They also highlight the possibility of using lithium-free plated cathodes which when combined with a lithium metal anode eliminates the issues associated with high energy density anodes, such as, Si and Ge, that become embrittled and rapidly lose capacity on cycling. Lithium-free cathodes described include MoS_2 [447], FeS_2 [459], and V_2O_5 [460].

3D printing technology or additive manufacturing is another potential option to achieve 3D structured microbatteries. The technique can be utilized to deposit established battery materials or potentially provide novel energy storage solutions as described in a comprehensive review [461]. An example of 3D printing capabilities has been reported for microbattery cells consisting of $Li_4Ti_5O_{12}$ and $LiFePO_4$ as the anode and cathode, respectively [290] and shown in Fig. 29a). The printed electrodes were annealed at 600 °C in an inert gas to remove the organic additives and promote nanoparticle sintering. A poly(methyl methacrylate) (PMMA) preform was laser cut and placed around the microbattery before sealing with poly(dimethyl siloxane) (PDMS) gel cured at 150 °C. The assembly was then filled with liquid electrolyte and sealed with a small glass cover and PDMS. The equipment utilized had a minimum resolution of 1 μm and was capable of printing interdigitated electrodes over 1 mm^2 to 1 m^2 in area. For the cells reported, the electrode width was 60 μm processed using a 30 μm diameter nozzle. In an eight-layer full cell tested with lithium perchlorate in EC/DMC solvent the energy density was 2.7 mWh cm^{-2} for the 30 cycles reported. As the printing technology and more printing inks become available it is likely that we will see further developments in this additive processing to achieve bespoke solutions for particular energy storage options, such as on flexible substrates.

The use of LiPON as the solid-state electrolyte of choice for thin-film microbatteries was based on introducing a nitriding step into the use of lithium phosphate electrolytes which resulted in an electrolyte with increased ionic conductivity and cycling stability. First principles analysis shows that many of the solid-state electrolytes investigated to date are thermodynamically unstable with respect to both electrodes and it is the development of *in situ* formed protective films or deliberately deposited protective layers, and in some cases, the resulting improved kinetic effects which offers the possibility of their use [463–465]. An approach to develop appropriate interlayers has been the use of combinatorial high-throughput physical vapour deposition (PVD) techniques to provide a range of electrolyte/cathode interlayer materials [466]. In that work, compositions of a series of amorphous, as-deposited LiNbTa films were crystallised over a range of temperatures. The resulting film properties were examined for optimised conductivity and dielectric component, and fast charge transfer reactions at the interface in a 5 V class of all-solid-state lithium batteries.

For the majority of the microbattery materials under investigation, interface nanoengineering is a viable option, as they are thin-film and solid-state and potentially well-suited to ALD or chemical processing. In addition to improving interface compatibility, some unexpected benefits may arise, such as that shown in recent work which utilised ALD alumina on $LiCoO_2$ particles for analysis in standard organic solvent electrolyte [462]. The nanoscale alumina, shown in Fig. 29b), maintained the capacity of the cathode and significantly improve the reaction kinetics, it was postulated, by aluminium doping into the $LiCoO_2$ cathode material at the interface. They also argued that the protective film suppressed the high potential phase transition of the cathode and decreased any potential Co dissolution. Over 80 % of the discharge capacity was accessible at 20C discharge rates for samples subjected to a 3 nm alumina layer process by comparison with less than 15 % in the absence of the alumina at the same discharge rate. The differences in rate capability only became significant at those above 1C. Sputter deposited thin-films of $LiCoO_2$ also showed an improvement in output characteristics when subjected to an ALD alumina coating [467]. When tested in standard EC/diethyl carbonate (DEC) electrolyte the alumina coating permitted cycling to 4.4 V for the $LiCoO_2$ without loss of activity and enabled greater than 80 % of the capacity to be accessed at 2.7C. Even with this high potential limit for the cathode, 61 % of the capacity was accessed at cycle 500 for the high discharge rate.

A similar benefit of interface engineering was shown recently for a plated V_2O_5 cathode. In that case, 1 nm coatings with ALD alumina were sufficient to enhance the cycle life against a lithium metal anode and rate capabilities for the cathode when tested in organic solvent, ionic liquid or polymer gel ionic liquid-based electrolytes [467]. The polymer gel ionic liquid (PGIL) electrolyte was prepared by mixing the ionic liquid 1-butyl-1-methylpyrrolidinium bis(trifluoromethylsulfonyl)imide (C4mpyrTFSI), LiTFSI and poly(vinylidene difluoride-co-hexafluoropropylene) (PVDF-HFP) [468]. The alumina coated V_2O_5 retained 93.5 % capacity to cycle 800 for a 1C discharge rate with a lithium metal anode indicating the potential for ionic liquid gel electrolytes which have similar conductivities to standard organic solvents to be used rather than ceramic or glassy all-solid-state electrolytes for microbatteries.

Although most research has been focused on the lithium-based microbatteries discussed so far, sodium microbatteries provide an alternative solution to the problem of microenergy storage with unique advantages and challenges. Often considered the bulky and inefficient analogue of lithium, sodium's main benefits are its natural abundance and resulting low cost. In their latest 2023 report, the European Commission has recognized lithium as a critical raw material both in terms of its supply risk and also its economic importance [469]. While sodium cannot compete with lithium for high end energy storage performance, its cost effectiveness could render it an excellent alternative for particular applications [470].

The similarities between sodium and lithium and potential electrolyte/cathode materials means it is as close to a 'drop-in replacement' as possible in manufacturing technology requiring minimal processing equipment modifications [401]. Compatible materials include the use of layered oxides or phosphate analogues as cathodes [471]. For microbatteries sodium metal would be the anode of choice and its use may also require the use of solid-state or nearly solid electrolytes. Solid-state NASICON or b-alumina electrolytes have higher ionic conductivity than solid-state lithium electrolytes [470] and offer an opportunity for development of the microbattery format with higher power capabilities. As is the case for larger batteries, the thermodynamic stability of aluminium with respect to sodium at low potentials, means that it can be used as the low-cost current collector for both electrodes, further reducing cost by replacing the more expensive copper required for lithium systems. Aluminium is also a material that has been used in microelectronics applications for many decades and significant expertise exists for its deposition and patterning. Sodium microbattery designs based on 1D, 2D, and 3D architectures have been reported [472,473]. The 1D architectures include coaxial, twisted and parallel electrode configurations [409,474]. However, 2D planar and 3D designs are more common, as observed for lithium systems. Although the number of articles on sodium-ion batteries is growing each year, much of the discussion is focused on large scale storage with relatively few focused on the development on full cell sodium microbatteries.

The European Union project Nereid (Nanoelectronics Roadmap for Europe) [475] included a chapter dedicated to energy harvesting which included an analysis of microbattery energy storage. The assessment concluded that in the short term (to 2026) microbatteries will be deployed for internal use in factory environments and externally to power autonomous sensors. The first deployment in healthcare systems is envisaged in medical patches. In the longer term (to 2033) the roadmap suggests that they will be employed in the home, extensively in agriculture and in implantable devices for each of the three cases. In terms of areal energy density, it was suggested that the realized 5 mWh cm^{-2} would be achieved by 2023. Incremental increases to 6. 5, 8 and then 10 mWh cm^{-2} were foreseen for the years 2026, 2029 and 2033, respectively. It is anticipated that these improvements will occur due to new and optimized deposition techniques, multilayer processing and novel electrode and electrolyte materials combinations.

10.3. Applications

Microbatteries have long been perceived as the option to power microdevices and the recent focus on ‘internet of things’ (IoT) devices and applications, facilitated by advances in communications technologies, is providing a large potential or target market for rechargeable microbatteries integrated with energy harvesting. There are cases where IoT devices do not require an energy storage option, such as for RFID chips or those which can be powered solely by harvested energy. However, a significant proportion of the IoT devices will require energy for operation beyond that provided by ambient harvesting sources or require energy when none is available for harvesting. Stored energy can also assist with optimization of device functionality and operation during periods of high energy requirements, such as, during sensing or external communication.

As with many new technologies one of the first technology applications to explore the potential use of thin-film solid-state microbatteries was the space industry. Key drivers for that technology are decreased weight and appropriately sourced energy provision. On-chip integrated microbatteries can minimize unnecessary cabling by co-locating the microbatteries and electronic chips to provide point-of-use power, reduce device weight and packaging and match the energy requirements of the system with the capacity of the rechargeable battery. Some early work in this area showed the potential to pattern and size microbatteries as required, such as, by their connection in series (Fig. 28b) or parallel to match the microspacecraft applications and a specific example of a switch array microsystem [425,476].

In addition to the basic needs for the energy source, many space applications have requirements that are inherently aligned with thin-film microbatteries including the ability to operate safely without leakage over a wide temperature range. The robust all-solid-state microbatteries have also shown high reliability, very low self-discharge and long cycle-life which is a requirement for space applications or missions where the energy source cannot be easily replaced.

Similar baseline characteristics apply to batteries for medical wearable or implantable devices. These two sectors are the least cost sensitive application domains for which the market may support more early adoption and costly fabrication and packaging options than those of more mainstream energy storage markets. A key requirement for their more general use is to match the available energy which can be harvested or supplied by short term wireless power transfer with the stored energy of the microbattery and minimization of the energy required by the microdevice for operation. This requires innovative circuit design and specifically developed ultra-low power management integrated circuit chips.

Options to integrate miniaturized photovoltaic (PV) cells from 0.07 to 1 mm^2 have been described for use in intraocular pressure

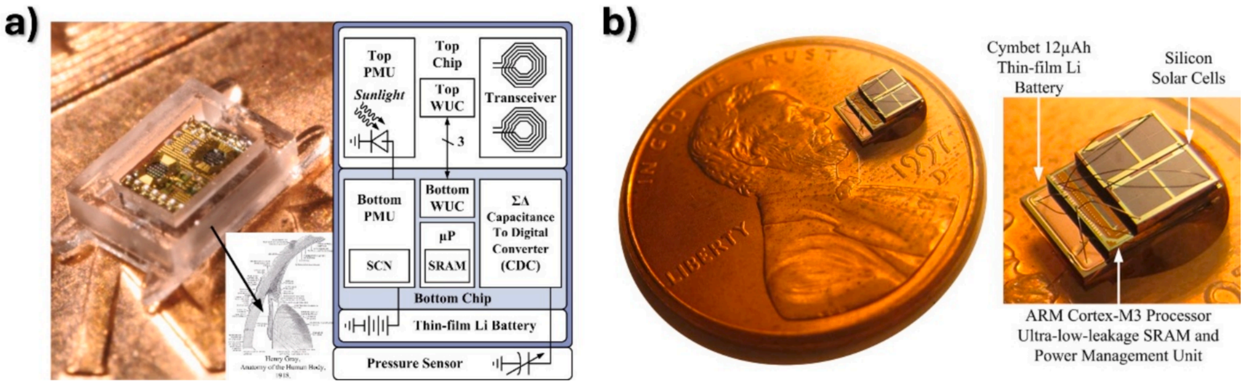

Fig. 30. A) 1.5 mm^3 size MEMS pressure sensor with PV cell, microbattery, antennae and integrated electronics. Reproduced from Ref. [477] with permission from IEEE, Copyright 2011. b) 8.75 mm^3 temperature sensor in three layers with PC cell, integrated circuits and thin-film microbattery. Reproduced from Ref. [478]. with permission from IEEE, Copyright 2013.

sensors (1.5 mm^3) [477] and for a wireless temperature sensor [478]. In both cases the electronics and energy harvester were integrated in microsystems with Cymbet supplied microbatteries. In the first case the microbattery was custom made with 1 μAh capacity. This was fabricated for the miniature device application limited by the acceptable incision dimensions for the device implant, the curvature of the cornea and dilation of the pupil. The electronic circuits included a wireless transceiver, capacitance to digital converter (CDC), a DC-DC switched capacitor network (SCN), microcontroller, and the memory was fabricated in 0.18 μm complementary metal oxide semiconductor (CMOS) as shown in Fig. 30a). The custom made microbattery demonstrates a significant advantage of these thin-film microbatteries which can be varied in footprint simply by changing the mask designs for the thin-film deposition. They can be fabricated in irregular or elongated shapes to match scenarios that require specific dimensions such as a narrow but long battery maintaining the stored energy density. This may be true of many medical device applications, particularly implantables for future sensors.

In the case of the 200 nW temperature sensor they developed a larger 8.75 mm^3 microsystem using 1 mm^2 PV energy harvesting cells, a 12 μAh thin-film microbattery from Cymbet and ultra-low-power circuits integrating an ARM Cortex-M3 microcontroller Fig. 30b). The microsystem consumed 7.7 W in active mode and 550 pW in standby mode between measurements. The microsystem was capable of processing temperature data hourly for 5 years using only the initial energy stored in the battery or had indefinite lifetime using the energy harvesting of the PV cells to recharge the battery for long-life autonomous operation.

To increase the energy density for implantable devices where size can be critically constrained one option is to increase the thickness of the electrodes [479]. Using a 20 μm sputter deposited $LiCoO_2$ cathode the authors achieved an energy density of ~ 3.3 mWh cm^{-2} at device level. In this cell they utilized a 3 μm LiPON electrolyte and a ‘lithium-free’ anode. The 3.1 × 1.7 mm^2 thin-film microbatteries which were 95 μm in total thickness had a discharge capacity of 25 μAh and were capable of maintaining 60 % of this value at 0.25 mA or 10C discharge rate. This flexibility of design again illustrates the potential for thin-film microbatteries for medtech applications.

A further, more recent development in solid state microbattery fabrication for commercial applications that maintains the areal dimensions has been the demonstration of stacked cells that go beyond the placement of cells in a pyramidal format one over the other to increase capacity [480]. Ilika in the UK [481] extended their portfolio by developing processes to stack the Stereax M50 or 50 μAh capacity cell which has a 5.5 × 3.5 mm footprint and a normalised energy density of 0.9 mWh cm^{-2}. The six cell stack of the Stereax M300 product can deliver 5.45 mWh cm^{-2} in a package which is still under 1 mm in height. This is potentially a key development as models of solid state and/or 3D microbatteries which consist of poor electronic conducting active materials and low ionic conductivity in the electrolyte have shown that they will have non-uniformity issues except at very low current drain or C-rates [436,482–484]. Most of the applications envisaged for microbatteries require the periodic delivery of high currents during sensing operations or data transmission. This multilayer option is directed towards applications in the medical device or implant sectors.

An alternative to the vacuum deposited solid-state batteries discussed so far is the recently introduced multilayered fabricated batteries using techniques similar to multilayer co-fired ceramic capacitor fabrication for surface mount component assemblies. The

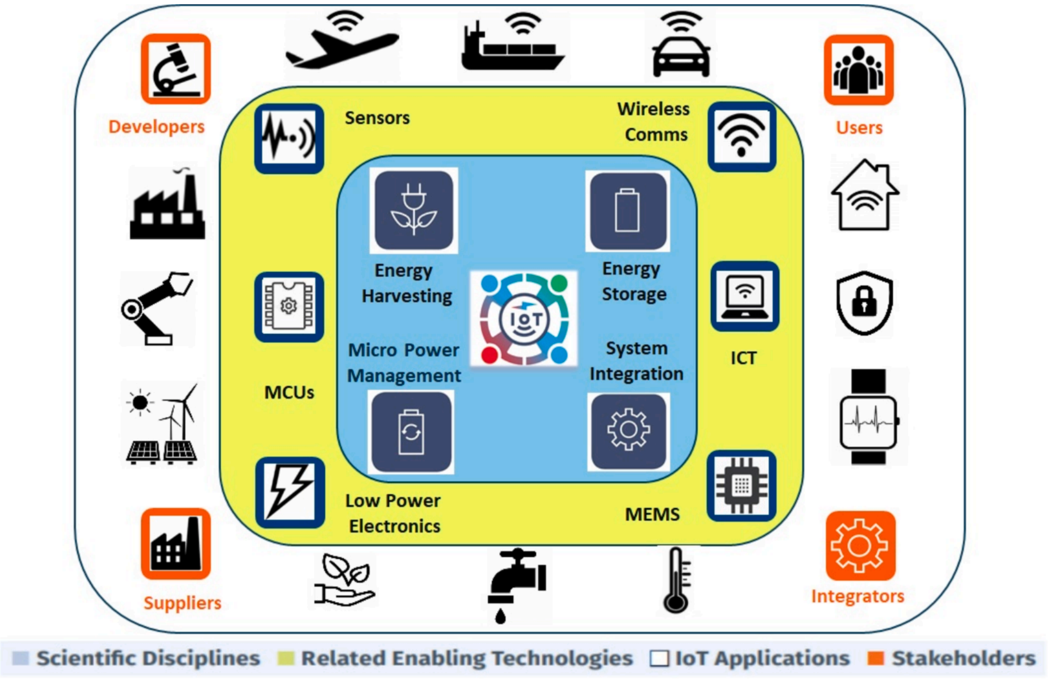

Fig. 31. Powering the IoT ecosystem including scientific disciplines, enabling technologies, IoT applications and stakeholders. Adapted from Ref. [487] with permission from IEEE, Copyright 2019.

initial product developed by TDK [485] is a multilayer packaged battery in a standard 1812 format (4.5 mm × 3.2 mm × 1.1 mm) which has a capacity of 100 μAh at a rated voltage of 1.5 V giving an areal energy density of ∼ 1 mWh cm^{-2}. It is solid-state, ceramic based, and therefore compatible with solder reflow typical of surface mount devices and initially targeted at the IoT application space. It is less energy dense with a lower rated voltage and, therefore, likely to service the higher volume and more cost sensitive IoT markets in conjunction with energy harvesting technologies.

Providing energetic autonomy to electronic devices for remote monitoring is seen as a large potential market for sensor networks and IoT devices:

- Where a simple primary battery is not sufficient
- If using power cables significantly increases the cost or complexity (i.e., avionics, or space applications)
- If devices are so numerous that changing batteries increases the maintenance cost and the logistics become unmanageable
- In harsh environments where electronic devices cannot be accessed easily

In these cases, remote monitoring can eliminate breakdowns and productivity losses by identifying failure modes or condition monitoring to increase lifetime or tracking of assets. The integration of energy storage with developing energy harvesting technologies also has the potential benefit of improving the sustainability of the energy solution. Less primary batteries would be required and disposed of at the end of their short lifetime. There is also a significant focus on the use of more sustainable or plentiful materials that are safe and readily recyclable to support a circular economy.

An international workshop (https://www.enerharv.com) dedicated to the development and promotion of the energy harvesting, storage and micropower management circuits was established in 2018 and the third biennial event took place in June 2024 in Perugia, Italy. The community and related workshops are dedicated to ‘Powering the IoT’ ecosystem [486,487], with the various contributors outlined in Fig. 31. The ecosystem consists of stakeholders to assist with integration of these fields of research for new materials, devices and systems with developers for applications, and end-users and to accelerate the roll-out of IoT devices. The goal is to create awareness and foster collaborations that will result in demonstrators/products aligned with technology roadmaps, and provide options to realize the development of standardized, interoperable and system-optimized IoT solutions.

10.4. Conclusions and future challenges

Microbatteries for energy storage, particularly for IoT applications or integrated in electronic devices, have areal energy densities of ∼ 5 mWh cm^{-2} when used with μm scale lithium-based thin-film materials. They can be cycled thousands of times with little capacity fade, particularly when the depth of discharge is minimized. Solid-state materials offer advantages in terms of safety, cycle life and energy per electrode thickness. Based of the early research on solid-state lithium microbatteries including lithium metal-based cells, research is now being extended for their potential use in larger cell formats appropriate to EV applications. This increased interest in solid-state electrolytes, interface improvement and novel analysis including operando studies [488] and potentially microelectrodes for undistorted and high-rate analysis [489–491] will assist with developments at all scales and all materials combinations for energy storage applications. A particular area of interest is in the electrolytes given that the ionic conductivity of the all-solid-state options is still significantly lower than the more common liquid-based electrolytes of current commercial lithium-ion batteries. Solid-state electrolytes offer enhanced safety by eliminating organic solvents of typical lithium-ion batteries and optimized charge times with thinner active electrode and electrolyte materials.

The analysis above has described how, despite efforts to 1D or 3D structure microbatteries, 2D stacking of individual microbattery unit cells is most likely the preferred realistic option to increase the energy and power density in the same footprint while maintaining the advantages of the thin-film format. Laminated ceramic components under development for multilayer stacked microbatteries are just now entering the market and may play a significant role in solderable surface mount devices for integrated electronics and IoT applications. With higher energy density materials, their use may be extended to other larger scale applications.

Significant efforts are underway to utilize more sustainable, safe and lower cost materials as the active battery components, or in particular cases, even using biodegradable materials and substrates for batteries in distributed sensors. In the latter case, with less energy dense materials, larger cell formats may be required. As with lithium-ion chemistries it is desirable to exclude cobalt in the cathode and ultimately move towards the more abundant sodium-based analogues of the benchmark lithium systems. Alternative electrolyte materials tending towards near solid-state are of interest with optimization of polymer, ceramic or gel-based electrolytes. Those were intensively investigated in the early days of lithium-ion development but can now include the developing field of ionic liquids or their polymer gel analogues. The desire is to include the benefits of the nearly solid-state materials while maintaining the ionic conductivity at current lithium-ion solvent system levels. Interface nanoengineering which is also now possible through a variety of processing options, including ALD, is also a developing field of research to minimize unwanted interfacial reactions while permitting low interfacial contact resistance with novel electrolytes and therefore, enhanced kinetics with extended cycle life.

Microbatteries can assist with the enhanced performance of distributed sensors. Ongoing research is required to integrate appropriately sized storage elements with energy harvesting options and power management systems to optimize the offering for the anticipated billions of sensor devices in the predicted future IoT scenario. An even more integrated option for future devices could be the use of photobatteries or those in which active battery materials can be recharged directly. Recent analysis of such materials in a dedicated test cell demonstrated that photo-charging is feasible when the conduction band quasi-Fermi level is positioned above the anode intercalation/plating potential [492]. Simulations and models describing microbattery characteristics have provided guidance for the architectures and fabrication of the devices. These will require updates to assist with design and optimization of the new specific active architectures, dimensions, electrode materials, interfaces and electrolytes.

11. Smart capabilities for the different battery systems

Smart materials are revolutionizing lithium batteries by enhancing efficiency, durability, and adaptability while paving the way for sustainable, flexible, and shape-adjustable battery designs [493]. These innovations include self-healing polymers, shape-memory alloys [494], and adaptive nanostructures [495], which significantly improve performance and lifespan as represented in Fig. 32.

For instance, self-healing materials allow to repair micro-cracks that develop during charging cycles, reducing capacity loss and extending operational life [496,497]. Smart coatings and separators adapt to environmental changes, such as overheating, by altering their properties to prevent thermal runaway [498]. Flame-retardant materials, such as phosphate-based compounds [499] and ceramic-coated separators [500], suppress combustion and enhance safety. Advanced electrolyte additives and modified cathode or anode coatings further boost safety by reducing flammability and mitigating lithium dendrite growth, all while maintaining high energy density and performance. In critical scenarios, built-in safety mechanisms ensure secure operation [501]; for example, separator membranes can melt at extreme temperatures to block ion flow [502], or built-in circuits can disconnect power if voltage, current, or temperature exceeds safe thresholds [503]. These innovations make lithium batteries more reliable, versatile, and suitable for demanding applications like electric vehicles and renewable energy storage.

Self-sensing to enhance life and safety through status monitoring and prediction is another capability of next-generation batteries. The Fiber Optic Bragg Grating (FBG), Distributed Fiber Optic Sensors (DFOS) sensors and a thin-film resistance temperature detectors allows to assess temperature, strength, and displacement at the cell level [504,505].

12. Circular economy and recycling issues

12.1. Introduction

The environmental problems that contemporary society faces, have become prevalent and important social concerns. These problems, especially those related to air quality and climate change, are mostly caused by the economy's heavy reliance on fossil fuels. As the transition from a fossil fuel powered society to a society strongly relying on renewable energy requires an increasing use of energy storage systems, the reuse and recycling of those systems also becomes a critical issue, since it promotes the idea of a circular economy, reduces the need to extract additional resources and strongly contributes to the reduction of the associated environmental impact.

In fact, the drive to achieve a net zero emission by 2050 has brought about a surge in the utilization of energy from renewable sources. Due to the intermittent nature of the predominant renewable energy sources such as solar and wind, energy storage systems has become an integral part of the solution to emission reduction of greenhouse gases (GHG) [506]. Rechargeable batteries, also known as secondary batteries, are currently the dominant energy storage systems. The installed capacity of energy storage batteries in the world increased from 9.6 GW h in 2020 to 50.8 GW h in 2022 and is projected to reach 288.3 GW h by 2025. This represents a

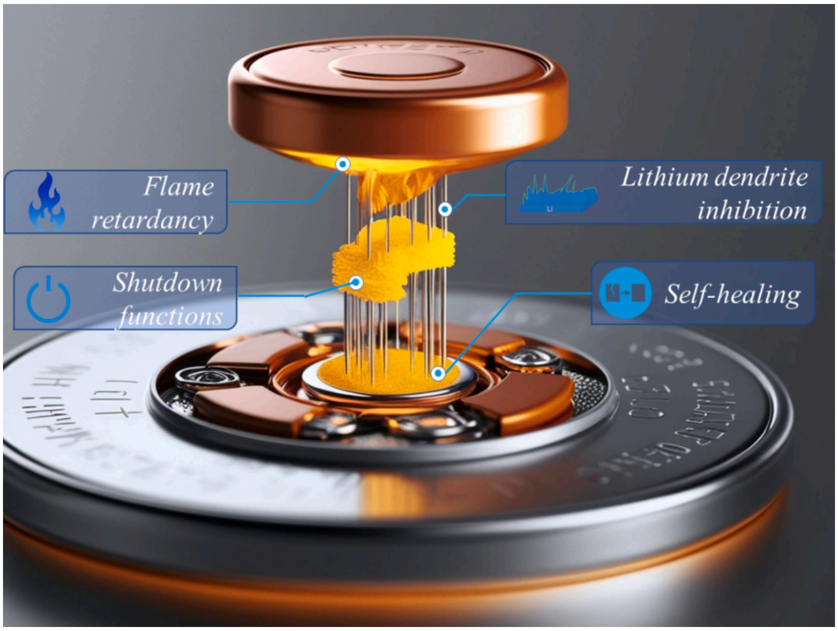

Fig. 32. Smart capabilities for the next generation of battery systems.

compound annual growth rate of more than 100 % from 2020 to 2025 [507].

There are a variety of secondary batteries in the market, ranging from the very common and traditional lead-acid batteries, to nickel–metal hydride battery (NiMH) and Lithium-ion polymer batteries (LiPo). However, since its commercialization in the early 1990 s, lithium-ion battery technology (LIB) has dominated the secondary battery market due to their high energy and power densities, as well as their cycle stability [508]. The large-scale production of electric vehicles (EV) has further accelerated the growth of the LIB industry. The global production capacity of LIBs has increased from 25.6 GWh in 2009 to 218 GWh in 2019 and predicted to be more than 2500 GWh in 2030 [509]. With a life span of 3 – 8 years for LIBs used on mobile devices and 10 – 15 years for the EV power battery packs, the quantity of LIBs reaching their end of life (EoL) has also been increasing over the years. The spent LIB capacity is expected to reach 300 GWh by 2030, as shown in Fig. 33 [510–512].

Regardless of their chemistries, all secondary batteries contain transition metals such as cobalt (Co), nickel (Ni), manganese (Mn), iron (Fe) and lead (Pb). A direct consequence of the sharp increase in the production of secondary batteries is the huge demand on transition metals. In the conventional linear economy (LE) where manufacturing industry takes the form of take-make-waste/discard, such a growth cannot be sustained with the finite natural resources on planet Earth [513]. Furthermore, concentration of some transition metal reserves only in a limited number of countries, particularly those for cobalt and nickel, makes their supply vulnerable. Many economically developed regions have classified them as critical materials [514].

It’s long been recognized that the significant quantity of transition metals in the spent LIBs is valuable secondary resources for their future manufacturing. This, coupled with the fact that the electrolyte in the spent LIBs is a potent contaminant to the environment if directly discarded, necessitates recycling of spent LIBs [509,515].

Reviews on LIB recycling are extensive; notable ones include Yang et al.[61] and Li et al.[516]. Most of the reviews focus on the technologies and their progresses for the materials recovery from the spent LIBs [510]. This review will, using LIB as a case study, take a holistic approach to assess the development of secondary battery industry as a whole from a sustainability and circular economy (CE) perspective. The review will start with a brief summary of the currently used recycling and materials recovery technologies. The emphasis is on the new technology developments, particularly the use of deep eutectic solvents (DESs) in the extraction of metals that has started to attract serious research attention only in recent years. It will then outline some major issues and challenges currently faced in battery recycling. The review will discuss how the CE and sustainability principles can be applied to the design of battery cells and systems before concluding with recommendations.

12.2. Recycling and material recovery technologies

Recycling of spent batteries starts with battery collection and transportation to sorting and preliminary processing stations or centers. These steps are important to the overall recycling process and will be discussed briefly in other sections in the context of the efficiencies and economics of the whole recycling process. This section will only discuss the development of technologies for the

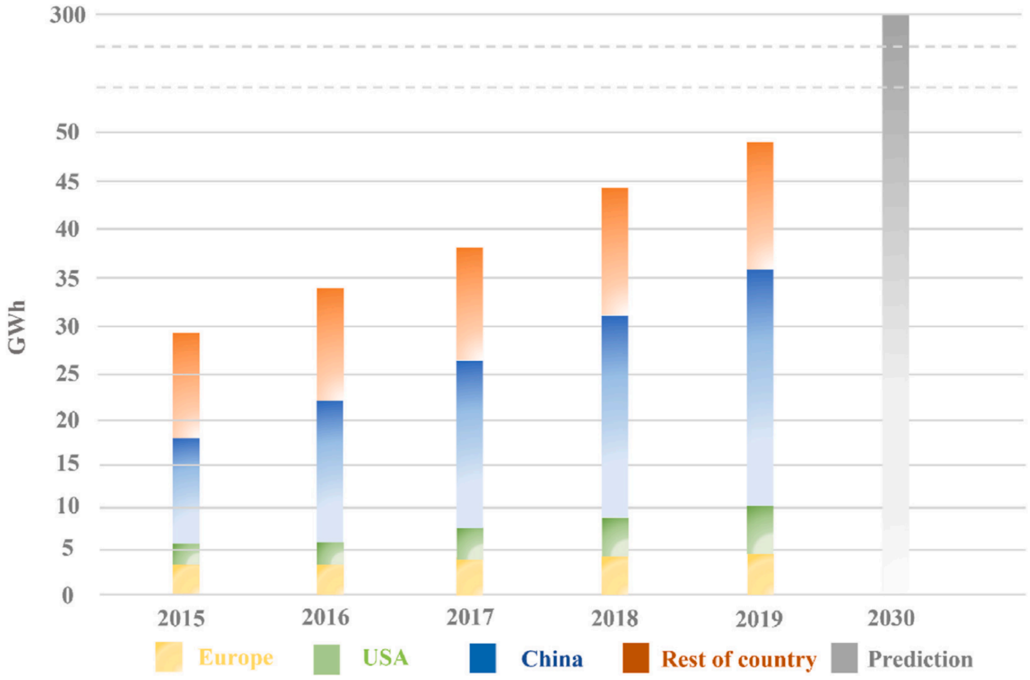

Fig. 33. Quantity of spent LIBs and its projection to 2030. Reproduced from Ref. [512] with permission from American Association for the Advancement of Science, Copyright 2021.

recovery of materials from the recycled spent LIBs.

The technologies that have been used for the recovery of materials from the spent LIBs can be broadly classified into three categories, namely, direct recycling, pyrometallurgy and hydrometallurgy. Fig. 34 shows the process steps each of the technologies goes through.

Except the pyrometallurgical method, both direct recycling and hydrometallurgical method require pre-processing the recycled spent LIBs to obtain the active electrode materials, termed the 'black mass' in industry, as the feed material. The pre-processing steps include discharging, dismantling, crushing, sieving, and physical separation [517–520].

Discharging removes the residual energy from the spent batteries to avoid short circuit current of the charged electrodes during the dismantling step, which could cause explosive reactions due to the presence of flammable electrolyte [521]. Discharging of a battery pack or a module from an EV is often achieved by connecting it to an external load which can harvest energy from the batteries. For individual battery cells, or sometimes the small-sized modules, discharging is done by submerging the batteries in electrolyte solutions such as sodium chloride (NaCl), sodium carbonate (Na_2CO_3), manganese sulphate ($MnSO_4$), sodium sulphate (Na_2SO_4), ferrous (II) sulphate ($FeSO_4$) [522]. The batteries are then crushed into pieces up to millimetres in size [519]. The crushed materials are separated using different separation methods including sieving, magnetic, eddy current, electrostatic, gravity separation, and froth flotation [522] to obtain the final product of the pre-processing, namely, the black mass.

12.2.1. *Direct recycling*

One of the main degradation mechanisms for LIBs is the loss of lithium ions from the cathode. This is caused by the repeated charging-discharging cycles that eventually lead to changes in the crystal structure that can no longer accommodate the chemical reinsertion of the lithium ion back into the cathode materials [514]. Direct recycling is essential to relithiate the cathode material to restore the LIB functionality.

Various techniques have been employed in the direct regeneration of spent cathode materials including chemical relithiation [523], hydrothermal relithiation [524], solid-state sintering [525], electrochemical relithiation [526], molten salt relithiation [527], and ionothermal relithiation [528]. These methods involve exposing the spent cathode material to an environment rich in lithium and utilizing both physical and chemical processes to reintegrate lithium ion into the crystal structure of the cathode material. Further, the lithium loss, due to a capacity loss of the LIBs, denotes that a proportion of the transition metals in the cathode material are permanently in the higher valence state. Consequently, the regeneration process also necessitates the reduction of this portion of the transition metals back to their lower valence state [529].

Chemical relithiation and hydrothermal relithiation, along with solid-state sintering, operate at lower temperatures in lithium-rich solutions with the assistance of a reductant, whereas hydrothermal relithiation requires a high pressure [523,524]. Solid-state sintering mimics the cathode material production process by embedding lithium ions back into the crystal structure of the cathode material under high-temperature conditions, resulting in high crystallinity and ideal stoichiometry [525]. Electrochemical regeneration, recognized as a sustainable and environmentally friendly technology, drives lithium ions back into cathode materials through electrochemical means for direct regeneration. Ionic liquids with good thermal stability can serve as effective reaction or flux media for cathode material regeneration under mild conditions [528]. A eutectic salt mixture has also been used as a medium to provide a lithium source for cathode relithiation. When heated to a sufficiently high temperature, the molten salt facilitates enhanced lithium-

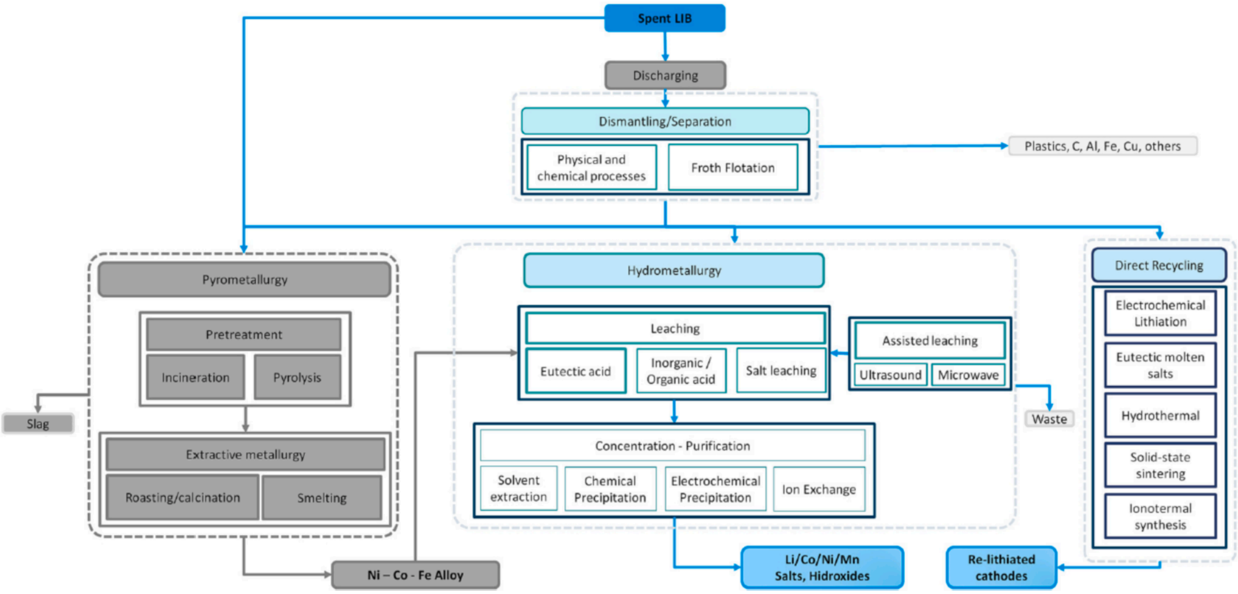

Fig. 34. Process steps of typical materials recovery technologies. Reproduced from Ref. [514] with permission from Elsevier, Copyright 2024.

ion diffusion, thereby aiding in the regeneration of cathode materials [527]. The residual lithium source left after the cathode regeneration reaction is easily soluble and recoverable for future use.

12.2.2. Pyrometallurgical processes

Pyrometallurgy is a traditional process to recover metals from the spent battery wastes using high temperature processes such as incineration, smelting, drossing, sintering, and melting [530,531]. Heat treatment in air is typically conducted in incinerators, blast furnace, or plasma arc furnace, where the volatile matter and other organic constituents (e.g. plastics) are removed as gases [530]. Heat treatment under reducing conditions results in the formation of pure metals, metal alloys and metals containing slag [519]. To recover and selectively separate the metals, pyrometallurgical process is often followed by hydrometallurgical and electrochemical processes. The pyrometallurgical process for LIB recycling has been industrialized by Umicore where the spent batteries are incinerated to produce a metal alloy, which are then fed into a hydrometallurgical process to recover 95 % of the cobalt, copper and nickel [532].

The biggest advantage of pyrometallurgical approach for the recovery of materials from the spent LIBs is its ability to treat the batteries without the delicate dismantling and battery crushing processes described before. However, due to the inherent high temperature nature of this approach, it consumes a significant amount of energy, which translates to a high carbon footprint. This method also releases toxic gases (e.g. dioxins) and a process waste stream [519,533]. Several modifications (e.g. metal extraction with vacuum, ultrasonic assisted pyrometallurgical metal recovery, addition of ammoniation in the pyrolysis step) have been proposed to improve the conventional pyrometallurgical process to reduce waste emission and increase recovery efficiency [526,530].

12.2.3. Hydrometallurgical processes

Hydrometallurgical processes involve dissolution of metals/metal oxides from the black mass using a leaching agent, which is the most critical process step that determines the overall efficiency of this approach. The agents can broadly be categorized into three groups, namely, inorganic acids, organic acids and DESs. Fig. 35 compares the various advantages and disadvantages of the leaching agents used for materials recovery from spent LIBs. From the figure, DESs are seen to be the best owing to their higher biocompatibility and biodegradability, improved dissolution kinetics and lower costs of their synthesis compared to the traditional inorganic and organic acids [534–538]. To date, however, only strong inorganic acids are used at industrial scale. For example, Umicore Valéas (Bruxelles, Belgium) used sulphuric acid (H_2SO_4) to leach the alloy from its pyrometallurgical process to recover primarily Co and Ni from spent LIBs [532]. The use of organic acids and DESs, together with bio-based leaching agents, is still at the lab scale research stage and the use of salt as a leaching agent depicted in Fig. 35 is in fact uncommon.

Details on the use of strong inorganic acids (e.g. H_2SO_4, HCl, HNO_3, aqua regia), organic acids (e.g. malonic, tartaric, oxalic citric, salicylic glycolic, succinic, lactic acid etc.) and alkalis (e.g. NaOH, NH_3) for the extraction of metals from the recycled spent LIBs are available in extensive reviews by Pradhan et al. [536] and P. Li et al. [516]. Interested readers are referred to those papers for further information. Further, P. Li, et al. [516], Zhao et al. [510] and Millian et al. [514] provided detailed summaries on bioleaching while Yu et al. [539] presented a comprehensive review on process intensification for the hydrometallurgical processes. This section will only provide a brief review on the leaching of black mass from the recycled LIBs using a DES, which has emerged as very promising and attracted significant research interests in recent years.

A DES is a mixture that contains a hydrogen bond acceptor and a hydrogen bond donor [534]. The ability of a DES to extract metals from the ores and electronic wastes was reported in the mid-2000 but application of DES to extract metals from the black mass from spent LIBs was not studied intensively until 2019 [534]. Although DES leaching of metals does not strictly belong to hydrometallurgy as DESs do not naturally contain water, it is often classified as hydrometallurgy due to its extraction of metals in a liquid state at a relatively low temperature.

Depending on the hydrogen bond donor and acceptor used, various DESs with different physicochemical properties can be prepared. The ability of a DES to leach metals depends on its reducibility and acidity, whereas the kinetics of the leaching process depends

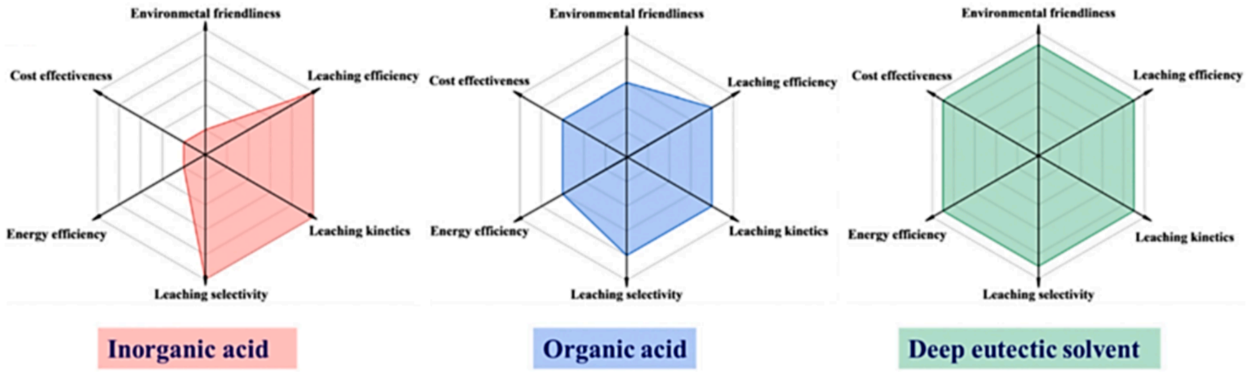

Fig. 35. Spider chart of hydrometallurgical recycling from different solutions. Reproduced from Ref. [529] with permission from Elsevier, Copyright 2021.

on its viscosity [534]. The reducibility of the DES is determined by its Fukui function, which can be calculated with DFT, and ionization potential [540,541]. A low ionization potential would indicate a strong reducing DES, which is beneficial to the recovery of transition metals [541]. The acidity of a DES is governed by the hydrogen bond donor used. Generally, higher acidity DESs are reported to be better in dissolving most of the metal oxides.

Most studies on DESs have used choline chloride or betaine as the hydrogen bond acceptor to pair with various hydrogen bond donors such as thiourea, glucose, fructose, xylose, citric acid, tartaric acid, malonic acid, glycerol, oxalic acid [529]. The viscosity of most of the DES was found to be $>$ 100 cP at ambient temperature [542]. This is high and limits mass transfer processes, resulting in low leaching kinetics. It can be reduced by 10–30 times through addition of water [543]. However, the amount of water added has to be limited as it significantly affects the hydrogen bonding in the DES, which in turn affects the leaching kinetics and dissolution processes [543].

Compared with those on hydrophilic DESs, investigations on the utilization of hydrophobic DESs, which usually have a low polarity, high viscosity and lower ionic conductivity, are limited [544,545]. Osch et al [546] showed the possibility to selectively remove transition metals from water using decanoic acid and lidocaine. Since then, several more hydrophobic DESs have been developed and used to extract In and Au. However, no application of hydrophobic DESs to the recycling of batteries has been reported, which could be a fruitful research direction to pursue [547,548].

In addition to tuning the properties of the DESs, researchers have also attempted other means to improve the DES leaching efficiency. For example, Chen *et al* (2021) [549] showed that Co, Li and Mn could be recovered together in a two-step process where formic acid was first used to selectively extract Li, followed by DES extraction of Co and Mn before the final separation step using Na_2CO_3 as the precipitation reagent. Peeters *et al* [550] showed that the addition of Al or Cu could reduce Co(III) in the black mass to Co(II), thus improving the leaching efficiency. Application of UV light to DES leaching was shown to affect the leaching efficiency which can be attributed to the absorption of UV light of Choline compounds [551]. Exposure of DES leaching to microwave irradiation was also shown to improve leaching kinetics [552]. However, due to its high energy density, microwave could cause DES to decompose. As this would affect the reusability of DES, the mechanism by which the leaching kinetics is improved needs to be carefully assessed.

To recover the leached metal ions from DES, precipitation is the preferred method. The addition of oxalic acid to the DES after leaching results in precipitation of the transition metals of Co, Ni and Mn in the LIBs in the form of their respective oxalates, which is further oxidized to produce their oxides [553–555]. Other reagents such as NaOH and Na_2CO_3 have also been used to precipitate the different metal oxides [534,540,556,557]. In contrast, little has been investigated of metal/metal oxide recovery from DES using electrodeposition wherein mainly metals and their alloys could be recovered [558,559].

Although studies have shown that DESs are an excellent media to leach various metal ions from the black mass, issues related to recovery, reuse of DES in the process remain a challenge. For electrochemical recovery, due to the limited electrochemical potential window, not all the metal ions can be electrodeposited [534]. The precipitation technique usually leads to a change in the hydrogen bonding and therefore the performance of DES deteriorates in its reuse. The maximum number of reuses of an oxalic acid-based DES was shown to be 15 [555]. For other DESs, it would be even lower. Therefore, a combination of precipitation, electrochemical recovery and solvent extraction might be required to improve the recovery of metals/metal oxides from DES while minimizing changes to the DES to allow its reuse for further leaching.

12.2.4. *Comparison of industrial recycling processes*

Industrial scale recycling efficiencies of companies using the three materials recovery technologies discussed before are shown in Table 3. These are much lower than the reported lab-scale leaching efficiencies where near 100 % of the metals in the black mass have been reported to be extracted into the solution. This is expected as the recycling efficiency of a whole multi-step process would always be lower than the efficiency of any single step process and, in the case of an industrial scale recycling efficiency, the effect of scaling-up also comes into play. Nevertheless, it is evident that, from both the data shown in Table 3 and literature results from lab scale research, the efficiency of hydrometallurgy is the highest while that of pyrometallurgy is the lowest.

A spider chart comparison of the three technologies on other performance measures such as cost, requirement on pre-treatment, process maturity/reliability, and waste generation is shown in Fig. 36a) [539]. Considering process maturity and requirements on pre-treatment, pyrometallurgical process is favourable. From the perspective of waste generation and the recovery rates of critical materials, direct recycling is better. Taking all performance measures into consideration as a whole, as well as process profitability that is now included in the chart, however, hydrometallurgy is the best.

Many studies confirmed that producing LIBs from recycled materials is environmentally less intensive than producing them from virgin materials/ores, despite that recycling processes themselves generate net emissions [511]. One example of such studies on emission from recycling processes is shown in Fig. 36b). It can be seen that CO_2 equivalent emissions from the recycling processes

Table 3
Industrial recycling processes in Europe and their recycling efficiency.

Name	Group	Recycling efficiency	Reference
Akkuser Oy	Direct physical full process	50–90 %	[535,560]
Duesenfeld GmbH	Direct physical full process	72 %	[561]
Umicore	Pyro-metallurgical refinement	50–61 %	[562]
Duesenfeld GmbH	Hydro-metallurgical full process	91 %	[563]

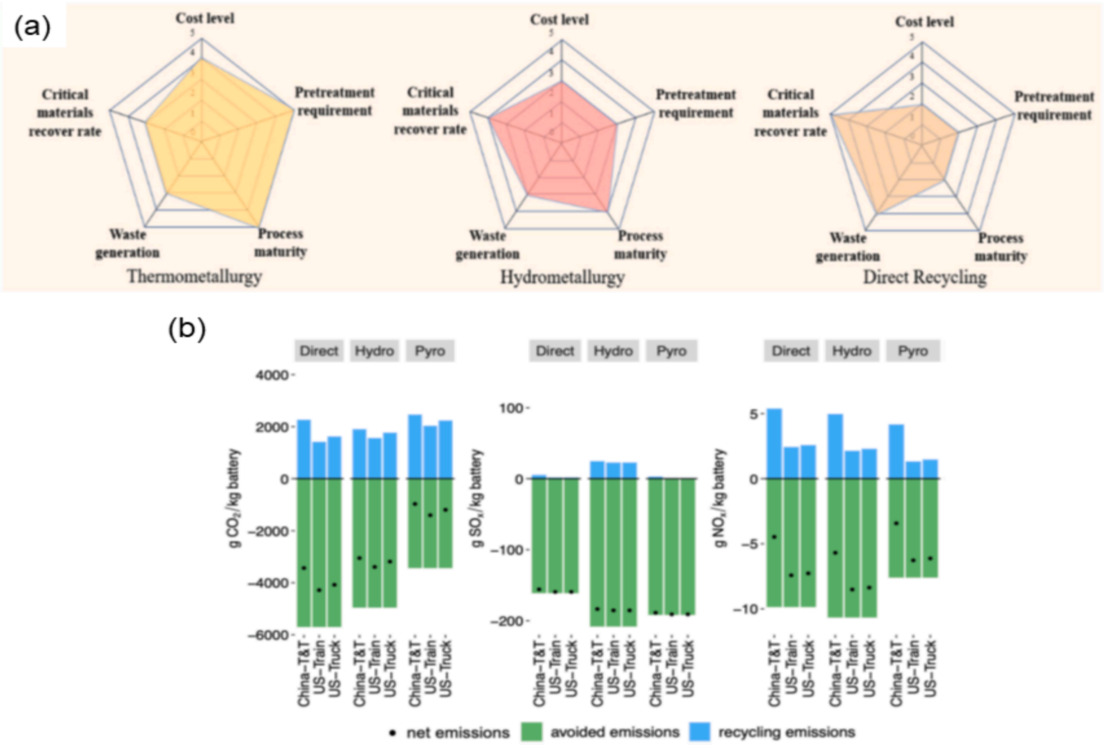

Fig. 36. Comparison of industrial recycling processes in terms of (a) performance measures (b) environmental impact. Reproduced from Refs. [511,539] with permission from Elsevier, Copyright 2022 and 2024.

themselves differ among the technologies investigated. Pyrometallurgical process generates more CO$_2$ emission than the two other recycling processes, whereas hydrometallurgical process results in higher SO$_x$ emissions [564]. It should also be noted that, for the same recycling technology, the CO$_2$ and NO$_x$ emissions in China are lower than those in the US. These results agree with those of Ciez and Whitacre [564] wherein pyrometallurgical recycling route was shown to result in the most emissions on treating both cylindrical and pouch cells.

12.3. Issues and challenges

Despite the fact that recycling of LIBs has been implemented at industrial scale in China, Korea, USA and Europe, it is still at its early stages and is facing many challenges including the economic feasibility and sustainability of the materials recovery processes themselves [511,564].

Accurate data on recycling rates are difficult to obtain and some disagreements exist in literature on their estimates. It is certain, however, that recycling rates vary significantly from region to region and are overall low [508,565]. The rate is strongly dependent on the locally applicable government policies and regulations [565]. Higher recycling rates are associated with clear and strict recycling policies and related government supports. As the major LIB manufacturing countries, China and South Korea have respectively developed a series of policies for the treatment and recycling of spent LIBs [566]. Similarly, as the major consumers and developed countries with strict environmental protection acts, the US, EU and Japan also have specific policies on spent LIBs and EV batteries [567]. Summaries of some of the typical policies on spent LIB recycling can be found in several reviews [61,568]. It should be noted that policies concerning battery recycling are frequently reviewed and revised. A typical example that is often cited is the 2019 Proposal for a Regulation of the European Parliament and of the Council, which is a modification of a 1991 Directive, namely, Council Directive 91/157/EEC [513,569].

Another significant challenge in the recycling of spent LIBs from the EVs is the dismantling of the modules and packs, and the opening of individual battery cells. As can be observed from Fig. 37, the LIBs used in the current EVs are produced in three different shapes, namely, cylindrical, prismatic and pouch. They are also packed in different ways into modules that are connected into a battery pack. In addition to the shape differences, the size of the individual cells is also different. These differences makes it difficult to dismantle the battery module into individual cells that they are largely done manually [567]. Not only is this a slow and low efficient process but it also poses dangers to the workers performing the duty due to possible residual charges in the battery cells.

In pursuit of performance improvements of the LIBs, researchers and manufacturers have constantly been changing the chemistry of the batteries, particularly that of the active cathode materials, from the first commercial LCO to the current NMC of different ratios and NCA [516]. This has created an additional layer of complexity for the recycling and materials recovery processes as different

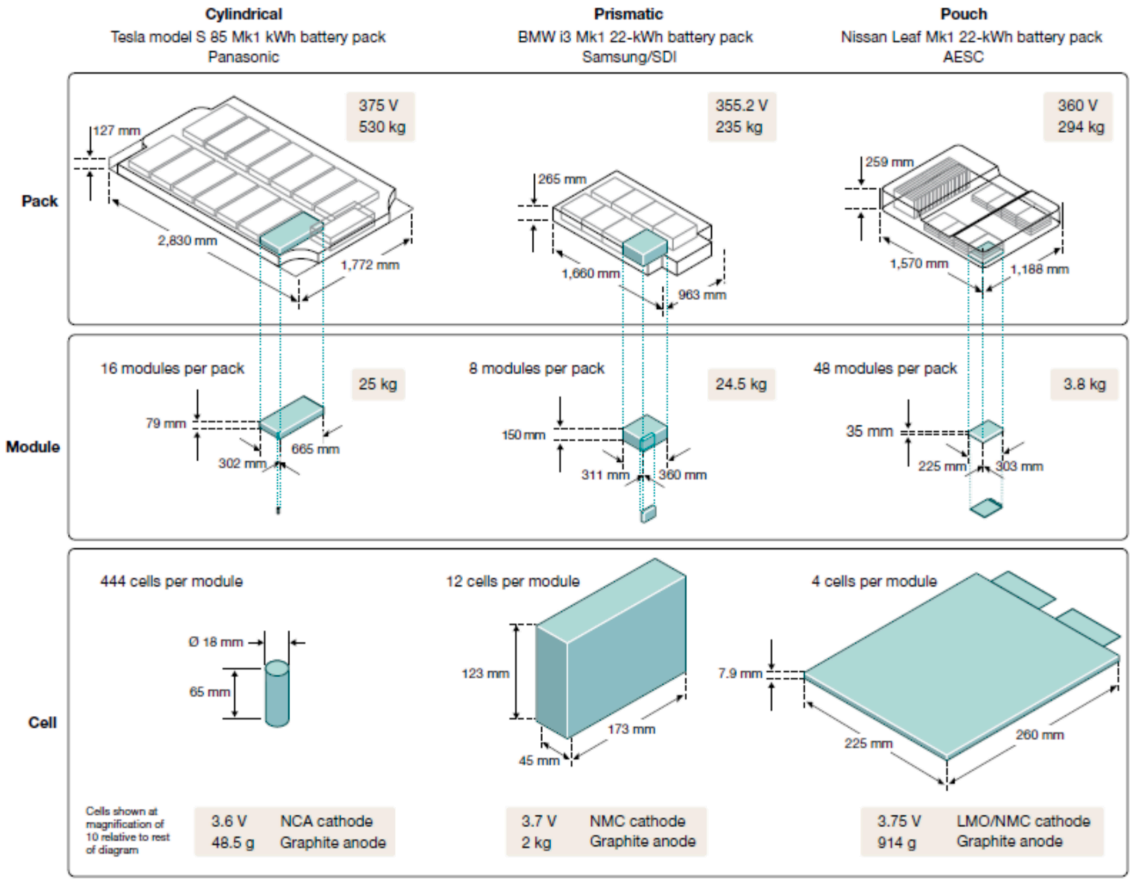

Fig. 37. Different battery types and battery packs used in automobile industries. Reproduced from Ref. [571] with permission from Nature, Copyright 2019.

electrode materials require different recovery processes. At present, there is no compulsory labelling of LIBs to provide their chemical compositions. It is therefore highly probable to mix spent LIBs of very different chemistries from different sources and have them go through the same processing technology for materials recovery, which renders the recovery process inefficient [513].

As mentioned before, life cycle assessment (LCA) studies conducted on the three technologies used at commercial scale reported that, in absolute terms, all technologies used for material recovery consume substantial amount of energy and release sizeable effluents. Significant improvements can be made to reduce the secondary pollution from the materials recovery processes themselves [570].

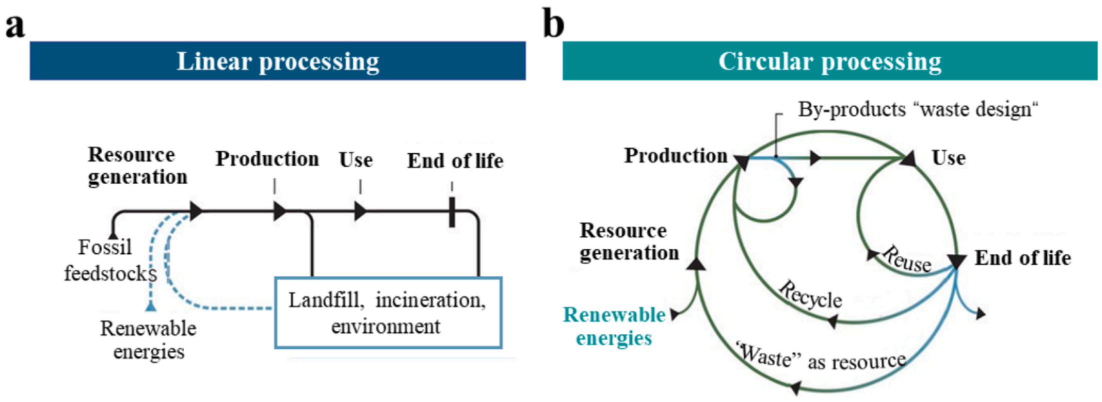

Fig. 38. Principles of (a) Linear; and (b) Circular Economy. Reproduced from Ref- [572] with permission from American Association for the Advancement of Science, Copyright 2020.

12.4. Circular economy, sustainability and battery design

In a conventional and currently dominant linear economy (LE), the mode of development is succinctly described as largely "take-make-discard". The process is illustrated in Fig. 39a) [572]. New products are developed to satisfy the needs of the society and are produced mostly with virgin raw materials from non-renewable natural reserves. The focus is on their functionalities. When they reach the end of their useful life, the product is discarded as waste. Some efforts have been devoted recently to using energy from renewable sources and recycling the end-of-life products, as illustrated in the blue dotted lines in Fig. 38a). While these efforts have achieved some successes in reducing natural resource depletion and negative environmental impacts, it's far from realizing the UN's sustainable development goals [513].

An alternative development model, circular economy (CE), was proposed to counter this unsustainable practice. The core principles of a CE are to (1) design out waste and pollution, (2) use products and materials for a longer period, and (3) re-generate natural ecosystems [573]. The implementation of a CE involves making the product go through different options to keep the material flow in a closed loop, as shown in Fig. 38b). Applied to the LIB industry, or secondary battery industry in general, the loops in Fig. 38b) represent the cascaded uses of LIBs (Reuse), recovering materials from recycled spent LIBs for the production of new LIBs (Recycle), and, recovering materials from recycled spent LIBs for the production of other products, e.g. functional materials ("Waste" as resource).

Clearly, the shorter the loop, the more sustainable the development as it involves fewer processing steps thus consumes less energy. Consequently, implementation of a CE for the battery industry should consider improvements on the extended usage (Reuse) in preference to the recycling of LIBs at the end of their useful lives. To date, however, much of the efforts in research and commercialization are on the materials recovery from the spent LIBs, particularly the "Recycle" loop in Fig. 38b) where a majority of the recovered materials are used as the feeds for the production of new LIBs [508]. Cascaded uses of LIBs, in comparison, received limited attention [570]. In fact, only continued use of LIBs retired from the EV power packs for other purposes that have less stringent demand on the power from the LIBs such as power systems, termed "second life" (SL), was considered [569]. Further, SL is often considered in the context of an alternative to recycling for materials recovery instead of as the primary intent. This is because, even though SL for the retired EV LIBs is an excellent idea, its implementation on the currently retired EV LIBs using technologies available to date encounters numerous challenges. Among them, the accurate determination of the state of the health (SoH) and the remaining life span of the retired EV batteries, degradation and therefore performance variations of individual battery cells within each pack/module, and difficulties in removing individual non-performing battery cells from a module to restore the performance of the module have been identified as issues that need to be addressed urgently [567–570].

From a technical perspective, most of the difficulties mentioned in the SL of retired EV LIBs, and the recycling of the spent individual battery cells, can be overcome if the battery cells, and battery systems (e.g. modules and packs) are designed with the intention to have cascaded uses and recycling at the end. Further, the impacts of battery design on the sustainability of a battery system (cell, module or pack) are also reflected in the quantity of energy and materials required, and emissions generated, during the manufacturing process; the useful life of the battery; the energy consumption and emission during the use phase; and the recyclability and potential pollution to the environment from recycling at the end of its life.

There are three levels of design for EV batteries with the most fundamental one being at the battery cell level [61,569]. To design out waste and pollution, battery chemistry must be selected using green chemistry principles. This approach dictates the use of least toxic and recyclable materials as feedstock while aiming to achieve maximum functionality (e.g. power density, safety and cycle

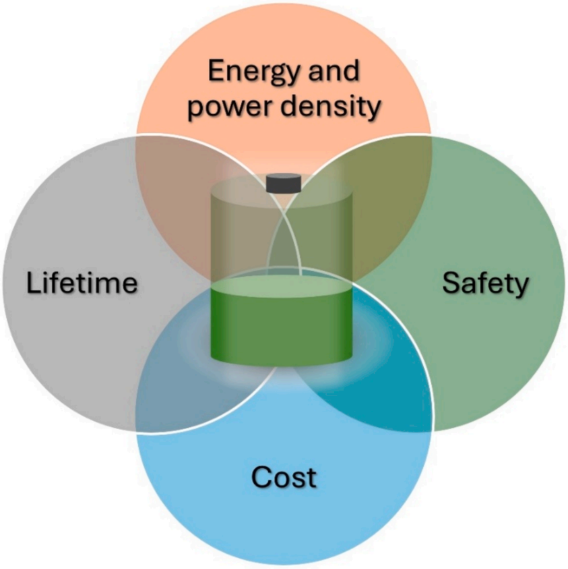

Fig. 39. Important issues that need to be improved in battery systems.

stability) with minimum hazards [508]. The materials are not limited only to those for active electrodes and electrolytes, but also include the binders and separators. Physical geometry and structure of the cells that facilitate the automation of cell opening are also essential for industrial scale operation of battery recycling [569].

At the battery module and pack levels, better designs of connectivity between battery cells in a module and that between modules in a pack are required for the automation of dissembling of individual cells from modules and modules from the pack [567,569]. A new design that uses a rigid busbar to mechanically connect the blade battery cells in a battery pack, which avoided the use of flexible cables thus significantly simplifies the disassembly process, has been proposed and implemented by the Chinese EV producer BYD [574].

Sensors and diagnostic technologies are essential to ensure the safety of the battery cells and systems [568]. They are also becoming increasingly important in improving the sustainability of the LIB industry. Embedment of diagnostic sensors in cells enables real-time monitoring of state of charge (SoC) and SoH of the individual cells during the use phase. This information would also aid the automatic and rapid sorting of battery cells for cascaded use. Inclusion of an electronic ID in each battery cell would facilitate the identification of the cells including their chemistry, size and safety precautions, which is required for the determination on material recovery routes at the end their useful lives [569].

It must be noted that, similar to the situation for SL of the retired EV LIBs, research on purposely recovering the materials from recycled spent LIBs for other uses, i.e. the “Waste as resource” loop in Fig. 38b), is also very limited. However, from both the sustainability and economic benefit perspective, this route could be just as beneficial as the “Recycle” loop. In an excellent and comprehensive review, Yu *et al.* [539] presented detailed potential applications of the recovered materials from spent LIBs, which include production of different types of catalysts, absorbents and electrode materials for other battery types, e.g. sodium ion batteries. Further research efforts in this direction will certainly be fruitful.

In a study investigating the development of circular business models (CBMs) for LIBs, Wrålsen et al. [575] surveyed 45 experts from business and academia as panel members and identified that the most critical driver for CBMs for the LIB industry is national and international regulations and policies; the most critical barrier is financial viability; and the most critical stakeholders are governments and EV manufacturers [575]. True sustainability, or a circular economy, cannot be achieved without concerted efforts from governments across the globe, and close collaborations between the governments, manufacturers, recyclers and end-users. Among these stakeholders, the governments play the most critical role in driving the development and implementation of a CE. In addition to development and enforcement of clear and consistent recycling policies, they must facilitate the establishment of recycling networks and supply chains for spent batteries, as well as provide subsidies and incentives to improve the financial profitability of the recycling process [567]. For the manufacturers, one of the priorities must be the development of industry-wide standards that enable automation of disassembly of battery modules and packs, and the sorting and opening of individual battery cells [570]. Close collaborations of recyclers with manufacturers and end-users are required to achieve optimal cascaded uses of serviceable batteries and recycling of end-of-life batteries, and to minimize illegal accumulation or disposal of spent batteries [61,513,576].

12.5. Conclusion and future prospects

Continued increase in the production and use of secondary batteries has brought about two immediate consequences, namely, the ever-increasing demand on the raw materials for the manufacturing of the batteries and the rapid accumulation of batteries reaching their end of useful lives. Recycling of spent secondary batteries offer a great opportunity to recover the valuable materials and energy while minimizing environmental pollutions. However, significant challenges remain in the sustainability of the secondary battery industry. Using LIBs as a case study, this review presents the following conclusions and future prospects, which are equally applicable to the broader secondary battery industry as a whole.

13. Conclusions

1. The quantity of spent LIBs is accumulating at an increasing pace. The processing capacity of commercial scale recycling of spent LIBs is lagging far behind. There are many contributing factors to this situation including a lack of established spent LIB supply chains, and technical challenges posed by ever changing battery chemistries and varying battery system designs. However, the biggest barrier is its low financial viability.
2. Most of the spent LIB recycling companies use a combination of direct recycling and hydrometallurgical processes with some simple initial stage thermal treatments to recover the valuable metals. Pyrometallurgical processes, in contrast, have been used to treat large quantities of spent LIBs, due to their ability to process them without crushing the cells. However, they often only recover the metals from the spent LIBs in forms of low-grade alloys and require hydrometallurgical processes to upgrade.
3. Governments of different levels play a key role in influencing the recycling of spent batteries, particularly the recycling rates and the financial viability of the recycling operators. The means that they can use to achieve that include implementing clear policies to ban unlawful disposal of spent batteries; offering incentives for wider public participation and providing investment in infrastructure for spent battery collection and preliminary processing, and subsidies to commercial recycling operators to improve their profitability.
4. Research on the technical aspects of materials recovery from spent LIBs has been very active. Most of the research works focus on one or two processing steps, such as leaching, purification and separation, in the multi-step materials recovery process. Much of the current research emphasis is on developing recovery processes with minimum secondary pollutions from the process itself.

Hydrometallurgical treatments of active electrode materials from spent LIBs using cheap organic agents including agroindustry wastes and deep eutectic solvents as the leaching lixiviant are currently attracting the most attention.

5. CE is a better model than the existing LE for the sustainable development of society. It involves many phases in the course of a product life including extended/cascaded use phase and recycling is the last phase that closes the material circulation loop. While commercial recycling of spent LIBs is gathering momentum, cascaded use of retired EV LIBs faces many technical and economic challenges and is yet to reach a meaningful scale.
6. The impacts of design of a product on its sustainability far outweigh those from the recycling of the product at the end of its useful life. The present spent LIBs were designed and produced largely for their functionalities with little consideration on their sustainability, particularly their recyclability at the end of their useful lives. Attention to design to improve the sustainability of the LIB industry is growing with calls for a paradigm shift at the design phase to incorporate green chemistry principles at the cell level and CE principles at the module and pack levels for the EV batteries.

14. Future prospects

1. Achieving a true circular economy for the secondary battery industry requires concerted efforts from and close collaborations between the governments, manufacturers, recyclers and end-users. Among these stakeholders, the governments play the most critical role. In addition to development and enforcement of clear and consistent recycling policies, they must facilitate the establishment of recycling networks and supply chains for spent batteries, as well as provide subsidies and incentives to improve the financial profitability of the recycling process. For the manufacturers, one of the priorities must be the development of industry-wide standards that enable automation of disassembly of battery modules and packs, and the sorting and opening of individual battery cells. Close collaborations of recyclers with manufacturers and end-users are required to achieve optimal cascaded uses of serviceable batteries and recycling of end-of-life batteries, and to minimize illegal accumulation or disposal of spent batteries.
2. Cascaded use of retired LIBs from EVs is a major option in a CE but is an area that is less explored. This option faces many challenges such as accurate determination of the SoH and prediction of the remaining lifetime. However, the most challenging factor is the rapid price decrease of new LIBs. With much reduced uncertainties in their performances, low price virgin LIBs markedly diminish the economic benefits of the used but serviceable LIBs. Practicable criteria need to be developed to maximize the usage of EV LIBs before being recycled for materials recovery.
3. Economically viable sensor technologies that can be applied at the battery cell level and readily integrated into the module and pack levels are becoming increasingly important. Information to be gathered include SoC, SoH and cell temperature, as well as identification of cell chemistry. While many technologies are technically capable to perform such tasks, their applicability economically at a large scale to the harsh working conditions in an EV battery pack is yet to be demonstrated.
4. For the foreseeable future, hydrometallurgical approach will continue to be the dominant means for materials recovery from the spent LIBs. Although the use of organic agents and DESs proved to be more environmentally friendly, its economic viability and the prospect of its integration into the overall recovery process need to be assessed at the commercial scale.
5. Open loop or “Waste to resource” recycling, is also a fruitful option for the spent batteries. Areas of potential applications of the materials thus recovered include catalysts, absorbents and sensors. This option needs to be examined more closely and compared against the close loop recycling.

Secondary battery technologies are still at their early developing stage. The industry is evolving with many industry-wide standards yet to be established. It will take some time for the industry to mature and build an industry ecosystem that includes cascaded uses of the batteries and recycling of the spent batteries at the end of their useful lives.

15. Conclusions

The energy transition, the need to power a growing number of diverse portable electronic devices, the quick adoption of electric cars, and other pertinent factors have made research and technology in the field of energy storage systems a rapidly developing field. Batteries are one of the most fascinating systems in this regard, for a variety of uses.

There are different batteries including lithium-ion batteries, beyond lithium-ion batteries, solid state batteries, printed batteries, structural batteries, flexible batteries, microbatteries, and biodegradable batteries, among others, that have been extensively covered in this review, indicating also the main areas for improvement, as represented in Fig. 39.

For each type of battery, the most used materials, geometries, performance parameters and applications have been presented. Furthermore, each chapter on battery types discusses future challenges where innovations are being applied and/or needed at many levels, primarily through the use of novel materials for the various battery components to enhance performance and safety while lowering environmental impact. Additionally, novel concepts emerge such as batteries specifically designed for particular application, in which the performance parameters are just the ones needed for a successful functional response. Thus, overall performance can be reduced while improving sustainability. Overall, the present review demonstrates a living and rapidly evolving field, essential for the energy transition required for a more sustainable society and economy.

Orcid

Carlos M. Costa, Orcid ID: 0000–0001-9266–3669.

Manuel Salado: Orcid ID: 0000–0001-5276–6233.

Chiara Ferrara, Orcid ID: 0000–0002-5834–8646.

Riccardo Ruffo, Orcid ID: 0000–0001-7509–7052.
Piercarlo Mustarelli, Orcid ID: 0000–0001-9954–5200.
Rui Mao, Orcid ID: 0000–0003-0264–5665.
Sheng Feng, Orcid ID: 0000–0001-8402–8139.
Yuxiang Shang, Orcid ID: 0000–0003-3875-277X.
Xiaochen Wang, Orcid ID: 0000–0002-8529–2473.
Zhenkun Lei, Orcid ID: 0000–0002-4077–4305.
Ruixiang Bai, Orcid ID: 0009–0000-0712–8558.
Cheng Yan, Orcid ID: 0000–0002-4909-439X.
Kwon-Hyung Lee, Orcid ID: 0000–0003-4868–5937.
Sang-Woo Kim, Orcid ID: 0000–0002-0079–5806.
Tae-Hee Kim, Orcid ID: 0000–0002-6650–0134.
Sang-Young Lee, Orcid ID: 0000–0001-7153–0517.
Long Kong, Orcid ID: 0000–0002-6284–9478.
Qiang Zhang, Orcid ID: 0000–0002-3929–1541.
Harsha Devnani, Orcid ID: 0009–0005-0187-779X.
Shikha Gupta, Orcid ID: 0000–0003-3734–4045.
James F. Rohan, Orcid ID: 0000–0003-0415–1140.
Neil Curtis, Orcid ID: 0000–0002-6565–6807.
Abhishek Lahiri, Orcid ID: 0000–0001-8264–9169.
Yinghe He, Orcid ID: 0000–0003-4252–5414.
S. Lanceros-Mendez, Orcid ID: 0000–0001-6791–7620.

CRediT authorship contribution statement

Carlos M. Costa: Writing – review & editing, Writing – original draft, Investigation, Conceptualization. **Manuel Salado:** Writing – review & editing, Writing – original draft, Investigation. **Chiara Ferrara:** Writing – review & editing, Writing – original draft, Investigation. **Riccardo Ruffo:** Writing – review & editing, Writing – original draft, Investigation. **Piercarlo Mustarelli:** Writing – review & editing, Writing – original draft, Investigation. **Rui Mao:** Writing – review & editing, Writing – original draft, Investigation. **Sheng Feng:** Writing – review & editing, Writing – original draft, Investigation. **Yuxiang Shang:** Writing – review & editing, Writing – original draft, Investigation. **Xiaochen Wang:** Writing – review & editing, Writing – original draft, Investigation. **Zhenkun Lei:** Writing – review & editing, Writing – original draft, Investigation. **Ruixiang Bai:** Writing – review & editing, Writing – original draft, Investigation. **Cheng Yan:** Writing – review & editing, Writing – original draft, Investigation. **Kwon-Hyung Lee:** Writing – review & editing, Writing – original draft, Investigation. **Sang-Woo Kim:** Writing – review & editing, Writing – original draft, Investigation. **Tae-Hee Kim:** Writing – review & editing, Writing – original draft, Investigation. **Sang-Young Lee:** Writing – review & editing, Writing – original draft, Investigation. **Long Kong:** Writing – review & editing, Writing – original draft, Investigation. **Qiang Zhang:** Writing – review & editing, Writing – original draft, Investigation. **Harsha Devnani:** Writing – review & editing, Writing – original draft, Investigation. **Shikha Gupta:** Writing – review & editing, Writing – original draft, Investigation. **James F. Rohan:** Writing – review & editing, Writing – original draft, Investigation. **Neil S. Curtis:** Writing – review & editing. **Abhishek Lahiri:** Writing – review & editing, Writing – original draft, Investigation. **Yinghe He:** Writing – review & editing, Writing – original draft, Investigation. **S. Lanceros-Mendez:** Writing – review & editing, Writing – original draft, Investigation, Conceptualization.

Declaration of competing interest

The authors declare that they have no known competing financial interests or personal relationships that could have appeared to influence the work reported in this paper.

Acknowledgements

The authors thank the Fundação para a Ciência e Tecnologia (FCT) for financial Support under the framework of Strategic Funding UID/ 04650: Physics Centre of Minho and Porto Universities (CF-UM-UP), UIDB/04650/2020, UID/FIS/04650/2020, UID/EEA/ 04436/2020, and UID/QUI/00686/2020 and under projects POCI-01-0247-FEDER-046985, and 2022.03931. PTDC funded by national funds through FCT and by the ERDF through the COMPETE2020—Programa Operacional Competitividade e Internacionalização (POCI). NGS-New Generation Storage, C644936001-00000045, supported by IAPMEI (Portugal) with funding from the European Union NextGenerationEU (PRR). The author also thank the FCT for financial support under FCT investigator 2020.04028. CEECIND (DOI:10.54499/2020.04028.CEECIND/CP1600/CT0018) (C.M.C.). M.S acknowledges the funding from the European Union H2020 Program under the Marie Curie global fellowship (ROCHE, 101026163). This study forms part of the Advanced Materials program and was supported by MCIN with funding from European Union NextGenerationEU (PRTR-C17.I1) and by the Basque Government under the IKUR program and Elkartek programs. The authors thank for technical and human support provided by SGIker (UPV/EHU/ ERDF, EU).

This work was supported by the Basic Science Research Program through the National Research Foundation of Korea (NRF) funded by the Ministry of Science and ICT (RS-2024-00344021). The authors thank BBSRC (BB/X011445/1) for financial support. Cheng Yan appreciate the financial support from two ARC Discovery Projects (DP250102887 and DP250102885).

The authors also acknowledge support from the Science Foundation Ireland (SFI)/Research Ireland (RI) Connect Research Centre project co-funded by the European Regional Development Fund under Grant Number 13/RC/2077_P2, and the Sustainable Energy Authority of Ireland (SEAI) BatterySense project under Grant Number RDD 864.

Data availability

Data will be made available on request.

References

[1] Holechek JL, Geli HME, Sawalhah MN, Valdez R. A Global Assessment: Can Renewable Energy Replace Fossil Fuels by 2050? Sustainability 2022;14(8):4792.

[2] Abbasi T, Abbasi SA. Decarbonization of fossil fuels as a strategy to control global warming. Renew Sustain Energy Rev 2011;15(4):1828–34.

[3] Al-Ghussain L. Global warming: review on driving forces and mitigation. Environ Prog Sustain Energy 2019;38(1):13–21.

[4] Zhang L, Jia C, Bai F, Wang W, An S, Zhao K, et al. A comprehensive review of the promising clean energy carrier: Hydrogen production, transportation, storage, and utilization (HPTSU) technologies. Fuel 2024;355:129455.

[5] I.B. Boa Morte, O.d.Q.F. Araújo, C.R.V. Morgado, J.L. de Medeiros, Electrification and decarbonization: a critical review of interconnected sectors, policies, and sustainable development goals, Energy Storage and Saving 2(4) (2023) 615-630.

[6] Hassan Q, Algburi S, Sameen AZ, Salman HM, Jaszczur M. A review of hybrid renewable energy systems: Solar and wind-powered solutions: Challenges, opportunities, and policy implications. Results Eng 2023;20:101621.

[7] Sayed ET, Olabi AG, Alami AH, Radwan A, Mdallal A, Rezk A, et al. Renewable Energy and Energy Storage Systems. Energies 2023;16(3):1415.

[8] El Haj Assad M, Khosravi A, Malekan M, Rosen MA, Nazari MA. Chapter 14 - Energy storage. In: Assad MEH, Rosen MA, editors. Design and Performance Optimization of Renewable Energy Systems. Academic Press; 2021. p. 205–19.

[9] Yoo HD, Markevich E, Salitra G, Sharon D, Aurbach D. On the challenge of developing advanced technologies for electrochemical energy storage and conversion. Mater Today 2014;17(3):110–21.

[10] De Carne G, Maroufi SM, Beiranvand H, De Angelis V, D'Arco S, Gevorgian V, et al. The role of energy storage systems for a secure energy supply: A comprehensive review of system needs and technology solutions. Electr Pow Syst Res 2024;236:110963.

[11] Amir M, Deshmukh RG, Khalid HM, Said Z, Raza A, Muyeen SM, et al. Energy storage technologies: An integrated survey of developments, global economical/environmental effects, optimal scheduling model, and sustainable adaption policies. J Storage Mater 2023;72:108694.

[12] Noori A, El-Kady MF, Rahmanifar MS, Kaner RB, Mousavi MF. Towards establishing standard performance metrics for batteries, supercapacitors and beyond. Chem Soc Rev 2019;48(5):1272–341.

[13] Yang F, Song X, Dong G, Tsui K-L. A coulombic efficiency-based model for prognostics and health estimation of lithium-ion batteries. Energy 2019;171:1173–82.

[14] Ramasubramanian B, Ling J, Jose R, Ramakrishna S. Ten major challenges for sustainable lithium-ion batteries. Cell Rep Phys Sci 2024;5(6).

[15] Finkelstein SH, Ricci M, Bötticher T, Schmidt-Rohr K. How lithium-ion batteries work conceptually: thermodynamics of Li bonding in idealized electrodes. PCCP 2024;26(36):24157–71.

[16] Meng J, Guo H, Niu C, Zhao Y, Xu L, Li Q, et al. Advances in Structure and Property Optimizations of Battery Electrode Materials. Joule 2017;1(3):522–47.

[17] Heard DM, Lennox AJJ. Electrode Materials in Modern Organic Electrochemistry. Angew Chem Int Ed 2020;59(43):18866–84.

[18] Fleischmann J, Hanicke M, Horetsky E, Ibrahim D, Jautelat S, Linder M, et al. Battery 2030: Resilient, sustainable, and circular. McKinsey & Company 2023:2–18.

[19] Njema GG, Ouma RBO, Kibet JK. A Review on the Recent Advances in Battery Development and Energy Storage Technologies. Journal of Renewable Energy 2024;2024(1):2329261.

[20] Lehtimäki H, Karhu M, Kotilainen JM, Sairinen R, Jokilaakso A, Lassi U, et al. Sustainability of the use of critical raw materials in electric vehicle batteries: A transdisciplinary review. Environ Challenges 2024;16:100966.

[21] Chen Y, Kang Y, Zhao Y, Wang L, Liu J, Li Y, et al. A review of lithium-ion battery safety concerns: The issues, strategies, and testing standards. Journal of Energy Chemistry 2021;59:83–99.

[22] Machín A, Morant C, Márquez F. Advancements and Challenges in Solid-State Battery Technology: An In-Depth Review of Solid Electrolytes and Anode Innovations. Batteries 2024;10(1):29.

[23] Mottaghi M, Pearce JM. A Review of 3D Printing Batteries. Batteries 2024;10(3):110.

[24] Costa CM, Gonçalves R, Lanceros-Méndez S. Recent advances and future challenges in printed batteries. Energy Storage Mater 2020;28:216–34.

[25] Barbosa JC, Fidalgo-Marijuan A, Dias JC, Gonçalves R, Salado M, Costa CM, et al. Molecular design of functional polymers for organic radical batteries. Energy Storage Mater 2023;60:102841.

[26] Jin T, Singer G, Liang K, Yang Y. Structural batteries: Advances, challenges and perspectives. Mater Today 2023;62:151–67.

[27] Ghasemi Yeklangi A, Ghafari A, Asgari Sima F, Akbari S. Advancing lithium-ion battery manufacturing: novel technologies and emerging trends. J Appl Electrochem 2024;54(12):2653–82.

[28] IEA, Global EV Outlook 2024, IEA, Paris https://www.iea.org/reports/global-ev-outlook-2024, Licence: CC BY 4.0, 2024.

[29] Li J, Fleetwood J, Hawley WB, Kays W. From Materials to Cell: State-of-the-Art and Prospective Technologies for Lithium-Ion Battery Electrode Processing. Chem Rev 2022;122(1):903–56.

[30] Toki GFI, Hossain MK, Rehman WU, Manj RZA, Wang L, Yang J. Recent progress and challenges in silicon-based anode materials for lithium-ion batteries. Ind Chem Mater 2024;2(2):226–69.

[31] Kim T. The origin of the aggressive degradation of Ni-rich transition metal oxide cathodes for high-energy density lithium-ion batteries. J Solid State Chem 2022;310:123040.

[32] Tagawa K, Brodd RJ. Production Processes for Fabrication of Lithium-Ion Batteries. In: Yoshio M, Brodd RJ, Kozawa A, editors. Lithium-Ion Batteries: Science and Technologies. New York, New York, NY: Springer; 2009. p. 181–94.

[33] Sharma R, Kumar H, Kumar G, Sharma S, Aneja R, Sharma AK, et al. Progress and challenges in electrochemical energy storage devices: Fabrication, electrode material, and economic aspects. Chem Eng J 2023;468:143706.

[34] Ryu M, Hong Y-K, Lee S-Y, Park JH. Ultrahigh loading dry-process for solvent-free lithium-ion battery electrode fabrication. Nat Commun 2023;14(1):1316.

[35] Heidbüchel M, Schultz T, Placke T, Winter M, Koch N, Schmuch R, et al. Enabling Aqueous Processing of Ni-Rich Layered Oxide Cathode Materials by Addition of Lithium Sulfate. ChemSusChem 2023;16(2):e202202161.

[36] Lippke M, Ohnimus T, Frankenberg F, Schilde C, Kwade A. Drying and calendering of Lithium Ion battery electrodes: A combined simulation approach. Powder Technol 2024;444:119984.

[37] Jin W, Song G, Yoo J-K, Jung S-K, Kim T-H, Kim J. Advancements in Dry Electrode Technologies: Towards Sustainable and Efficient Battery Manufacturing. ChemElectroChem 2024;11(17):e202400288.

[38] Sun X, Zhou Y, Li D, Zhao K, Wang L, Tan P, et al. A review of electrospun separators for lithium-based batteries: Progress and application prospects. Carbon Energy 2024;6(9):e539.

[39] Liang Z, Li T, Chi H, Ziegelbauer J, Sun K, Wang M, et al. Solvent-Free Manufacturing of Lithium-Ion Battery Electrodes via Cold Plasma. Energy Environ Mater 2024;7(1):e12503.

[40] Liu X, Zeng Y, Yuan W, Zhang G, Zheng H, Chen Z. Advances in multi-scale design and fabrication processes for thick electrodes in lithium-ion batteries. Energy Rev 2024;3(2):100066.

[41] Deng J, Ren X, Lin H, Hu L, Bai Y, Yu X, et al. Functionally gradient materials for sustainable and high-energy rechargeable lithium batteries: Design principles, progress, and perspectives. Journal of Energy Chemistry 2024;99:426–49.

[42] Zhang X, Hui Z, King ST, Wu J, Ju Z, Takeuchi KJ, et al. Gradient Architecture Design in Scalable Porous Battery Electrodes. Nano Lett 2022;22(6):2521–8.

[43] Pfleging W. A review of laser electrode processing for development and manufacturing of lithium-ion batteries. Nanophotonics 2018;7(3):549–73.

[44] Ju Z, Zheng T, Calderon J, Checko S, Zhang B, Yu G. Scalable Fast-Charging Aligned Battery Electrodes Enabled by Bidirectional Freeze-Casting. Nano Lett 2023;23(18):8787–93.

[45] Dixit MB, Zaman W, Bootwala Y, Zheng Y, Hatzell MC, Hatzell KB. Scalable Manufacturing of Hybrid Solid Electrolytes with Interface Control. ACS Appl Mater Interfaces 2019;11(48):45087–97.

[46] W. Pfleging, Ultrafast laser structuring of electrodes to boost electrochemical performance of lithium-ion batteries, Procédés Laser Pour L'Industrie Conférences (PLI 2023), Rennes, Frankreich, 27.09. 2023–28.09. 2023, 2023.

[47] Huo S, Sheng L, Su B, Xue W, Wang L, Xu H, et al. 3D Printing Manufacturing of Lithium Batteries: Prospects and Challenges toward Practical Applications. Adv Mater 2024;36(8):2310396.

[48] T. B.. Lithium Battery Equipmnet: Everything You Need to Know! 2023.

[49] Naseri F, Gil S, Barbu C, Cetkin E, Yarimca G, Jensen AC, et al. Digital twin of electric vehicle battery systems: Comprehensive review of the use cases, requirements, and platforms. Renew Sustain Energy Rev 2023;179:113280.

[50] Salado M, Lizundia E, Oyarzabal I, Salazar D. The Role of Critical Raw Materials for Novel Strategies in Sustainable Secondary Batteries, physica status solidi (a) 2022;219(15):2100710.

[51] M.a. Markets, Lithium-ion battery market size, share and growth analysis, 2024.

[52] Nitta N, Wu F, Lee JT, Yushin G. Li-ion battery materials: present and future. Mater Today 2015;18(5):252–64.

[53] Xie J, Lu Y-C. A retrospective on lithium-ion batteries. Nat Commun 2020;11(1):2499.

[54] Goodenough JB, Park K-S. The Li-Ion Rechargeable Battery: A Perspective. J Am Chem Soc 2013;135(4):1167–76.

[55] Gören A, Costa CM, Silva MM, Lanceros-Méndez S. State of the art and open questions on cathode preparation based on carbon coated lithium iron phosphate. Compos B Eng 2015;83:333–45.

[56] Mishra AK, Monika BSP. A review on recent advances in anode materials in lithium ion batteries. Mater Today Electron 2024;7:100089.

[57] Wu Q, Zhang B, Lu Y. Progress and perspective of high-voltage lithium cobalt oxide in lithium-ion batteries. Journal of Energy Chemistry 2022;74:283–308.

[58] Costa CM, Gonçalves R, Lanceros-Méndez S. Advances in Cathode Nanomaterials for Lithium-Ion Batteries. In: Zhen Q, Bashir S, Liu JL, editors. Nanostructured Materials for Next-Generation Energy Storage and Conversion: Advanced Battery and Supercapacitors. Berlin Heidelberg, Berlin, Heidelberg: Springer; 2019. p. 105–45.

[59] Britala L, Marinaro M, Kucinskis G. A review of the degradation mechanisms of NCM cathodes and corresponding mitigation strategies. J Storage Mater 2023; 73:108875.

[60] Costa CM, Lee Y-H, Kim J-H, Lee S-Y, Lanceros-Méndez S. Recent advances on separator membranes for lithium-ion battery applications: From porous membranes to solid electrolytes. Energy Storage Mater 2019;22:346–75.

[61] Yang Y, Okonkwo EG, Huang G, Xu S, Sun W, He Y. On the sustainability of lithium ion battery industry – A review and perspective. Energy Storage Mater 2021;36:186–212.

[62] Narayan R, Laberty-Robert C, Pelta J, Tarascon J-M, Dominko R. Self-Healing: An Emerging Technology for Next-Generation Smart Batteries. Adv Energy Mater 2022;12(17):2102652.

[63] Vegge T, Tarascon J-M, Edström K. Toward Better and Smarter Batteries by Combining AI with Multisensory and Self-Healing Approaches. Adv Energy Mater 2021;11(23):2100362.

[64] Fichtner M, Edström K, Ayerbe E, Berecibar M, Bhowmik A, Castelli IE, et al. Rechargeable Batteries of the Future—The State of the Art from a BATTERY 2030 + Perspective. Adv Energy Mater 2022;12(17):2102904.

[65] Moradi Z, Lanjan A, Tyagi R, Srinivasan S. Review on current state, challenges, and potential solutions in solid-state batteries research. J Storage Mater 2023; 73:109048.

[66] Ahmed MD, Maraz KM. Revolutionizing energy storage: Overcoming challenges and unleashing the potential of next generation Lithium-ion battery technology. Materials Engineering Research 2023;5(1):265–78.

[67] Yang Y, Yang S, Xue X, Zhang X, Li Q, Yao Y, et al. Inorganic All-Solid-State Sodium Batteries: Electrolyte Designing and Interface Engineering. Adv Mater 2024;36(1):2308332.

[68] Ahmad H, Kubra KT, Butt A, Nisar U, Iftikhar FJ, Ali G. Recent progress, challenges, and perspectives in the development of solid-state electrolytes for sodium batteries. J Power Sources 2023;581:233518.

[69] Rudola A, Sayers R, Wright CJ, Barker J. Opportunities for moderate-range electric vehicles using sustainable sodium-ion batteries. Nat Energy 2023;8(3): 215–8.

[70] Kim J-S, Yoon G, Kim S, Sugata S, Yashiro N, Suzuki S, et al. Surface engineering of inorganic solid-state electrolytes via interlayers strategy for developing long-cycling quasi-all-solid-state lithium batteries. Nat Commun 2023;14(1):782.

[71] Körber N, Lu Y, Friess B, Birke KP. Meso-scale mechanical characterization of polymeric, oxidic and sulfidic solid-state electrolytes until failure. J Storage Mater 2024;83:110643.

[72] Yang W, Wang J, Jian J. Metal organic framework-based materials for metal-ion batteries. Energy Storage Mater 2024;66:103249.

[73] Zheng M, Li X, Sun J, Wang X, Liu G, Yu W, et al. Research progress on chloride solid electrolytes for all-solid-state batteries. J Power Sources 2024;595: 234051.

[74] Zampardi G, La Mantia F. Open challenges and good experimental practices in the research field of aqueous Zn-ion batteries. Nat Commun 2022;13(1):687.

[75] Li G, Sun L, Zhang S, Zhang C, Jin H, Davey K, et al. Developing Cathode Materials for Aqueous Zinc Ion Batteries: Challenges and Practical Prospects. Adv Funct Mater 2024;34(5):2301291.

[76] Wei J, Zhang P, Sun J, Liu Y, Li F, Xu H, et al. Advanced electrolytes for high-performance aqueous zinc-ion batteries. Chem Soc Rev 2024;53(20):10335–69.

[77] Ge H, Xie X, Xie X, Zhang B, Li S, Liang S, et al. Critical challenges and solutions: quasi-solid-state electrolytes for zinc-based batteries. Energ Environ Sci 2024; 17(10):3270–306.

[78] Kim SC, Gao X, Liao S-L, Su H, Chen Y, Zhang W, et al. Solvation-property relationship of lithium-sulphur battery electrolytes. Nat Commun 2024;15(1):1268.

[79] Wu X, Zhao Y, Li H, Zhou C, Wang X, Du L. Sulfurized polyacrylonitrile as cathodes for advanced lithium–sulfur batteries: advances in modification strategies. Nanoscale 2024;16(10):5060–78.

[80] Zhao M, Peng H-J, Li B-Q, Huang J-Q. Kinetic Promoters for Sulfur Cathodes in Lithium–Sulfur Batteries. Acc Chem Res 2024;57(4):545–57.

[81] Zhou J, Sun A. Redox mediators for high performance lithium-sulfur batteries: Progress and outlook. Chem Eng J 2024;495:153648.

[82] Anchieta CG, Francisco BAB, Júlio JPO, Trtik P, Bonnin A, Doubek G, et al. LiOH Decomposition by NiO/ZrO2 in Li-Air Battery: Chemical Imaging with Operando Synchrotron Diffraction and Correlative Neutron/X-Ray Computed-Tomography Analysis. Small Methods 2024;8(10):2301749.

[83] Zhang X, Zhang G, Yang R, Zhang D, Lian G, Hou C, et al. Lattice-dependent activation of highly efficient SnTe cathode catalyst for Li–air batteries. Energy Storage Mater 2024;69:103392.

[84] Pan K, Li M, Wang W, Xing S, Dou Y, Gao S, et al. A leap by the rise of solid-state electrolytes for Li-air batteries. Green Energy Environ 2023;8(4):939–44.

[85] Zhou T, Shan H, Yu H, Zhong CA, Ge J, Zhang N, Chu W, Yan W, Xu Q, Wu HA, Wu C, Xie Y. Nanopore Confinement of Electrocatalysts Optimizing Triple Transport for an Ultrahigh-Power-Density Zinc–Air Fuel Cell with Robust Stability. Adv Mater 2020;32(47):2003251.

[86] Xu M, Cao R, Hao B, Wang D, Luo D, Dou H, et al. Single-Anion Conductive Solid-State Electrolytes with Hierarchical Ionic Highways for Flexible Zinc-Air Battery. Angew Chem Int Ed 2024;63(36):e202407380.
[87] Wang X, Xi B, Ma X, Feng Z, Jia Y, Feng J, et al. Boosting Zinc-Ion Storage Capability by Effectively Suppressing Vanadium Dissolution Based on Robust Layered Barium Vanadate. Nano Lett 2020;20(4):2899–906.
[88] Adil M, Sarkar A, Sau S, Muthuraj D, Mitra S. Non-aqueous rechargeable calcium-ion batteries based on high voltage zirconium-doped ammonium vanadium oxide cathode. J Power Sources 2022;541:231669.
[89] Chen J, Zhao Z, Niu R, Yao Y, Liang M, Huang Q, et al. Highly stabilized FeS2 cathode design and energy storage mechanism study for advanced aqueous FeS2–Cu battery. J Power Sources 2024;621:235240.
[90] Leung OM, Gordon LW, Messinger RJ, Prodromakis T, Wharton JA, Ponce de León C, et al. Solid Polymer Electrolytes with Enhanced Electrochemical Stability for High-Capacity Aluminum Batteries. Adv Energy Mater 2024;14(8):2303285.
[91] Greim P, Solomon AA, Breyer C. Assessment of lithium criticality in the global energy transition and addressing policy gaps in transportation. Nat Commun 2020;11(1):4570.
[92] Picatoste A, Schulz-Mönninghoff M, Niero M, Justel D, Mendoza JMF. Comparing the circularity and life cycle environmental performance of batteries for electric vehicles. Resour Conserv Recycl 2024;210:107833.
[93] Liu Y-K, Zhao C-Z, Du J, Zhang X-Q, Chen A-B, Zhang Q. Research Progresses of Liquid Electrolytes in Lithium-Ion Batteries. Small 2023;19(8):2205315.
[94] Kainat S, Anwer J, Hamid A, Gull N, Khan SM. Electrolytes in Lithium-Ion Batteries: Advancements in the Era of Twenties (2020's). Mater Chem Phys 2024;313:128796.
[95] Liu M, Zeng Z, Wu Y, Zhong W, Lei S, Cheng S, et al. Reviewing recent progress of liquid electrolyte chemistry for mitigating thermal runaway in lithium–ion batteries. Energy Storage Mater 2024;65:103133.
[96] Zheng Y, Shen Y, Guo J, Li J, Wang J, Ning D, et al. Recent advances in solid-state lithium batteries based on anode engineering. Nano Research Energy 2024;3:e9120118.
[97] Wu M, Han S, Liu S, Zhao J, Xie W. Fire-safe polymer electrolyte strategies for lithium batteries. Energy Storage Mater 2024;66:103174.
[98] Nguyen A-G, Lee M-H, Kim J, Park C-J. Construction of a High-Performance Composite Solid Electrolyte Through In-Situ Polymerization within a Self-Supported Porous Garnet Framework. Nano-Micro Letters 2024;16(1):83.
[99] Sau K, Takagi S, Ikeshoji T, Kisu K, Sato R, dos Santos EC, et al. Unlocking the secrets of ideal fast ion conductors for all-solid-state batteries. Communications Materials 2024;5(1):122.
[100] Raza S, Bashir T, Hayat A, Abd-Rabboh HSM, Shen L, Orooji Y, et al. Recent progress and fundamentals of solid-state electrolytes for all solid-state rechargeable batteries: Mechanisms, challenges, and applications. J Storage Mater 2024;92:112110.
[101] Ko JS, Hamann T, Fortunato J, Augustyn V. Recent Advances in Electrolytes for Enabling Lithium-Ion Batteries across a Wide Temperature Range. J Phys Chem C 2024;128(8):3113–26.
[102] He P, Tang Y, Tan Z, Lei C, Qin Z, Li Y, et al. Solid-state batteries encounter challenges regarding the interface involving lithium metal. Nano Energy 2024;124:109502.
[103] BATTERIES EUROPE SECRETARIAT D3.6-KPIs Benchmarking & Target KPIs. .
[104] Quartarone E, Mustarelli P. Review—Emerging Trends in the Design of Electrolytes for Lithium and Post-Lithium Batteries. J Electrochem Soc 2020;167(5):050508.
[105] Agrawal RC, Pandey GP. Solid polymer electrolytes: materials designing and all-solid-state battery applications: an overview. J Phys D Appl Phys 2008;41(22):223001.
[106] Yang H, Wu N. Ionic conductivity and ion transport mechanisms of solid-state lithium-ion battery electrolytes: A review. Energy Sci Eng 2022;10(5):1643–71.
[107] Galiński M, Lewandowski A, Stępniak I. Ionic liquids as electrolytes. Electrochim Acta 2006;51(26):5567–80.
[108] Armand M. The history of polymer electrolytes. Solid State Ion 1994;69(3):309–19.
[109] Quartarone E, Mustarelli P, Magistris A. PEO-based composite polymer electrolytes. Solid State Ion 1998;110(1):1–14.
[110] Jagan M, Vijayachamundeeswari SP. The significance of fillers in composite polymer electrolytes for optimizing lithium battery. Ionics 2024;30(2):647–75.
[111] D.K. Maurya, B. Bazri, P. Srivastava, J.-Y. Huang, Y.-T. Hung, W.-T. Huang, D.-H. Wei, R.-S. Liu, Ceramic Rich Composite Electrolytes: An Overview of Paradigm Shift toward Solid Electrolytes for High-Performance Lithium-Metal Batteries, Advanced Energy Materials n/a(n/a) 2402402.
[112] Song JY, Wang YY, Wan CC. Review of gel-type polymer electrolytes for lithium-ion batteries. J Power Sources 1999;77(2):183–97.
[113] Aruchamy K, Ramasundaram S, Divya S, Chandran M, Yun K, Oh TH. Gel Polymer Electrolytes: Advancing Solid-State Batteries for High-Performance Applications. Gels 2023;9(7):585.
[114] Gentili V, Panero S, Reale P, Scrosati B. Composite gel-type polymer electrolytes for advanced, rechargeable lithium batteries. J Power Sources 2007;170(1):185–90.
[115] Fergus JW. Ceramic and polymeric solid electrolytes for lithium-ion batteries. J Power Sources 2010;195(15):4554–69.
[116] Wang Z, Luo S-H, Zhang X, Guo S, Li P, Yan S. Glass and glass ceramic electrodes and solid electrolyte materials for lithium ion batteries: A review. J Non Cryst Solids 2023;619:122581.
[117] Yin J-H, Zhu H, Yu S-J, Dong Y-B, Wei Q-Y, Xu G-Q, et al. Recent Advances of LATP and Their NASICON Structure as a Solid-State Electrolyte for Lithium-Ion Batteries. Adv Eng Mater 2023;25(20):2300566.
[118] Luo C, Yi M, Cao Z, Hui W, Wang Y. Review of Ionic Conductivity Properties of NASICON Type Inorganic Solid Electrolyte LATP. ACS Appl Electron Mater 2024;6(2):641–57.
[119] Wang Y, Chen Z, Jiang K, Shen Z, Passerini S, Chen M. Accelerating the Development of LLZO in Solid-State Batteries Toward Commercialization: A Comprehensive Review. Small 2024;20(35):2402035.
[120] Wang J-C, Li Y, Li Z-X, Wang P-F, Zhu Y-R, Sun Y, et al. Review on Interface Issues between a Garnet Li7La3Zr2O12 Solid Electrolyte and Li Anode: Advances and Perspectives. Energy Fuel 2024;38(14):12528–45.
[121] Z. Zou, Z. Xiao, Z. Lin, B. Zhang, C. Zhang, F. Wei, Lithium Phosphorous Oxynitride as an Advanced Solid-State Electrolyte to Boost High-Energy Lithium Metal Battery, Advanced Functional Materials n/a(n/a) 2409330.
[122] Dai W, Qiao Y, Ma Z, Wang T, Fu Z. All-solid-state thin-film batteries based on lithium phosphorus oxynitrides. Materials Futures 2022;1(3):032101.
[123] Goodenough JB, Hong HYP, Kafalas JA. Fast Na+-ion transport in skeleton structures. Mater Res Bull 1976;11(2):203–20.
[124] Hong HYP. Crystal structure and ionic conductivity of Li14Zn(GeO4)4 and other new Li+ superionic conductors. Mater Res Bull 1978;13(2):117–24.
[125] Krauskopf T, Culver SP, Zeier WG. Bottleneck of Diffusion and Inductive Effects in Li10Ge1–xSnxP2S12. Chem Mater 2018;30(5):1791–8.
[126] Kamaya N, Homma K, Yamakawa Y, Hirayama M, Kanno R, Yonemura M, et al. A lithium superionic conductor. Nat Mater 2011;10(9):682–6.
[127] Ohara K, Mitsui A, Mori M, Onodera Y, Shiotani S, Koyama Y, et al. Structural and electronic features of binary Li2S-P2S5 glasses. Sci Rep 2016;6(1):21302.
[128] Warren Z, Rosero-Navarro NC. Solution-Based Suspension Synthesis of Li2S–P2S5 Glass-Ceramic Systems as Solid-State Electrolytes: A Brief Review of Current Research. ACS Omega 2024;9(29):31228–36.
[129] Kato Y, Hori S, Saito T, Suzuki K, Hirayama M, Mitsui A, et al. High-power all-solid-state batteries using sulfide superionic conductors. Nat Energy 2016;1(4):16030.
[130] Kanno R, Murayama M. Lithium Ionic Conductor Thio-LISICON: The Li2 S - GeS2 - P 2 S 5 System. J Electrochem Soc 2001;148(7):A742.
[131] Luo M, Wang C, Duan Y, Zhao X, Wang J, Sun X. Surface Coating Enabling Sulfide Solid Electrolytes with Excellent Air Stability and Lithium Compatibility. Energy Environ Mater 2024;7(6):e12753.
[132] Zhen Y, Yang W, Qin Z, Ji M, Qie Y, Li J, et al. Improved ionic conductivity and air stability of Li7P3S11 by SnSe2 doping and two-step pressing sintering method. Electrochim Acta 2024;503:144888.
[133] Yang J, Jiang Z, Liu C, Li L, Li S, Wu Z, et al. Tin-based dual-modification enabling enhanced air stability and electrochemical performance for Li5.5PS4.5Cl1.5 in all-solid-state lithium metal batteries. Chem Eng J 2024;500:157027.

[134] Helm B, Strotmann K, Böger T, Samanta B, Banik A, Lange MA, et al. Reducing the Defect Formation Energy by Aliovalent Sn(+IV) and Isovalent P(+V) Substitution in Li3SbS4 Promotes Li+ Transport. ACS Appl Energy Mater 2024;7(5):1735–47.
[135] Zhang N, He Q, Zhang L, Zhang J, Huang L, Yao X. Homogeneous Fluorine Doping toward Highly Conductive and Stable Li10GeP2S12 Solid Electrolyte for All-Solid-State Lithium Batteries. Adv Mater 2024;36(36):2408903.
[136] Wang Q, Zhou Y, Wang X, Guo H, Gong S, Yao Z, et al. Designing lithium halide solid electrolytes. Nat Commun 2024;15(1):1050.
[137] Li X, Kim JT, Luo J, Zhao C, Xu Y, Mei T, et al. Structural regulation of halide superionic conductors for all-solid-state lithium batteries. Nat Commun 2024;15(1):53.
[138] Chen S, Yu C, Chen S, Peng L, Liao C, Wei C, et al. Enabling ultrafast lithium-ion conductivity of Li2ZrCl6 by indium doping. Chin Chem Lett 2022;33(10):4635–9.
[139] Rosa C, Ravalli M, Pianta N, Mustarelli P, Ferrara C, Quartarone E, et al. Aliovalent Substitution in Li3InCl6: A Combined Experimental and Computational Investigation of Structure and Ion Diffusion in Lithium-Halide Solid State Electrolytes. ACS Appl Energy Mater 2024;7(10):4314–23.
[140] Banik A, Samanta B, Helm B, Kraft MA, Rudel Y, Li C, et al. Exploring Layered Disorder in Lithium-Ion-Conducting Li3Y1–xInxCl6. Inorg Chem 2024;63(19):8698–709.
[141] Liu X-K, Zhou Y-X, Mi F-H, Ma X-L, Sun C-W. Superionic halide solid electrolyte Li1.7Zr0.7Ta0.3Cl6 for durable all-solid-state lithium batteries. Energy Storage Mater 2024;72:103737.
[142] Miyazaki R, Yamaguchi G, Yagi E, Yoshida T, Tomita T. Enhancement of the Li+ Conductivity of Li3AlF6 for Stable All-Solid-State Lithium-Ion Batteries. ACS Appl Energy Mater 2024;7(6):2533–41.
[143] Sun A, Tu H, Sun Z, He Z, Wang Y, Wang J, et al. Dual-Halide Interphase Enabling High-Performance Lithium Metal Batteries in Wide-Temperature Range. ACS Energy Lett 2024;9(6):2545–53.
[144] Chen HM, Maohua C, Adams S. Stability and ionic mobility in argyrodite-related lithium-ion solid electrolytes. PCCP 2015;17(25):16494–506.
[145] Park J-S, Jo C-H, Myung S-T. Comprehensive understanding on lithium argyrodite electrolytes for stable and safe all-solid-state lithium batteries. Energy Storage Mater 2023;61:102869.
[146] Deiseroth H-J, Kong S-T, Eckert H, Vannahme J, Reiner C, Zaiß T, et al. Li6PS5X: A Class of Crystalline Li-Rich Solids With an Unusually High Li+ Mobility. Angew Chem Int Ed 2008;47(4):755–8.
[147] Adeli P, Bazak JD, Park KH, Kochetkov I, Huq A, Goward GR, et al. Boosting Solid-State Diffusivity and Conductivity in Lithium Superionic Argyrodites by Halide Substitution. Angew Chem Int Ed 2019;58(26):8681–6.
[148] Kraft MA, Ohno S, Zinkevich T, Koerver R, Culver SP, Fuchs T, et al. Inducing High Ionic Conductivity in the Lithium Superionic Argyrodites Li6+xP1–xGexS5I for All-Solid-State Batteries. J Am Chem Soc 2018;140(47):16330–9.
[149] Yu C, Zhao F, Luo J, Zhang L, Sun X. Recent development of lithium argyrodite solid-state electrolytes for solid-state batteries: Synthesis, structure, stability and dynamics. Nano Energy 2021;83:105858.
[150] Wang J, Chen F, Hu L, Ma C. Alternate Crystal Structure Achieving Ionic Conductivity above 1 mS cm–1 in Cost-Effective Zr-Based Chloride Solid Electrolytes. Nano Lett 2023;23(13):6081–7.
[151] Tanaka Y, Ueno K, Mizuno K, Takeuchi K, Asano T, Sakai A. New Oxyhalide Solid Electrolytes with High Lithium Ionic Conductivity >10 mS cm−1 for All-Solid-State Batteries. Angew Chem Int Ed 2023;62(13):e202217581.
[152] Hu L, Wang J, Wang K, Gu Z, Xi Z, Li H, et al. A cost-effective, ionically conductive and compressible oxychloride solid-state electrolyte for stable all-solid-state lithium-based batteries. Nat Commun 2023;14(1):3807.
[153] Quartarone E, Mustarelli P. Electrolytes for solid-state lithium rechargeable batteries: recent advances and perspectives. Chem Soc Rev 2011;40(5):2525–40.
[154] Xi G, Xiao M, Wang S, Han D, Li Y, Meng Y. Polymer-Based Solid Electrolytes: Material Selection, Design, and Application. Adv Funct Mater 2021;31(9):2007598.
[155] Sanchez J-Y, Alloin F, Saunier J. Chapter 14 - PVdF-based polymers for lithium batteries. In: Nakajima T, Groult H, editors. Fluorinated Materials for Energy Conversion. Amsterdam: Elsevier Science; 2005. p. 305–33.
[156] Meyer WH. Polymer Electrolytes for Lithium-Ion Batteries. Adv Mater 1998;10(6):439–48.
[157] Gao J, Wang C, Han D-W, Shin D-M. Single-ion conducting polymer electrolytes as a key jigsaw piece for next-generation battery applications. Chem Sci 2021;12(40):13248–72.
[158] Raphael E, Avellaneda CO, Manzolli B, Pawlicka A. Agar-based films for application as polymer electrolytes. Electrochim Acta 2010;55(4):1455–9.
[159] Wang Z-L, Tang Z-Y. A novel polymer electrolyte based on PMAML/PVDF-HFP blend. Electrochim Acta 2004;49(7):1063–8.
[160] Croce F, Persi L, Ronci F, Scrosati B. Nanocomposite polymer electrolytes and their impact on the lithium battery technology. Solid State Ion 2000;135(1):47–52.
[161] Chen S, Wen K, Fan J, Bando Y, Golberg D. Progress and future prospects of high-voltage and high-safety electrolytes in advanced lithium batteries: from liquid to solid electrolytes. J Mater Chem A 2018;6(25):11631–63.
[162] Fenton DE, Parker JM, Wright PV. Complexes of alkali metal ions with poly(ethylene oxide). Polymer 1973;14(11):589.
[163] Marzantowicz M, Dygas JR, Krok F, Florjańczyk Z, Zygadło-Monikowska E. Influence of crystalline complexes on electrical properties of PEO:LiTFSI electrolyte. Electrochim Acta 2007;53(4):1518–26.
[164] Halder B, Mohamed MG, Kuo S-W, Elumalai P. Review on composite polymer electrolyte using PVDF-HFP for solid-state lithium-ion battery. Mater Today Chem 2024;36:101926.
[165] Armand M, Axmann P, Bresser D, Copley M, Edström K, Ekberg C, et al. Lithium-ion batteries – Current state of the art and anticipated developments. J Power Sources 2020;479:228708.
[166] Hoang Huy VP, So S, Hur J. Inorganic Fillers in Composite Gel Polymer Electrolytes for High-Performance Lithium and Non-Lithium Polymer Batteries. Nanomaterials 2021;11(3):614.
[167] Zhou S, Zhong S, Dong Y, Liu Z, Dong L, Yuan B, et al. Composition and Structure Design of Poly(vinylidene fluoride)-Based Solid Polymer Electrolytes for Lithium Batteries. Adv Funct Mater 2023;33(20):2214432.
[168] Wieczorek W, Florjanczyk Z, Stevens JR. Composite polyether based solid electrolytes. Electrochim Acta 1995;40(13):2251–8.
[169] Fu J, Li Z, Zhou X, Guo X. Ion transport in composite polymer electrolytes. Mater Adv 2022;3(9):3809–19.
[170] Huo H, Chen Y, Luo J, Yang X, Guo X, Sun X. Rational Design of Hierarchical "Ceramic-in-Polymer" and "Polymer-in-Ceramic" Electrolytes for Dendrite-Free Solid-State Batteries. Adv Energy Mater 2019;9(17):1804004.
[171] Han L, Lehmann ML, Zhu J, Liu T, Zhou Z, Tang X, et al. Recent Developments and Challenges in Hybrid Solid Electrolytes for Lithium-Ion Batteries. Front Energy Res 2020;8.
[172] Gao H, Grundish NS, Zhao Y, Zhou A, Goodenough JB. Formation of Stable Interphase of Polymer-in-Salt Electrolyte in All-Solid-State Lithium Batteries. Energy Mater Adv 2021;2021.
[173] Zhao T, Gai Q, Deng X, Ma J, Gao H. A new type of LATP doped PVDF-HFP based electrolyte membrane with flame retardancy and long cycle stability for solid state batteries. J Storage Mater 2023;73:108576.
[174] Wang C, Bai G, Yang Y, Liu X, Shao H. Dendrite-free all-solid-state lithium batteries with lithium phosphorous oxynitride-modified lithium metal anode and composite solid electrolytes. Nano Res 2019;12(1):217–23.
[175] Capiglia C, Mustarelli P, Quartarone E, Tomasi C, Magistris A. Effects of nanoscale SiO2 on the thermal and transport properties of solvent-free, poly(ethylene oxide) (PEO)-based polymer electrolytes. Solid State Ion 1999;118(1):73–9.
[176] Pandian AS, Chen XC, Chen J, Lokitz BS, Ruther RE, Yang G, et al. Facile and scalable fabrication of polymer-ceramic composite electrolyte with high ceramic loadings. J Power Sources 2018;390:153–64.
[177] Chen A, Qu C, Shi Y, Shi F. Manufacturing Strategies for Solid Electrolyte in Batteries. Front Energy Res 2020;8.

[178] Song Z, Chen F, Martinez-Ibañez M, Feng W, Forsyth M, Zhou Z, et al. A reflection on polymer electrolytes for solid-state lithium metal batteries. Nat Commun 2023;14(1):4884.
[179] Chen L, Li Y, Li S-P, Fan L-Z, Nan C-W, Goodenough JB. PEO/garnet composite electrolytes for solid-state lithium batteries: From "ceramic-in-polymer" to "polymer-in-ceramic". Nano Energy 2018;46:176–84.
[180] McLachlan DS. Measurement and analysis of a model dual-conductivity medium using a generalised effective-medium theory. J Phys C Solid State Phys 1988;21(8):1521.
[181] Hailu Mengesha T, Lemma Beshahwured S, Wu Y-S, Wu S-H, Jose R, Yang C-C. A polydopamine-modified garnet–based polymer-in-ceramic hybrid solid electrolyte membrane for high-safety lithium metal batteries. Chem Eng J 2023;452:139340.
[182] Wang Q, Wang S, Lu T, Guan L, Hou L, Du H, et al. Ultrathin Solid Polymer Electrolyte Design for High-Performance Li Metal Batteries: A Perspective of Synthetic Chemistry. Adv Sci 2023;10(1):2205233.
[183] Bonizzoni S, Ferrara C, Berbenni V, Anselmi-Tamburini U, Mustarelli P, Tealdi C. NASICON-type polymer-in-ceramic composite electrolytes for lithium batteries. PCCP 2019;21(11):6142–9.
[184] Colombo F, Bonizzoni S, Ferrara C, Simonutti R, Mauri M, Falco M, et al. Polymer-in-Ceramic Nanocomposite Solid Electrolyte for Lithium Metal Batteries Encompassing PEO-Grafted TiO2 Nanocrystals. J Electrochem Soc 2020;167(7):070535.
[185] Jiang H, Wu Y, Ma J, Liu Y, Wang L, Yao X, et al. Ultrathin polymer-in-ceramic and ceramic-in-polymer bilayer composite solid electrolyte membrane for high-voltage lithium metal batteries. J Membr Sci 2021;640:119840.
[186] Wang Z, Liu R, Ba Z, Xu K, Li X, Dong J, et al. Built-in garnet-rich composite solid electrolyte towards fast ion transport and dendrite-free for high-energy lithium batteries. Compos Commun 2024;47:101871.
[187] Zhang X, Wang S, Xue C, Xin C, Lin Y, Shen Y, et al. Self-Suppression of Lithium Dendrite in All-Solid-State Lithium Metal Batteries with Poly(vinylidene difluoride)-Based Solid Electrolytes. Adv Mater 2019;31(11):1806082.
[188] Callegari D, Bonizzoni S, Berbenni V, Quartarone E, Mustarelli P. Is It Possible to Obtain Solvent-Free, Li+-Conducting Solid Electrolytes Based on Pure PVdF? Comment on "Self-Suppression of Lithium Dendrite in All-Solid-State Lithium Metal Batteries with Poly(vinylidene difluoride)-Based Solid Electrolytes". Adv Mater 2020;32(14):1907375.
[189] Vallana N, Carena E, Ceribelli N, Mezzomo L, Di Liberto G, Mauri M, et al. Host–Guest Interactions and Transport Mechanism in Poly(vinylidene fluoride)-Based Quasi-Solid Electrolytes for Lithium Metal Batteries. ACS Appl Energy Mater 2024;7(4):1606–17.
[190] Carena E, Mezzomo L, Vallana N, Ceribelli N, Di Liberto G, Mostoni S, et al. PVDF-HFP Based, Quasi-Solid Nanocomposite Electrolytes for Lithium Metal Batteries. Small 2024;20(30):2311805.
[191] Nguyen A-G, Park C-J. Insights into tailoring composite solid polymer electrolytes for solid-state lithium batteries. J Membr Sci 2023;675:121552.
[192] He R, Kyu T. Effect of Plasticization on Ionic Conductivity Enhancement in Relation to Glass Transition Temperature of Crosslinked Polymer Electrolyte Membranes. Macromolecules 2016;49(15):5637–48.
[193] Zhang H, Oteo U, Zhu H, Judez X, Martinez-Ibañez M, Aldalur I, et al. Enhanced Lithium-Ion Conductivity of Polymer Electrolytes by Selective Introduction of Hydrogen into the Anion. Angew Chem Int Ed 2019;58(23):7829–34.
[194] Qiao L, Rodriguez Peña S, Martínez-Ibañez M, Santiago A, Aldalur I, Lobato E, et al. Anion π–π Stacking for Improved Lithium Transport in Polymer Electrolytes. J Am Chem Soc 2022;144(22):9806–16.
[195] Zhu X, Wang K, Xu Y, Zhang G, Li S, Li C, et al. Strategies to Boost Ionic Conductivity and Interface Compatibility of Inorganic - Organic Solid Composite Electrolytes. Energy Storage Mater 2021;36:291–308.
[196] Chi S-S, Liu Y, Zhao N, Guo X, Nan C-W, Fan L-Z. Solid polymer electrolyte soft interface layer with 3D lithium anode for all-solid-state lithium batteries. Energy Storage Mater 2019;17:309–16.
[197] Yang C, Xie H, Ping W, Fu K, Liu B, Rao J, et al. An Electron/Ion Dual-Conductive Alloy Framework for High-Rate and High-Capacity Solid-State Lithium-Metal Batteries. Adv Mater 2019;31(3):1804815.
[198] Tang J, Wang L, Tian C, Huang T, Zhang J, Zeng L, et al. Multilayer structure solid-state electrolyte composite membranes for long-life quasi-solid-state battery. J Alloy Compd 2023;960:170736.
[199] Hu Y, Li W, Zhu J, Hao S-M, Qin X, Fan L-Z, et al. Multi-layered electrolytes for solid-state lithium batteries. Next Energy 2023;1(3):100042.
[200] Nie K, Hong Y, Qiu J, Li Q, Yu X, Li H, et al. Interfaces Between Cathode and Electrolyte in Solid State Lithium Batteries: Challenges and Perspectives. Front Chem 2018;6.
[201] Xiao Y, Miara LJ, Wang Y, Ceder G. Computational Screening of Cathode Coatings for Solid-State Batteries. Joule 2019;3(5):1252–75.
[202] Khan K, Fu B, Xin H, Beshiwork BA, Hanif MB, Wu J, et al. Composite polymer electrolyte incorporating WO3 nanofillers with enhanced performance for dendrite-free solid-state lithium battery. Ceram Int 2023;49(3):4473–81.
[203] Li G, Monroe CW. Dendrite nucleation in lithium-conductive ceramics. PCCP 2019;21(36):20354–9.
[204] Gaines L, Cuenca R. Costs of lithium-ion batteries for vehicles. IL (US): Argonne National Lab; 2000.
[205] Ahuis M, Doose S, Vogt D, Michalowski P, Zellmer S, Kwade A. Recycling of solid-state batteries. Nat Energy 2024;9(4):373–85.
[206] Bauer A, Song J, Vail S, Pan W, Barker J, Lu Y. The Scale-up and Commercialization of Nonaqueous Na-Ion Battery Technologies. Adv Energy Mater 2018;8(17):1702869.
[207] Saw LH, Ye Y, Tay AAO. Integration issues of lithium-ion battery into electric vehicles battery pack. J Clean Prod 2016;113:1032–45.
[208] Lin J, Liu X, Li S, Zhang C, Yang S. A review on recent progress, challenges and perspective of battery thermal management system. Int J Heat Mass Transf 2021;167:120834.
[209] Huang S, Wang Z, Von Lim Y, Wang Y, Li Y, Zhang D, et al. Recent Advances in Heterostructure Engineering for Lithium–Sulfur Batteries. Adv Energy Mater 2021;11(10):2003689.
[210] Hu Y, Chen W, Lei T, Jiao Y, Huang J, Hu A, et al. Strategies toward High-Loading Lithium–Sulfur Battery. Adv Energy Mater 2020;10(17):2000082.
[211] Chen Y, Xu J, He P, Qiao Y, Guo S, Yang H, et al. Metal-air batteries: progress and perspective. Science Bulletin 2022;67(23):2449–86.
[212] Pan J, Xu YY, Yang H, Dong Z, Liu H, Xia BY. Advanced Architectures and Relatives of Air Electrodes in Zn–Air Batteries. Adv Sci 2018;5(4):1700691.
[213] Liu Q, Pan Z, Wang E, An L, Sun G. Aqueous metal-air batteries: Fundamentals and applications. Energy Storage Mater 2020;27:478–505.
[214] Borchardt L, Oschatz M, Kaskel S. Carbon Materials for Lithium Sulfur Batteries—Ten Critical Questions, Chemistry – A. European Journal 2016;22(22):7324–51.
[215] Liu Q, Lin Y, Zong Z, Sun G, Li Q. Lightweight design of carbon twill weave fabric composite body structure for electric vehicle. Compos Struct 2013;97:231–8.
[216] Snyder JF, Wong EL, Hubbard CW. Evaluation of Commercially Available Carbon Fibers, Fabrics, and Papers for Potential Use in Multifunctional Energy Storage Applications. J Electrochem Soc 2009;156(3):A215.
[217] Snyder J, Carter R, Wong E, Nguyen P, Xu K, Ngo E, et al. Multifunctional Structural Composite Batteries, International SAMPE Technical Conference 2007:18.
[218] Wong E, Baechle D, Xu K, Carter R, Snyder J, Wetzel E. Design and Processing of Structural Composite Batteries. International SAMPE Symposium and Exhibition (Proceedings) 2007;52:20.
[219] South JT, Carter RH, Snyder JF, Hilton CD, O'Brien DJ, Wetzel ED. Multifunctional Power-Generating and Energy-Storing Structural Composites for U.S. Army Applications. MRS Online Proc Libr 2004;851(1):269–80.
[220] Johannisson W, Zenkert D, Lindbergh G. Model of a structural battery and its potential for system level mass savings. Multifunct Mater 2019;2(3):035002.
[221] Hopkins BJ, Long JW, Rolison DR, Parker JF. High-Performance Structural Batteries. Joule 2020;4(11):2240–3.
[222] Galos J, Best AS, Mouritz AP. Multifunctional sandwich composites containing embedded lithium-ion polymer batteries under bending loads. Mater Des 2020;185:108228.
[223] Chen J, Zhou Y, Islam MS, Cheng X, Brown SA, Han Z, et al. Carbon fiber reinforced Zn–MnO2 structural composite batteries. Compos Sci Technol 2021;209:108787.
[224] Pyo J, Park H-W, Jang M-S, Choi J-S, Sathish Kumar SK, Kim C-G. Tubular laminated composite structural battery. Compos Sci Technol 2021;208:108646.

[225] Mao Y-Q, Dong G-H, Fu Y-T, Li Y-Q, Huang P, Fu S-Y. High performance shape-adjustable structural lithium-ion battery based on hybrid fiber reinforced epoxy composite. Compos Struct 2023;325:117598.
[226] Thakur A, Dong X. Printing with 3D continuous carbon fiber multifunctional composites via UV-assisted coextrusion deposition. Manuf Lett 2020;24:1–5.
[227] Pappas JM, Thakur AR, Dong X. Effects of cathode doping on 3D printed continuous carbon fiber structural battery composites by UV-assisted coextrusion deposition. J Compos Mater 2021;55(26):3893–908.
[228] Qian J, Chen Q, Hong M, Xie W, Jing S, Bao Y, et al. Toward stretchable batteries: 3D-printed deformable electrodes and separator enabled by nanocellulose. Mater Today 2022;54:18–26.
[229] Chaudhary R, Xu J, Xia Z, Asp LE. Unveiling the Multifunctional Carbon Fiber Structural Battery. Advanced Materials n/a(n/a) 2024:2409725.
[230] Xu J, Geng Z, Johansen M, Carlstedt D, Duan S, Thiringer T, et al. A multicell structural battery composite laminate. EcoMat 2022;4(3):e12180.
[231] Kjell MH, Jacques E, Zenkert D, Behm M, Lindbergh G. PAN-Based Carbon Fiber Negative Electrodes for Structural Lithium-Ion Batteries. J Electrochem Soc 2011;158(12):A1455.
[232] Ladpli P, Nardari R, Kopsaftopoulos F, Chang F-K. Multifunctional energy storage composite structures with embedded lithium-ion batteries. J Power Sources 2019;414:517–29.
[233] Moyer K, Boucherbil NA, Zohair M, Eaves-Rathert J, Pint CL. Polymer reinforced carbon fiber interfaces for high energy density structural lithium-ion batteries. Sustainable Energy Fuels 2020;4(6):2661–8.
[234] Moyer K, Meng C, Marshall B, Assal O, Eaves J, Perez D, et al. Carbon fiber reinforced structural lithium-ion battery composite: Multifunctional power integration for CubeSats. Energy Storage Mater 2020;24:676–81.
[235] Choi J-S, Park H-W, Noh J-E, Cha J, Jang W-H, Kim C-G. Composite-fabric-based structure-integrated energy storage system. Compos Struct 2023;310:116757.
[236] Hahn M, Buqa H, Ruch PW, Goers D, Spahr ME, Ufheil J, et al. A Dilatometric Study of Lithium Intercalation into Powder-Type Graphite Electrodes. Electrochem Solid St 2008;11(9):A151.
[237] Qi Y, Guo H, Hector LG, Timmons A. Threefold Increase in the Young's Modulus of Graphite Negative Electrode during Lithium Intercalation. J Electrochem Soc 2010;157(5):A558.
[238] Zhang P, Ma Z, Wang Y, Zou Y, Sun L, Lu C. Lithiation-induced interfacial failure of electrode-collector: A first-principles study. Mater Chem Phys 2019;222:193–9.
[239] Zhao Y, Stein P, Bai Y, Al-Siraj M, Yang Y, Xu B-X. A review on modeling of electro-chemo-mechanics in lithium-ion batteries. J Power Sources 2019;413:259–83.
[240] Verma A, Kotaka T, Tabuchi Y, Mukherjee PP. Mechano-Electrochemical Interaction and Degradation in Graphite Electrode with Surface Film. J Electrochem Soc 2018;165(10):A2397.
[241] Jacques E, Hellqvist Kjell M, Zenkert D, Lindbergh G, Behm M. Expansion of carbon fibres induced by lithium intercalation for structural electrode applications. Carbon 2013;59:246–54.
[242] Mao R, Lei Z, Liu X, Li Q, Zhong J, Bai R, et al. Study on electrochemical lithiation stress model of graphite-carbon fiber bilayer electrode. Carbon 2024;226:119214.
[243] Park H-W, Jang M-S, Choi J-S, Pyo J, Kim C-G. Characteristics of woven carbon fabric current collector electrodes for structural battery. Compos Struct 2021;256:112999.
[244] Zhou G, Li F, Cheng H-M. Progress in flexible lithium batteries and future prospects. Energy Environmental Science 2014;7(4):1307–38.
[245] Xu K. Electrolytes and interphases in Li-ion batteries and beyond. Chem Rev 2014;114(23):11503–618.
[246] Asp LE, Johansson M, Lindbergh G, Xu J, Zenkert D. Structural battery composites: a review. Funct Compos Struct 2019;1(4):042001.
[247] Tikekar MD, Archer LA, Koch DL. Stabilizing electrodeposition in elastic solid electrolytes containing immobilized anions. Sci Adv 2016;2(7):e1600320.
[248] Liu P, Sherman E, Jacobsen A. Design and fabrication of multifunctional structural batteries. J Power Sources 2009;189(1):646–50.
[249] Dong G-H, Mao Y-Q, Yang G-M, Li Y-Q, Song S-F, Xu C-H, et al. High-Strength Poly (ethylene oxide) Composite Electrolyte Reinforced with Glass Fiber and Ceramic Electrolyte Simultaneously for Structural Energy Storage. ACS Appl Energy Mater 2021;4(4):4038–49.
[250] Shirshova N, Bismarck A, Carreyette S, Fontana QP, Greenhalgh ES, Jacobsson P, et al. Structural supercapacitor electrolytes based on bicontinuous ionic liquid–epoxy resin systems 2013;1(48):15300–9.
[251] Shirshova N, Bismarck A, Greenhalgh ES, Johansson P, Kalinka G, Marczewski MJ, et al. MJTJoPCC Wienrich, Composition as a means to control morphology and properties of epoxy based dual-phase structural electrolytes 2014;118(49):28377–87.
[252] Ihrner N, Johannisson W, Sieland F, Zenkert D, Johansson M. Structural lithium ion battery electrolytes via reaction induced phase-separation. J Mater Chem A 2017;5(48):25652–9.
[253] Johannisson W, Ihrner N, Zenkert D, Johansson M, Carlstedt D, Asp LE, et al. Multifunctional performance of a carbon fiber UD lamina electrode for structural batteries. Composites Science Technology 2018;168:81–7.
[254] D. Carlstedt, W. Johannisson, D. Zenkert, P. Linde, L.E. Asp, Conceptual design framework for laminated structural battery composites, Proc. 18th Eur. Conf. Compos. Mater., Athens, Greece, 2018, pp. 24-8.
[255] Schneider LM, Ihrner N, Zenkert D, Johansson M. Bicontinuous electrolytes via thermally initiated polymerization for structural lithium ion batteries. ACS Appl Energy Mater 2019;2(6):4362–9.
[256] Asp LE, Bouton K, Carlstedt D, Duan S, Harnden R, Johannisson W, et al. A structural battery and its multifunctional performance. Advanced Energy Sustainability Research 2021;2(3):2000093.
[257] Dong G-H, Mao Y-Q, Guo F-L, Li Y-Q, Huang P, Fu S-Y. Structural battery composites with remarkable energy storage capabilities via system structural design. Compos Struct 2023;306:116615.
[258] Scholz AE, Hermanutz A, Hornung M. Feasibility analysis and comparative assessment of structural power technology in all-electric composite aircraft. Deutscher Luft-und Raumfahrtkongress; 2018.
[259] Thomas JP, Qidwai SM, Pogue WR, Pham GT. Multifunctional structure-battery composites for marine systems. J Compos Mater 2012;47(1):5–26.
[260] Han Z, Zhu J, Feng Y, Zhang W, Xiong Y, Zhang W. Manufacturing carbon fabric composite structural batteries using spray with high-pressure and high-temperature and vacuum-bag assisted infusion techniques. Compos Sci Technol 2024;245:110321.
[261] Landowski M, Strugała G, Budzik M, Imielińska K. Impact damage in SiO2 nanoparticle enhanced epoxy – Carbon fibre composites. Compos B Eng 2017;113:91–9.
[262] Eskizeybek V, Avcı A, Gülce A. Preparation and mechanical properties of carbon nanotube grafted glass fabric/epoxy multi-scale composites. Adv Compos Mater 2017;26(2):169–80.
[263] Sahraei E, Hill R, Wierzbicki T. Calibration and finite element simulation of pouch lithium-ion batteries for mechanical integrity. J Power Sources 2012;201:307–21.
[264] D.J. O'Brien, D.M. Baechle, E.D. Wetzel, Performance Metrics for Structural Composite Capacitiors, ASME 2010 Conference on Smart Materials, Adaptive Structures and Intelligent Systems, 2010, pp. 215-221.
[265] O'Brien DJ, Baechle DM, Wetzel ED. Design and performance of multifunctional structural composite capacitors. J Compos Mater 2011;45(26):2797–809.
[266] Snyder JF, Gienger EB, Wetzel ED. Performance metrics for structural composites with electrochemical multifunctionality. J Compos Mater 2015;49(15):1835–48.
[267] Carlstedt D, Asp LE. Performance analysis framework for structural battery composites in electric vehicles. Compos B Eng 2020;186:107822.
[268] Pejman R, Gorman J, Najafi AR. Multi-physics design of a new battery packaging for electric vehicles utilizing multifunctional composites. Compos B Eng 2022;237:109810.
[269] Woellert K, Ehrenfreund P, Ricco AJ, Hertzfeld H. Cubesats: Cost-effective science and technology platforms for emerging and developing nations. Adv Space Res 2011;47(4):663–84.
[270] CubeSats, NASA, https://www.nasa.gov/mission_pages/cubesats/index.html.

[271] Thomas JP, Qidwai MA. The design and application of multifunctional structure-battery materials systems. JOM 2005;57(3):18–24.

[272] Qidwai S, Baucom J, Thomas J, Horner D. Multifunctional Applications of Thin Film Li Polymer Battery Cells. Materials Science Forum - MATER SCI FORUM 2005;492–493:157–62.

[273] Riboldi Carlo ED, Trainelli L, Biondani F. Structural Batteries in Aviation: A Preliminary Sizing Methodology. J Aerosp Eng 2020;33(4):04020031.

[274] Di Mauro G, Corcione S, Cusati V, Marciello V, Guida M, Nicolosi F. The Potential of Structural Batteries for Commuter Aircraft Hybridization. J Mater Eng Perform 2023;32(9):3871–80.

[275] Karadotcheva E, Nguyen SN, Greenhalgh ES, Shaffer MSP, Kucernak ARJ, Linde P. Structural Power Performance Targets for Future Electric Aircraft. Energies 2021.

[276] Nguyen SN, Millereux A, Pouyat A, Greenhalgh ES, Shaffer MSP, Kucernak ARJ, et al. Conceptual Multifunctional Design, Feasibility and Requirements for Structural Power in Aircraft Cabins. J Aircr 2021;58(3):677–87.

[277] Kim J, Campbell AS, de Ávila B-E-F, Wang J. Wearable biosensors for healthcare monitoring. Nat Biotechnol 2019;37(4):389–406.

[278] Lim H-R, Kim HS, Qazi R, Kwon Y-T, Jeong J-W, Yeo W-H. Advanced Soft Materials, Sensor Integrations, and Applications of Wearable Flexible Hybrid Electronics in Healthcare, Energy, and Environment. Adv Mater 2020;32(15):1901924.

[279] Park J, Lee Y, Cho S, Choe A, Yeom J, Ro YG, et al. Soft Sensors and Actuators for Wearable Human–Machine Interfaces. Chem Rev 2024;124(4):1464–534.

[280] Armand M, Tarascon JM. Building better batteries. Nature 2008;451(7179):652–7.

[281] Choi K-H, Ahn DB, Lee S-Y. Current Status and Challenges in Printed Batteries: Toward Form Factor-Free. Monolithic Integrated Power Sources, ACS Energy Letters 2018;3(1):220–36.

[282] Ahn DB, Lee K-H, Lee S-Y. Printed solid-state electrolytes for form factor-free Li-metal batteries. Curr Opin Electrochem 2022;32:100889.

[283] Ahn DB, Lee S-S, Lee K-H, Kim J-H, Lee J-W, Lee S-Y. Form factor-free, printed power sources. Energy Storage Mater 2020;29:92–112.

[284] Lyu Z, Lim GJH, Koh JJ, Li Y, Ma Y, Ding J, et al. Design and Manufacture of 3D-Printed Batteries. Joule 2021;5(1):89–114.

[285] Lee K-H, Ahn DB, Kim J-H, Lee J-W, Lee S-Y. Printed Built-In Power Sources. Matter 2020;2(2):345–59.

[286] Lewis JA. Colloidal Processing of Ceramics. J Am Ceram Soc 2000;83(10):2341–59.

[287] Fairhurst D. An Overview of the Zeta Potential Part 3: Uses and Applications. Americal Parmaceutical Review 2013.

[288] Kim S-H, Choi K-H, Cho S-J, Yoo J, Lee S-S, Lee S-Y. Flexible/shape-versatile, bipolar all-solid-state lithium-ion batteries prepared by multistage printing. Energ Environ Sci 2018;11(2):321–30.

[289] Singh N, Galande C, Miranda A, Mathkar A, Gao W, Reddy ALM, et al. Paintable Battery. Sci Rep 2012;2(1):481.

[290] Sun K, Wei T-S, Ahn BY, Seo JY, Dillon SJ, Lewis JA. 3D Printing of Interdigitated Li-Ion Microbattery Architectures. Adv Mater 2013;25(33):4539–43.

[291] Sarma Choudhury S, Katiyar N, Saha R, Bhattacharya S. Inkjet-printed flexible planar Zn-MnO2 battery on paper substrate. Sci Rep 2024;14(1):1597.

[292] Lee K-H, Lee S-S, Ahn DB, Lee J, Byun D, Lee S-Y. Ultrahigh areal number density solid-state on-chip microsupercapacitors via electrohydrodynamic jet printing. Sci Adv 2020;6(10):eaaz1692.

[293] Choi K-H, Kim H-W, Lee S-S, Yoo J, Lee D-G, Lee S-Y. All-Hand-Drawn Zn–Air Batteries: Toward User-Customized On-the-Fly Power Sources. Adv Sustainable Syst 2018;2(5):1700132.

[294] Lei Y, Zhao W, Zhu Y, Buttner U, Dong X, Alshareef HN. Three-Dimensional Ti3C2Tx MXene-Prussian Blue Hybrid Microsupercapacitors by Water Lift-Off Lithography. ACS Nano 2022;16(2):1974–85.

[295] Liu Z, Wu Z-S, Yang S, Dong R, Feng X, Müllen K. Ultraflexible In-Plane Micro-Supercapacitors by Direct Printing of Solution-Processable Electrochemically Exfoliated Graphene. Adv Mater 2016;28(11):2217–22.

[296] Shi X, Wu Z-S, Qin J, Zheng S, Wang S, Zhou F, et al. Graphene-Based Linear Tandem Micro-Supercapacitors with Metal-Free Current Collectors and High-Voltage Output. Adv Mater 2017;29(44):1703034.

[297] Kim S-W, Kang K-N, Min J-W, Jang J-H. Plotter-assisted integration of wearable all-solid-state micro-supercapacitors. Nano Energy 2018;50:410–6.

[298] Nardekar SS, Krishnamoorthy K, Manoharan S, Pazhamalai P, Kim SJ. Two Faces Under a Hood: Unravelling the Energy Harnessing and Storage Properties of 1T-MoS2 Quantum Sheets for Next-Generation Stand-Alone Energy Systems. ACS Nano 2022;16(3):3723–34.

[299] Kim S-W, Lee K-H, Lee Y-H, Youe W-J, Gwon J-G, Lee S-Y. Transparent and Multi-Foldable Nanocellulose Paper Microsupercapacitors. Adv Sci 2022;9(34):2203720.

[300] Li J, Shi Q, Shao Y, Hou C, Li Y, Zhang Q, et al. Cladding nanostructured AgNWs-MoS2 electrode material for high-rate and long-life transparent in-plane micro-supercapacitor. Energy Storage Mater 2019;16:212–9.

[301] Li C, Bu F, Wang Q, Liu X. Recent Developments of Inkjet-Printed Flexible Energy Storage Devices. Adv Mater Interfaces 2022;9(34):2201051.

[302] Wei T-S, Ahn BY, Grotto J, Lewis JA. 3D Printing of Customized Li-Ion Batteries with Thick Electrodes. Adv Mater 2018;30(16):1703027.

[303] Cao D, Xing Y, Tantratian K, Wang X, Ma Y, Mukhopadhyay A, et al. 3D Printed High-Performance Lithium Metal Microbatteries Enabled by Nanocellulose. Adv Mater 2019;31(14):1807313.

[304] Lacey SD, Kirsch DJ, Li Y, Morgenstern JT, Zarket BC, Yao Y, et al. Extrusion-Based 3D Printing of Hierarchically Porous Advanced Battery Electrodes. Adv Mater 2018;30(12):1705651.

[305] Kim S-H, Kim J-H, Cho S-J, Lee S-Y. All-Solid-State Printed Bipolar Li–S Batteries. Adv Energy Mater 2019;9(40):1901841.

[306] Ma J, Zheng S, Chi L, Liu Y, Zhang Y, Wang K, et al. 3D Printing Flexible Sodium-Ion Microbatteries with Ultrahigh Areal Capacity and Robust Rate Capability. Adv Mater 2022;34(39):2205569.

[307] Ahn DB, Kim W-Y, Lee K-H, Lee S-S, Kim S-H, Park S, et al. Enabling On-Demand Conformal Zn-Ion Batteries on Non-Developable Surfaces. Adv Funct Mater 2023;33(18):2211597.

[308] Shi G, Peng X, Zeng J, Zhong L, Sun Y, Yang W, et al. A Liquid Metal Microdroplets Initialized Hemicellulose Composite for 3D Printing Anode Host in Zn-Ion Battery. Adv Mater 2023;35(25):2300109.

[309] Choi K-H, Yoo J, Lee CK, Lee S-Y. All-inkjet-printed, solid-state flexible supercapacitors on paper. Energ Environ Sci 2016;9(9):2812–21.

[310] Tang X, Zhou H, Cai Z, Cheng D, He P, Xie P, et al. Generalized 3D Printing of Graphene-Based Mixed-Dimensional Hybrid Aerogels. ACS Nano 2018;12(4):3502–11.

[311] Shen K, Ding J, Yang S. 3D Printing Quasi-Solid-State Asymmetric Micro-Supercapacitors with Ultrahigh Areal Energy Density. Adv Energy Mater 2018;8(20):1800408.

[312] Gao T, Zhou Z, Yu J, Zhao J, Wang G, Cao D, et al. 3D Printing of Tunable Energy Storage Devices with Both High Areal and Volumetric Energy Densities. Adv Energy Mater 2019;9(8):1802578.

[313] Zhang C, McKeon L, Kremer MP, Park S-H, Ronan O, Seral-Ascaso A, et al. Additive-free MXene inks and direct printing of micro-supercapacitors. Nat Commun 2019;10(1):1795.

[314] Fan Z, Wei C, Yu L, Xia Z, Cai J, Tian Z, et al. 3D Printing of Porous Nitrogen-Doped Ti3C2 MXene Scaffolds for High-Performance Sodium-Ion Hybrid Capacitors. ACS Nano 2020;14(1):867–76.

[315] Wang Z, Lee Y-H, Kim S-W, Seo J-Y, Lee S-Y, Nyholm L. Why Cellulose-Based Electrochemical Energy Storage Devices? Adv Mater 2021;33(28):2000892.

[316] Fu K, Wang Y, Yan C, Yao Y, Chen Y, Dai J, et al. Graphene Oxide-Based Electrode Inks for 3D-Printed Lithium-Ion Batteries. Adv Mater 2016;28(13):2587–94.

[317] Tagliaferri S, Nagaraju G, Panagiotopoulos A, Och M, Cheng G, Iacoviello F, et al. Aqueous Inks of Pristine Graphene for 3D Printed Microsupercapacitors with High Capacitance. ACS Nano 2021;15(9):15342–53.

[318] Kim S-H, Choi K-H, Cho S-J, Choi S, Park S, Lee S-Y. Printable Solid-State Lithium-Ion Batteries: A New Route toward Shape-Conformable Power Sources with Aesthetic Versatility for Flexible Electronics. Nano Lett 2015;15(8):5168–77.

[319] Hwang J-Y, Myung S-T, Sun Y-K. Sodium-ion batteries: present and future. Chem Soc Rev 2017;46(12):3529–614.

[320] Delmas C. Sodium and Sodium-Ion Batteries: 50 Years of Research. Adv Energy Mater 2018;8(17):1703137.

[321] Yabuuchi N, Kubota K, Dahbi M, Komaba S. Research Development on Sodium-Ion Batteries. Chem Rev 2014;114(23):11636–82.

[322] Tang B, Shan L, Liang S, Zhou J. Issues and opportunities facing aqueous zinc-ion batteries. Energ Environ Sci 2019;12(11):3288–304.

[323] Fang G, Zhou J, Pan A, Liang S. Recent Advances in Aqueous Zinc-Ion Batteries. ACS Energy Lett 2018;3(10):2480–501.
[324] Kang H, Kim S-H, Ahn DB, Wang X, Wu Z-S, Lee S-Y. Liquid Metal-Skinned Zn Powder Anodes Enabled by Capillary Suspension. ACS Energy Lett 2024;9(6):2816–25.
[325] Lee S-S, Choi K-H, Kim S-H, Lee S-Y. Wearable Supercapacitors Printed on Garments. Adv Funct Mater 2018;28(11):1705571.
[326] Yun Y, Nandanapalli KR, Choi J-H, Son W, Choi C, Lee S. Extremely flexible and mechanically durable planar supercapacitors: High energy density and low-cost power source for E-skin electronics. Nano Energy 2020;78:105356.
[327] Lee K-H, Jeon J, Cho W, Kim S-W, Moon H, Wie JJ, et al. Light-triggered autonomous shape-reconfigurable and locomotive rechargeable power sources. Mater Today 2022;55:56–65.
[328] Wang S, Liu N, Tao J, Yang C, Liu W, Shi Y, et al. Inkjet printing of conductive patterns and supercapacitors using a multi-walled carbon nanotube/Ag nanoparticle based ink. J Mater Chem A 2015;3(5):2407–13.
[329] Hu L, Wu H, Cui Y. Printed energy storage devices by integration of electrodes and separators into single sheets of paper. Appl Phys Lett 2010;96(18).
[330] Lee K-H, Kim S-W, Kim M, Ahn DB, Hong Y-K, Kim S-H, et al. Folding the Energy Storage: Beyond the Limit of Areal Energy Density of Micro-Supercapacitors. Adv Energy Mater 2023;13(20):2204327.
[331] Jiang Y, Xu Z, Huang T, Liu Y, Guo F, Xi J, et al. Direct 3D Printing of Ultralight Graphene Oxide Aerogel Microlattices. Adv Funct Mater 2018;28(16):1707024.
[332] Wang Z, Zhang QE, Long S, Luo Y, Yu P, Tan Z, Bai J, Qu B, Yang Y, Shi J, Zhou H, Xiao Z-Y, Hong W, Bai H. Three-Dimensional Printing of Polyaniline/Reduced Graphene Oxide Composite for High-Performance Planar Supercapacitor. ACS Appl Mater Interfaces 2018;10(12):10437–44.
[333] Yao B, Chandrasekaran S, Zhang J, Xiao W, Qian F, Zhu C, et al. Efficient 3D Printed Pseudocapacitive Electrodes with Ultrahigh MnO2 Loading. Joule 2019;3(2):459–70.
[334] Tang X, Zhu C, Cheng D, Zhou H, Liu X, Xie P, et al. Architectured Leaf-Inspired Ni0.33Co0.66S2/Graphene Aerogels via 3D Printing for High-Performance Energy Storage. Adv Funct Mater 2018;28(51):1805057.
[335] Yang W, Yang J, Byun JJ, Moissinac FP, Xu J, Haigh SJ, et al. 3D Printing of Freestanding MXene Architectures for Current-Collector-Free Supercapacitors. Adv Mater 2019;31(37):1902725.
[336] Zhang C, Kremer MP, Seral-Ascaso A, Park S-H, McEvoy N, Anasori B, et al. Stamping of Flexible, Coplanar Micro-Supercapacitors Using MXene Inks. Adv Funct Mater 2018;28(9):1705506.
[337] Banerjee A, Wang X, Fang C, Wu EA, Meng YS. Interfaces and Interphases in All-Solid-State Batteries with Inorganic Solid Electrolytes. Chem Rev 2020;120(14):6878–933.
[338] Zhao Q, Stalin S, Zhao C-Z, Archer LA. Designing solid-state electrolytes for safe, energy-dense batteries. Nat Rev Mater 2020;5(3):229–52.
[339] McOwen DW, Xu S, Gong Y, Wen Y, Godbey GL, Gritton JE, et al. 3D-Printing Electrolytes for Solid-State Batteries. Adv Mater 2018;30(18):1707132.
[340] Ping W, Wang C, Wang R, Dong Q, Lin Z, Brozena AH, et al. Printable, high-performance solid-state electrolyte films. Sci Adv 2020;6(47):eabc8641.
[341] Nam YJ, Cho S-J, Oh DY, Lim J-M, Kim SY, Song JH, et al. Bendable and Thin Sulfide Solid Electrolyte Film: A New Electrolyte Opportunity for Free-Standing and Stackable High-Energy All-Solid-State Lithium-Ion Batteries. Nano Lett 2015;15(5):3317–23.
[342] Lee S-S, Kim S-H, Ahn DB, Lee K-H, Jo Y, Jeong S, et al. All-Direct-Ink-Writing of Artistic Supercapacitors: Toward On-Demand Embodied Power Sources. Adv Funct Mater 2022;32(34):2202901.
[343] He Y, Chen S, Nie L, Sun Z, Wu X, Liu W. Stereolithography Three-Dimensional Printing Solid Polymer Electrolytes for All-Solid-State Lithium Metal Batteries. Nano Lett 2020;20(10):7136–43.
[344] Oh K-S, Kim J-H, Kim S-H, Oh D, Han S-P, Jung K, et al. Single-Ion Conducting Soft Electrolytes for Semi-Solid Lithium Metal Batteries Enabling Cell Fabrication and Operation under Ambient Conditions. Adv Energy Mater 2021;11(38):2101813.
[345] Chae C, Han JH, Lee SS, Choi Y, Kim T-H, Jeong S. A Printable Metallic Current Collector for All-Printed High-Voltage Micro-Supercapacitors: Instantaneous Surface Passivation by Flash-Light-Sintering Reaction. Adv Funct Mater 2020;30(25):2000715.
[346] Jo Y, Park HJ, Kim Y-B, Lee SS, Lee SY, Kim S-K, et al. Form-Factor Free 3D Copper Circuits by Surface-Conformal Direct Printing and Laser Writing. Adv Funct Mater 2020;30(45):2004659.
[347] Owens CE, Headrick RJ, Williams SM, Fike AJ, Pasquali M, McKinley GH, et al. Substrate-Versatile Direct-Write Printing of Carbon Nanotube-Based Flexible Conductors, Circuits, and Sensors. Adv Funct Mater 2021;31(25):2100245.
[348] Manthiram A, Yu X, Wang S. Lithium battery chemistries enabled by solid-state electrolytes. Nat Rev Mater 2017;2(4):16103.
[349] Lee Y-G, Fujiki S, Jung C, Suzuki N, Yashiro N, Omoda R, et al. High-energy long-cycling all-solid-state lithium metal batteries enabled by silver–carbon composite anodes. Nat Energy 2020;5(4):299–308.
[350] Kil E-H, Choi K-H, Ha H-J, Xu S, Rogers JA, Kim MR, et al. Imprintable, Bendable, and Shape-Conformable Polymer Electrolytes for Versatile-Shaped Lithium-Ion Batteries. Adv Mater 2013;25(10):1395–400.
[351] Choi K-H, Kim S-H, Ha H-J, Kil E-H, Lee CK, Lee SB, et al. Compliant polymer network-mediated fabrication of a bendable plastic crystal polymer electrolyte for flexible lithium-ion batteries. J Mater Chem A 2013;1(17):5224–31.
[352] Kwon YW, Ahn DB, Park Y-G, Kim E, Lee DH, Kim S-W, et al. Power-integrated, wireless neural recording systems on the cranium using a direct printing method for deep-brain analysis. Sci Adv 2024;10(14):eadn3784.
[353] Sun P, Li X, Shao J, Braun PV. High-Performance Packaged 3D Lithium-Ion Microbatteries Fabricated Using Imprint Lithography. Adv Mater 2021;33(1):2006229.
[354] Wang S, Li L, Zheng S, Das P, Shi X, Ma J, et al. Monolithic integrated micro-supercapacitors with ultra-high systemic volumetric performance and areal output voltage. Natl Sci Rev 2022;10(3).
[355] Bae J, Oh S, Lee B, Lee CH, Chung J, Kim J, et al. High-performance, printable quasi-solid-state electrolytes toward all 3D direct ink writing of shape-versatile Li-ion batteries. Energy Storage Mater 2023;57:277–88.
[356] Shao Y, Wei L, Wu X, Jiang C, Yao Y, Peng B, et al. Room-temperature high-precision printing of flexible wireless electronics based on MXene inks. Nat Commun 2022;13(1):3223.
[357] Park J, Ahn DB, Kim J, Cha E, Bae B-S, Lee S-Y, et al. Printing of wirelessly rechargeable solid-state supercapacitors for soft, smart contact lenses with continuous operations. Sci Adv 2019;5(12):eaay0764.
[358] Kim J-H, Hwang I, Kim S-H, Park J, Jin W, Seo K, et al. Voltage-tunable portable power supplies based on tailored integration of modularized silicon photovoltaics and printed bipolar lithium-ion batteries. J Mater Chem A 2020;8(32):16291–301.
[359] Yin L, Cao M, Kim KN, Lin M, Moon J-M, Sempionatto JR, et al. A stretchable epidermal sweat sensing platform with an integrated printed battery and electrochromic display. Nat Electron 2022;5(10):694–705.
[360] Ryou M-H, Kim S-H, Kim S-W, Lee S-Y. A microgrid-patterned silicon electrode as an electroactive lithium host. Energ Environ Sci 2022;15(6):2581–90.
[361] Lim GJH, Lyu Z, Zhang X, Koh JJ, Zhang Y, He C, et al. Robust pure copper framework by extrusion 3D printing for advanced lithium metal anodes. J Mater Chem A 2020;8(18):9058–67.
[362] Park S, Shi B, Shang Y, Deng K, Fu K. Structured Electrode Additive Manufacturing for Lithium-Ion Batteries. Nano Lett 2022;22(23):9462–9.
[363] Park S, Cao Z, Sung DH, Fu KK. High-Loaded Electrode Filaments for Additive Manufacturing of Structural Batteries. Adv Energy Mater 2023;13(38):2301704.
[364] Lee K-H, Lee S-Y. Cell architecture designs towards high-energy-density microscale energy storage devices. Nano Research Energy 2024;3:e9120101.
[365] Gao Y, Guo Q, Zhang Q, Cui Y, Zheng Z. Fibrous Materials for Flexible Li–S Battery. Adv Energy Mater 2021;11(15):2002580.
[366] Kong L, Tang C, Peng H-J, Huang J-Q, Zhang Q. Advanced energy materials for flexible batteries in energy storage: A review. SmartMat 2020;1(1):1–35.
[367] Shi Q, Dong B, He T, Sun Z, Zhu J, Zhang Z, et al. Progress in wearable electronics/photonics—Moving toward the era of artificial intelligence and internet of things. InfoMat 2020;2(6):1131–62.
[368] Choi JW, Aurbach D. Promise and reality of post-lithium-ion batteries with high energy densities. Nat Rev Mater 2016;1(4):16013.
[369] Zhang X, Cheng X, Zhang Q. Nanostructured energy materials for electrochemical energy conversion and storage: A review. Journal of Energy Chemistry 2016;25(6):967–84.

[370] Xu C, Niu Y, Ka-Man Au V, Gong S, Liu X, Wang J, et al. Recent progress of self-supported air electrodes for flexible Zn-air batteries. Journal of Energy Chemistry 2024;89:110–36.

[371] Jia SK, Yang BZ, Zhao CF, Zhang ZY, Yin YH, Liu XB, et al. Tab engineering-mediated resistance of flexible lithium-ion batteries for high output current. Journal of Energy Chemistry 2021;58:264–70.

[372] Wang Y, Zhu J, Chen A, Guo X, Cui H, Chen Z, et al. Spider Silk-Inspired Binder Design for Flexible Lithium-Ion Battery with High Durability. Adv Mater 2023;35(47):2303165.

[373] Nishide H, Oyaizu K. Toward Flexible Batteries. Science 2008;319(5864):737–8.

[374] Peng J, Snyder GJ. A figure of merit for flexibility. Science 2019;366(6466):690–1.

[375] Ashby MF. The deformation of plastically non-homogeneous materials, The Philosophical Magazine: A Journal of Theoretical Experimental and Applied. Physics 1970;21(170):399–424.

[376] Kong L, Peng H-J, Huang J-Q, Zhang Q. Review of nanostructured current collectors in lithium–sulfur batteries. Nano Res 2017;10(12):4027–54.

[377] Ye Y, Chou L-Y, Liu Y, Wang H, Lee HK, Huang W, et al. Ultralight and fire-extinguishing current collectors for high-energy and high-safety lithium-ion batteries. Nat Energy 2020;5(10):786–93.

[378] Yang W, Yang W, Zeng J, Chen Y, Huang Y, Liu J, et al. Biopolymer-based gel electrolytes for electrochemical energy Storage: Advances and prospects. Prog Mater Sci 2024;144:101264.

[379] Li X, Wang D, Ran F. Key approaches and challenges in fabricating advanced flexible zinc-ion batteries with functional hydrogel electrolytes. Energy Storage Mater 2023;56:351–93.

[380] Deimede V, Elmasides C. Separators for Lithium-Ion Batteries: A Review on the Production Processes and Recent Developments. Energ Technol 2015;3(5):453–68.

[381] Zhuang T-Z, Huang J-Q, Peng H-J, He L-Y, Cheng X-B, Chen C-M, et al. Rational Integration of Polypropylene/Graphene Oxide/Nafion as Ternary-Layered Separator to Retard the Shuttle of Polysulfides for Lithium–Sulfur Batteries. Small 2016;12(3):381–9.

[382] Li B-Q, Zhang S-Y, Wang B, Xia Z-J, Tang C, Zhang Q. A porphyrin covalent organic framework cathode for flexible Zn–air batteries. Energ Environ Sci 2018;11(7):1723–9.

[383] Wang H-F, Tang C, Wang B, Li B-Q, Cui X, Zhang Q. Defect-rich carbon fiber electrocatalysts with porous graphene skin for flexible solid-state zinc–air batteries. Energy Storage Mater 2018;15:124–30.

[384] Peng H-J, Huang J-Q, Zhang Q. A review of flexible lithium–sulfur and analogous alkali metal–chalcogen rechargeable batteries. Chem Soc Rev 2017;46(17):5237–88.

[385] Jin J, Cai W, Cai J, Shao Y, Song Y, Xia Z, et al. MOF-derived hierarchical CoP nanoflakes anchored on vertically erected graphene scaffolds as self-supported and flexible hosts for lithium–sulfur batteries. J Mater Chem A 2020;8(6):3027–34.

[386] Li H, Tang Z, Liu Z, Zhi C. Evaluating Flexibility and Wearability of Flexible Energy Storage Devices. Joule 2019;3(3):613–9.

[387] Song Z, Ma T, Tang R, Cheng Q, Wang X, Krishnaraju D, et al. Origami lithium-ion batteries. Nat Commun 2014;5(1):3140.

[388] Song Z, Wang X, Lv C, An Y, Liang M, Ma T, et al. Kirigami-based stretchable lithium-ion batteries. Sci Rep 2015;5(1):10988.

[389] Liu W, Chen J, Chen Z, Liu K, Zhou G, Sun Y, et al. Stretchable Lithium-Ion Batteries Enabled by Device-Scaled Wavy Structure and Elastic-Sticky Separator. Adv Energy Mater 2017;7(21):1701076.

[390] Shi C, Wang T, Liao X, Qie B, Yang P, Chen M, et al. Accordion-like stretchable Li-ion batteries with high energy density. Energy Storage Mater 2019;17:136–42.

[391] Chen X, Liu B, Zhong C, Liu Z, Liu J, Ma L, et al. Ultrathin Co3O4 Layers with Large Contact Area on Carbon Fibers as High-Performance Electrode for Flexible Zinc–Air Battery Integrated with Flexible Display. Adv Energy Mater 2017;7(18):1700779.

[392] Zhu Y-H, Yang X-Y, Liu T, Zhang X-B. Flexible 1D Batteries: Recent Progress and Prospects. Adv Mater 2020;32(5):1901961.

[393] Liao M, Wang C, Hong Y, Zhang Y, Cheng X, Sun H, et al. Industrial scale production of fibre batteries by a solution-extrusion method. Nat Nanotechnol 2022;17(4):372–7.

[394] Xi Z, Zhang X, Ma Y, Zhou C, Yang J, Wu Y, et al. Recent Progress in Flexible Fibrous Batteries. ChemElectroChem 2018;5(21):3127–37.

[395] Wang L, Chen D, Jiang K, Shen G. New insights and perspectives into biological materials for flexible electronics. Chem Soc Rev 2017;46(22):6764–815.

[396] Juqu T, Willenberg SC, Pokpas K, Ross N. Advances in paper-based battery research for biodegradable energy storage. Adv Sens Energy Mater 2022;1(4):100037.

[397] Senthilkumar ST, Abirami M, Kim J, Go W, Hwang SM, Kim Y. Sodium-ion hybrid electrolyte battery for sustainable energy storage applications. J Power Sources 2017;341:404–10.

[398] Ani PC, Nzereogu PU, Agbogu AC, Ezema FI, Nwanya AC. Cellulose from waste materials for electrochemical energy storage applications: A review. Appl Surf Sci Adv 2022;11:100298.

[399] Wu M, Zhang Y, Xu L, Yang C, Hong M, Cui M, et al. A sustainable chitosan-zinc electrolyte for high-rate zinc-metal batteries. Matter 2022;5(10):3402–16.

[400] Ali AMM, Subban RHY, Bahron H, Yahya MZA, Kamisan AS. Investigation on modified natural rubber gel polymer electrolytes for lithium polymer battery. J Power Sources 2013;244:636–40.

[401] Abraham KM. How Comparable Are Sodium-Ion Batteries to Lithium-Ion Counterparts? ACS Energy Lett 2020;5(11):3544–7.

[402] Colò F, Bella F, Nair JR, Destro M, Gerbaldi C. Cellulose-based novel hybrid polymer electrolytes for green and efficient Na-ion batteries. Electrochim Acta 2015;174:185–90.

[403] Chen HY, Keller A, Conn AT, Rossiter J. GelBat: An Edible Gelatin-Based Battery. IEEE International Conference on Soft Robotics (RoboSoft) 2023;2023:1–6.

[404] Gouda A, Masson A, Hoseinizadeh M, Soavi F, Santato C. Biosourced quinones for high-performance environmentally benign electrochemical capacitors via interface engineering. Communications Chemistry 2022;5(1):98.

[405] Rahmanudin A, Mohammadi M, Isacsson P, Li Y, Seufert L, Kim N, et al. Stretchable and biodegradable plant-based redox-diffusion batteries. Mater Horiz 2024;11(18):4400–12.

[406] Sun L, Yao Y, Dai L, Jiao M, Ding B, Yu Q, et al. Sustainable and high-performance Zn dual-ion batteries with a hydrogel-based water-in-salt electrolyte. Energy Storage Mater 2022;47:187–94.

[407] Leong KW, Pan W, Yi X, Luo S, Zhao X, Zhang Y, et al. Next-generation magnesium-ion batteries: The quasi-solid-state approach to multivalent metal ion storage. Sci Adv 2023;9(32):eadh1181.

[408] Tsang M, Armutlulu A, Martinez AW, Allen SAB, Allen MG. Biodegradable magnesium/iron batteries with polycaprolactone encapsulation: A microfabricated power source for transient implantable devices. Microsyst Nanoeng 2015;1(1):15024.

[409] Mei T, Wang C, Liao M, Li J, Wang L, Tang C, et al. A biodegradable and rechargeable fiber battery. J Mater Chem A 2021;9(16):10104–9.

[410] Luo P, Zheng C, He J, Tu X, Sun W, Pan H, et al. Structural Engineering in Graphite-Based Metal-Ion Batteries. Adv Funct Mater 2022;32(9):2107277.

[411] Noh SH, Kwon C, Hwang J, Ohsaka T, Kim B-J, Kim T-Y, et al. Self-assembled nitrogen-doped fullerenes and their catalysis for fuel cell and rechargeable metal–air battery applications. Nanoscale 2017;9(22):7373–9.

[412] Jiang Z, Zhao Y, Lu X, Xie J. Fullerenes for rechargeable battery applications: Recent developments and future perspectives. Journal of Energy Chemistry 2021;55:70–9.

[413] Zhu S, Sheng J, Chen Y, Ni J, Li Y. Carbon nanotubes for flexible batteries: recent progress and future perspective. Natl Sci Rev 2020;8(5).

[414] Ning J, Jiang T, Men K, Dai Q, Li D, Wei Y, et al. Syntheses, Characterizations, and Applications in Lithium Ion Batteries of Hierarchical SnO Nanocrystals. J Phys Chem C 2009;113(32):14140–4.

[415] Muraliganth T, Vadivel Murugan A, Manthiram A. Facile synthesis of carbon-decorated single-crystalline Fe3O4nanowires and their application as high performance anode in lithium ion batteries. Chemical Communications (47) 2009:7360–2.

[416] Yao B, Zhang J, Kou T, Song Y, Liu T, Li Y. Paper-Based Electrodes for Flexible Energy Storage Devices. Adv Sci 2017;4(7):1700107.

[417] Sampaio PGV, González MOA, de Oliveira Ferreira P, da Cunha Jácome P, Vidal JPP, Pereira HR, et al. Overview of printing and coating techniques in the production of organic photovoltaic cells. Int J Energy Res 2020;44(13):9912–31.

[418] R. Szentgyörgyvölgyi, E. Novotny, M. Weimert, DETERMINING AND SELECTING SCREEN PRINTING FORM PARAMETERS FOR PRINTING ON PAPER AND TEXTILE, 2018.

[419] A. C, Łuszczyńska B, Dupont B, Sieradzki Z. Inkjet Printing Technique and Its Application in Organic Light Emitting Diodes †. Display and Imaging 2017;2:339–58.

[420] Wang Y, Pan W, Kwok HYH, Zhang H, Lu X, Leung DYC. Liquid-free Al-air batteries with paper-based gel electrolyte: A green energy technology for portable electronics. J Power Sources 2019;437:226896.

[421] Navarro-Segarra M, Tortosa C, Ruiz-Díez C, Desmaële D, Gea T, Barrena R, et al. A plant-like battery: a biodegradable power source ecodesigned for precision agriculture. Energ Environ Sci 2022;15(7):2900–15.

[422] Edström K, Brandell D, Gustafsson T, Nyholm L. Electrodeposition as a Tool for 3D Microbattery Fabrication. The Electrochemical Society Interface 2011;20(2):41.

[423] Jones SD, Akridge JR, Shokoohi FK. Thin film rechargeable Li batteries. Solid State Ion 1994;69(3):357–68.

[424] Jones SD, Akridge JR. A thin-film solid-state microbattery. J Power Sources 1993;44(1):505–13.

[425] West WC, Whitacre JF, White V, Ratnakumar BV. Fabrication and testing of all solid-state microscale lithium batteries for microspacecraft applications. J Micromech Microeng 2002;12(1):58.

[426] J.B. Bates, N.J. Dudney, G.R. Gruzalski, C.F. Luck, Thin film battery and method for making same, 1994.

[427] Bates JB, Gruzalski GR, Luck CF. Rechargeable solid state lithium microbatteries. Proceedings IEEE Micro Electro Mechanical Systems 1993;1993:82–6.

[428] Bates JB, Dudney NJ, Gruzalski GR, Zuhr RA, Choudhury A, Luck CF, et al. Fabrication and characterization of amorphous lithium electrolyte thin films and rechargeable thin-film batteries. J Power Sources 1993;43(1):103–10.

[429] Bates JB, Dudney NJ, Lubben DC, Gruzalski GR, Kwak BS, Yu X, et al. Thin-film rechargeable lithium batteries. J Power Sources 1995;54(1):58–62.

[430] Neudecker BJ, Dudney NJ, Bates JB. "Lithium-Free" Thin-Film Battery with In Situ Plated Li Anode. J Electrochem Soc 2000;147(2):517.

[431] Wenzel S, Randau S, Leichtweiß T, Weber DA, Sann J, Zeier WG, et al. Direct Observation of the Interfacial Instability of the Fast Ionic Conductor Li10GeP2S12 at the Lithium Metal Anode. Chem Mater 2016;28(7):2400–7.

[432] Yoon K, Kim J-J, Seong WM, Lee MH, Kang K. Investigation on the interface between Li10GeP2S12 electrolyte and carbon conductive agents in all-solid-state lithium battery. Sci Rep 2018;8(1):8066.

[433] Murugan R, Thangadurai V, Weppner W. Fast Lithium Ion Conduction in Garnet-Type Li7La3Zr2O12. Angew Chem Int Ed 2007;46(41):7778–81.

[434] Liu X, Garcia-Mendez R, Lupini AR, Cheng Y, Hood ZD, Han F, et al. Local electronic structure variation resulting in Li 'filament' formation within solid electrolytes. Nat Mater 2021;20(11):1485–90.

[435] Jiang Z, Han Q, Wang S, Wang H. Reducing the Interfacial Resistance in All-Solid-State Lithium Batteries Based on Oxide Ceramic Electrolytes. ChemElectroChem 2019;6(12):2970–83.

[436] Hart RW, White HS, Dunn B, Rolison DR. 3-D Microbatteries. Electrochem Commun 2003;5(2):120–3.

[437] Long JW, Dunn B, Rolison DR, White HS. Three-Dimensional Battery Architectures. Chem Rev 2004;104(10):4463–92.

[438] Enerchip, Enerchip CBC050 datasheet DS-72-01 Rev10 www.Cymbet.com 2009., 2009.

[439] Patrissi CJ, Martin CR. Sol-Gel-Based Template Synthesis and Li-Insertion Rate Performance of Nanostructured Vanadium Pentoxide. J Electrochem Soc 1999;146(9):3176.

[440] Sides CR, Martin CR. Nanostructured Electrodes and the Low-Temperature Performance of Li-Ion Batteries. Adv Mater 2005;17(1):125–8.

[441] Ortiz GF, Hanzu I, Djenizian T, Lavela P, Tirado JL, Knauth P. Alternative Li-Ion Battery Electrode Based on Self-Organized Titania Nanotubes. Chem Mater 2009;21(1):63–7.

[442] Roberts M, Johns P, Owen J, Brandell D, Edstrom K, El Enany G, et al. 3D lithium ion batteries—from fundamentals to fabrication. J Mater Chem 2011;21(27):9876–90.

[443] Wang C, Taherabadi L, Jia G, Madou M, Yeh Y, Dunn B. C-MEMS for the Manufacture of 3D Microbatteries. Electrochem Solid St 2004;7(11):A435.

[444] Hasan M, Chowdhury T, Rohan JF. Nanotubes of Core/Shell Cu / Cu2O as Anode Materials for Li-Ion Rechargeable Batteries. J Electrochem Soc 2010;157(6):A682.

[445] Perre E, Taberna PL, Mazouzi D, Poizot P, Gustafsson T, Edström K, et al. Electrodeposited Cu2Sb as anode material for 3-dimensional Li-ion microbatteries. J Mater Res 2010;25(8):1485–91.

[446] Vullum F, Teeters D. Investigation of lithium battery nanoelectrode arrays and their component nanobatteries. J Power Sources 2005;146(1):804–8.

[447] Nathan M, Golodnitsky D, Yufit V, Strauss E, Ripenbein T, Shechtman I, et al. Three-dimensional thin-film Li-ion microbatteries for autonomous MEMS. J Microelectromech Syst 2005;14(5):879–85.

[448] Notten PHL, Roozeboom F, Niessen RAH, Baggetto L. 3-D Integrated All-Solid-State Rechargeable Batteries. Adv Mater 2007;19(24):4564–7.

[449] Baggetto L, Niessen RAH, Roozeboom F, Notten PHL. High Energy Density All-Solid-State Batteries: A Challenging Concept Towards 3D Integration. Adv Funct Mater 2008;18(7):1057–66.

[450] A.V. Jeyaseelan, J.F. Rohan, Fabrication of three-dimensional substrates for Li microbatteries on Si, Applied Surface Science 256(3, Supplement) (2009) S61-S64.

[451] Chamran F, Yeh Y, Min HS, Dunn B, Kim CJ. Fabrication of High-Aspect-Ratio Electrode Arrays for Three-Dimensional Microbatteries. J Microelectromech Syst 2007;16(4):844–52.

[452] Pikul JH, Gang Zhang H, Cho J, Braun PV, King WP. High-power lithium ion microbatteries from interdigitated three-dimensional bicontinuous nanoporous electrodes. Nat Commun 2013;4(1):1732.

[453] Ning H, Pikul JH, Zhang R, Li X, Xu S, Wang J, et al. Holographic patterning of high-performance on-chip 3D lithium-ion microbatteries. Proc Natl Acad Sci 2015;112(21):6573–8.

[454] Behboudikhiavi S, Omale JO, Babu B, Piraux L, Vlad A. Electrodeposition of Li-Ion Cathode Materials: The Fascinating Alternative for Li-Ion Micro-Batteries Fabrication. J Electrochem Soc 2023;170(2):020509.

[455] Zhang H, Ning H, Busbee J, Shen Z, Kiggins C, Hua Y, et al. Electroplating lithium transition metal oxides. Sci Adv 2017;3(5):e1602427.

[456] Johns P, Roberts M, Owen J. Conformal electrodeposition of manganese dioxide onto reticulated vitreous carbon for 3D microbattery applications. J Mater Chem 2011;21(27):10153–9.

[457] Armstrong E, McNulty D, Geaney H, O'Dwyer C. Electrodeposited Structurally Stable V2O5 Inverse Opal Networks as High Performance Thin Film Lithium Batteries. ACS Appl Mater Interfaces 2015;7(48):27006–15.

[458] Chen Y, Tarascon J-M, Guéry C. Electrochemically assisted growth of LiFePO4 in ionic liquid media. Electrochem Commun 2011;13(7):673–6.

[459] Yufit V, Freedman K, Nathan M, Burstein L, Golodnitsky D, Peled E. Thin-film iron sulfide cathodes for lithium and Li-ion/polymer electrolyte microbatteries. Electrochim Acta 2004;50(2):417–20.

[460] McGrath LM, Rohan JF. High-Rate Lithium-Ion Cycling in Electrodeposited Binder-Free Thin-Film Vanadium Oxide Cathodes with Lithium Metal Anodes in Ionic Liquid and Polymer Gel Analogue Electrolytes. Batteries Supercaps 2021;4(3):485–92.

[461] Egorov V, Gulzar U, Zhang Y, Breen S, O'Dwyer C. Evolution of 3D Printing Methods and Materials for Electrochemical Energy Storage. Adv Mater 2020;32(29):2000556.

[462] Teranishi T, Yoshikawa Y, Yoneda M, Kishimoto A, Halpin J, O'Brien S, et al. Aluminum Interdiffusion into LiCoO2 Using Atomic Layer Deposition for High Rate Lithium Ion Batteries. ACS Appl Energy Mater 2018;1(7):3277–82.

[463] Janek J, Zeier WG. A solid future for battery development. Nat Energy 2016;1(9):16141.

[464] Zhu Y, He X, Mo Y. First principles study on electrochemical and chemical stability of solid electrolyte–electrode interfaces in all-solid-state Li-ion batteries. J Mater Chem A 2016;4(9):3253–66.

[465] Zhu Y, He X, Mo Y. Origin of Outstanding Stability in the Lithium Solid Electrolyte Materials: Insights from Thermodynamic Analyses Based on First-Principles Calculations. ACS Appl Mater Interfaces 2015;7(42):23685–93.
[466] Yada C, Lee CE, Laughman D, Hannah L, Iba H, Hayden BE. A High-Throughput Approach Developing Lithium-Niobium-Tantalum Oxides as Electrolyte/Cathode Interlayers for High-Voltage All-Solid-State Lithium Batteries. J Electrochem Soc 2015;162(4):A722.
[467] O'Donoghue A, Shine M, Povey IM, Rohan JF. Nanoengineering of Thin Film V2O5 Cathode Interfaces via Atomic Layer Deposition for use with Polymer Gel Ionic Liquid Electrolytes. Batteries Supercaps 2024;7(1):e202300447.
[468] McGrath LM, Jones J, Carey E, Rohan JF. Ionic Liquid Based Polymer Gel Electrolytes for Use with Germanium Thin Film Anodes in Lithium Ion Batteries. ChemistryOpen 2019;8(12):1429–36.
[469] E. Commission, I. Directorate-General for Internal Market, Entrepreneurship, SMEs, M. Grohol, C. Veeh, Study on the critical raw materials for the EU 2023 – Final report, Publications Office of the European Union2023.
[470] Usiskin R, Lu Y, Popovic J, Law M, Balaya P, Hu Y-S, et al. Fundamentals, status and promise of sodium-based batteries. Nat Rev Mater 2021;6(11):1020–35.
[471] Tarascon J-M. Na-ion versus Li-ion Batteries: Complementarity Rather than Competitiveness. Joule 2020;4(8):1616–20.
[472] Moghadami M, Massoudi A, Nangir M. Unveiling the recent advances in micro-electrode materials and configurations for sodium-ion micro-batteries. J Mater Chem A 2024;12(29):17923–57.
[473] Qu Z, Zhu M, Tang H, Liu L, Li Y, Schmidt OG. Towards high-performance microscale batteries: Configurations and optimization of electrode materials by in-situ analytical platforms. Energy Storage Mater 2020;29:17–41.
[474] Wang Y, Kong D, Huang S, Shi Y, Ding M, Von Lim Y, et al. 3D carbon foam-supported WS2 nanosheets for cable-shaped flexible sodium ion batteries. J Mater Chem A 2018;6(23):10813–24.
[475] NEREID, 2019 NEREID roadmap. , 2019. www.nereid-h2020.eu/roadmap.
[476] Sukumar V, Alahmad M, Buck K, Hess H, Li H, Cox D, et al. Switch array system for thin film lithium microbatteries. J Power Sources 2004;136(2):401–7.
[477] Chen G, Ghaed H, Haque RU, Wieckowski M, Kim Y, Kim G, Fick D, Kim D, Seok M, Wise K, Blaauw D, Sylvester D. A cubic-millimeter energy-autonomous wireless intraocular pressure monitor. 2011 IEEE International Solid-State Circuits Conference 2011:310–2.
[478] Fojtik M, Kim D, Chen G, Lin YS, Fick D, Park J, et al. A Millimeter-Scale Energy-Autonomous Sensor System With Stacked Battery and Solar Cells. IEEE J Solid State Circuits 2013;48(3):801–13.
[479] R.S. S. Oukassi, A. Bazin, C. Secouard, I. Chevalier, S. Poncet,, J.-M.B. S. Poulet, F. Geffraye, J. Brun, 2019 IEEE International Electron Devices Meeting (IEDM), IEEE, San Francisco, CA, USA 2019, pp. 26.1.1–26.1.4., 2019.
[480] Baba M, Kumagai N, Fujita H, Ohta K, Nishidate K, Komaba S, et al. Multi-layered Li-ion rechargeable batteries for a high-voltage and high-current solid-state power source. J Power Sources 2003;119–121:914–7.
[481] Ilika, Ilika Stereax M300 2024. www.ilika.com/micro-solid-state-batteries 2024.
[482] Danilov D, Niessen RAH, Notten PHL. Modeling All-Solid-State Li-Ion Batteries. J Electrochem Soc 2011;158(3):A215.
[483] Raijmakers LHJ, Danilov DL, Eichel RA, Notten PHL. An advanced all-solid-state Li-ion battery model. Electrochim Acta 2020;330:135147.
[484] Clancy TM, Rohan JF. Simulations of 3D nanoscale architectures and electrolyte characteristics for Li-ion microbatteries. J Storage Mater 2019;23:1–8.
[485] TDK, TDK Ceracharge 2024. www.tdk.com/en/tdknext/solution/cera_charge/index.html 2024.
[486] Ramadass YK. Powering the Internet of Things. In: 2014 IEEE/ACM International Symposium on Low Power Electronics and Design (ISLPED); 2014. p. 375–80.
[487] Hayes M, Donnelly J, Fagas G, Salot R, Savelli G, Spies P, et al. EnABLES: European Infrastructure Powering the Internet of Things. In: Smart Systems Integration; 13th International Conference and Exhibition on Integration Issues of Miniaturized Systems; 2019. p. 1–8.
[488] Popovic J. The importance of electrode interfaces and interphases for rechargeable metal batteries. Nat Commun 2021;12(1):6240.
[489] Pletcher D, Rohan JF, Ritchie AG. Microelectrode studies of the lithium/propylene carbonate system—Part I. Electrode reactions at potentials positive to lithium deposition, Electrochimica Acta 1994;39(10):1369–76.
[490] Pletcher D, Rohan JF, Ritchie AG. Microelectrode studies of the lithium/propylene carbonate system—part II. studies of bulk lithium deposition and dissolution. Electrochim Acta 1994;39(13):2015–23.
[491] Boyle DT, Kong X, Pei A, Rudnicki PE, Shi F, Huang W, et al. Transient Voltammetry with Ultramicroelectrodes Reveals the Electron Transfer Kinetics of Lithium Metal Anodes. ACS Energy Lett 2020;5(3):701–9.
[492] Pujari A, Kim B-M, Abbasi H, Lee M-H, Greenham NC, De Volder M. What Makes a Photobattery Light-Rechargeable? ACS Energy Lett 2024;9(8):4024–31.
[493] Ou Y, Zhou P, Hou W, Ma X, Song X, Yan S, et al. Smart materials for safe lithium-ion batteries against thermal runaway. Journal of Energy Chemistry 2024;94:360–92.
[494] Li Y, Bai M, Zhou Z, Wu W-T, Wei L, Hu C, et al. Zero-energy nonlinear temperature control of lithium-ion battery based on a shape memory alloy. Energy Storage Mater 2024;68:103351.
[495] Riad A, Ben Zohra M, Alhamany A. Enhancing electric car lithium-ion batteries by using adaptive materials to improve heat transfer and reduce fatigue, Progress in Engineering. Science 2024;1(4):100025.
[496] Tsai W-T, Lu Y-H, Liu Y-L. In Situ Self-Healing of Gel Polymer Electrolytes Enhancing the Cycling Stability of Lithium Ion Batteries. ACS Sustain Chem Eng 2024;12(20):7894–902.
[497] Lv H, Chu X, Zhang Y, Liu Q, Wu F, Mu D. Self-healing solid-state polymer electrolytes for high-safety and long-cycle lithium-ion batteries. Mater Today 2024;78:181–208.
[498] J.H. Yang, Y.K. Jeong, W. Kim, M.A. Lee, J.W. Choi, H.-s. Kim, K.J. Kim, Dual Flame-Retardant Mechanism-Assisted Suppression of Thermal Runaway in Lithium Metal Batteries with Improved Electrochemical Performances, Advanced Energy Materials n/a(n/a) 2304366.
[499] Li X, Li Z, Zhang W, Jiang X, Han L, Wang X, et al. Flame-retardant in-situ formed gel polymer electrolyte with different valance states of phosphorus structures for high-performance and fire-safety lithium-ion batteries. Chem Eng J 2024;490:151568.
[500] Roh Y, Kim D, Jin D, Kim D, Han C, Choi J, et al. Enhanced safety of lithium ion batteries through a novel functional separator with encapsulated flame retardant and hydroxide ceramics. Chem Eng J 2023;474:145937.
[501] Lan Y, Xiang L, Zhou J, Jiang S, Ge Y, Wang C, et al. Thermal Warning and Shut-down of Lithium Metal Batteries Based on Thermoresponsive Electrolytes. Adv Sci 2024;11(31):2400953.
[502] Tong B, Li X. Towards separator safety of lithium-ion batteries: a review. Mater Chem Front 2024;8(2):309–40.
[503] Zheng X, Luo Z, An J, Yang S, Li B. Built-in hybrid intercalation cations facilitated fast lithium-ion conduction of lamellar montmorillonite for safety lithium-metal batteries. J Storage Mater 2024;86:111269.
[504] Li Y, Wang W, Yang X-G, Zuo F, Liu S, Lin C. A smart Li-ion battery with self-sensing capabilities for enhanced life and safety. J Power Sources 2022;546:231705.
[505] An C, Zheng K, Wang S, Wang T, Liu H, Lin L, et al. Advances in sensing technologies for monitoring states of lithium-ion batteries. J Power Sources 2025;625:235633.
[506] Jacob M, Wissel K, Clemens O. Recycling of solid-state batteries—challenge and opportunity for a circular economy? Materials Futures 2024;3(1):012101.
[507] Men L, Feng S, Zhang J, Luo X, Zhou Y. A systematic review of efficient recycling for the cathode materials of spent lithium-ion batteries: process intensification technologies beyond traditional methods. Green Chem 2024;26(3):1170–93.
[508] Song D, Yu J, Wang M, Tan Q, Liu K, Li J. Advancing recycling of spent lithium-ion batteries: From green chemistry to circular economy. Energy Storage Mater 2023;61:102870.
[509] Mrozik W, Rajaeifar MA, Heidrich O, Christensen P. Environmental impacts, pollution sources and pathways of spent lithium-ion batteries. Energ Environ Sci 2021;14(12):6099–121.
[510] Zhao Q, Sun K, Wang X, Wang Q, Wang J. Examining green-sustainable approaches for recycling of lithium-ion batteries. DeCarbon 2024;3:100034.
[511] Dunn J, Kendall A, Slattery M. Electric vehicle lithium-ion battery recycled content standards for the US – targets, costs, and environmental impacts. Resour Conserv Recycl 2022;185:106488.

[512] Melin HE, Rajaeifar MA, Ku AY, Kendall A, Harper G, Heidrich O. Global implications of the EU battery regulation. Science 2021;373(6553):384–7.
[513] Goyal M, Singh K, Bhatnagar N. Circular economy conceptualization for lithium-ion batteries- material procurement and disposal process. Chem Eng Sci 2023;281:119080.
[514] Milian YE, Jamett N, Cruz C, Herrera-León S, Chacana-Olivares J. A comprehensive review of emerging technologies for recycling spent lithium-ion batteries. Sci Total Environ 2024;910:168543.
[515] Niu B, Xu Z, Xiao J, Qin Y. Recycling Hazardous and Valuable Electrolyte in Spent Lithium-Ion Batteries: Urgency. Progress, Challenge, and Viable Approach, Chemical Reviews 2023;123(13):8718–35.
[516] Li P, Luo S, Zhang L, Liu Q, Wang Y, Lin Y, et al. Progress, challenges, and prospects of spent lithium-ion batteries recycling: A review. Journal of Energy Chemistry 2024;89:144–71.
[517] Duan X, Zhu W, Ruan Z, Xie M, Chen J, Ren X. Recycling of Lithium Batteries—A Review. Energies 2022;15(5):1611.
[518] Khodadadmahmoudi G, Javdan Tabar K, Homayouni AH, S.. Chehreh Chelgani, Recycling spent lithium batteries – an overview of pretreatment flowsheet development based on metallurgical factors. Environ Technol Rev 2023;12(1):2248559.
[519] Kim S, Bang J, Yoo J, Shin Y, Bae J, Jeong J, et al. A comprehensive review on the pretreatment process in lithium-ion battery recycling. J Clean Prod 2021;294:126329.
[520] Garole DJ, Hossain R, Garole VJ, Sahajwalla V, Nerkar J, Dubal DP. Recycle, Recover and Repurpose Strategy of Spent Li-ion Batteries and Catalysts: Current Status and Future Opportunities. ChemSusChem 2020;13(12):3079–100.
[521] Xiao J, Guo J, Zhan L, Xu Z. A cleaner approach to the discharge process of spent lithium ion batteries in different solutions. J Clean Prod 2020;255:120064.
[522] Wang M, Liu K, Dutta S, Alessi DS, Rinklebe J, Ok YS, et al. Recycling of lithium iron phosphate batteries: Status, technologies, challenges, and prospects. Renew Sustain Energy Rev 2022;163:112515.
[523] Wu C, Hu J, Ye L, Su Z, Fang X, Zhu X, et al. Direct Regeneration of Spent Li-Ion Battery Cathodes via Chemical Relithiation Reaction. ACS Sustain Chem Eng 2021;9(48):16384–93.
[524] Jing Q, Zhang J, Liu Y, Zhang W, Chen Y, Wang C. Direct Regeneration of Spent LiFePO4 Cathode Material by a Green and Efficient One-Step Hydrothermal Method. ACS Sustain Chem Eng 2020;8(48):17622–8.
[525] Ji G, Wang J, Liang Z, Jia K, Ma J, Zhuang Z, et al. Direct regeneration of degraded lithium-ion battery cathodes with a multifunctional organic lithium salt. Nat Commun 2023;14(1):584.
[526] Zhou S, Du J, Xiong X, Liu L, Wang J, Fu L, et al. Direct recovery of scrapped LiFePO4 by a green and low-cost electrochemical re-lithiation method. Green Chem 2022;24(16):6278–86.
[527] Liu L, Zhang Y, Zhao Y, Jiang G, Gong R, Li Y, et al. Surface Growth and Intergranular Separation of Polycrystalline Particles for Regeneration of Stable Single-Crystal Cathode Materials. ACS Appl Mater Interfaces 2022;14(26):29886–95.
[528] Wang T, Luo H, Bai Y, Li J, Belharouak I, Dai S. Direct Recycling of Spent NCM Cathodes through Ionothermal Lithiation. Adv Energy Mater 2020;10(30):2001204.
[529] Fan X, Tan C, Li Y, Chen Z, Li Y, Huang Y, et al. A green, efficient, closed-loop direct regeneration technology for reconstructing of the LiNi0.5Co0.2Mn0.3O2 cathode material from spent lithium-ion batteries. J Hazard Mater 2021;410:124610.
[530] Chen X, Luo C, Zhang J, Kong J, Zhou T. Sustainable Recovery of Metals from Spent Lithium-Ion Batteries: A Green Process. ACS Sustain Chem Eng 2015;3(12):3104–13.
[531] Gavrilescu M. Microbial recovery of critical metals from secondary sources. Bioresour Technol 2022;344:126208.
[532] Umicore, https://brs.umicore.com/en/recycling/ (accessed 17/08/2024), 2024.
[533] Jin Y, Zhang T, Zhang M. Advances in Intelligent Regeneration of Cathode Materials for Sustainable Lithium-Ion Batteries. Adv Energy Mater 2022;12(36):2201526.
[534] Wang J, Lyu Y, Zeng R, Zhang S, Davey K, Mao J, et al. Green recycling of spent Li-ion battery cathodes via deep-eutectic solvents. Energ Environ Sci 2024;17(3):867–84.
[535] Velázquez-Martínez O, Valio J, Santasalo-Aarnio A, Reuter M, Serna-Guerrero R. A Critical Review of Lithium-Ion Battery Recycling Processes from a Circular Economy Perspective. Batteries 2019;5(4):68.
[536] Pradhan S, Nayak R, Mishra S. A review on the recovery of metal values from spent nickel metal hydride and lithium-ion batteries. Int J Environ Sci Technol 2022;19(5):4537–54.
[537] Baum ZJ, Bird RE, Yu X, Ma J. Lithium-Ion Battery Recycling─Overview of Techniques and Trends. ACS Energy Lett 2022;7(2):712–9.
[538] Gaida B, Brzęczek-Szafran A. Insights into the Properties and Potential Applications of Renewable Carbohydrate-Based Ionic Liquids: A Review. Molecules 2020;25(14):3285.
[539] Yu H, Yang H, Chen K, Yang L, Huang M, Wang Z, et al. Non–closed–loop recycling strategies for spent lithium–ion batteries: Current status and future prospects. Energy Storage Mater 2024;67:103288.
[540] Wang S, Zhang Z, Lu Z, Xu Z. A novel method for screening deep eutectic solvent to recycle the cathode of Li-ion batteries. Green Chem 2020;22(14):4473–82.
[541] Hua Y, Sun Y, Yan F, Wang S, Xu Z, Zhao B, et al. Ionization potential-based design of deep eutectic solvent for recycling of spent lithium ion batteries. Chem Eng J 2022;436:133200.
[542] Ling JKU, Hadinoto K. Deep Eutectic Solvent as Green Solvent in Extraction of Biological Macromolecules: A Review. Int J Mol Sci 2022;23(6):3381.
[543] Ma C, Laaksonen A, Liu C, Lu X, Ji X. The peculiar effect of water on ionic liquids and deep eutectic solvents. Chem Soc Rev 2018;47(23):8685–720.
[544] Makoś-Chełstowska P, Kaykhaii M, Płotka-Wasylka J, de la Guardia M. Magnetic deep eutectic solvents – Fundamentals and applications. J Mol Liq 2022;365:120158.
[545] Kivelä H, Salomäki M, Vainikka P, Mäkilä E, Poletti F, Ruggeri S, et al. Effect of Water on a Hydrophobic Deep Eutectic Solvent. J Phys Chem B 2022;126(2):513–27.
[546] van Osch DJGP, Zubeir LF, van den Bruinhorst A, Rocha MAA, Kroon MC. Hydrophobic deep eutectic solvents as water-immiscible extractants. Green Chem 2015;17(9):4518–21.
[547] Martins MAR, Crespo EA, Pontes PVA, Silva LP, Bülow M, Maximo GJ, et al. Tunable Hydrophobic Eutectic Solvents Based on Terpenes and Monocarboxylic Acids. ACS Sustain Chem Eng 2018;6(7):8836–46.
[548] Cao J, Su E. Hydrophobic deep eutectic solvents: the new generation of green solvents for diversified and colorful applications in green chemistry. J Clean Prod 2021;314:127965.
[549] Chen L, Chao Y, Li X, Zhou G, Lu Q, Hua M, et al. Engineering a tandem leaching system for the highly selective recycling of valuable metals from spent Li-ion batteries. Green Chem 2021;23(5):2177–84.
[550] Peeters N, Binnemans K, Riaño S. Solvometallurgical recovery of cobalt from lithium-ion battery cathode materials using deep-eutectic solvents. Green Chem 2020;22(13):4210–21.
[551] Wang C, Yang H, Yang C, Liu Y, Bai L, Yang S. A novel recycling process of LiFePO4 cathodes for spent lithium-ion batteries by deep eutectic solvents. J Mater Cycles Waste Manage 2023;25(4):2077–86.
[552] Zhu A, Bian X, Han W, Wen Y, Ye K, Wang G, et al. Microwave-ultra-fast recovery of valuable metals from spent lithium-ion batteries by deep eutectic solvents. Waste Manag 2023;156:139–47.
[553] Xiong C, Kan K, Xie Z, Wang C, Li X, Xu Y, et al. A Green and Efficient Solvent for Simultaneously Leaching Co and Li from Spent Li-Ion Batteries: Dicarboxylated Polyethylene Glycol. ACS Sustain Chem Eng 2023;11(39):14367–75.
[554] Ma W, Liu M, Zhang X, Zhao Q, Liang Z. An Efficient and Precipitant-Free Approach to Selectively Recover Lithium Cobalt Oxide Made for Cathode Materials Using a Microwave-Assisted Deep Eutectic Solvent. Energy Fuel 2023;37(1):724–34.
[555] Tang S, Feng J, Su R, Zhang M, Guo M. New Bifunctional Deep-Eutectic Solvent for In Situ Selective Extraction of Valuable Metals from Spent Lithium Batteries. ACS Sustain Chem Eng 2022;10(26):8423–32.

[556] Łukomska A, Wiśniewska A, Dąbrowski Z, Kolasa D, Luchcińska S, Domańska U. Separation of cobalt, lithium and nickel from the “black mass” of waste Li-ion batteries by ionic liquids. DESs and organophosphorous-based acids extraction, Journal of Molecular Liquids 2021;343:117694.
[557] Tran MK, Rodrigues M-T-F, Kato K, Babu G, Ajayan PM. Deep eutectic solvents for cathode recycling of Li-ion batteries. Nat Energy 2019;4(4):339–45.
[558] Wang H, Li M, Garg S, Wu Y, Nazmi Idros M, Hocking R, et al. Cobalt Electrochemical Recovery from Lithium Cobalt Oxides in Deep Eutectic Choline Chloride +Urea Solvents. ChemSusChem 2021;14(14):2972–83.
[559] Landa-Castro M, Aldana-González J, Montes de Oca-Yemha MG, Romero-Romo M, Arce-Estrada EM, Palomar-Pardavé M. Ni–Co alloy electrodeposition from the cathode powder of Ni-MH spent batteries leached with a deep eutectic solvent (reline). J Alloy Compd 2020;830:154650.
[560] A. Oy, How the collected batteries are recycled?, https://www.akkuser.fi/en/home/, 2024.
[561] Duesenfeld, https://www.duesenfeld.com/index_de.html, 2024.
[562] Tytgat J. The Recycling Efficiency of Li-ion EV batteries according to the European Commission Regulation, and the relation with the End-of-Life Vehicles Directive recycling rate. World Electric Vehicle Journal 2013;6(4):1039–47.
[563] Tan DHS, Chen Z. Sustainable design of fully recyclable all solid-state batteries. MRS Bull 2020;45(12):990–1.
[564] Ciez RE, Whitacre JF. Examining different recycling processes for lithium-ion batteries. Nat Sustainability 2019;2(2):148–56.
[565] Golmohammadzadeh R, Faraji F, Jong B, Pozo-Gonzalo C, Banerjee PC. Current challenges and future opportunities toward recycling of spent lithium-ion batteries. Renew Sustain Energy Rev 2022;159:112202.
[566] Zhang Q, Gao X-W, Liu X, Gu Q, Mu J, Luo W-B. Economical and Ecofriendly Lithium-Ion Battery Recycling: Material Flow and Energy Flow. ACS Sustain Chem Eng 2024;12(7):2511–30.
[567] Neumann J, Petranikova M, Meeus M, Gamarra JD, Younesi R, Winter M, et al. Recycling of Lithium-Ion Batteries—Current State of the Art, Circular Economy, and Next Generation Recycling. Adv Energy Mater 2022;12(17):2102917.
[568] Wang Y, Hu F, Wang Y, Guo J, Yang Z, Jiang F. Revolutionizing the Afterlife of EV Batteries: A Comprehensive Guide to Echelon Utilization Technologies. ChemElectroChem 2024;11(4):e202300666.
[569] Harper GDJ, Kendrick E, Anderson PA, Mrozik W, Christensen P, Lambert S, et al. Roadmap for a sustainable circular economy in lithium-ion and future battery technologies. Journal of Physics: Energy 2023;5(2):021501.
[570] Ferrara C, Ruffo R, Quartarone E, Mustarelli P. Circular Economy and the Fate of Lithium Batteries: Second Life and Recycling. Adv Energy Sustainability Res 2021;2(10):2100047.
[571] Harper G, Sommerville R, Kendrick E, Driscoll L, Slater P, Stolkin R, et al. Recycling lithium-ion batteries from electric vehicles. Nature 2019;575(7781):75–86.
[572] Zimmerman JB, Anastas PT, Erythropel HC, Leitner W. Designing for a green chemistry future. Science 2020;367(6476):397–400.
[573] Konietzko J, Baldassarre B, Brown P, Bocken N, Hultink EJ. Circular business model experimentation: Demystifying assumptions. J Clean Prod 2020;277:122596.
[574] BYD, https://www.byd.com/eu/blog/BYDs-revolutionary-Blade-Battery-all-you-need-to-know, 2024.
[575] Wrålsen B, Prieto-Sandoval V, Mejia-Villa A, O’Born R, Hellström M, Faessler B. Circular business models for lithium-ion batteries - Stakeholders, barriers, and drivers. J Clean Prod 2021;317:128393.
[576] Ali H, Khan HA, Pecht M. Preprocessing of spent lithium-ion batteries for recycling: Need, methods, and trends. Renew Sustain Energy Rev 2022;168:112809.

Carlos M. Costa graduated in Physics in 2005 and obtained his Master Degree in Materials Engineering in 2007. In 2014, he received the Ph.D. in Physics from the Science School of the University of Minho. Currently, he is Associate Researcher at the same institution. He has been visiting scientist at the “La Sapienza” University of Rome, Ulsan National Institute of Science and Technology (UNIST) and Indian Institute of Technology Jodhpur (IITJ). His work is mainly focused on the development electroactive polymer based porous membranes, anode and cathode materials for energy storage applications, including lithium-ion batteries, sodium-ion batteries and printed batteries. It is also interested in the processing, characterization and optimization of nanostructured polymers and porous polymer nanocomposites. He has published over 250 scientific publications, 18 books chapters and is co-editor of three books, one on printed batteries, one on multifunctional materials and one on sustainable energy systems. https://scholar.google.com/citations?user=ax3i9sAAAAAJ&hl=pt-PT. ORCID iD: https://orcid.org/0000-0001-9266-3669. https://www.researchgate.net/profile/Carlos_Costa10

S. Lanceros-Mendez is Ikerbasque Professor at BCMaterials, Basque Center for Materials, Applications and Nanostructures, Leioa, Spain, where he is the Scientific Director. He is Associate Professor at the Physics Department of the University of Minho, Portugal (on leave), where also belongs to the Center of Physics. He graduated in Physics at the University of the Basque Country, Leioa, Spain and obtained his Ph.D. degree at the Institute of Physics of the Julius-Maximilians-Universität Würzburg, Germany. He has been Associated Researcher to the International Iberian Nanotechnology Laboratory and visiting researcher at Montana State University, US, Pennsylvania State University, US and University of Potsdam, Germany, among others., His work is focused in the development of smart and multifunctional materials for sensors and actuators, energy, environmental and biomedical applications. He has published over 990 scientific articles, edited 6 books, filed 12 patents, supervised over 140 MsC and 50 PhD students and four Spin-off companies have been created based on technologies developed in his research group. https://scholar.google.com/citations?user=AbLpTrkAAAAJ&hl=pt. ORCID iD: http://orcid.org/0000-0001-6791-7620. https://www.researchgate.net/profile/Senentxu_Lanceros-Mendez